Discrete Rate Simulation Framework for Narrow Vein Mining Performance Optimization Based on Geological Variability Modelled by Geostatistical Simulation

Javier Alejandro Órdenes Alegría

Department of Mining and Materials Engineering

McGill University, Montreal, QC, Canada

February 2025

A thesis submitted to McGill University in partial fulfillment of the requirements of the degree of Doctor of Philosophy

Abstract

One of the primary challenges facing the mining industry is the geological uncertainty associated with the variability of minerals within deposits. This variability can have significant implications for every stage of the mining process, from exploration and resource estimation to mine planning and mineral processing. The purpose of this research is to enhance the implementation of data-driven frameworks for evaluating mining projects, incorporating stochastic simulation to develop digital tools that support management decisions. The aim is to create a quantitative framework that integrates geological and geometallurgical models, enabling a deeper understanding of how various variables influence the overall performance of mining systems. A common practice in mining is to generate a single mining plan based on a deterministic resource model, where all inputs and outcomes are derived from a single prediction of values at unsampled locations on a grid, often overlooking the inherent random variability of in-situ grades and other geology-dependent variables. One of the main limitations of this approach is its inability to assess the risks caused by geological uncertainty, such as variability in ore grade and tonnage. Significant changes in the geological characteristics of the ore can also severely affect the efficiency and outcomes of mining operations. Minerals are inherently complex and exhibit significant variability due to their geological and mineralogical characteristics, which directly influence plant performance. Consequently, a mine is expected to experience significant variations in mineral characteristics over its lifetime. Understanding these problems and their impacts is crucial for optimizing the operations involved in the value chain, thereby reducing costs and minimizing potential environmental impacts. These insights enable the development of predictive models that anticipate how minerals will behave, thereby reducing the risks associated with variability and improving overall operational efficiency in mining projects.

In mining companies there is a justified effort in the characterization and grades control, where a large amount of economic and human resources are focused on the characterization and quantification of the metal contained, but in concrete terms, this represents a small part of the total mass that will enter the processing plant - in the best of cases 3 to 5% of the total ore mined; underestimating the potential problems for the process in the remaining portion of mass that enters the process. This dissertation presents a quantitative approach to take advantage of the information

obtained from geometallurgical sampling campaigns to optimize reagent consumption and the overall performance in gold and silver ore processing plants in the context of underground mining. Based on a clear and intelligent definition of mineral classification and stockpile control policies, changes in modes of operation are triggered by observed variation and forecasted inventory levels. The resulting modes of operation provide an integrated response to geological and geometallurgical variability; demonstrated through the simulation of discrete events/rates. It is critical that strategic decisions in the evaluation of mineral deposits take into account this geological uncertainty. The mining systems dynamics framework uses mass balance in conjunction with discrete event/rate simulation, a subset of Monte Carlo simulations, to connect geological data with alternative downstream resource configurations. The use of discrete rate simulation assays in combination with stochastic simulations can provide a better understanding of the dynamics of geological variability and mineral processing variables within a mining system by optimizing the balance of incoming ore. The use of simulations provides reliable inputs for modeling geological uncertainty by testing the possible values of the sample dataset while respecting their probability of occurrence (histogram distribution). This approach allows the benefits of each configuration to be compared, along with the corresponding capital investments, for example to calculate the net present value (NPV). This research emphasizes that stockpiles management policies are crucial to maximizing plant yield and metal production, and therefore the bottom line in the cash flow of a specific project. Additionally, highlights that these policies should be considered in long- and medium-term mine planning due to their potential benefits to system performance. However, these policies need to be carefully estimated, as the beneficial effects of increasing the target stock level are limited. A high target level can restrict the system, reducing its flexibility and potentially having a negative effect on overall mining system performance.

Resumé

L'un des principaux défis auxquels fait face l'industrie minière est l'incertitude géologique associée à la variabilité des minéraux dans les gisements. Cette variabilité peut avoir des répercussions importantes à chaque étape du processus minier, de l'exploration et de l'estimation des ressources à la planification et au traitement des minéraux. Cette recherche vise à améliorer la mise en œuvre de cadres axés sur les données pour l'évaluation des projets miniers, en intégrant la simulation stochastique afin de développer des outils numériques soutenant les décisions de gestion. L'objectif est de créer un cadre quantitatif qui intègre des modèles géologiques et géométallurgiques, permettant une compréhension plus approfondie de la façon dont diverses variables influencent la performance globale des systèmes miniers. Une pratique courante dans le secteur minier consiste à générer un seul plan d'exploitation minière basé sur un modèle de ressources déterministe, où toutes les entrées et tous les résultats sont dérivés d'une seule prédiction de valeurs à des emplacements non échantillonnés sur une grille, négligeant souvent la variabilité aléatoire inhérente des teneurs in situ et d'autres variables dépendantes de la géologie. L'une des principales limites de cette approche est son incapacité à évaluer les risques causés par l'incertitude géologique, comme la variabilité de la teneur et du tonnage du minerai. Des changements importants dans les caractéristiques géologiques du minerai peuvent également affecter gravement l'efficacité et les résultats des opérations minières. Les minéraux sont intrinsèquement complexes et présentent une variabilité importante en raison de leurs caractéristiques géologiques et minéralogiques, qui influencent directement le rendement des plantes. Par conséquent, on s'attend à ce qu'une mine connaisse des variations importantes dans les caractéristiques minérales au cours de sa durée de vie. La compréhension de ces problèmes et de leurs impacts est cruciale pour optimiser les opérations impliquées dans la chaîne de valeur, réduisant ainsi les coûts et minimisant les impacts environnementaux potentiels. Ces informations permettent de développer des modèles prédictifs qui anticipent le comportement des minéraux, réduisant ainsi les risques associés à la variabilité et améliorant l'efficacité opérationnelle globale des projets miniers.

Dans les entreprises minières, il y a un effort justifié dans la caractérisation et le contrôle de la teneur du minerai, où une grande partie des ressources économiques et humaines est concentrée sur la caractérisation et la quantification du métal contenu, mais concrètement, cela représente une

petite partie de la masse totale qui entrera dans l'usine de traitement - dans le meilleur des cas 3 à 5% du minerai total extrait ; sous-estimer les problèmes potentiels pour le processus dans la partie restante de la masse qui entre dans le processus. Cette thèse présente une approche quantitative permettant de tirer parti des informations obtenues lors des campagnes d'échantillonnage géométallurgique afin d'optimiser la consommation de réactifs et la performance globale des usines de traitement de minerai d'or et d'argent dans le contexte de l'exploitation minière souterraine. Grâce à une classification claire et rigoureuse des minéraux et des politiques de gestion des stocks, les changements de modes de fonctionnement sont déclenchés par les variations observées et les niveaux de stock prévus. Les modes de fonctionnement qui en résultent apportent une réponse intégrée à la variabilité géologique et géométallurgique ; démontré par la simulation d'événements/taux discrets. Il est essentiel que les décisions stratégiques dans l'évaluation des gisements minéraux tiennent compte de cette incertitude géologique. Le cadre de dynamique des systèmes miniers utilise le bilan de masse en conjonction avec la simulation d'événements/taux discrets, un sous-ensemble des simulations de Monte Carlo, pour relier les données géologiques à d'autres configurations de ressources en aval. L'utilisation d'analyses de simulation à taux discrets combinée à des simulations stochastiques peut fournir une meilleure compréhension de la dynamique de la variabilité géologique et des variables de traitement des minéraux au sein d'un système minier en optimisant l'équilibre du minerai entrant. L'utilisation de simulations fournit des données fiables pour modéliser l'incertitude géologique en testant les valeurs possibles de l'ensemble de données de l'échantillon tout en respectant leur probabilité d'occurrence (distribution de l'histogramme). Cette approche permet de comparer les avantages de chaque configuration, ainsi que les investissements en capital correspondants, par exemple pour calculer la valeur actuelle nette (VAN). Cette recherche souligne que les politiques de gestion des stocks sont essentielles pour maximiser le rendement de l'usine et la production de métaux, et donc le résultat net dans le flux de trésorerie d'un projet spécifique. De plus, souligne que ces politiques devraient être prises en compte dans la planification minière à long et à moyen terme en raison de leurs avantages potentiels pour le rendement du système. Cependant, ces politiques doivent être évaluées avec soin, car les effets bénéfiques d'une augmentation du niveau de stock cible sont limités. Un niveau cible élevé peut restreindre le système, réduire sa flexibilité et avoir un effet négatif sur les performances globales du système de minage.

Acknowledgements

I would like to express my sincerest gratitude to Prof. Alessandro Navarra for giving me the opportunity to join the Mining System Dynamics group as his doctoral candidate. Your relentless guidance, motivation, availability, and trust have been fundamental in starting my journey as a researcher. Thank you for helping me strive to become the best version of myself, for always seeing the best in me, highlighting my strengths, and helping me improve on my weaknesses. My heartfelt thanks also go to my fellow members of the Mining System Dynamics group for all the discussions, shared experiences, collaborations, successes, failures, and memories we have shared throughout our studies. A special thanks to Aldo Quelopana for all your help, especially when we first arrived in Canada—your kindness and the warmth of your family meant so much to us. To Ryan Wilson, thank you for your invaluable help when I started my courses and understanding life in Canada, and for your valuable help in the final days in the university. Your friendship is something I will always treasure. I want to extend my gratitude to my dear colleague Roberto Retamal for his support with geostatistical analysis and modeling. Also, those telematic conversations and messages were of great help during my research. In these brief words.

I want to pay tribute to my family, who have shared this tremendous life experience with me. To my beloved spouse, Marcela—your constant support and advice have been crucial in helping me stay on course and remain steadfast in my goals. To my sons, Diego and Bruno—thank you for the many good moments we shared, for allowing me to witness your growth, and for being a part of my daily life. And to my dear daughter Catalina, who thrived during our time in Canada, thank you for your strength and resilience. Also, want to dedicate some words to Marcela's family for their tremendous help and emotional support to my wife, without them this would be much harder. To my parents, Audilia and Orlando, without whose support this venture would not have been possible. To my mother—thank you for always believing in me and my project, for all your love and understanding, and for traveling to be with us. And to my father, whom I lost during the pandemic—thank you for helping to care for my family when I was away in 2020. I wish you could have shared this experience with us, but fate had other plans. I know you are with me, watching over us.

Thank you all for being a part of this tremendous journey……..…Javier.

Contribution of Authors

This thesis is written in a traditional format, and includes work completed between January 2020 and June 2024 as part of the author's PhD studies in mining engineering at McGill University. The work resulted in a series of four peer-reviewed publications, each of which is associated with a specific section in Chapter 4. The author contributions (following the CRediT taxonomy) corresponding to each manuscript are as follows:

Paper #1: Órdenes, J., Wilson, R., Peña-Graf, F. & Navarra, A., 2021. Incorporation of geometallurgical input into gold mining system simulation to control cyanide consumption. Minerals, 11(1023), pp. 1–16. Conceptualization, J.Ó., R.W., F.P.-G., and A.N.; Methodology, J.Ó. and A.N.; Data curation, J.Ó.; Investigation, J.Ó. and F.P.-G.; Writing—original draft preparation, J.Ó. and A.N., Writing—reviewing and editing, R.W. and A.N.; Supervision, A.N.; Funding acquisition, J.Ó. and A.N. All authors have read and agreed to the published version of the manuscript. Funding acquisition, A.N and J.Ó.

Paper #2: Órdenes, J.; Toro, N.; Quelopana, A.; Navarra, A. Data-Driven Dynamic Simulations of Gold Extraction Which Incorporate Head Grade Distribution Statistics. Metals 2022, 12, 1372. https://doi.org/10.3390/met12081372 Conceptualization, J.Ó., N.T. and A.N.; Methodology, J.Ó. and A.N.; Data curation, J.Ó.; Investigation, J.Ó. and A.Q.; Writing—original draft preparation, J.Ó. and A.N.; Writing—reviewing and editing, A.Q. and A.N.; Supervision, N.T. and A.N.; All authors have read and agreed to the published version of the manuscript Funding acquisition, J.Ó. and A.N.

Paper #3: Órdenes, J.; Pearce, K.; Bai, J.; Peña-Graf, F. and Navarra, A. (Under revision). Sequential Gaussian Simulation Incorporated into Dynamic Mass Balance for Simulation-based Control of Cyanide Consumption. Conceptualization, J.Ó and A.N.; Methodology, J.Ó. and A.N.; Data curation, J.Ó. and A.N.; Investigation, J.Ó. and A.N.; Formal analysis, J.Ó. and A.N.; Validation, J.Ó. and A.N.; Visualization, J.Ó., K.P, J.B and A.N.; Writing–original draft preparation, J.Ó., K.P, J.B. and A.N.; Writing–reviewing and editing, J.Ó.,., K.P, J.B. and A.N.; Supervision, A.N.; Funding acquisition, J.Ó. and A.N.

Paper #4: Órdenes, J.; Retamal, R.; Mroz, M.; Quelopana, A.; Zbadi, G and Navarra, A. (Accepted). Discrete Rate Simulation for Geostatistically Informed Economical Evaluation of Narrow Vein Au-Ag Mining and Processing. CIM Journal. Conceptualization, J.Ó and A.N.; Methodology, J.Ó; Data curation, J.Ó; Investigation, J.Ó., R.R. and A.Q.; Formal analysis, J.Ó; Validation, J.Ó. and A.N.; Visualization, J.Ó., Z.G; Writing–original draft preparation, J.Ó., M.M, and A.N.; Writing–reviewing and editing, J.Ó., M.M, G.Z. and A.N.; Supervision, A.N.; Funding acquisition, J.Ó. and A.N.

Table of Contents

List of Figures

List of Tables

List of Abbreviations

AD	Anderson-Darling
AG	Autogenous
AI	Artificial intelligence
CAPEX	Capital Expenses
CCDF	Conditional Cumulative Distribution Functions
CDF	Cumulative Density Function
DES	Discrete Event Simulations
DPP	Discounted Payback Period
DRS	Discrete Rate Simulations
GOF	Goodness of Fit
HOS	Higher Order Statistics
IRR	Internal Rate of Return
KPI	Key Performance Index
KS	Kolmogorov–Smirnov
LUD	Lower Upper Decomposition
MB	Mass Balance
MCS	Monte Carlo Simulations
NPV	Net Present Value
R&P	Room and Pillar
REE	Rare Earth Element
RF	Random Function
RNG	Random Number Generators
SA	Simulated Annealing
SAG	Semi-Autogenous
SGS	Sequential Gaussian Simulation
SIS	Sequential Indicator Simulation
TBM	Turning Bands Method

Chapter 1

Introduction

1.1 Overview

Mining is an interconnected sequence of systems and sub-systems involving geological, mining and mineral processing variables. One of the most challenging problems for managers is developing a process that effectively provides the information on key performance indicators necessary to evaluate a project, plan strategically, and improve operational efficiency (McGrath, 2005). The assessment of a mining project begins with the collection of geological, mining, and mineral processing data to obtain the economical parameters of the global process. As well as to establish the economic metrics that will help determine whether the project is viable. These information is related; therefore, the variables that can influence project results- both positively and negatively - can be at different stages and impact level on the final cash flow (Bassan & Knights,2008). The mining industry is facing a new cycle for metal prices, wind tailed by the world demand to obtain raw materials useful to developed new technology to fight against carbon emissions and climate change. Concerns associated with the attempt to reduce greenhouse gas emissions by changing fossil fuels in favor of cleaner energies, have driven steady progress towards to environmentally friendly technologies. In this context, the mining industry will be the main pillar in meeting this growing demand for green technologies metals which are essential components for electric vehicles, energy storage systems, and other applications crucial to the transition to a future low-carbon economy.

As the demand for greener technologies is rising fast, the challenge for the mining sector is how scale up operations to ensure a steady supply of these critical materials. Expanding mines currently in production, opening new mines (slow and costly process), requires investing in technologies to increase efficiency. In parallel, operations must reduce energy consumption, water usage, and greenhouse gas emissions in the extraction and processing for the obtention of green technology metals. A key challenge of the low carbon transition with respect to the minerals and

metals requirement, is understanding the scope of this growing demand, and ensuring the supply of these materials while minimizing any negative environmental, social and economic impacts (Laing & Pinto, 2023). Some of the key green metals include lithium, cobalt, nickel, copper, rare earth elements (REE), and precious metals. For example, lithium, nickel, manganese, and cobalt are critical for electric vehicle batteries for lithium-ion batteries (Mills, R, 2023), while copper is a fundamental component in electric wiring, and silver is a key component for solar panels. However, expected supply from existing mines and projects under construction is estimated to meet only half of projected lithium and cobalt requirements and 80% of copper needs by 2030 (Birol, 2022).

Ore deposits exploited by traditional mining methods remain the main source for obtaining the raw materials needed, but currently worldwide, mining is suffering from depletion of its large shallow deposits. This implies that mining is migrating into new sources for the obtention of the materials need to the electromobility and the evolution of the global energy market. From the mining industry perspective large open pit operations will be replaced by underground extraction methods (Vives, 2015) for increase the current global production rates, opening an opportunity to medium and small-scale mining be another player in the "Low- Carbon Revolution". In the search for new extraction areas, whether deeper or farther from depleted zones—and consequently more distant from existing facilities in operational mines—drastic changes in geology are to be expected. These can significantly impact mineral processing, requiring a rigorous evaluation to ensure continued operational efficiency and profitability.

Within modern mines, there is an emerging need for intelligent coordination and the development of interdisciplinary expertise with increasing automation (Navarra, 2019). Therefore, innovation in specialized digital tools development to simulate mining operations and project evaluation are an attractive alternative, considering the green economy context. These developments can help to plan, design, and optimize faster several aspects of mining by incorporating real-time data and historical data patterns to improve mining operations. This integration allows for more accurate and dynamic simulations and through this companies can better predict future trends, potential risks, project outcomes and new business opportunities.

1.2 Mining Dynamics Simulation Frameworks

Mining Dynamics Simulation frameworks are software tools designed to model and analyze complex systems. These platforms can provide a comprehensive and dynamic representation of several aspects of mining operations, including equipment performance, worker activities, and environmental conditions. They can be utilized to design and test alternative approaches to integrated management, encompassing aspects such as scheduling, resource allocation, and operational planning over different timeframes. Furthermore, these simulation platforms facilitate scenario analysis, allowing mining companies to evaluate the potential impacts of various operational strategies before been implemented. Simulation frameworks in mining are used to model mining processes including the simulation of drilling, blasting, loading, hauling, and other operations. The frameworks can model equipment performance, workforce efficiency, and the impact of different mining methods and mineral processing. Furthermore, are useful to evaluate the economic feasibility of mining projects by considering factors like commodity prices, capital and operational costs, and expected revenues and also, for the assessment of environmental impact of mining operations, including land disturbance, water usage, and pollution. Likewise, can incorporate geological information allowing for the assessment of resource potential and exploration strategies and the assessment random natural variability associated to mineral resources also known as geological uncertainty. For mining and mineral processing systems, these platforms can be initially developed using mass balancing in conjunction with discrete event/rate simulation (DES/DRS), and then detailed in later engineering phases by hierarchically embedding models and sub-models to represent critical risks and opportunities (Navarra, 2023).

One of the main challenges confronting the mining industry is the geological uncertainty associated with increased variability and complexity of mineral distributions within the deposits. A common practice in mining is generate a single mine plan based on a deterministic resource model, where all mine plan inputs and outcomes are based on the calculation of a single prediction of values in the unsampled location in a grid, ignoring the random variability in-situ of grades (Goovaerts, 1997; Chiles and Delfiner, 1999). One of the main limitations of this approach is the inability to assess the risk caused by geological uncertainty (i.e., the variability of ore grade and tonnage). Significative changes in mineralogy can affect severally the efficiency and outcomes of both mining and plant operations. Understanding these changes and their impacts is crucial for

optimizing mineral processing operations, reducing costs and potential environmental impacts. Minerals are inherently complex and exhibit significant variability due to their geological and mineralogical characteristics, which influence plant performance. Therefore, it is expected indeed that a mine can experience significant variations in mineral characteristics over its life in production. These insights also enable the development of predictive models that anticipate how minerals will behave in various processing scenarios, thereby reducing the risks associated with variability and improving overall operational efficiency in mining projects. It is therefore critical that strategic decisions to develop a mineral deposit evaluation take this geological uncertainty into account (Navarra et al., 2018). Navarra (2016) developed a mining systems dynamics framework were by using mass balancing in conjunction with discrete event simulation (DES) a sub-from of Montecarlo simulations (MCS), connecting geological data to alternate configurations of the downstream resources, hence comparing the benefit of each configuration, and the corresponding capital investments to finally calculate the net present value (NPV). With this approach it is possible to address the geological uncertainty by incorporating stochastic modelling and mine planning algorithms as they simultaneously consider several geological scenarios generated by conditional simulation in an open pit mine. With the advancement of knowledge, new approaches to ore prospecting have been incorporated, including the evaluation of variables that can affect mineral processes and plant performance (e.g. hardness and reagent consumption). The aim of this research is the development of quantitative tools that enable informed decisions to address the complexities related to abrupt changes in the characteristics of the minerals entering the processing plant.

1.3 Research Objectives and Thesis Structure

The emergence of new digital technologies has opened the door to opportunities for developing new tools to accelerate the process of re/evaluation of mining assets effectively and in a context of constant economic uncertainty. The nature of the mining industry is closely related to risk; nevertheless, identifying the uncertainties of a given project, estimating and analyzing its impact, establishing controls are vital to find new business opportunities. The present research delves into the implementation of digital frameworks for data-driven mining project evaluation, incorporating stochastic simulation to develop digital tools that support management decisions. The objective of this research is to develop a quantitative framework for mining project evaluation that incorporates

geological, geometallurgical, and economic models to understand the influence of various variables on the overall performance of mining systems. This report includes a preliminary literature review with a general overview of the methodologies that support the present research providing an immersion of all the pertinent topics addressed in this thesis. This includes a broad introduction into mineral deposits and related underground methods, a Montecarlo simulations overview, the principles of conditional simulation in geostatistics, mining systems dynamics, and introduction to mining project evaluation (Chapter 2). Description of the main methodologies applied to the DRS framework implementation (Chapter 3). This is followed by different case studies in the context of underground mining, which evaluates the influence of different geological contexts on throughput, head grades and reagent consumption (Chapter 4); a discussion based on the case studies to relate the simulation frameworks and the effects on the performance outcomes of the different mining systems presented, and considerations for future work and the evolution alternatives for the developed framework and the incorporation of supplementary methods (Chapter 5). Lastly, the summary and final conclusions (Chapter 6). The overall thesis structure and chapters overview are shown in Figure 1.3.1.

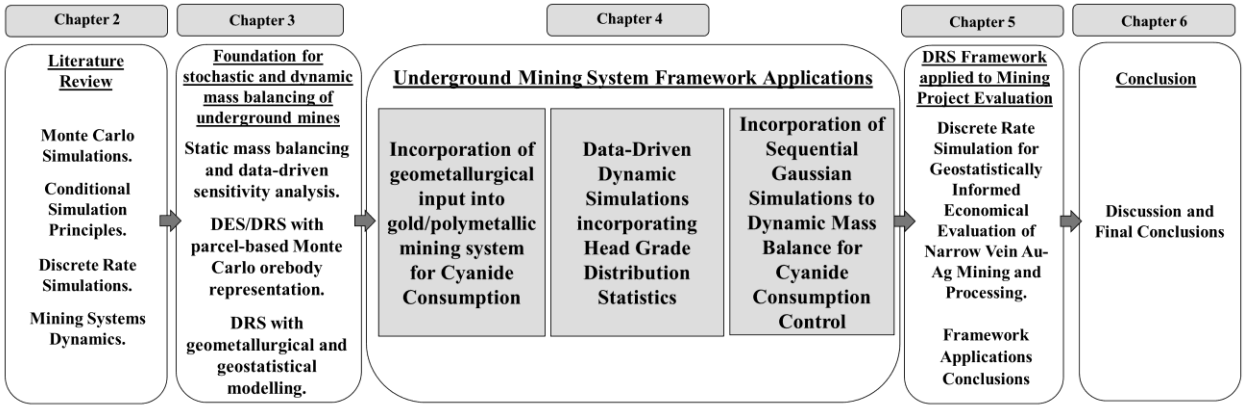

Figure 1.3.1: Schematic flow chart of overall thesis structure and chapters overview.

1.4 Contribution to Original Knowledge

The current thesis has made a number of contributions to original knowledge through the development of a series of case studies focused on the integration of Montecarlo Simulations, Conditional Simulation and Mining Systems Dynamics. Following the earlier work by Navarra et al. (2019):

(1) The DRS framework was extended to input new variables, with this in addition to evaluating the feed tonnage and final yield, it is also possible to calculate the output statistics of head grades, reagent consumption.

(2) Probability distribution models and data analysis for a variable have been incorporated based on the simulation framework extension previously developed. This study applies data-driven simulation modeling, to represent standardized operational modes and the impact of the variable on the operational performance.

(3) The scope of the simulation framework has been extended to be able to impute the added variables, but in this case, based on block models generated by stochastic simulation. This contribution is a significant improvement; allows to feeding simulation frameworks with spatially located information. Therefore, this extension allows high-cost geological information to be processed through advanced geostatistical methodologies and can be used as a source of information for mining project evaluations. This has a high potential impact on the mining industry, as it allows the identification of possible risks associated with the execution of a mining project, anticipating problems in the plant such as unexpected variations in processing parameters and reagent consumption caused by the mineralogical variability of different ore types.

(4) This research aims to show that quantitative frameworks based on Monte Carlo simulation are a suitable way for the development of digital tools that can contribute to automation and Mining Industry 4.0. These tools can be applied in project optimization and the development of process controls, which make decisions based on data. In addition, the fact that the data feed is linked to a spatial location means making it possible to use it in different time horizons of mine planning.

Chapter 2

Literature Review

2.1 Monte Carlo Simulations (MCS)

Monte Carlo simulation is a mathematical technique that allows for the modeling of complex systems and the assessment of uncertainty in various scenarios based on random experimentations. Emerged from the researchers on the Manhattan Project, named after the Monte Carlo Casino in Monaco due to its use of randomness. Monte Carlo simulations have been applied in several fields such as finance, engineering, and even in areas like climate modeling. For engineering disciplines, a common use is estimating reliability of mechanical components, effective life of pressure vessels in reactors (Raychaudhuri, 2008). MCS is helpful to understand how probable a phenomenon is to happen, due to is possible to run various virtual experiments giving a stochastic insight of a process. Monte Carlo simulation is one of the main applications involving the use of random number generators (RNG). By the use of random numbers, we can get sampled values based on the distribution of one or more variables, and then calculate the function by putting these samples into the model. Also, is one of the best technics for randomness testing generators properties, through the comparison of results from simulations using different generators. Many widely used generators that perform well in standard statistical tests are shown to fail these Monte Carlo tests (Coddington, 1993).

The method uses repeated random sampling to obtain numerical results for problems that might be deterministic in principle. The aim of the method is to determine how the lack of knowledge, random variation, or error affects the sensitivity or performance of the system that is being modelled (Wittwer, 2004). MCS method is a powerful modelling tool for the analysis of complex systems, due to its capability of achieving a closer adherence to reality (Zio, 2013). Real-world data not always fit perfectly into a gaussian distributions (a.k.a. Normal), for this reason, Monte Carlo method is very powerful because a wide variety of distributions can be inputted into the simulation framework (e.g., uniform, triangular, binomial, etc.). This methodology

incorporates variability and uncertainty directly into the calculations, which makes Monte Carlo frameworks a suitable tool for model phenomenon that have a high unpredictability, instead of giving a single deterministic answer to a problem. Monte Carlo methods provide a range of possible outcomes and the probabilities they will occur, a good approach for risk analysis and decision-making. One of the disadvantages of this method is simulations require many iterations to get accurate results, this implies are computationally expensive, time-consuming and may not be feasible for all problems. Also, not always is the optimal choice for some problematics, deterministic technics or other forms of simulations might be a more suitable and efficient alternative. The quality of the results strongly depends on the quality of the data used for modelling, poorly controlled samples, incorrect assumptions, or biased data, will result in a likely incorrect output or not informative (garbage in, garbage out). Figure 2.2.1 summarizes the principles of the Monte Carlo methods.

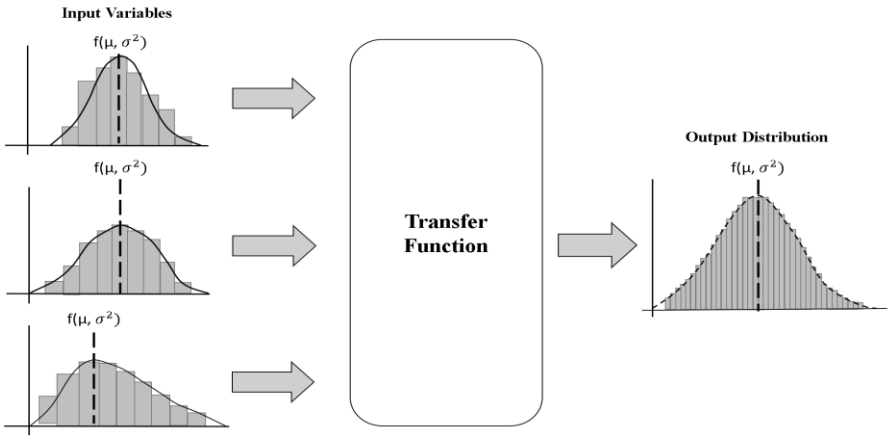

Figure 2.1.1 Principles of the Monte Carlo methods scheme.

In the mining industry, is widely spread the use Monte Carlo methods in risk modelling, perform sensitivity analysis and optimizing parameters (Kleijnen, 2012). In literature, there is several applications of this technic in mining related research, in areas such as resource geology, mine operation and equipment assessment, geotechnics and ground support, mineral processing and mine safety, all pointing towards support managers for decision-making.

Samis and Davis (2014) evaluated a financing proposal in a small gold project KuisebSun in Africa. The mine used traditional static (single value) and Monte Carlo discounted cash flow methods to evaluate the proposal and then compare it with a real option of the proposal which

relies on market-based signals of price risk. The Monte Carlo method was performed to quantify the effect of technical default risk and the ability of creditors to recover lost cash flows via a loan shortfall facility. The Monte Carlo simulation was also able to produce default probabilities and expected creditor losses. Kumral and Sari (2017) propose an extraction sequencing approach in which the net present value of a mining project was maximized. They combine chance-constrained programming with MCS to solve the gold mine extraction sequencing of an open-pit mine in a context of financial and technical uncertainties generated by grades. Mathey (2022) used the Monte Carlo technique to production planning and daily economic decision making in mine production management, with an example of underground production with miners and truck haulage. The study was based on the availability of equipment and personnel are the predominant variables influencing mine output and productivity and that those variables be represented by binomial probability distributions. Cardozo et al. (2022) present an application of the Monte Carlo method as a procedure of risk analysis in the economic evaluation of a gold mine project in Brazil, exploited through the long hole underground mining method. Deterministic evaluation methodologies were compared with the probabilistic output generated by MCS, evaluating the impact of different variables (e.g., ore content, tonnage, metal price) input into the economic model. The proposed methodology was applied to the conceptual and pre-feasibility studies for underground mining, evaluating the impact of uncertainty as varying parameters (reserve, production, and depth) related to CAPEX and OPEX.

Bueno et al. in 2011 used geometallurgical information to minimize the risk in the design of a comminution circuit. They use Monte Carlo simulations to analyze the effects that orebody variability has on the circuit performance and the probabilities they will occur, i.e; the likelihood of achieving design throughput or not. This methodology is an alternative way of applying geometallurgy and multi-scenario simulation in the design of a circuit featuring AG/SAG mills. The method relies in using statistics to analyze geometallurgical and mining data to model the variability of specific energy requirements of SAB (SAG and ball mill) and SABC (SAG and ball mill with-pebble crushing) circuits for mill design purposes. Ultimately, an example was presented to demonstrate the application of this method, and that it can be used to evaluate and minimize design risks.

Monte Carlo simulation is an effective alternative for analyzing processes where the probability of the occurrence of the phenomena studied can help to assess risks and make better informed and data-driven decisions. Within simulation frameworks, integrating techniques based on the Monte Carlo method marks a substantial evolution in project evaluation and in obtaining solutions to potential challenges that may arise over the life of a mine. This approach and every method based on the Monte Carlo approach improves the ability to predict and manage the complexities and uncertainties inherent in mining operations.

2.2 Conditional Simulation Principles

Mining projects are a risky endeavor, due to the significant initial investment capital and a series of unpredictable external factors such as global economy and metal prices. A large number of different concepts should be weighed to find the optimal alternative for developing a mining project. The viability of an investment depends on a series of complex engineering decisions based on the information provided from a geological model, constructed with limited information derived from geological field work, surface sampling and drilling campaigns.

The most common approach used in the mining industry to mineral resources evaluation is block scale grade estimation using a deterministic model (Chiquini, 2018), mineral resources calculated with this method are a smooth representation of the actual distribution of grades at block scale (Journel & Kyriakidis, 2004). During deterministic modeling and variable estimation, geologists and engineers use their previous knowledge of a deposit for describing and interpreting its geological controls, to understand geometry and grades distribution. In contrast, stochastic simulations take into account the uncertainty of the related input parameters, considering them as a variable. From the simulation point of view the input variables and outcomes have an expected value with a maximum and minimum possible. This leads to a high level of unpredictability regarding grades and other variables within ore body, therefore, the uncertainty associated with the material to be extracted is not adequately informing the decisions of a mining project. In contrast, stochastic models take into account the uncertainty of the related input parameters considering them a variable. In this context, conditional simulations (based on the deterministic methods with additional considerations) appear as a better geostatistical approach to addressed this problematic.

Conditional simulation (a.k.a. stochastic interpolation, stochastic simulation or stochastic imaging) is a technic for describing the variability in spatial fields (Journel, 1974; Journel, 1996) often used in geostatistics, hydrology, environmental science, and other fields to generate spatial or temporal distributions. Matheron, G. (1963) is considered the founder of geostatistics, in the 1960s laid the foundation for many geostatistical techniques, including kriging and conditional simulation. Journel and Huijbregts (1978) presents a seminal book in geostatistics titled "Mining Geostatistics", providing a comprehensive treatment on conditional simulation methodologies. Like the kriging estimation method, simulations theory has been detailed by authors such as Deutsch and Journel (1997) and Chilès and Delfiner (2012). Conditional simulation is widely used in the oil and gas industry for modeling reservoir properties such as porosity, permeability, and saturation; groundwater modeling to generate spatial distributions of hydraulic conductivity or contaminant concentrations. Recently, with the growing capability of computers to generate many millions of calculations, is gaining more space in the mining industry with a variety of simulation techniques for obtaining conditionally simulated models.

Geostatistical simulation aims to reproduce the variability of the real underlying phenomena (Ortiz & Deutsch, 2004). Kriging algorithm generates a single representation of the modeled variable, with conditional bias, and underestimation of high values and overestimation of low ones; conversely, conditional simulation provides multiple, equally likely realizations of a spatial phenomenon, given known values at certain locations in the same form the values are randomly drawn emulating the Monte Carlo simulation (Matheron, 1973; Journel, 1974;Goovaerts, 1997).This mathematical procedure constructs synthetic realizations of a random function that holds the same spatial statistics (first and second order moments) as the sampled data of a specific variable (Dungan, 1999). Therefore, is a suitable algorithm for spatial modelling because emphasizes the main statistical attributes of a spatial field, such as histogram and variance, to find the hidden spatial pattern in a given dataset. The main pilar of simulation (as well for estimation) is the random function, any variable distributed in space and described in two or three dimensions is called a regionalized variable, and regionalized variables are often modeled as realizations from a random function. The main idea is constructing the different realizations that will share a spatial structure governed by the relationships of pairs of points (two-point statistics) imposed by the variogram or infer pattens from multiple points (multiple-point statistics) (Ortiz, 2020).

Understanding the mathematical background of these methods is critical to making informed choices when selecting a technique for a specific application, for example risk-characterization (Vann et al. 2002). There is a long list of different simulation methods, each of these methods has its own strengths and is suited to specific types of problems. The choice of method depends on the characteristics of the data and the specific objectives of the analysis. The most important simulation methods will be described:

1) Turning Bands (TB) was the first large-scale 3D Gaussian simulation algorithm implemented (Journel, 1974). The technique was developed in the early 1980s, with foundational contributions by Matheron (1982). The Turning Bands technique is based on the decomposition of a 2D or 3D random field into a superposition of 1D random functions, oriented in various directions. The turning bands method generates 3-D simulation results from several independent 1-D simulations along lines that can be rotated in 3-D space (Ren, 2005). By turning these bands or profiles in various directions, the spatial variability of the field can be simulated. The method is very efficient for generating non-conditional simulations and particularly good at replicating the variogram, due to a clear geometrical interpretation allowing for the simulation of anisotropic fields. Some limitations of this technique are related to the non-exact reproduction of the variogram (which can be addressed asymptotically by increasing the number of bands) and to the production of high contrasts artifacts if not enough bands are used.
2) Sequential Gaussian simulation (SGS) is a pixel-based gaussian method. This technic is widely used in the mining industry. Journel, A. G., & Huijbregts, C. J. (1978) published "Mining Geostatistics" which provides foundational theory of this method. SGS is a stochastic simulation methodology that aims to create multiple equiprobable representations of a spatial variable based on its statistical properties (mean, variance) and spatial continuity (defined by the variogram or the covariance function). The implementation of this methods proceeds sequentially, at every unsampled point in the grid or node, the sample values within a neighborhood as well as the previously simulated nodes in the neighborhood, are used to compute the kriging estimate and variance (in Gaussian transformed units). To avoid artifacts due to the use of a regular

grid of simulation points (and the screening effect of kriging), a random path is created to visit the nodes in a random order in each realization (Ortiz, 2020).

3) Sequential indicator simulation (SIS) is a pixel based non- parametric method for simulating categorical variables. This method is based on the concept of indicator kriging, where continuous variables are transformed into categorical indicators before simulation. The SIS is appropriate when there is uncertainty in the geometry of the geological body, and the continuity is well described by variograms (Pyrcz & Deutsch, 2014). Conditional simulation generates equiprobable realizations that honor the data inputs. Each realization is a possible outcome of the random function (Mizuno & Deutsch, 2022). The method involves the use of indicator variograms and the conditional cumulative distribution functions (ccdf) to simulate the presence or absence of a particular class at unsampled locations, then build a model using one of the indicator kriging approaches.
4) Truncated Gaussian simulations (TGS) is a method that is used for simulating sequentially ordered lithofacies by truncating a Gaussian random function (GRF) (Galli et al., 1994). The bounds of the interval are calculated to match the proportions of the various lithotypes, following the spatial characteristics of the GRF are related to those of the lithotype indicators which are described by their experimental variograms. When the lithotype organization is not ordered by a sequence is necessary to consider several GRFs, in that case, the method called pluriGaussian (Beucher & Renard, 2016). They also have other possible applications for grade simulation, when the grade distribution is highly correlated to lithotype.
5) Lower-Upper Decomposition (LUD) is a methodology to solve linear systems of equations systematically. In geostatistics, LU decomposition is an important mathematical tool for efficiently solving linear systems, especially in Kriging and geological simulations. If the Kriging matrix satisfies the condition of being symmetric and positive definite, by applying the LUD it is possible to obtain a numerically stable and simple solution for simulating problems with large number of data (Davis, 1987). With a low number of samples, the number of unsampled points in the grid to be simulated is small (less than a few hundred) and a large number of

realizations wants to be computed, the fastest solution is simulated through the LU decomposition of the covariance matrix (Alabert, 1987; Davis, 1987; Fogg et al., 1991; Glacken, 1996), in other words, these method suffer from efficiency limitations related to the size of the matrices to be handled and essentially used for small simulations.

6) Simulated annealing (SA) is multiple point geostatistical simulation, that has gained ground over the past decade, especially in the petroleum industry (Deutsch & Cockerham, 1994). Was proposed by Deutsch in his Ph.D. thesis (Deutsch, 1992 Simulated annealing is a probabilistic technique for find the closest approximation of the global optima of a given function. The first step is generating an initial image based on the prior knowledge (sampled data points) and all remaining nodes are inputted by random values from the user-specified histogram (Deutsch and Journel, 1997). The initial image is slightly perturbed by redrawing the value at a randomly selected grid node, and an objective function is defined to evaluate the quality of any solution between desired spatial and features and those of the realization (Ortiz and Peredo, 2010). The acceptance criteria is founded on a decision rule to accept non favourable perturbations based on the Boltzmann distribution (Wells, 2002). The Simulated Annealing process appears to be inefficient, in that up to a million perturbations may be required to obtain an image that contains the prespecified spatial structure (Deutsch & Cockerham, 1994).

Conditional simulation can provide grade statistics at the highly selective scale required, for example, by narrow vein mining, which makes it a more useful tool for short to medium term planning than linear estimation methods such as kriging (Khosrowshahi & Shaw, 2001). Fowler and Davis (2011) perform a conditional simulation, of the Augusta mine in central Victoria in Australia, using grade and width of narrow-vein deposits reproduce the observed features of the mineralization, they model these variables using SGS in 2D to produce realizations of veins from a reference plane. This study allows calculate grade statistics at the highly selective scale required by narrow vein mining. The uncertainty in ore body geometry, where thickness and grade were quantified in terms that can be used directly for mine planning. Richmond (2012) uses conditional simulation to simulate the spatial distribution of gold grades controlled by quartz vein sets in a

folded lode-style gold deposit. For this case study, lithology was dealt with using a modified SIS algorithm that accounts implicitly for interpreted locally varying anisotropy, due to the financial implications that relies in locate and define spatially the individual lodes. By considering lode geometry uncertainty, significantly greater downside risk and upside potential was present in the gold deposit than previously recognized by simply considering gold grade uncertainty within a deterministic wireframe.

Jackson et al. (2003) presents a case study that quantifies both geological and grade risk in an underground gold mine at Stawell in western Victoria, Australia. Assessing the size and geological controls of the Golden Gift deposit at an early stage previous to an extensive underground drilling program. In addition, the project needed quantified characterization of the main resource risks, in a context of high dislocated complex structurally controlled shear-hosted quartz-pyrite-arsenopyrite veins. They demonstrated that whilst the risk derived from geological interpretation and geological risk at early stages could easily have a dramatic impact on financial outcomes. Murphy et al. (2004) quantifies the resource risk based on constraining envelopes for resource classification nickel grade and ore-thickness (a proxy for ore tonnage) for Koniambo nickel laterite project in New Caledonia. Ore-thickness intercepts were created from vertical drilling and converted to 2D point data. One hundred 2D sequential indicator conditional simulations were generated for each attribute on a 10 m by 10 m grid for the three deposit areas. Tonnages were computed for each panel from the mean simulation thickness and deposit-average bulk density. The drilling grid adequately defined the nickel grade; however, tonnage risk was considered to be high on a panel-by-panel basis. Rescaling the risk to quarterly and annual production periods revealed that the annual risk was acceptable, but that close-spaced drilling would be required to increase the confidence in tonnage.

2.3 Discrete Event/Rate Simulation (DES/DRS)

Discrete event simulation (DES) is probably the most widely used simulation technique in operational research, considered a subclass of Monte Carlo simulation (Altiok and Melamed, 2007). DES conceptualizes a process as a sequence of discrete events, wherein entities transition between different states over time, in other words, this means that entities are thought of as moving between different states as time passes (Maidstone, 2012). DES models systems as a network of

queues and activities, where state changes occur at discrete points of time (Brailsford & Hilton, 2001). A key characteristic of DES is that state changes occur at discrete time points, enabling precise control over the timing and sequencing of events. Objects are individually represented and can be tracked through the system and specific attributes are assigned to each individual and determine what happens to them throughout the simulation. DES allow researchers and engineers to study the behavior of complex systems under different conditions and scenarios, evaluating system performance, and make predictions. DES are commonly used to model and analyze queueing systems, where entities (e.g., customers) arrive, wait in a queue, and are served by one or more service providers. Discrete Event Simulation has evolved as a powerful decision-making tool after the appearance of fast and inexpensive computing capacity (Upadhyay et al., 2015). Another key characteristic of DES is that incorporates randomness or stochastic processes. This randomness can be used to model uncertainties, variability, or probabilistic events within the system, helping capture real-world complexity and randomness.

This methodology has many applications such as health care, financial, manufacturing and many others and started to be adopted by the mining industry from the late 1950's when a train transportation system was modeled and investigated by hand calculation for the Kiruna underground iron ore mine (Panagiotou 1999). In modern mining operations, maximizing productivity by effective decision making is essential. Discrete event simulation is used to conduct "what if" analysis supporting mining engineers and management in decision making (Fahl, 2017). Discrete event simulations are typically used to analyze queuing problems, but fits to many applications in mining, for example optimization of the load-haul-dump cycle, one of the most important activities in mining production chain and is critical to optimize for achieving higher efficiency and cost reduction (Fahl, 2017). The purposes of DES include the improvement of equipment utilization, reducing waiting and queuing time, to evaluate cost reduction initiatives, to minimize the effects of breakdowns, to understand the impact of mixed fleet interactions (Price, 2014). Additional areas in mining operations and mineral processing that can be modeled with DES will require further research (Dindarloo & Siami-Irdemossa, 2016). New applications are found in the literature such as energy efficiency in mining, which can be achieved by optimized shovel utilization (Awuah-Offei 2012). Moreover, there are equipment subsystems investigated by the use of availability and reliability data of mining equipment (Gbadam et al. 2015) and geological

uncertainty on production scheduling is examined by means of DES (Shishvan & Benndorf 2014). Pamparana et al. (2017) evaluated the benefits of coupling solar radiation energy with a semi-autogenous grinding (SAG) mill and Navarra et al. (2017), consider discrete event simulation (DES) an appropriate framework for the plant-wide analysis of copper smelters.

A powerful aspect of DES is the ability to simulate hundreds or thousands of days of operation in order to analyze various processes and identify any potential deficiencies (e.g., bottlenecks) (Navarra, 2020). As a result, tactical decisions can be made to introduce operational buffers, such as stockpiles, ore blending or pre-treatment processes. Additional simulations are then run to observe any potential effects from the adjusted policies. DES essentially creates a form of 'virtual reality' of the operations that can help identify and mitigate risk prior to investing significant resources into a sub-optimal or possibly unviable project (Navarra, 2020).

Another type in the field of simulation is Discrete rate simulation (DRS). DRS is used to model linear continuous systems, hybrid systems, and any other high speed/large volume system that involves the rate-based movement or flow of material from one location to another (Damiron and Krahl, 2015). The primary objective of DRS is to increase the movement as much as possible through the system, essentially aiming to 'maximize' the flow. (Damiron & Nastasi, 2008). Instead of focusing on a single occurrence like traditional discrete event simulations (DES), DRS considers the rates at which materials are in movement through a system (Muravjovs et al., 2016), in other words, continuous processes in which the rate of change of the continuous variables (for example, liquid in a tank, coal in a barge) was constant or changed at discrete points in time.

This approach becomes necessary when dealing with a process that involves a large number of fast-moving objects and for reasons of efficiency calculation fails discrete approach (Giel et al. 2017). Speed improvements in comparison to discrete event simulation (DES) can be achieved, when the model perform flows-based calculations rather than in individual entities, this approach helps to prevent the emergence of invalid system states, a challenge often faced in system dynamics. (Reggelin and Tolujew 2011). The primary characteristic of discrete rate modeling lies in the stationary nature of the flows. (Muravjovs et al., 2016). This new method developed in 1990's, simulates continuous-linear flow, rate-based systems, and hybrid systems (combining continuous and discrete event) (Damiron & Nastasi, 2008), where continuous and discrete event

simulation were not suited or not adaptable to those issues (Damiron & Krahl, 2015). Numerous physical systems can be classified as hybrids, especially in scenarios involving the manufacturing or transfer of bulk or liquid products among containers. This approach can be particularly useful for systems such as chemical processes, manufacturing, traffic, pipelines, and high speed/large volume processes and other scenarios where flow rates play an important role. In mining for example, haulage and bulk material handling can be modeled through this methodology.

The steps for the Implementation of a DES/DRS framework are (1) Outline the system, defining the flows and levels (i.e. in chemical processing “rates" and "tank levels"; (2) System initialization, setting initial conditions, such as timers, levels and rates and define the event list or priority queue to manage future events; (3) Main simulation loop in which retrieve the next event from the event list, update the simulation clock to the time of this event, update system state based on this event, schedule new events if necessary and add them to the event list(4) Data collection and result analysis of system related variables statistics like average waiting times, throughput, or any other metric of interest; (5)After the simulation completes, analyze these statistics to derive insights.

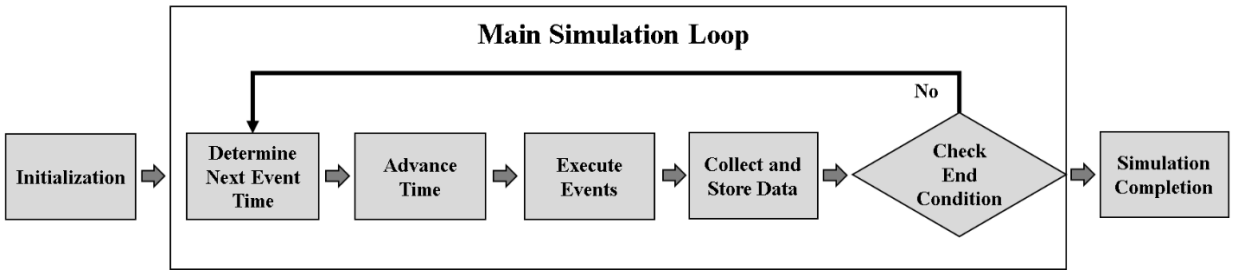

Figure 2.3.1: Workflow for the Implementation of a DES/DRS framework.

Muravjovs et al. (2016) develop an inventory control system model on the basis of “discrete rate” paradigm. Employing fragments built on the discrete event principle, supply chain uses the same elementary strategy for inventory control. The structure of simulated system comprises four elements that are interconnected with material flows: supplier, transportation channel, warehouse, and customer. There are information flows shown in the structure of the system such as the pull of demand for simulated daily demand, information about the inventory level in stock, and information, which the supply manager, sends to the supplier as a replenishment order. Pull of demand was simulated as a uniform random variable, reorder level, namely threshold level of

inventory – allows to make a purchase order when this level reached a specific unit number level, for an operation simulation run length for 30 days. The aim was not to study a certain inventory control system, but to demonstrate the method can be implemented with different paradigms for simulation modelling of processes, which includes DRS. Terlunen et al. (2014) expanded this simulation approach by incorporating modeling and material flow control mechanisms. This enhancement facilitates straightforward implementation and simulation of various tactical supply chain planning tasks. To effectively assess different planning decisions within this framework, numerous simulation runs are required, highlighting the demand for rapid simulation methods. The researchers formally demonstrate that models based on discrete rate-based simulation can typically be computed faster than the more traditional discrete event-based simulation models.

2.4 Mining Systems Dynamics (MSD)

System dynamics (SD) is a computer simulation modeling technique and methodology for framing, understanding, and discussing complex issues and problems. Originally developed in the 1950's to help corporate managers improve their understanding of industrial processes (Radzicki & Taylor, 2008). This methodology studies the dynamic behavior of a complex system by considering that each process is part of the whole system rather than in isolation. SD is a field of knowledge that encompasses the change and complexity over time of a dynamic system, in other words, this approach helps to represent and understand, simulate, and observe trends over time. Systems thinking must consider all the components and variables that interact and influence the dynamics of the complex system. This methodology is based on the feedback concepts of the control theory developed by Forrester (1968), is considered the most proper technique to handle and improve systemic thinking and learning (Bala et al., 2017). SD deals with interaction of various elements within a system in time, capturing the dynamic characteristic by incorporating concepts such as stock, flows, feedback and delays, and thereby provides an insight into the dynamic behavior of systems over time (Tang and Vijay, 2001). Figure 2.3.1 summarized the workflow for system dynamics methods development.

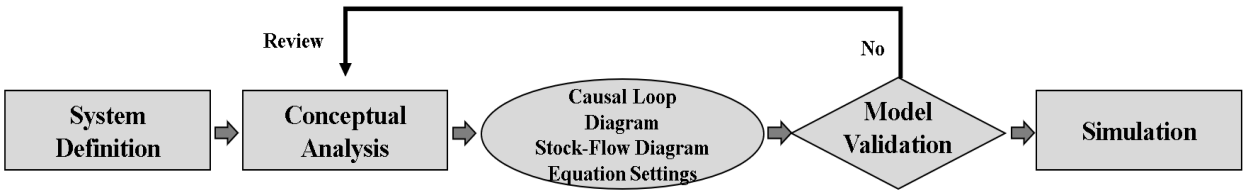

Figure 2.4.1: Workflow for implementation of system dynamics.

The foundation of this methodology relies on the feedback systems derived from control theory and is able to manage the non-linearity and time-delay and the multi-loop structures of the complex and dynamic systems (Bala et al., 2017). The objective of system dynamics is comprehending the fundamental structure of a system, and followed, understand the potential behaviors it can generate (Radzicki & Taylor, 2008). The principles of system dynamics are predicated on two major systems principles, (1) The first is that stocks, flows, and delays determine system behavior and (2) the second is bounded rationality (Simon, 1957), to perform a simulation with realistic parameters.

The implementation of system dynamics in the mining industry is not a novel concept, Montaldo (1977) publish a study applying this methodology in underground mining operation. The model includes an underground operation with milling sectors, together with cash flow and finances. Likewise, pay attention to the feedback relation between all the components, showing how individual processes interact and affect the overall system performance. The use of feedback theory differentiates the model from a "basic" econometric simulation and helps to design a stronger management policy towards improving mining company performance.

Alpagut and Çelebi (2003) present research about two different applications of system dynamics in the mining industry. They provide examples for the usage of this methodology in the mining sector to illustrate SD as an alternative approach to system comprehension. Like most other systems, mining systems can be represented as complex information-feedback systems, in a manner that the result of each mining operation affects itself back at the next point in time. The first example was a SD mine planning model, that identifies the colliery as a feedback system, in which the coalfaces and their associated development works are operated to reach a target output, under geological and manpower availability fluctuations. The second model presented was the application of SD in equipment selection to choose the optimum blinker- conveyor belt system for

haulage in a coal longwall mine. The two study cases described suggest that a mine can be described as a dynamic feedback system.

O'regan and Moles (2006) research the impact of environmental policy on the investment and development strategies of the mining industry within the broader context of government minerals policy. They developed a computer simulation model grounded in system dynamics for a quantitative evaluation of existing data within the context of sustainable development, the underlying assumptions used as a basis for corporate decisions. They constructed several interlinked system dynamics sub-models where the mining firm is viewed as a particular case of a typical business entity, which is assumed to have the objective of maximizing profits. These sub-models are designed to understand the critical decision-making frameworks of the company, particularly in terms of reinvestment of profits into new exploration and development activities.

Navarra et al. (2017) present a hierarchical discrete event simulation (DES) framework to analyze copper smelter operation of the Hernán Videla Lira (HVL) smelter (a major asset of the *Empresa Nacional de Minería* which is National Mining Company, under the acronym in Spanish ENAMI), located in the small town of Paipote in the north of Chile. The DES framework integrates thermochemical aspects of copper smelters to examine the analyze the operational system dynamics, especially in the context of sulfur dioxide (SO_2) emissions and meteorological factors that adversely impact air quality. The model was developed in phases due to the complexity of the problematic, incorporating feedback from personnel who have different perspectives The mass and heat balancing parameters were used to estimate converter cycle time so that the DES framework could assess the tradeoff between copper production and environmental risk.

Lui et al. (2019) incorporate an SD application to extend real options (RO) valuation for the decision-making of a mining project, using the methodology in Hongwei uranium deposit in China. SD hybrid simulations were used to visualize numerous techno-economic factors that are contained in mining operation systems and their interactions during the valuation process of mining projects. The simulation results were able to accurately estimate influencing factors and provide a deeper assessment for mining investment decision-making projects. The methods presented improve the accuracy of valuation of mining projects and help decision-makers make science-based decisions for mining investment projects.

Chapter 3

Foundation for stochastic and dynamic mass balancing of underground mines

The foundation for stochastic and dynamic mass balancing in underground mines is to develop a data-driven and responsive framework that can adapt to the inherent uncertainties, constantly changing conditions and complex dynamics of underground mining operations. In mining, mass balance is crucial, as it provides assurance that the tracking and accounting of materials entering and leaving the process are accurately executed. Mass balance miscalculations can result in erroneous estimations of vital operational metrics, such as production rates, recovery and economic losses. These imprecisions could cause the misallocation of vital resources and operational inefficiencies, which could lead to substantial operational failures and financial and/or environmental consequences for the mining project(e.g. incorrect estimates of the amount of recoverable mineral, affecting the profitability of the mining operation; faster depletion of the ore reserve/resources than anticipated, potentially shortening the life of the mine (LOM); increase the footprint of the waste disposal areas, potentially leading to more severe environmental contamination and increased risk of tailings dam failures, and a long etc.). Herein lies the value of extensible simulation frameworks focusing on mass balance. They can be developed initially to support broad ranges of realistic data (Boom et al., 2015; Mittal et al., 2008) and then successively detail the operational aspects that are the most critical for attaining support for sampling campaigns and metallurgical studies. DRS is perhaps the simplest approach for encapsulating dynamic mass balances (Navarra et al., 2019; Peña-Graf et al., 2021; Peña-Graf et al., 2022; Wilson et al., 2022a), from which context-specific feed variations can be developed in phases so that the corresponding risks can be quantified, as well as opportunities for improvement. As Figure 2.3.1 describes, DRS is a particular type of DES in which incoming and outgoing material flows undergo discrete jumps over the simulated timeline. DES/DRS frameworks are also extensible, i.e., they can be successively extended in response to management concerns (Figure 3.1) via the incorporation of models, sub-models, ‘sub-sub-models’, etc. For example, if an existing gold mine experiences

feeds with increasing portions of copper sulfides, there may be a case for building a flotation circuit that would produce a copper concentrate parallel to the cyanidation process; however, management would be uncertain about the partitioning criteria that would divide marginal ore into the flotation feed versus the cyanidation feed (Hedley & Tabachnick, 1958). In this case, the DES/DRS framework can be extended with models using published data (Hedley & Tabachnick [1958] and/or Guo et al. [2014], for example), demonstrating the potential benefits of the processing upgrade so that management can ideally approve a detailed metallurgical study to refine the model parameters with site-specific data. Suppose that the proposed metallurgical study is not approved due to a series of criticisms from management. These criticisms are used to guide the next iteration of model development (Figure 3.1a), which is then integrated into the next version of the simulation.

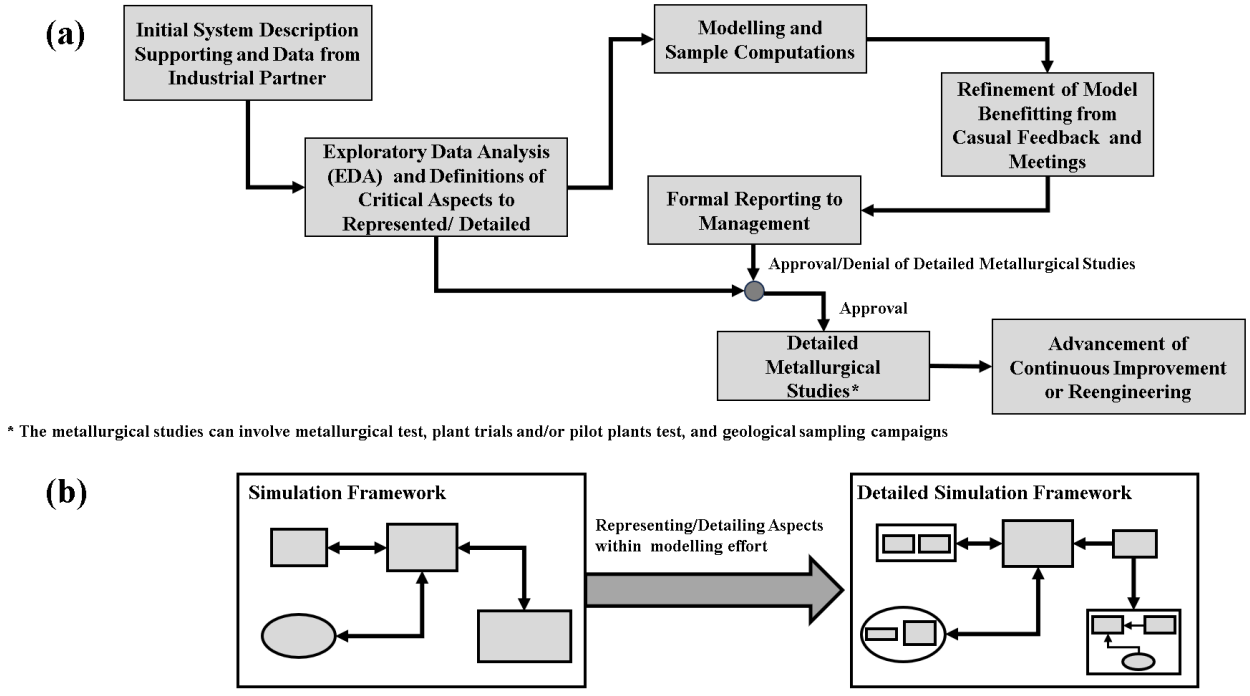

Figure 3.1: Development of an extensible simulation framework prior to the approval of metallurgical studies: (a) interaction with management leading to approval; (b) simulation framework detailing via the incorporation of models and sub-models.

3.1 Dynamic mass balancing and data-driven sensitivity analysis

Mass balance (a.k.a. material balance [MB]) is a method for continuously tracking and accounting for materials in a system (Himmelblau, 1967). MB for materials accounting requires that the system boundary be defined in space and time, stocks and flows be expressed in consistent physical

units, and mass and energy be in balance across transformation, distribution and storage processes in the system (Baccini & Brunner, 1991; Brunner & Rechberger, 2004). Essentially, MBs are accounting procedures: the total mass entering must be accounted for at the end of the process, even if it experiences heating, mixing, drying, fermentation or any other operation (except nuclear reaction) in the system (Doran, 2013). Traditional mass balancing is typically conceptualized as an optimization problem; the aim is to minimize the residual by modifying the assay values to achieve MB; in other words, MB is the requirement that the adjusted values are as close to the measured values as possible (Anderson, 2021). Currently, data acquisition and mass balancing are increasingly computerized and automated. Mass balancing techniques have been improved from the well-known two-product formula to advanced computerized statistical algorithms that can handle different scenarios and problems when engineers perform an MB calculation (Wills & Finch, 2016). In the mining context, MB aims to control the movement through various stages of the material extraction, transport and ore processing operations (Simony et al., 2023). MB is a powerful tool in engineering analysis for solving and simplifying many complex calculations by investigating the movement of mass and relating what comes out to what goes in (Doran, 2013). MB plays a crucial role in mining processes' design and operation, closely interacting with every aspect of a mining operation's development (e.g., mine design, environmental impact and business economics) (Figure 3.1.1). This methodology is essential for controlling and optimizing the efficiency of mining processes, ensuring resource utilization and meeting a business's key performance indexes (KPI), as well as environmental and regulatory requirements.

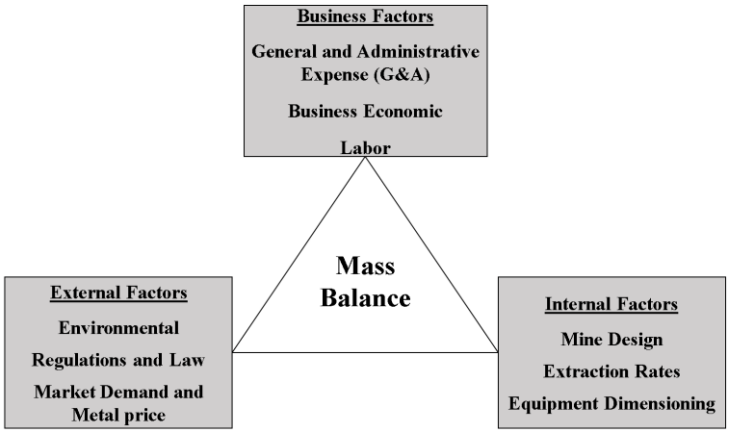

Figure 3.1.1: Interactions of a mass balance in mining project.

A mining operation is a unified system in which each component functions synergistically to form a whole. To perform an efficient MB, this structure must be subdivided into different levels. At the highest level, there is the breakdown of the entire system into sub-processes (in mining blasting, excavation, haulage and plant), allowing engineers to prioritize what should be included in the MB and establish appropriate boundaries (Simony et al., 2023). At a more detailed MB level, there are analyses of each sub-system's key data and characteristics, such as ore tonnage processed, overburden hauled, tailing mass flow and other relevant data. Such analyses may reveal the key factors affecting the performance of each sub-process as well as highlight which to prioritize when allocating resources for more detailed investigation or additional evaluation. Moreover, a detailed analysis of mass flows for specific plants and equipment, modelling the effects of changes in loading, vehicle mass, speeds, tunnel slopes (in underground mining), drilling capacity and plant production rates (to calculate comminution energy, tailing dam capacities and potential environmentally harmful elements) and waste dump capacity.

Performing an MB is similar in principle to accounting; this methodology accounts for what happens in each of the system's components. Through this methodology, which is possible tally for materials entering and exiting a system, MB techniques enable the identification of material flows that might have previously been unknown or difficult to measure. MBs are applicable to any system with defined boundaries, regardless of whether its nature is physical, chemical, or abstract. These balances serve as fundamental tools in systems analyses; when studying a system, or a portion of a system, it is essential to establish the system's boundaries. The extent to which a unit or part is included or excluded from the system under consideration must be delineated based on the process or processes being analyzed.

The underlying principle common to all these applications revolves around the fundamental concept of mass conservation (Himmelblau, 1967). The 'conservation of mass' law states that mass cannot be created or destroyed (Lavoisier, 1789), therefore the total mass of materials entering a system must be equal to the total mass of material leaving the system, less any accumulation. In other words, mass within a system must remain constant over time, forming the basis for accurate and effective MB analyses. The principle of mass conservation is utilized as a comprehensive material balance equation to account for the total mass of all the components involved in the process.

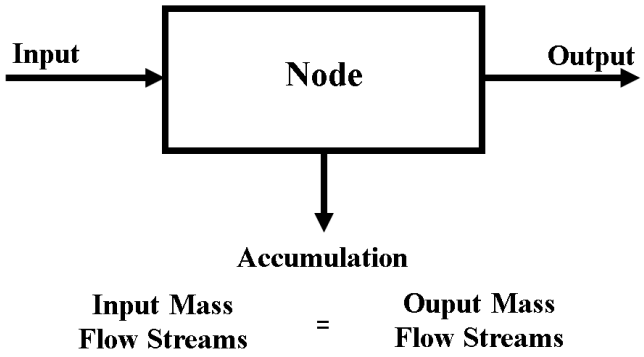

Figure 3.1.2: Principle of mass conservation in material balance.

Generalizing for MB, it is crucial to recognize that the variables characterizing process streams are diverse in nature (volume flows, temperatures, composition, pH, electric conductivity, etc.). Therefore, it is important to transform the primary data into balancing variables, which allows for a more uniform and coherent analysis within the mass balance framework. In general, a mass balance can be calculated as follows:

$$\text{Input} = \text{Accumulation} + \text{Generation} - \text{Output} - \text{Consumption} \quad (3.1.1)$$

Based on how the process varies with time, MB can be classified into the following two types:

(1) A steady-state process is one that does not change over time. This means that the variables have the same values at every snapshot of the system. A general balance equation can be written for any material that enters or leaves any system, and it can be applied to the total mass of this material or to any molecular/atomic species involved in the process. Mathematically, the mass balance for a system in a steady state (with no chemical reaction occurring) is as follows:

$$\text{Accumulation} = \text{Input} - \text{Output} \quad (3.1.2)$$

(2) An unsteady-state (or transient) process deals with time-variant system conditions. Variables have different values from the initial ones, depending on where a snapshot is taken. For transient balances, the quantities involved in a given system are a function of time. MB for a transient system is as follows:

$$\int_{m_i}^{m_t} dM = \int_{t_i}^{t_f} m_{in} dt - \int_{t_i}^{t_f} m_{out} dt \quad (3.1.3)$$

Where:

m_{in}, m_{out}, are the mass flows in and out of the system.
M is the total mass in the system at a given time.

To effectively perform a dynamic MB, whether in the context of reservoir engineering, chemical processing or any industry in which fluid or material flow dynamics are crucial, you can follow a systematic procedure. (1) Define the system boundaries (area or equipment being analyzed, volumes, levels, etc.) and identify system components or systems that will be included in the balance (clearly define the relevant parts of the system, such as a single reactor, a production facility or one or a series of stockpiles). (2) Collect data on inputs, outputs and internal transfers of mass or volume over time (production rates, feed compositions and operational changes). (3) Develop the balance equations for each component or stream and write equations that represent the conservation of mass, including accumulation stages. (4) Establish the system's degrees of freedom for determining whether it is solvable and identify whether the number of unknowns in a system can be determined based on the available equations and specified conditions. (5) Solve the equations by choosing an appropriate method (analytical methods, numerical simulations or computational software).

3.1.1 Dynamic Mass Balance for mining systems

In the context of mining operations, mass balancing (MB) is critical for monitoring the mass flows of ore and waste, as well as metal content and ore grades. This process ensures that all materials are accurately reported throughout the mining and plant processing stages. To achieve effective mass balancing in mining operations, it is essential to integrate temporal changes into the material balance equations, continuously updating the balance equations to reflect the dynamic nature of mining activities over time. This involves tracking variations in mined mass over time and meticulously accounting for the diverse inflows and outflows of materials. The implementation of an MB equation in the mining process is outlined as follows:

Run of Mine Ore (Input)= Plant Feed (Output) + Stockpiles (Accumulation) (3.1.4)

The dynamic material balance equation for an ore stockpile can be generally expressed as a function of time, where the rate of change in mass in a mining system is equal to the mass added minus the mass removed:

Where:

$$dM(t)dt=I(t)-O(t)\text{dt} \tag{3.1.5}$$

$M(t)$ = Mass of ore at time t.

$I(t)$ = Mass inflow rate at time t (from mining or other sources).

$O(t)$ = Mass outflow rate at time t (to processing plants).

These equations are crucial for optimizing ore handling and processing schedules, managing stockpile size, waste and tail dams, and planning future mining and processing activities. There are some detailed considerations when an DMB is performed in the mining context. (1) Inputs can vary based on mining production rates, which might be influenced by operational schedules, equipment constraints and/or geological variability (may also include material transferred from other stockpiles), which in an underground mining context can be enhanced by several operational considerations such as ventilation, ground support, material handling (ore and back fill). (2) Outputs are controlled based on the processing plant's capacity and ore quality requirements; therefore, adjustments might be made to manage the blending of different ore grades to optimize mineral process performance.

3.1.2 Data Driven Sensitivity Analysis

SA is defined as the study of how variations in input variables affect the outputs of numerical models and reliability by identifying which inputs have the most significant impact on the results (Iooss & Saltelli, 2017). This analytical approach is increasingly used in different research areas, highlighting its importance in enhancing the interpretability and credibility of complex models, making it a fundamental tool in scientific and engineering research (Saltelli, 2002; Pianosi et al., 2015). The system can be developed by single or a set of mathematical models, employing computer software, that simulates a real-world system (Razavi et al., 2021). Such mathematical models can be data-driven (also called statistical), directly mapping inputs to outputs (Engelbrecht et al., 1995; Rodriguez et al., 2010). In an advanced stage, is possible to assess these input data distributions through a data-driven sensitivity analysis gaining insights into which variables are

most influential, instead of relying on analytical or model-based approaches by the use of actual data to understand the relationships and sensitivities (Figure 3.1.4). By employing statistical random distributions in combination with sensitivity analysis (SA), analysts can effectively simulate a wide range of possible scenarios. This process not only highlights the most sensitive parameters but also guides efforts in data collection and model refinement, ensuring that the analysis focuses on the most impactful areas.

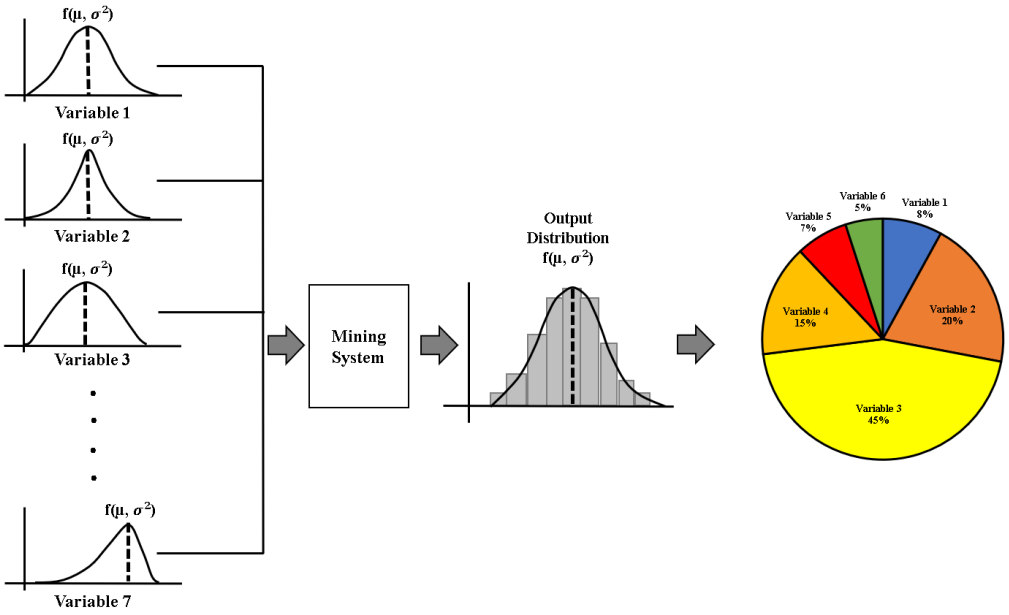

Figure 3.1.3: Schematic diagram of global sensitivity analysis (Based on Saltelli et al., 1999)

Data-driven sensitivity analysis is a method used to understand how variations in input parameters impact the outputs of a model. Using real-world data, this approach provides insights into the relationships between various factors and helps identify the most influential variables affecting a system's performance. DDSA is a modern approach that leverages large datasets and computational techniques used in modeling of systems and in support of decision making (Razavi et al., 2021). This technique is foundational for understanding the robustness of a model and identifying key variables that significantly impact the outcomes of any given system. By understanding which inputs have the most influence on the results, decision-makers can prioritize where to focus their efforts, refining certain measurements, improving processes, or making other strategic decisions. In particular, data-driven analysis is useful when the relationship between inputs and outputs is not easily captured by simple analytical expressions. Moreover, data-driven

modeling carries along a number of advantages, (1) Closeness to the real system: data-driven models tend to more accurately reflect the actual systems that they model (Wang et al., 2021). (2) Possibility to use other techniques such as Machine Learning (ML) and Artificial Intelligence (AI) for model enhancement: (Cavalcante et al., 2019).

Sensitivity analysis methods can be divided into three categories, namely screening methods, local sensitivity analysis methods, and global sensitivity analysis methods (Ascough et al., 2005; Emanuele, 2006). The first category, the screening method, is helpful in examining the relationship between input and output variables. This is used as a preliminary phase of analysis and is advantageous when the model requires a large number of parameters, allowing with a limited number of calculations the quick identification of those parameters that generate significant variability in the model output (Rivalin, 2018). By understanding these relationships is possible to reduce the complexity and computational cost of the model, helping to select an appropriate methodology that aligns with the specific requirements and characteristics of the model (Li et al., 2023). The local sensitivity method focuses on stablish the impact of a singular input parameter on a model result while the other input parameters are fixed, providing a detailed understanding of the individual contribution of each parameter to the overall output. Lastly, the global sensitivity analysis method is to study the collective influence of multiple input parameters on the model output and analyze the influence of the interaction between each parameter on offering a comprehensive view of how these combined influences shape the model output (Cai et al., 2008).

Data-driven sensitivity analysis often involves statistical methods such as correlation, multiple linear regression, nonparametric regression, among others (Iooss & Saltelli, 2017), these methods help in quantifying the sensitivity of the results to changes in the input variables. In advanced scenarios, techniques like Monte Carlo simulations can be used to model uncertainties and perform SA. The advantage of the data-driven approaches is that they are rooted in real-world scenarios, making the findings more relevant, identifying critical design parameters that affect the performance and reliability of a system. In a deterministic framework, models are inputted with specific values, exploring uncertainty by statistical approaches. In another hand, with a stochastic approach, inputs are considered as random variables $X = (X_1; : : : ; X_d) \in \mathbb{R}^d$, with random vector X has a known joint distribution, which represent the uncertainty of an input variable by the model function $Y= G(x)$. This can denote a system of differential equations, a program code, or any other

correspondence between *X* and *Y* values that can be calculated for a finite period. Therefore, the model output Y is also a random variable. In advanced approaches, when in a SA framework is dealing with models with a large number of inputs or when precise sensitivity results are required, is commonly employed MCS. With this methodology is possible to obtain more accurate sensibility results (Iooss & Saltelli, 2017). Finally, in dealing with real-geological data and computational techniques, empirically assessing the sensitivity of a model through SA becomes a more practical approach. This is particularly relevant in scenarios characterized by complex data relationships and where theoretical assumptions are difficult to substantiate. Sensitivity analysis can be integrated with other methods, such as Maximum Likelihood Estimation (MLE) and Goodness of Fit (GOF), to improve the robustness and interpretability of a statistical model. This integration is beneficial in several ways, due to helps to find potential weaknesses within the models, evaluates the impact of data variability on the estimates, and provides guidance in the process of model selection and refinement. By doing so, it ensures that the models are not only statistically robust but also resilient to variations in input data, thereby increasing their reliability and applicability in real-world scenarios.

3.2 DRS with parcel-based Monte Carlo Orebody Representation

Monte Carlo simulations (MCS) use probability distributions to represent input parameters, rather than deterministic values. This creates a more realistic representation of the system being simulated (Órdenes et al., 2022). The execution of an MCS consists of running numerous replicas, each based on a distinct instance of random number generation. This results in a distribution of possible behaviors, which can be used to understand the uncertainty associated with the system. In summary, Monte Carlo simulation (MCS) frameworks use random number generation to relate input probability distributions to output probability distributions. In broad terms, a Monte Carlo simulation framework considers:

- A set of input parameters that configure the system that is to be simulated;
- That one or more of the inputs are to be represented by probability distributions rather than deterministic values;

- That the execution of the simulation consists of numerous replicas, each based on an independent generation of random numbers following the input probability distributions;
- That the collection of outputs from the replicas approximate the distribution of possible system behaviors;
- Typically, the overall system performance can be assessed through the output distributions and quantified by so-called key performance indicators (KPIs).

Essentially, a Monte Carlo simulation uses random number generation (RNG) to convert input parameters and distributions into output distributions and KPIs. As illustrated in Figure 3.2.1, some of the input parameters can be used to parametrize the input distributions as well as for configuring the internal aspects of the framework. Similarly, certain KPIs can be drawn as summative evaluations of the output distributions, while others may be directly computed by the framework.

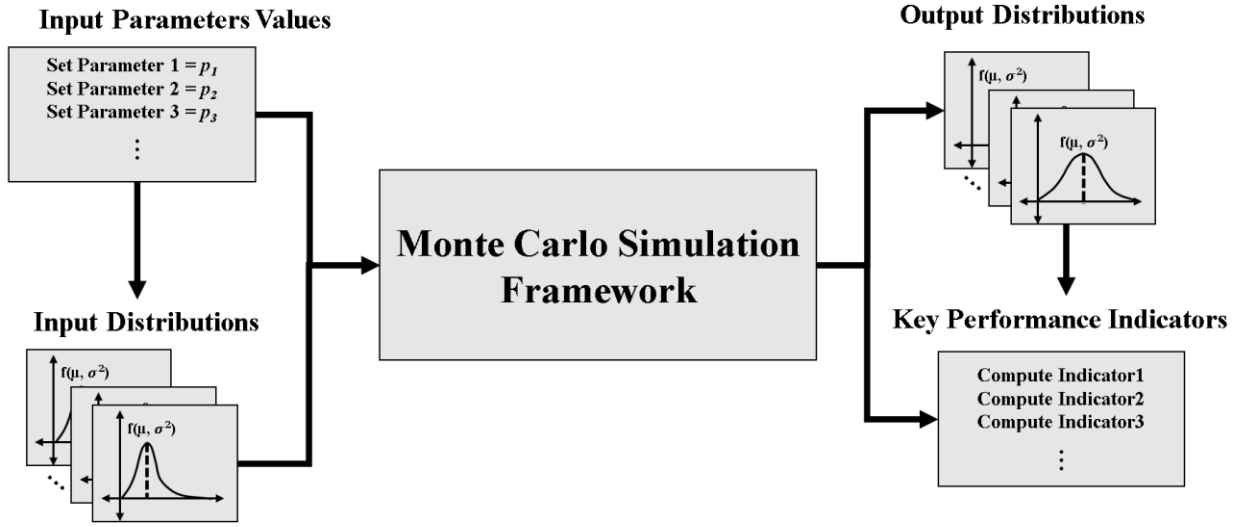

Figure 3.2.1: General representation of a Monte Carlo simulation framework.

Moreover, a discrete event simulation (DES) framework represents a dynamic system via input parameters and distributions as well as a collection of state variables that are updated at discrete points along a simulated timeline, hence, discrete events. Indeed, it is the simulated clock jumps from one discrete event to the next without explicitly representing the behavior between the events. An activity or condition that extends over a duration is represented by a discrete event that signals its beginning and a later discrete event that signals its end; within this duration, there may

be a series of discrete events, and possibly sub-activities, "sub-sub-activities", etc. depending on the level of detail. DES models can therefore be developed in iterative phases that incorporate hierarchical complexity, as per Figure 3.1, which define additional state variables and incrementally detail the system's activities, conditions, processes, etc. There are cases in which a purely deterministic DES may be of interest (e.g., for initial conception or later verification), but in practice, DES is seen as a type of Monte Carlo simulation (Figure 3.2.2), considering that the time between events can be the result of RNG and that the updating of state variables that occur at the events are generally the result of RNG.

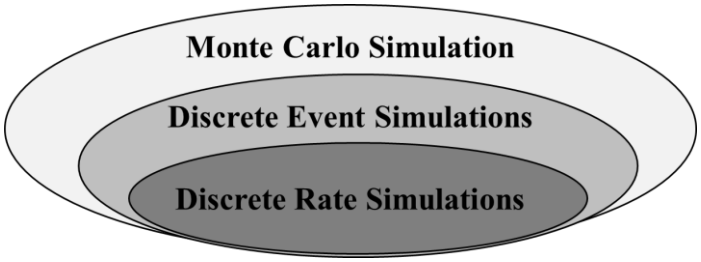

Figure 3.2.2: Relationship between Monte Carlo, discrete event, and discrete rate simulation.

Furthermore, a discrete rate simulation (DRS) is a particular kind of DES in which the state variables consist of pairs of levels and rates (l_j,r_j), and the discrete events consist of threshold crossings. Each level-rate pair represents a continuous variable that follows piecewise linear dynamics. The occurrence that such a continuous variable crosses a threshold is, itself, a discrete event (e.g., an ore stockpile level crossing below a critical value). When the *i*th threshold crossing event occurs at time t_i, the levels l_j are updated as per:

$$l_j = l_j + (t_j - l_{i-1})r_j \tag{3.2.1}$$

and, subsequently, the corresponding rates, r_j, are updated by model-specific formulas for $j \in \{1,2 \ldots ,nCSV\}$, in which nCSV is the number of continuous state variables. The model-specific updating of r_j can incorporate RNG, particularly in a mineral processing and extractive metallurgical context, when representing geological variation (Navarra et al., 2019; Ordenes et al. 2021; Peña-Graf et al., 2022, Peña-Graf et al., 2021; Wilson et al., 2022). These rate updates can also be the result of an operational policy that depends on the current configuration of the plant, as well as current and forecasted stockpile levels. Also, depending on the particular event, there

can also be discrete jumps in lj as well as in rj, for example, a corrective action can include an immediate injection of a certain reagent, as well as a change in the continuous feeding rate.

In DRS with parcel-based Monte Carlo orebody representation, the modelling is computed in the form of "parcels". Each parcel may be considered to represent a composite of several excavation zones, whereby at any given time a single "parcel" is being excavated containing a combination of waste rock and various types of ore. The depletion of this so-called parcel corresponds to a threshold crossing event (i.e. there is zero tonnes remaining in the current parcel), at which point the next parcel is randomly generated, containing a new blend of waste rock and ore; if the new parcel consists of the same blend of waste rock and ore, then the change in geological character is in comparison to the previous parcel based on local statistical variation, otherwise the contribution of new facies is generating using parcel is generated using global statistics. Previously, the parcels had been generated by elementary random number generation, without reference to an explicit orebody model and mine plan (Figure 3.2.3).

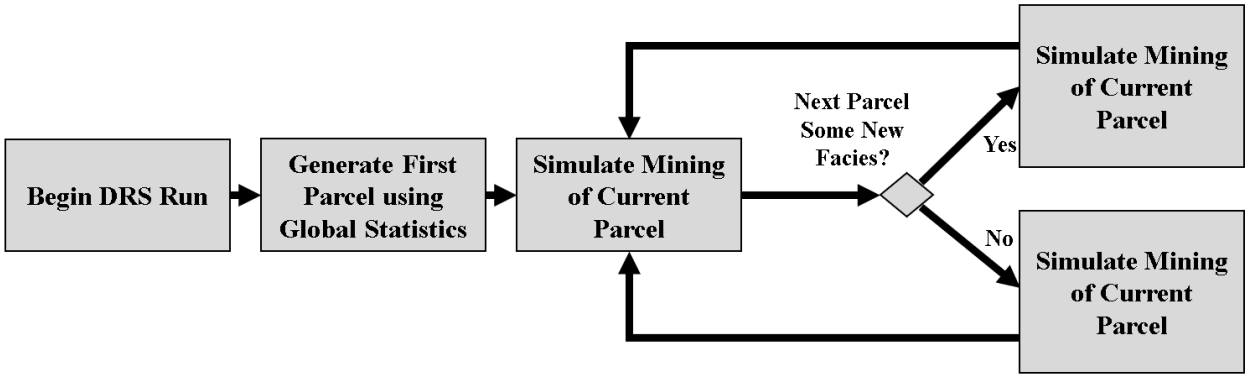

Figure 3.2.3: Simple Monte Carlo approach, which does not explicitly consider the spatial distribution of geological data. Within this approach, subsequent incoming tonnages (parcels) are generated during each DRS.

3.2.1 Maximum Likelihood Estimation of Distribution Parameter

Maximum likelihood estimation (MLE) is foundational to the data-driven parameterization of probability distributions (Altiok & Melamed, 2007; Montgomery & Runger, 2010) and precedes each of the goodness-of-fit (GOF) methods described in the following section (Figure 3.1.5). Supposing that a given set of numerical measurements, x_1, x_2, … x_n, follow a probability distribution, having density distribution $\boldsymbol{f}$, MLE determines the parametrization of $\boldsymbol{f}$ that would have been the most likely to have produced said measurements.

Using standard notation, the probability density function (pdf) can be expressed as a function $\boldsymbol{f}(x)$ in which x is a possible value; by definition, $\int_{-\infty}^{\infty} f(x)dx = 1$. To explicitly cite the distribution parameters, we may write $\boldsymbol{f}(x|\theta)$, in which θ is a tuple containing the list of parameters of the distribution. For example, a Gaussian distribution (also known as Normal distribution) can be expressed as $\boldsymbol{f}(x|\mu,\sigma^2)$, in which the parameters $\theta = (\mu,\sigma^2)$ are the mean and variance. MLE applies the principles of mathematical optimization and calculus to determine appropriate formulas (also known as "estimators") for estimating parameter values, as a function of the observed values. In the case of a Gaussian distribution, the parameter values are commonly taken to be $\mu \approx (\Sigma\, x_i/n) = \bar{X}$ and $\sigma^2 \approx (\Sigma\, (x_i - \bar{X})^2/(n-1))$; however, industrial measurements of head grade and other process variables do not follow a Gaussian distribution, hence requiring the broader concepts of MLE and goodness-of-fit testing (Altiok & Melamed, 2007,Devore, 2011; Massey, 1951; Anderson & Darling, 1954). Especially for gold head grades, it is advised that the distribution of the grade be represented, rather than using averages to define a deterministically constant grade since the variation effects process decisions and outcomes. Moreover, it is important to implement a truly representative distribution since the erroneous usage of a Gaussian process can again effect process decisions and outcomes.

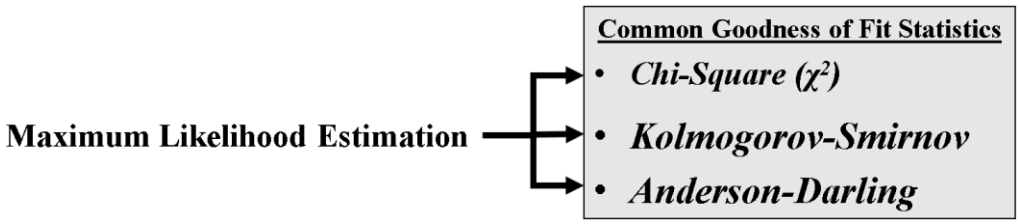

Figure 3.2.4: Maximum likelihood estimation is incorporated into common goodness-of-fit statistics, including Chi-Square ($\chi 2$), Kolmogorov–Smirnov, and Anderson–Darling.

Anecdotally, professionals within the mining and metallurgical industries are reluctant to consider distributions other than the familiar Gaussian; they are often unfamiliar with the concepts of MLE and goodness-of-fit testing, unless they have had particular training in continuous improvement methodologies, such as Six-Sigma or related statistics or industrial engineering. The current treatment is intended to be adequately brief but self-contained. Alternatively, many practitioners are prone to using group averages to represent the plant behavior, which does not represent lost productivity from a sudden departure away from the operating tolerances or, in the case of gold processing, spikes in cyanide consumption.

Consider a series of random measurements: X_1, X_2, …, X_n, which are made and are found to have values of x_1, x_2, … x_n, and have some degree of precision: $\delta > 0$. More explicitly, it has been found that $X_1 \in [x_1 - ½\delta, x_1 + ½\delta]$ and $X_2 \in [x_2 - ½\delta, x_2 + ½\delta]$, etc., and finally, that $X_n \in [x_n - ½\delta, x_n + ½\delta]$ for a small value $\delta > 0$. Supposing that these measurements follow a hypothetical distribution described by f, the probability that X_1 would have landed within the interval $[x_1 - ½\delta, x_1 + ½\delta]$ is estimated by the area of a rectangle of width δ and height $f(x_1)$, and similarly for the other measurements; hence, $P(X_1 \in [x_1 - ½\delta, x_1 + ½\delta]) \approx \delta \cdot f(x_1)$, $P(X_2 \in [x_2 - ½\delta, x_2 + ½\delta]) \approx \delta \cdot f(x_2)$, …, $P(X_n \in [x_n - ½\delta, x_n + ½\delta]) \approx \delta \cdot f(x_n)$. Assuming that the n samples are independent, the joint probability is given by the product:

$$P(X_1 \in [x_1 - ½\delta, x_1 + ½\delta], \dots, X_n \in [x_n - ½\delta, x_n + ½\delta]) \approx \delta^n \prod_{i=1}^{n} f(x_i) \qquad (3.2.2)$$

MLE maximizes this joint probability by adjusting the parameters of f, asking the question: which parameter values would have maximized the probability of having measured $X_1 \approx x_1$ and $X_2 \approx x_2$ and … and $X_n \approx x_n$?

Assuming that the degree of precision, δ, is sufficiently small, then it does not affect the maximization and can be ignored. Thus, as a proxy for the joint probability (Equation 3.2.2), we define the likelihood L(x), in which $x = (x_1, x_2, \dots x_n)$ is the tuple of measured values:

$$L(\boldsymbol{x}) = \prod_{i=1}^{n} f(x_i) \qquad (3.2.3)$$

To explicitly cite the distribution parameters $\boldsymbol{\theta} = (\theta_1, \theta_2, \dots \theta_p)$, we write:

$$L(\boldsymbol{x}|\boldsymbol{\theta}) = \prod_{i=1}^{n} f(x_i|\boldsymbol{\theta}) \qquad (3.2.4)$$

It is common to maximize the natural logarithm of L, rather than L itself, which converts the product of Equation (3.1.8) into a summation. The log-likeliness function is thus given by:

$$l(\boldsymbol{x}|\boldsymbol{\theta}) = \sum_{i=1}^{n} \ln(f(x_i|\boldsymbol{\theta})) \qquad (3.2.5)$$

and indeed, the maximization of l = ln (L), rather than L, does not change the result, considering that ln is a strictly increasing function. This transformation slightly simplifies the calculus to

parameterize common distributions, such as the Gaussian and exponential (Montgomery and Runger, 2010).

Moreover, it is standard to use a "hat" to denote the MLE estimates, i.e., the $\widehat{\boldsymbol{\theta}} = (\hat{\theta}_1, \hat{\theta}_2, .., \hat{\theta}_p)$ are the particular values of $\theta = (\theta_1, \theta_2, \ldots \theta_p)$ that maximize the joint probability (or equivalently the likelihood or log-likelihood) of having measured $X_1 \approx x_1$ and $X_2 \approx x_2$ and … and $X_n \approx x_n$. The MLE-parametrized density function is also denoted with a "hat", as in $\hat{f}(x) = f\left(x|\widehat{\boldsymbol{\theta}}\right)$, and similarly for the cumulative distribution function $F(x) = \int_{-\infty}^{x} f(u)du$; the MLE-parameterization is expressed as $\hat{F}(x) = F\left(x|\widehat{\boldsymbol{\theta}}\right) = \int_{-\infty}^{x} f\left(u|\widehat{\boldsymbol{\theta}}\right)du$.

Depending on the distribution, there may be constraints on certain parameter values, e.g., only positive σ2 values are allowed in the case of a Gaussian distribution. Therefore, the exercise of MLE is in general a constrained optimization:

$$\widehat{\boldsymbol{\theta}}(\boldsymbol{x}) = \underset{\boldsymbol{\theta}\in\Theta}{\operatorname{argmax}}\, L(\boldsymbol{x}|\boldsymbol{\theta}) = \underset{\boldsymbol{\theta}\in\Theta}{\operatorname{argmax}}\, l(\boldsymbol{x}|\boldsymbol{\theta}) \tag{3.2.6}$$

in which Θ is the feasible parameter space, $\Theta \subset \mathbb{R}p$, yet there are many practical cases in which the constraints do not affect the optimization. In practice, Θ can be taken as $\mathbb{R}p$ to apply unconstrained optimization techniques (calculus), and only if the resulting parametrization is infeasible is it necessary to consider a specialized constrained approach.

If $L(x|\theta)$ varies continuously with θ, then elementary differential calculus can be applied. For distributions with only one parameter, $\hat{\theta}$ is determined by setting $\partial L/\partial\theta$ to zero and solving for θ. Nearly all of the distributions under consideration, regarding the Minera Florida data, consist of two parameters, in which case $\widehat{\boldsymbol{\theta}} = (\hat{\theta}_1, \hat{\theta}_2)$ is determined by setting $\partial L/\partial\theta_1 = 0$ and $\partial L/\partial\theta_2 = 0$ and solving for two unknowns: θ_1 and θ_2. More generally, for p-parameter distributions, the calculus consists of solving p equations to obtain p unknowns (Montgomery & Runger, 2010).

However, prior to selecting a particular standard distribution to represent a particular variable (e.g., log-normal to represent the head grade), a litany of other potential distributions are also considered, which are each parameterized according to Equation (3.2.6), leading to distribution-specific estimation formulas. The idea is to compare the best Log-normal distribution to the best Gaussian distribution, and to the best Gamma distribution, and so on. In this case, "best" means

optimally parametrized in the sense of MLE. The distribution-specific estimators are usually programmed within software such as the input analyzer that is available with Rockwell Arena or the commonly used easy fit by Math Wave Technologies. In typical applications, it may not be necessary to derive or to work directly with the distribution-specific estimation formulas, relying instead on the software; however, the detailing of the DES/DRS framework has required that we directly program these estimators as an essential part of the data processing (Figure 4). It is prudent (and strongly recommended) to derive the formulas for any of the MLE estimators that are programmed into such a framework to be precisely sure of what the parameters represent. These calculus exercises are fairly basic and avoid errors that would later be very difficult to detect. As an example, once again, Equation (3.2.6) demands the mean of the logarithm rather than the logarithm of the mean. Consider further that an unapologetically deterministic simulation may be preferred over such an ill-conceived probabilistic model that gives false confidence.

In summary, MLE is the rigorous mathematical basis for data-driven parameterization. It provides the formulas to channel industrial measurements into the DES/DRS framework of Órdenes et al. (2021). The approach and experience that we have gained in the context of Minera Florida can be adapted to other mining contexts.

Figure 3.2.5: Data-driven representation of process variable distributions within a DES/DRS framework, using maximum likelihood estimation and goodness-of-fit ranking.

3.2.2 Chi-Squared, Kolmogorov–Smirnov, and Anderson–Darling Statistics

Critical process variables, such as head grades, recoveries and others can be observed with histograms and clearly do not follow Gaussian distributions. Yet, statistical concepts that are erroneously adapted to the Gaussian distributions are still commonly used. Even when metallurgical operators and engineers recognize this “non-Gaussianity”, they are left with the task of selecting other standard distributions which might be more appropriate, but without knowledge of a rigorous approach, the Gaussian distribution is nonetheless retained. This erroneous

application of the Gaussian process makes it difficult to justify a budget for detailed metallurgical studies (Figure 3.1). Particularly, in responding to critical variation, such as with gold head grade, any deterministic approach is inadequate, but an ill-adjusted probabilistic approach may be even less desirable since it provides false confidence.

In other industrial contexts, the typical approach is to rank the MLE parametrization for a list of candidate distributions according to goodness-of-fit (GOF) statistics (Figure 3.2.3). Given several hundred gold head grade measurements, for example, the preference to model these data as log-normal rather than as Gaussian involves a comparison of GOF metrics from the MLE-parameterized log-normal together with the GOF metrics of the MLE-parameterized Gaussian, with both parameterized with respect to the same given data. More broadly, software such as the Rockwell input analyzer and easy fit (of Math Wave Technologies) tabulate the GOF metrics for an extensive list of candidate distributions. The user of the software may then select the best-ranked distribution but, alternatively, may select another highly ranked distribution if it has fewer parameters and/or can be more effectively implemented or studied in computational experiments. This shall be further discussed below.

The chi-squared (χ^2) is the most widely known statistic that is used for GOF. Indeed, the χ^2 is described in elementary statistics textbooks such as (Ferguson and Erickson, 1988). Anecdotally, practitioners of extractive metallurgy may have a vague familiarity with χ^2, possibly for the construction of variance intervals of Gaussian-distributed variables or embedded within ANOVA tables in the evaluation of the F statistics (that compares variances of Gaussian-distributed variables (Devore, 2011)). In its classic use as a GOF statistic (dating to 1900, [26]), it is evaluated as a weighted sum of squares over k categories:

$$\chi^2 = \sum_{j=1}^{k} \left(\frac{1}{n_j^{\mathrm{Dist}}} \right) \left(n_j^{\mathrm{Obs}} - n_j^{\mathrm{Dist}} \right)^2 \tag{3.2.7}$$

in which n_j^{Obs} is the number of observed measurements that fall within category j, and n_j^{Dist} is the number of measurements predicted by the MLE-parametrized hypothetical distribution, noting that the $\frac{1}{n_j^{\mathrm{Dist}}}$ factors act as weighting; alterations of the classic χ^2 may consider different weightings. In general, according to Equation (3.2.1), distributions whose MLE-parametrization

have smaller differences ($n_j^{\text{Obs}} - n_j^{\text{Dist}}$) over the k categories will give smaller χ^2 values and are hence, a better fit.

One drawback of this use of chi-squared is the ambiguity in the definition of the k categories. Ad hoc approaches for evaluating discrete distributions are described in (Devore, 2011), including mergers of smaller categories resulting in larger categories that are adequately sampled and (ideally) are equiprobable. For continuous distributions such as Gaussian, log-normal, etc., the k categories correspond to a set of intervals, {(aj−1,aj]|j = 1… k}, and the equiprobable condition ($n_j^{\text{Dist}} = \frac{n}{k}$) is strictly enforced by setting:

$$a_j = \hat{F}^{-1}(j/k) \tag{3.2.8}$$

in which $\hat{F}^{-1}$ is the inverse of the MLE-parameterized cumulative distribution function. Thus, for continuous distributions, χ^2 is expressed in terms of the number of samples n:

$$\chi^2 = \left(\frac{k}{n}\right)\sum_{j=1}\left(n_j^{\text{Obs}} - \frac{n}{k}\right)^2 \tag{3.2.9}$$

Yet, even for continuous distributions, there is generally no optimal approach for fixing k since the optimal number of categories depends on the (unknown) distribution that underlies the data. A commonly used formula is:

$$k = \lfloor 1 + \log_2 n \rfloor \tag{3.2.10}$$

Alternatives to the $\chi 2$ include Kolmogorov–Smirnov (KS) and Anderson–Darling (AD) statistics, both of which avoid the artificial construction of categories. KS and AD both make use of the empirical cumulative distribution,

$$F_n(x) = \frac{|\{x_1, x_2, \ldots x_n\} \cap (-\infty, x]|}{n} \tag{3.2.11}$$

$F_n(x)$ is thus the portion of observed measurements whose value is smaller or equal to x, which forms a step function graph as illustrated in Figure 5. Herein the KS statistic is the largest absolute distance between F_n and $\hat{F}$. Formally:

$$\text{KS} = \sup_{x \in \mathbb{R}} \left| F_n(x) - \hat{F}(x) \right| \tag{3.2.12}$$

KS is an unweighted metric, i.e., there is no weighting w(x) that multiplies the absolute difference. A supremum operation (sup) is more appropriate than a maximum (max) to ensure the largest interpretation of $\left|F_n(x_i) - \hat{F}(x_i)\right|$ when evaluating the distance at the sample points xi, i.e., $\left|F_n(x_i) - \hat{F}(x_i)\right|$ is taken to be the larger of either the left limit $\lim_{x \to x_i^-} \left|F_n(x) - \hat{F}(x)\right|$ or the right limit $\lim_{x \to x_i^+} \left|F_n(x) - \hat{F}(x)\right|$ (Massey, 1951).

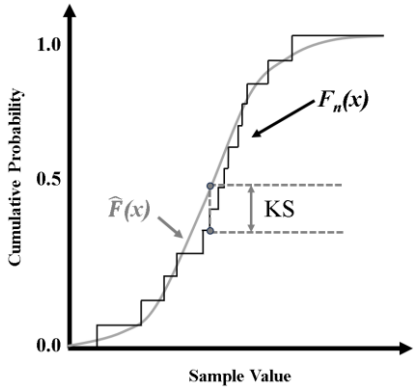

Figure 3.2.6: Kolmogorov–Smirnov statistic (KS) is the supremal distance between an empirical cumulative distribution and an MLE-parametrized cumulative distribution. A small KS indicates a good fit.

The Anderson–Darling statistic is conceived as a weighted integral of the squared difference of F_n and $\hat{F}(x)$,

$$\mathrm{AD} = n \int_{-\infty}^{\infty} \frac{\left(F_n(x) - \hat{F}(x)\right)^2}{\hat{F}(x)\left(1 - \hat{F}(x)\right)} d\hat{F}(x) \tag{3.2.13}$$

in which the weighting $\frac{1}{\hat{F}(x)(1-\hat{F}(x))}$ preferentially penalizes the deviations in the tails; in practice, AD is indeed more sensitive to tail deviations than either the χ^2 or the KS. Through a partial fraction decomposition of the integrand and the articulation of F_n as piecewise constant intervals, and a change of the integrating domain such that $d\hat{F}(x) = \hat{f}(x)dx$, Equation (3.2.7) is resolved as:

$$\mathrm{AD} = -n - \left(\frac{1}{n}\right) \sum_{i=1}^{n} (2i - 1)\left[\ln \hat{F}\left(x_{(i)}\right) + \ln\left[1 - \hat{F}\left(x_{(n+1-i)}\right)\right]\right] \tag{3.2.14}$$

in which $\{x_{(1)}, x_{(2)},\ldots x_{(n)}\}$ is the sorting of the sample data $\{x_1, x_2,\ldots x_n\}$ in ascending order, i.e., $x_{(1)} \leq x_{(2)} \leq \ldots \leq x_{(n)}$.

In developing data-driven industrial simulations, the χ^2, KS, and AD statistics are used to rank the MLE-parametrized distributions, indicating which distributions are representative of the various process variables. However, they often provide conflicting results, including the χ^2 rankings, which can change depending on how the categories are constructed. Moreover, common software such as easy fit and the Rockwell input analyzer consider an extensive list of distributions, many of which are obscure. For example, the top-ranked distribution according to KS may be a Johnson SU, which is a four-parameter transformation of the standard Gaussian; if a more commonly used distribution is nearly as good in KS ranking and is also favorable in the χ^2 and AD rankings, then the more common distribution is a better choice. Firstly, the more common distributions are prolific in published studies across many disciplines, allowing for cross-disciplinary comparisons. More importantly, the common distributions are better received in preparation for detailed studies (Figure 3.1a) that would ultimately allow more detailed modelling; the fitted distributions that are most impactful to the simulation may (or should) ultimately be replaced by mechanistic models (Figure 3.1b). The application of an obscure multiparameter distribution may be counter-productive since either (1) the process variable is critical and should genuinely be represented through a sub-model rather than an obscure distribution, or (2) the variable is not so critical and should rather be represented by a common distribution instead of being a point of unnecessary scrutiny for management.

An existing nuance is that the χ^2, KS, and AD rankings of MLE-parameterized distributions are descriptive in the sense of descriptive statistics; this is in contrast to inferential statistics, which relies on hypothesis testing to infer the properties of an underlying process, given a set of sample data. In the current context, it is understood that the process variables do not actually follow any of the idealized distributions listed by the fitting software; the task is to decide which of these distributions are best suited to argue for the next phase of simulation modelling, with the objective of efficiently directing the resources for further study (Figure 3.1) and ultimately for process improvement.

In a different context, whereby a systematic sweep of numerous candidate distributions is not involved, a GOF hypothesis test is applied when there is a hypothetical distribution that is specifically observed to be a possible description of the underlying process. For χ^2, KS, and AD tests, a null hypothesis is formulated as:

H_0: the measured sample data $\{x_1, x_2 \ldots x_n\}$ follows a distribution whose cumulative probability function is described by $F_0(x|\theta)$ having parameters θ.

The observed χ^2, KS, and AD can then be computed by applying Equations (3.2.9), (3.2.12), or (3.2.14), respectively, to the MLE-parametrized hypothetical cumulative probability function $\hat{F}_0$. For a significance level $\alpha \in (0, 1]$, the null hypothesis is rejected if the observed statistics exceed a critical value; such a rejection indicates a minimal confidence $(1-\alpha)$ level in which the underlying process does not follow the hypothetical distribution. For the χ^2 test, the test is formulated as:

$$\left(\chi^2 > \chi^2_{1-\alpha,k-m}\right) \Rightarrow (\text{Reject } H_0) \tag{3.2.15}$$

in which the critical value is $\chi^2_{1-\alpha,k-m}$ can be obtained from textbooks or from software (Excel, Minitab, etc.) considering $(k-p)$ degrees of freedom; p is the number of parameters within the hypothetical distribution, e.g., p = 2 for Gaussian and log-normal. The critical $KS_{1-\alpha}$ and $AD_{1-\alpha}$ are both distribution-specific (Massey, 1951; Anderson & Darling, 1954) and consider multiplicative adjustment factors that depend on the number of samples n.

$$(\text{KS} > \phi_n^{\text{KS}} \text{KS}_{1-\alpha}) \Rightarrow (\text{Reject } H_0) \tag{3.2.16}$$

$$(\text{AD} > \phi_n^{\text{AD}} \text{AD}_{1-\alpha}) \Rightarrow (\text{Reject } H_0) \tag{3.2.17}$$

For a hypothetical Gaussian distribution, the adjustment factors are $\phi_n^{\text{KS}} = \left(\sqrt{n} - 0.01 + \frac{0.85}{\sqrt{n}}\right)$ and $\phi_n^{\text{AD}} = \left(1 + \frac{4}{n} - \frac{25}{n^2}\right)$. For certain distributions, such as the exponential, the n-dependent adjustment includes an additive shift as well as a multiplicative factor (Massey, 1951). It is indeed customary to apply the tests of Equations (3.2.9) – (3.2.11) for the selected distribution, which incidentally may not be the top-ranked of all GOF metrics. But particular caution is required when interpreting the rejection of these hypotheses, especially when communicating to management

(Figure 3.1). In the descriptive statistical context of GOF ranking to support simulation modelling, the null hypothesis, H_0, is moot a priori unless there is a genuine expectation that the underlying process could follow the proposed distribution. The ultimate decision to accept a distribution-based representation of a process variable, or to replace it with a more detailed sub-model (i.e., to truly reject the distribution), must depend on how significant the process variable is to the engineering decision-making. Otherwise, the tendency is to focus erroneously on irrelevant aspects of the model that justifiably have a large statistical deviation from the observed data; in practice, it is typical that the unimpactful aspects (as determined by the approach in Figure 2) of the model remain less developed in favor of the more impactful aspects that should indeed be more developed. Therefore, simulation modelers must understand the notion of inferential statistical significance, especially to distinguish it from engineering decision-making significance. It is likely that all distribution-based representations should ideally be replaced by sub-models, "sub-sub-models", etc. (Figure 3.1b) from a statistical point-of-view with $\alpha \approx 0$. Yet, in practice, the budgetary and human resource limitations cause the modelling effort to prioritize those aspects which are truly critical to the advancement of the project (Figure 3.1a). This engineering-oriented prioritization is not reflected within the weightings of Equations (3.2.7), (3.2.12), and (3.2.13).

3.3 DRS with geostatistical modelling and geometallurgical input

The quantitative framework developed in this research aims to improve our understanding of geological variability by incorporating spatial uncertainty using geostatistical simulation methods. As mentioned in Chapter 2, these methods generate a series of equiprobable realizations that reflect the spatial variability of each variable, providing a solid basis for assessing the uncertainty inherent in mineral deposits. In addition, taking advantage of three-dimensional geological data collected early in the value chain, allowing to have for a simulated mineral processing stage response, contributing to the expansion of the capabilities of discrete event/rate frameworks. The SGS-DRS approach developed in the current work can be an important step within improvement projects in preparation for more elaborate efforts in which either SGS or DRS are eventually replaced by more advanced frameworks. In particular, the current research uses Sequential Gaussian Simulation to generate geospatially distributed variables, which is an adaptation of the discrete rate simulation (DRS) framework that was initially developed by Navarra et al. (Navarra, et al., 2019).

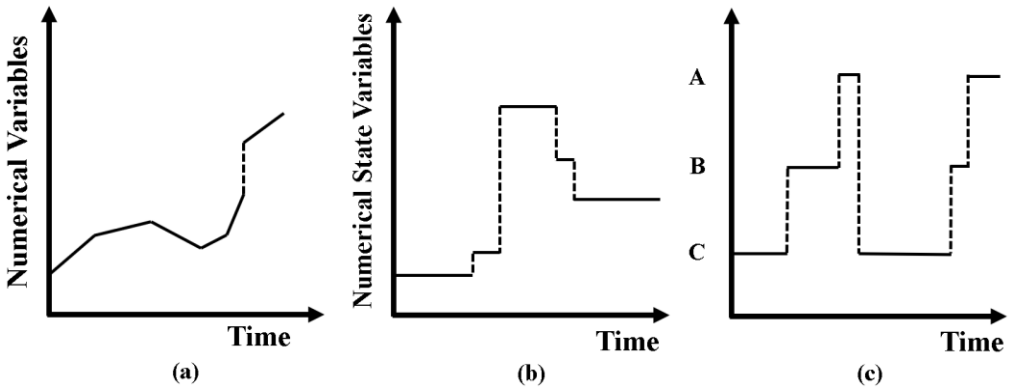

Figure 3.3.1: (a)State variable with linear dynamics evolution during simulation time frame (b) Discrete numerical state variable evolution during simulation time frame (c) Categorical state variables evolution during simulation time frame.

DRS is a kind of MC simulation that represents dynamic systems whose state variables have piecewise linear dynamics (Figure 3.3.1a). The state variables are represented over time by pairs of levels and rates (l_j, r_j), for j = 1, 2, … nSV in which nSV is the number of state variables. The simulation progresses through a series of discrete events, whereby the ith event causes an updating of the levels in accordance with continuous piecewise linear dynamics,

$$l_j := l_j + (t_i - t_{i-1}) r_j \tag{3.3.1}$$

as illustrated by the first five segments of Figure 3.3.1a, and can consider a discontinuous jump as described by

$$l_j := l_j + (t_i - t_{i-1}) r_j + \Delta_j \tag{3.3.2}$$

as illustrated by the vertical dotted line that leads into the sixth segment Figure 3.3.1a. The updating of the rates rj and the discrete jumps Δj are based on model-specific formulas that consider the values of state variables (lj', rj') possibly in conjunction with random number generation depending on other defined dependencies in a particular system. Figure 1b illustrates a discrete numerical state variable (i.e., with rj ≡ 0), and the changes are entirely due to discrete jumps Δj. This approach is easily adapted to consider categorical state variables which have a discrete range of values, e.g., the operating mode can have values of "A", "B", etc. as illustrated in Figure 3.3.1c, which may be interpreted as a mapping from numerical values, 1, 2, and so on.

Within equations (3.3.1) and (3.3.2), t_i denotes the time of event i, whereas ti-1 represents the time of the preceding event. In general, the time between events (ti – ti-1) can be the result of

random number generation. The formulation of (Navarra, et al., 2019) places particular emphasis on threshold crossing events, e.g., when a certain type of feed is exhausted, and the cyanidation process is therefore adjusted to accommodate a different blend. (Navarra, et al., 2019) and subsequent work such as (Wilson et al., 2021), (Wilson et al., 2022a), (Wilson et al., 2022b), (Órdenes et al., 2021), (Órdenes et al. 2022) and (Quelopana et al., 2023), used threshold crossing events to model geological variation.

In the geostatistical approach, the generation of the parcels is informed by the statically defined mine plan in conjunction with the corresponding block model constructed from Sequential Gaussian Simulation (SGS) generations (Figure 3.3.2). Each SGS replica produces a different scenario of what the orebody might be, which is then used within a DRS replica to simulate the operational response.

Figure 3.3.2: Geostatistical approach, in which geological data is generated prior to the execution of the DRS, through Sequential Gaussian Simulation.

Within the current model, the loading of a subsequent parcel immediately changes the mass balance and is observed as slope changes (i.e., changes in rates rj) in the progression of feed stockpile levels. A high-resolution representation would consider parcels containing low tonnages, e.g., 1,000 t, which would be rapidly excavated to allow a frequent succession of randomly generated parcels while retaining the ability to represent the geospatial aspects of the orebody as the excavation progresses from one zone to another and may be set up in such a way to inform or verify the mining sequence. This approach can be used to model mine phases starting from even the earliest stages of orebody development to examine approaches for minimizing grade variability and/or deleterious element variability.

The incorporation of SGS within DRS has relevance for the early phases of mining improvement projects. This relationship can be explained by on one hand; SGS is a well-known extension of variography and kriging (which are foundational to geostatistics), and on the other hand; DRS is arguably the most basic approach to dynamic and stochastic mass balancing. In the

case where SGS is poorly representative of the orebody, then an alternate conditional simulation such as SIS or higher order techniques may then take the place of SGS in the later phases of an improvement project. Similarly, DRS is a distinct form of Discrete Event Simulation (DES). The more general DES structure can support increasingly intricate operational dynamics including the discrete actions of individual equipment (e.g., load-haul-dumpers, scoops, etc.), thus addressing questions of fleet sizing and coordination. Application of DES are described within the mining context, e.g., by (Peña-Graf et al., 2022). However, these approaches do not make an explicit connection to geostatistical techniques.

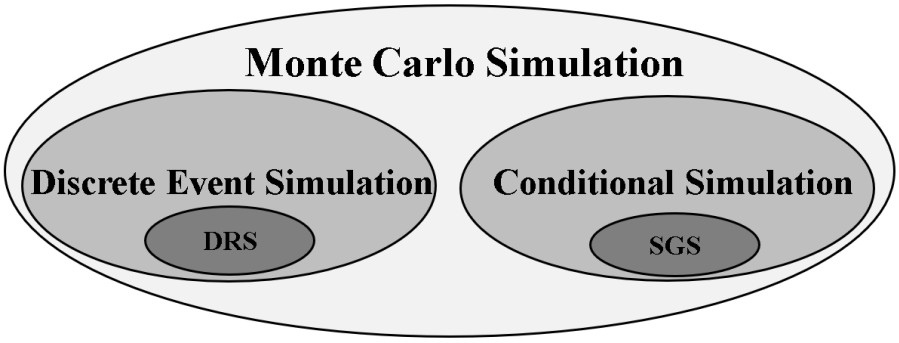

Figure 3.3.3: Monte Carlo Frameworks. On the left side, Discrete Event Simulation contains Discrete Rate Simulation as a subcategory, and on the right side, Conditional Simulation includes Sequential Gaussian Simulation as a subcategory.

3.3.1 Sequential Gaussian Simulation (SGS)

Sequential Gaussian Simulation (SGS) is a common method to stochastically populate a grid with a Gaussian random realization (Journel, 1989) and (Deutsch & Journel, 1992). This method is an efficient means of modelling spatial heterogeneity and has long been utilized in the oil reservoir and orebody modelling communities (Dimitrakopoulos & Fonseca, 2003). Sequential Gaussian Simulation has been pivotal within modern resource estimation, and from an epistemological perspective, it is the merger of DRS with the principles of Monte Carlo Simulation adapted to Normal (a.k.a. Gaussian) distributions. Indeed, there are computationally efficient methods for randomly generating data using a normal distribution $N[\mu , \sigma]$, such as the Box-Muller transform and the ziggurat algorithm (Driss, Addaim, & Abdessalam, 2018), which are incorporated into SGS. The current discussion is intended to be a concise overview of SGS, noting that more rigorous treatments are available.

Suppose there are nS sample points located in space $\{(x_i,y_i,z_i)|\ i = 1, 2, \ldots, nS\}$ where numerical measurements have been made resulting in so-called "hard data", and an additional nU unsampled points located at $\{(x_i,y_i,z_i)|\ i = (nS+1), (nS+2), \ldots, (nS + nU)\}$ at which measurements have not been made. SGS creates nG equiprobable geological scenarios by utilizing the nS measurements of a geological attribute to simulate values at the remaining nU sample points. The hard data is maintained within each of the nG scenarios, while the nU randomly generated data will each be different for each of the scenarios. The steps for SGS are:

- Normalize the sample data
- Model the variogram using the normalized data
- For $j = 1 \ldots n_G$
- Construct a random sequence to visit the n_U unsampled points
- For $i = (n_S+1)\ldots(n_S+n_U)$
    1. Use the variogram model to extend and solve the kriging system of equations
    2. Use kriging interpolation weights to compute the mean μ_i and variance σ_i^2
    3. Randomly generate a value from $N[\mu_i,\sigma_i]$ and assign it to the point (x_i,y_i,z_i)
    4. Include the newly simulated point value into the conditioning data
    5. Denormalize the data, hence completing scenario *j*

In this context "normalize" implies redistributing the data with respect to a standard Normal distribution N[0,1] and after each of the nU data have been generated, "denormalize" implies distributing the data back into the original scale. Moreover, the generated data is sensitive to the sequence in which the points are visited, as each generated value successively conditions the subsequent values; therefore, rather than having a fixed (hence biased) order in which the nU points are simulated, a different random sequence (permutation) is used in each of the nG scenarios, by applying a permutation method such as the Knuth shuffle (Roy et al., 2014).

SGS depends on kriging which, in turn, depends on variography, i.e., the plotting of inter-sample variation versus inter-sample distances a.k.a. lags (Figure 3.3.1). The SGS algorithm requires a variogram model which describes how a value at a specific location is conditioned (influenced) by neighbouring values. For instance, in an anisotropic field the value at a point may be more influenced by neighbours along a particular direction, hence favouring neighbourhoods

having an ellipsoidal character rather than spherical. For certain geological structures such as veins or domes, a variogram model may be more representative if the inter-sample distances are quantified within in a geometrically transformed ("folded") space, rather than the natural Cartesian space. A more complete discussion on variography is presented by (Wilson, et al., 2021) for example, but in general a variogram includes (1) an innate localized variation which constitutes the so-called nugget effect, (2) a range of inter-sample lags beyond which two sample points are deemed independent, and (3) a concave down curve used to model the transition from the localized variation toward the far field variation. Variogram modelling is something of an art form; nonetheless a proposed variogram can be validated through SGS if the data within the resulting scenarios capture the essential features of the orebody. In practice, this validation includes a visual assessment of the geological scenarios, and an inspection of histogram plots and other numerical and graphical aids.

Figure 3.3.4: Sequential Gaussian Simulation variography and kriging dependency.

There are two main forms of kriging that are commonly used within SGS, namely simple kriging (SK) and ordinary kriging (OK), both of which rely on least-squares optimization to attain an interpolated attribute value μi at a point (x_i,y_i,z_i) that, if appended to the previously available values (i.e. the conditioning data) at points $\{(x_i', y_i', z_i')\}|i'=1, 2\ldots (i-1)\}$, will yield minimal variance σ_i^2. Both SK and OK produce a system of linear equations in order to establish the kriging weights however, OK enforces an additional constraint that these weights should sum to 1 and is thus a form of constrained least-square optimization (which features a Lagrangian multiplier). More details for the SK, OK, and other kriging formulations are described in (Wilson et al., 2022a).

Given the kriging weights, the interpolated value μ_i is a weighted sum of the neighbouring conditioning data. As indicated in the preceding algorithm, these results (μ_i,σ_i) are used to parametrize a Gaussian random generation, and the resulting randomly generated value is considered as conditioning data for each of the remaining points $\{(x_{i'}, y_{i'}, z_{i'})\}|i'=i+1, nS+nU\}$.

An important nuance within the SGS algorithm is that the system is extended by one linear equation for each newly simulated point that is incorporated into the conditioning set. By applying

specialized matrix techniques, only a marginal amount of computational effort is required to solve the i^{th} kriging system as partial results from the preceding $(i-1)^{th}$ kriging system are successively utilized. These partial results constitute a lower triangular matrix known as a Cholesky factor Ki, and for SK, the i^{th} Cholesky factor contains the $(i-1)^{th}$ Cholesky factor Ki-1 as a submatrix, which in turn contains the $(i-2)^{th}$ Cholesky factor Ki-2, and so on. As described by (Deutsch and Journel, 1992), Cholesky decomposition is a particular form of the so-called LU decomposition (a.k.a. Lower–Upper decomposition) that allows efficient solution of symmetric linear equations, such as the SK and OK systems which are present within the SGS algorithm. Practical implementations of SGS depend on computationally efficient approaches to solving the kriging system. Notably, Generalized Sequential Gaussian Simulation (GSGS) arranges the kriging systems according to groups of points (Quigley, 2016), which reduces the computation time by a factor of 10, but also biases the sequence and results in a visual artifact known as the screening effect.

3.3.2 Turning Bands Method (TBM)

This technic was first presented in a strict mathematical format by Matheron (1973) and after was developed by Journel (1974; 1978). The TBM is used in geostatistics for simulating spatial random fields, the foundational concept is that a multidimensional spatial random field can be modelled by the superposition of several independent one-dimensional (1D) random profiles. These 1D functions are conceptually 'turned' in several directions across the multidimensional space, and they are distributed equally to represent the multidimensional field (Brooker,1985). By turning these bands or profiles in different directions, the spatial variability of the field can be captured, this method effectively simplifies the problem of simulating a spatial field in multiple dimensions by reducing it to the task of simulating several one-dimensional bands (Biermé et al., 2015). To jointly simulate the components of a vector RF, the field can be split into its constituent components. (Paravarzar, et al., 2015):

$$\forall x \in D\ , Y(x) = \sum_{s=1}^{s} y_S(x) \tag{3.3.3}$$

In accordance with the linear coregionalization model, Y_1,. . ., Y_s are considered as independent vector Gaussian random fields. Each of these fields has associated matrices $B_1\rho_1$,. . ., $B_s\rho_s$ that represent their direct and cross-covariance functions. Since each coregionalization matrix

is positive semi-definite, non-conditional simulations are carried out by decomposing each co-regionalization matrix, $\mathbf{B}_n$, as follows (Emery, 2008; Paravarzar, et al., 2015):

$$\mathrm{B}_n = A_n \mathrm{A}_n^T = Q_n \Delta_n \mathrm{Q}_n^T \tag{3.3.4}$$

Where Q_n is an orthogonal matrix eigenvectors, Δ_n is a diagonal matrix of eigenvalues, and $A_n = Q_s\sqrt{\Delta_s}$. The generated non-conditional realizations are converted through a kriging step into conditional realizations (Journel & Huijbregts, 1978). Let $\{\mathrm{Y_S(x)}, \mathrm{x} \in \mathrm{R}^3\}$ be a non-conditional simulation, in the stationary case (finite variance models), the random field defined by (Emery, 2006):

$$\forall x \in R^3 \, , y_{cs}(x) = y_s(x) + [y(x) - y_S(x)]^{sk} \tag{3.3.5}$$

Which reproduces the distribution of $[Y_s(x),\ x \in R^3]$ conditional to the Y-data. To summarize, the conditional simulation implementation is as follows:

(1) Draw a non-conditional realization at the target location x and at the data locations, via the turning bands method;

(2) Compute the deviations (residuals) between the data values and simulated values at the data locations;

(3) Perform a simple kriging of the residual from its values at the data locations

(4) Add the result to the non-conditional realization, in accordance with Equation (3.3.5).

This method has proven to be very efficient in the interpretation of ore body geometry, allowing simulated anisotropy with higher accuracy. Indeed, the TBM is often recognized for its efficiency in simulating spatial fields with a large number of points (Mantoglou, & Wilson, 1982). The limitations related to the TBM is firstly does not reproduce the exact variogram, and secondly, even though the use of more bands improves the approximation of the variogram (asymptotically) reducing artifacts, computational demands are increased. Therefore, a trade-off between achieving a more accurate simulation and maintaining computational efficiency needs to be performed.

3.3.3 Sequential Indicator Simulation (SIS)

Classical geostatistical simulation methods, such as Sequential Gaussian Simulation (SGS), introduced by Journel in the late 1980s (Gomez-Hernandez & Srivastava, 2021), rely on

the assumption that the underlying data follows a multivariate Gaussian distribution. In this algorithm, values are sequentially simulated conditioned on the original data and previously simulated values. The assumed Gaussian nature of the local conditional distributions significantly simplifies the process, as the mean and covariance derived from an ordinary or simple kriging system are sufficient to fully determine these distributions, which are subsequently randomly sampled to generate unique simulated point-scale values. However, this assumption can be problematic when dealing with non-gaussian random functions, such as continuous variables with spatially correlated extreme values, non-linear geological features or categorical variables representing lithological facies. In such cases, the assumption of Gaussianity is not suited since the local conditional distributions cannot be expressed analytically. Moreover, SGS tends to produce maximum-entropy solutions, which may not adequately capture the complex variability and patterns observed in geological systems (Journel and Deutsch, 1993).

The Sequential Indicator Simulation algorithm was introduced by Journel and Alabert in 1987 (Gomez-Hernandez & Srivastava, 2021) as a non-parametric statistical framework that can handle the complexity and variability inherent in geological systems without defaulting to assumptions of multiGaussianity. This simulation technique is variogram-based and categorical in nature, and as in SGS, follows the principle of sequential simulation (Journel 1993), where the joint probability distribution of a stationary ergodic random vector $\boldsymbol{Z} = (Z_1, Z_2, \dots, Z_N)^T$, associated with probability triple $(\Omega, \mathcal{F}, P)$, a set of categories $C = \{c_1, c_2, \dots, c_N\}$ such that $\boldsymbol{Z}: \Omega \rightarrow C^N$ and defined on a grid $D = \{\boldsymbol{x}_1, \boldsymbol{x}_2, \dots, \boldsymbol{x}_N\}$, $\boldsymbol{x} \in \mathbb{R}^n$, $n = 2,3$, can be decomposed into the product of univariate conditional distributions as follows:

$$P(Z_1 = c_1, Z_2 = c_2, \dots, Z_N = c_N | \boldsymbol{d}_n) = \prod_{i=2}^{N} P(Z_i = c_i | Z_1 = c_1, Z_2 = c_2, \dots, Z_{i-1} = c_{i-1}, \boldsymbol{d}_n) P(Z_1 = c_1 | \boldsymbol{d}_n) \quad (3.3.6)$$

Here, $\boldsymbol{d}_n = \{z_1, z_2, \dots, z_n\}$ denotes a set of conditioning data where lowercase z implies a realization of random vector Z. As such, the difficulty in SIS is in deriving the conditional distributions of Z at one node of grid D given the available data at other nodes. This can be done using the indicator formalism introduced in Journel and Alabert (1989). Without loss of generality, let $c_k = k, k = 1, \dots, K$ represent K different rock types. A categorical variable is encoded as a vector of K indicator variables:

$$i_k(Z_i) = \begin{cases} 1, & Z_i = k \\ 0, & Z_i \neq k \end{cases} \tag{3.3.7}$$

Then, any conditional probability for $\boldsymbol{Z}$ to the previously simulated nodes and given data within the local neighborhood of Z_i, represented by set $\boldsymbol{\lambda}_i$, can be written as a conditional expectation:

$$P(Z_i = k_i|\boldsymbol{\lambda}_i) = E\left[i_{k_i}(Z_i)|\boldsymbol{\lambda}_i\right] \tag{3.3.8}$$

Estimates of the conditional distributions at each grid node are given by indicator kriging using corresponding indicator variograms. To compute the conditional expectation in equation 3.3.8, the first-order linear approximation in equation 3.3.9 is used, where $\alpha_0$and α_1 are weights determined using simple or ordinary indicator kriging, and the covariance structure of the data (Hansen, 1992).

$$P(Z_i = k_i|\boldsymbol{\lambda}_i) = E\left[i_{k_i}(Z_i)|\boldsymbol{\lambda}_i\right] = \alpha_0 + \sum_{\beta \in \boldsymbol{\lambda}_i} \alpha_1(\beta) \times i_{k_i}(Z_\beta) \tag{3.3.9}$$

Note that since there are K different rock types, kriging systems must be solved K times for each Z_i associated with location $\boldsymbol{x}_i$.

Unlike SGS, SIS enables the incorporation of class-specific spatial continuity patterns by utilizing different indicator variogram models for each considered rock type k. Prior to variogram model fitting, experimental variograms are calculated from the indicators as follows:

$$\hat{\gamma}(\boldsymbol{h})_k = \frac{1}{2N(\boldsymbol{h})} \sum_{N(\boldsymbol{h})} \left[i_k\big(\boldsymbol{Z}(\boldsymbol{x})\big) - i_k\big(\boldsymbol{Z}(\boldsymbol{x}+\boldsymbol{h})\big)\right]^2 \; k = 1, \dots, K \tag{3.3.10}$$

Where $N(\boldsymbol{h})$ denotes the number of pairs of data points distanced by $\boldsymbol{h}$ units. The indicator variogram functions can vary depending on k. This allows for the modeling of different degrees of spatial correlation for each rock type, enabling a more precise representation of geological variability than with Gaussian methods. As described, the fundamental concept of SIS involves breaking down a multivariate spatial distribution into a series of conditional distributions. While the sequence by which nodes in the grid are visited can be arbitrary, a random order is usually adopted to prevent artifacts. At each visited node, conditional distributions are determined using indicator kriging, incorporating both the original data and previously simulated values (equation 3.3.9). To enhance computational efficiency, a search neighborhood restricts the conditioning data. A category is assigned to each location by randomly sampling from the local uncertainty model,

represented by a probability mass function of the possible rock types. This process continues until all nodes are simulated. Multiple equiprobable realizations can be generated by using different random numbers when sampling the distributions. Figure 3.3.5 summarizes the procedure.

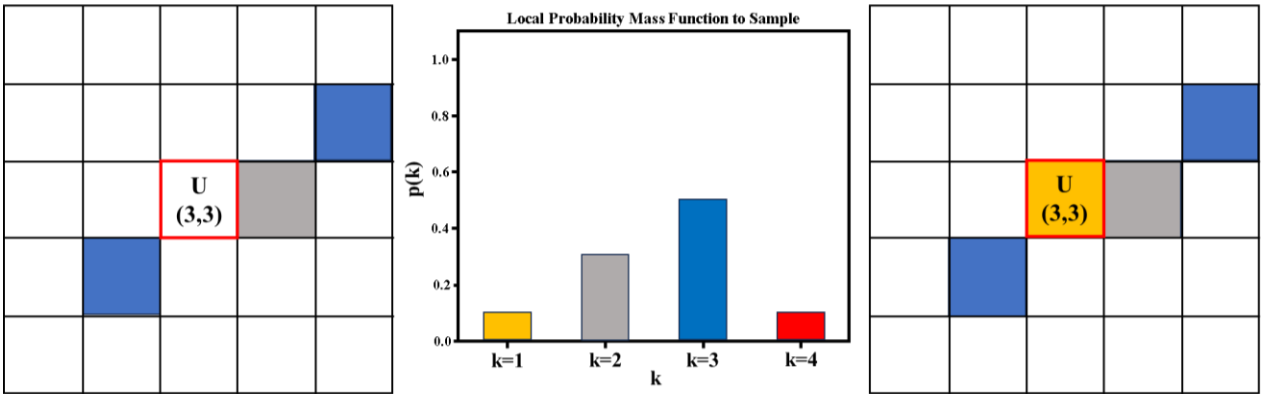

Figure 3.3.5: Summary of the SIS procedure of a grid, (a) random path, generated local uncertainty model at location (3,3) (b) a rock type k=1 is randomly sampled from the local uncertainty model based (c). Modeled node at the location (3,3).

The algorithm for generating conditional cumulative distribution functions (CCDF's) particularly in the context of conditional simulation offers several significant advantages (Alabert, 1987; Deutsch & Journel, 1992). SIS is particularly beneficial in scenarios where the geometry of geological bodies is not distinctly defined, and where the spatial continuity of the variables can be effectively characterized by variograms, i.e. geological formations that have significant diagenetic alteration (Pyrcz & Deutsch, 2014). By sequentially simulating each location or node, based on the local probabilistic framework provided by the variogram, SIS generates realistic and geologically likely representations of the spatial distribution of categorical variables, generating equiprobable realizations that honor a pre-defined structure and the data inputs (Mizuno & Deutsch, 2022).

3.3.4 Multiple Point Statistics (MPS) and Higher Order Stochastic Simulation (HOS).

The multiple-point statistics (MPS) was proposed in the early 1990s, and widely used in the petroleum industry (Srivastava, 2018). MPS is an advanced technique aimed at understanding the spatial relationship between multiple points in a given sample data. Variogram-based methods rely on two-point statistics, which only consider the relationship between pairs of data points at a time.

However, by describing only the correlations between two spatial locations, a variogram cannot capture mathematically the complexity of curvilinear geological features (Caers and Zhang 2004). In the MPS methods, the spatial statistics are not either extracted using variogram (two-point statistics paradigm), instead a conceptual tool named training image (TI) is used, which is an example of the spatial structure to be modelled by the available data (Tahmasebi, 2018). The role of the training images (TI, the most important input in this techniques) is to act as a conceptual model that captures the spatial patterns and structures expected in geological formations. Many of the major oil companies funded detailed quantitative studies of outcrops that could serve as good geological analogs for input in simulations (Srivastava, 2018). The concept of a training image (TI) in geostatistical modeling, particularly in the context of MPS, is centered around its role as a conceptual interpretation of the major spatial variations present in the studied area, which can be based on actual data, or on other exhaustive data set considered to be representative (Strebelle, 2000; Zhang, 2006). Three main methods are presented for constructing a TI:

(1) Outcrop Data: Outcrops are indeed one of the most valuable sources of information in geological surveys and field studies. Outcrops provide a direct and tangible view of the geological characteristics of an area, offering a firsthand look at the geology. They can show the layering, folding, faulting, and other structural aspects of rock formations, which are crucial to construct the geological model. By the information provided by outcrops, it is possible to interpret the three-dimensional arrangement, understand spatial patterns and structural relationships that can guide the creation of the training images that finally are inputted into the simulations.

(2) Object-based Methods: Another method for build structured categorical models is the object-based (or Boolean) method (Deutsch & Wang 1996; Skorstad et al. 1999). In this case, the trained image is defined based on geological features, such as shape, size, direction, and sinuosity. The results can be used within an iterative algorithm to provide any further alterations, but not always the best option (Srivastava, 2018).

(3) Process-based Methods: Process-based methods (Lancaster & Bras, 2002; Pyrcz et al. 2009) develop 3D models emulating the physical processes that generate a porous

medium. Even though the realism, they are computationally expensive and additive models, their result is oriented to a specific geological formation.

The comparison between pixel-based and pattern-based MPS methods highlights the trade-offs encountered in geostatistical modeling, particularly in the context of simulating complex geological structures. In the case of pixel-based methods have good precision on matching sample data, honoring the values at specific data points (e.g., well locations), ensuring that the simulated model aligns perfectly with the observed data at those points. Conversely, in complex geological scenarios, pixel-based may struggle to realistically replicate the intricate structures, producing artifacts or overly simplistic representations that do not capture the true complexity of the geology. In the other hand, pattern-based techniques accurately represent the subsurface model by the use of the training image, capturing the spatial relationships and structural complexities, leading to more realistic simulations, they may not always perfectly honor the data at specific locations (such as well data), leading to discrepancies between the model and observed data points.

A important technic in the MPS is the High-order stochastic simulation (HOS), these methods are amongst the latest developments in geostatistical simulation (Journel and Huijbregts 1978; Goovaerts 1997), developed in recent years, aiming to reproduce complex spatial patterns from the available data that cannot be efectibly captured by traditional two-point geostatistics. Initial simulation methods in geostatistics assumed that the variables being modeled followed a Gaussian (or normal) distribution and the use of second-order statistics, which involve the mean (first-order) and variance and covariance (second-order). (Journel & Huijbregts 1978; Goovaerts 1997). The most crucial second-order statistic in geostatistics is the variogram or the covariance function, which describes how spatial correlation changes with distance, this statistics provide a comprehensive statistical framework for Gaussian processes, but they fail when it comes to modeling geological phenomena, which commonly deviate from Gaussianity and exhibit complex, non-linear spatial patterns (Dimitrakopoulos et al. 2010). The spatial attributes of certain geological features among multiple locations can be characterized by the high-order spatial statistics defined by spatial cumulants or spatial moments (Dimitrakopoulos et al., 2010; De Iaco & Maggio 2011). Cumulants are combinations of statistical moments that allow the characterization of non-Gaussian random variables which are used to evaluate the dependence

structure of a spatially distributed random variable at an unsampled location, based on values at some sample locations in the neighborhood (Billinger & Rosenblatt, 1966; Rosenblatt 1985).

Let (Ω,ℑ, P) be a probability space and Z(x) be a real random field in R_n defined at the locations, $x_i \in D \subseteq R_n (n = 1, 2, 3)$ for i = 1 . . .N, where N is the number of points in a discrete grid $D \subseteq R_n$(Dimitrakopoulos et al., 2010). Assuming Z(x) is a zero-mean ergodic stationary random field in R_n, then the cumulants of Z(x) are defined by the MacLaurin expansion of the cumulant generating function (Rosenblatt, 1985):

$$K(\omega) = \ln\left(E[e^{\omega Z}]\right) \tag{3.3.13}$$

The high-order spatial moment of order r is:

$$Mom[Z(x), Z(x + h_1), \ldots, Z(x + h_{r-1})] = E\left[Z(x)Z(x + h_1) \ldots Z(x + h_{r-1})\right] \tag{3.3.14}$$

Similarly, the cumulants of the random field Z(x) up to order r can be expressed as

$$c_r^z(h_1, \ldots, h_{r-1})] = Cum\left[Z(x)Z(x + h_1) \ldots Z(x + h_{r-1})\right] \tag{3.3.15}$$

For example, cumulant order 1 is a mean of random field Z(x)

$$c_r^z = E\left[Z(x)\right] \tag{3.3.16}$$

Second-order cumulant of the random field Z(x) is known as covariance

$$c_2^z(h)] = E\left[Z(x)Z(x + h_1)\right] \tag{3.3.17}$$

Its third-order cumulant is given by

$$\begin{aligned} c_3^z(h_1, h_2)] = {} & E\left[Z(x)Z(x + h_1)Z(x + h_2)\right] - E\left[Z(x)\right]E\left[Z(x + h_1)Z(x + h_2)\right] \\ & - E\left[Z(x + h_1)\right]E\left[Z(x)Z(x + h_2)\right] - E\left[Z(x + h_2)\right]E\left[Z(x)Z(x\right. \\ & \left. + h_1)\right] - E\left[Z(x)\right]E\left[Z(x + h_1)\right]E\left[Z(x + h_2)\right] \end{aligned} \tag{3.3.18}$$

Some studies have highlighted limitations in the use of traditional geostatistical methods, particularly in the context of modeling complex geological phenomena that exhibit nonlinear and non-Gaussian behaviors, their shortcomings become evident when dealing with the intricacies of geological patterns (Journel & Zhang, 2006). In that context, multiple-point geostatistical simulation methods (MPS) were developed to counter the mentioned drawbacks for the traditional geostatistical methods becoming a suitable alternative for modelling complex scenarios (Mariethoz et al., 2010; Strebelle, 2002; Zhang et al., 2006).

Chapter 4

Underground Mining Systems DRS Applications

4.1 Incorporation of geometallurgical input into gold mining system simulation to control cyanide consumption.

In the last ten years, historic surges in precious metal prices have led to abundant mining opportunities, particularly in the gold sector. This increase in production directly impacts the consumption of sodium cyanide in the metallurgical extraction of precious metals. With gold mining companies investing capital into new grassroots exploration projects, re-evaluating low-grade deposits and prolonging activities at existing mines, there is an expected increase in market demand for sodium cyanide, which will likely result in increased cyanide prices (Verbrugge et al., 2021).

Understanding the metallurgical behaviour of ore and gangue material in plant feed is crucial to optimizing reagent consumption, process cost control and cash flow. Increases in required reagent dosages due to the presence of cyanide-consuming elements, such as copper and iron, can cause significant increases in plant operating costs. As a result, the development of tools to predict and simulate the system response to increases in reagent consumption is critical to identify and mitigate potential risks to gold mining operations.

In Chile, there are a large number and variety of gold deposit types, including porphyry copper-gold, iron-oxide-copper-gold (IOCG), and high-grade gold and silver hydrothermal veins (Sepúlveda, 2004). The Alhué gold mining district is located near the small village of Alhué in the Costa range of central Chile, approximately 70 km to the southwest of Santiago and 40 km southeast of Melipilla (Figure 4.1.1).

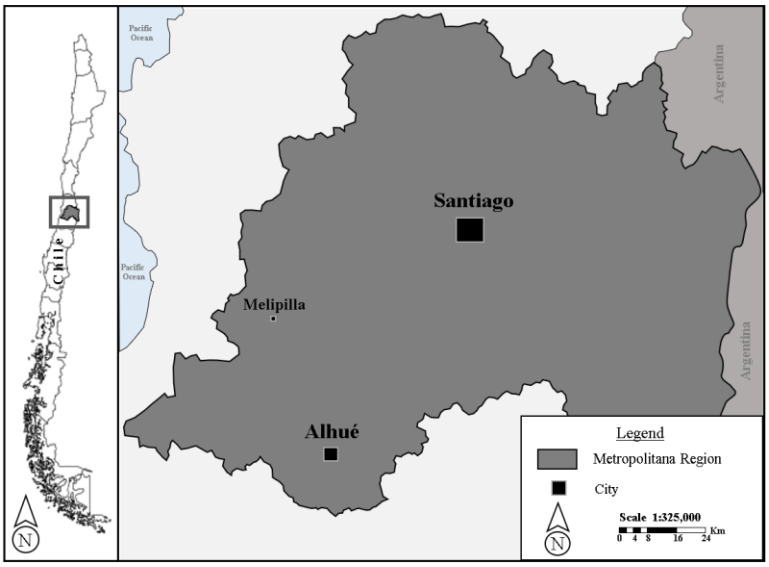

Figure 4.1.1: Location of the Alhué mining district in relation to the Chilean capital Santiago.

The Alhué deposit is a high-grade Au-Ag-Zn(-Pb) system in which veins exhibit mineralized gradients of base metal sulphides and are subject to faults that intersect the underground workings of the mine. Similar deposits can be found in the central zone of Chile, hosting polymetallic veins (Au, Ag, Cu, Pb and Zn) related to subvolcanic intrusive events, development of collapsed calderas and extensive hydrothermal alteration and pre- and syn-tectonic structural controlled veins, such as Bronces de Petorca, the Chancón mining district and Cerro Cantillana (Camus et. Al, 1991; Diaz, 1986). More specifically, the Florida Mine is located within the Alhué district. The quantity of copper (II) and iron (II) sulphides (CuS-FeS) entering the Florida plant is difficult to predict based on the actual mineral stockpile distribution due to heterogeneities inherent to the orebody. These base minerals are considered harmful to the extraction of precious metals as they are aggressive consumers of cyanide, thereby affecting the viability of the metallurgical process. Previous classification methods were based solely on head grade and did not consider the potential for high concentrations of impurities, such as CuS and FeS. Subsequent analysis showed that the geometallurgical variation and its impact on the beneficiation process can be managed by alternating between modes of operation that balance process mineralogy with strategic key performance indicators (KPIs) (Navarra, 2019). These modes of operation, each governed by separate operating policies and triggered by established thresholds, can then apply the necessary adjustments to effectively manage reagent addition.

The definition of appropriate geometallurgical units is paramount to properly plan and implement alternate modes of operation in response to imbalances of CuS-FeS contents in the ore feed. Furthermore, geometallurgical information should be routinely collected to complement the strategic planning of the mining process. Interpretation of this data can help define key criteria from which appropriate modes of operation and plant parameters can be established. From the experience at Florida Mine, the main factors that control copper and iron cyanide-soluble content include concentration, mineralogy and the oxidation-reduction (redox) state of the ore upon mining. These processed data are then converted into defined programs and decision-making criteria to implement changes in the plant's operational modes.

The current paper presents a quantitative approach to leverage the information obtained from process mineralogy to optimize cyanide consumption, in which mode changes are triggered by observed and forecasted changes in stockpile levels. The resulting operational modes provide an integrated response to the geological and geometallurgical variation; this is demonstrated through discrete event simulation (DES) following the two-mode formulation of Navarra et al. (Navarra, 2019).

4.1.1 Geological setting of the Alhué District

The Alhué district is known for gold-silver vein systems (Gómez, 2019). The veins are mainly hosted by volcanic rocks of the Las Chilcas Formation (Thomas, 1958; Carter, 1962), which are intruded by a batholith of monzogranitic composition and several minor subvolcanic bodies (e.g. andesitic domes and dykes). The Las Chilcas Formation is discordant to the underlying Lo Valle Formation. The Lo Valle Formation is comprised of an alternating succession of pyroclastic (tuffs and breccias) and lava flows, emplaced in a subaerial-continental setting (Thomas, 1958; Carter, 1962). The composition of the volcanic rocks varies from andesitic to dacitic, with the more acidic lavas dominant in the upper member of the stratigraphic sequence. Andesitic lavas are aphanitic to feldspar-porphyritic with variably clay-altered plagioclase phenocrysts. Common alteration minerals include chlorite and epidote, as well as later vuggy and vein-controlled zeolites.

The mineralized structures typically consist of a central vein composed of multiple types of quartz (grey, grey-green, green and lesser translucent white phases). The margins of the central vein tend to be flanked by hydrothermal breccia consisting of white to translucent-white quartz

with varying proportions of silicified (± epidotized) wall-rock fragments (Sepúlveda, 2004). An abundance of gold and silver-rich quartz veins occur in the district, with a total of 76 identified to date. The lengths and widths of these structurally controlled mineralized veins vary throughout the region (Gómez, 2019). The deepest levels of the hydrothermal system correspond to north-south trending structures (Maqui-type, Figure 4.1.2), which are dominated by calc-silicate minerals, magnetite and iron-rich sphalerite, and indicate a high-temperature deposition stage (Cotton, 1998).

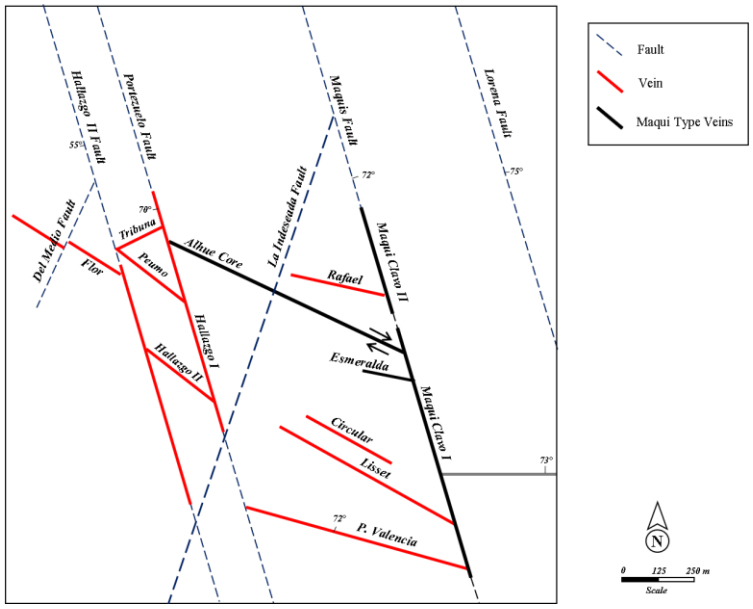

Figure 4.1.2: Schematic map of the Alhué district faulting and vein systems.

Veins such as Pedro Valencia, Cantillana and Circular represent earlier stages of mineralization that occurred at slightly lower temperatures, but still within the range of epithermal deposits (Cotton, 1998). Moreover, the vein-controlled gold mineralization occurs primarily as free electrum and native gold grains in quartz or associated to sulphides. The mineralization is commonly associated with magnetite and sulphides, including pyrite ± sphalerite-galena-chalcopyrite (Araya, 2001). The alteration assemblage in the veins mainly consists of quartz-epidote-chlorite-actinolite with lesser smectite, amphibole, and calcite-kaolinite-garnet (Matthews, 2018).

The process mineralogy can be subdivided based on redox conditions, which reflect the spatial interaction of the ore with the paleo-water table. This level indicates the depth to which oxygen affected the primary vein mineralogy by altering sulphides, leaching base metals, and transporting

them to lower levels. The geometry of the paleo-phreatic level has two main controls: 1) the landscape, along which the under-ground water level follows the shape of the surface topography; and 2) the intersection of veins with major faults. In both cases, this level is modified by these features reaching deeper levels. An example of this mineralogical contrast due to the reshaped paleo-water table level is the Flor vein, which interacts with the Del Medio fault system. Within just a few meters in the horizontal, there is a remarkable change in redox and related mineralogy due to the high permeability generated by the intersection of the vein with the fault system (Figure 4.1.3).

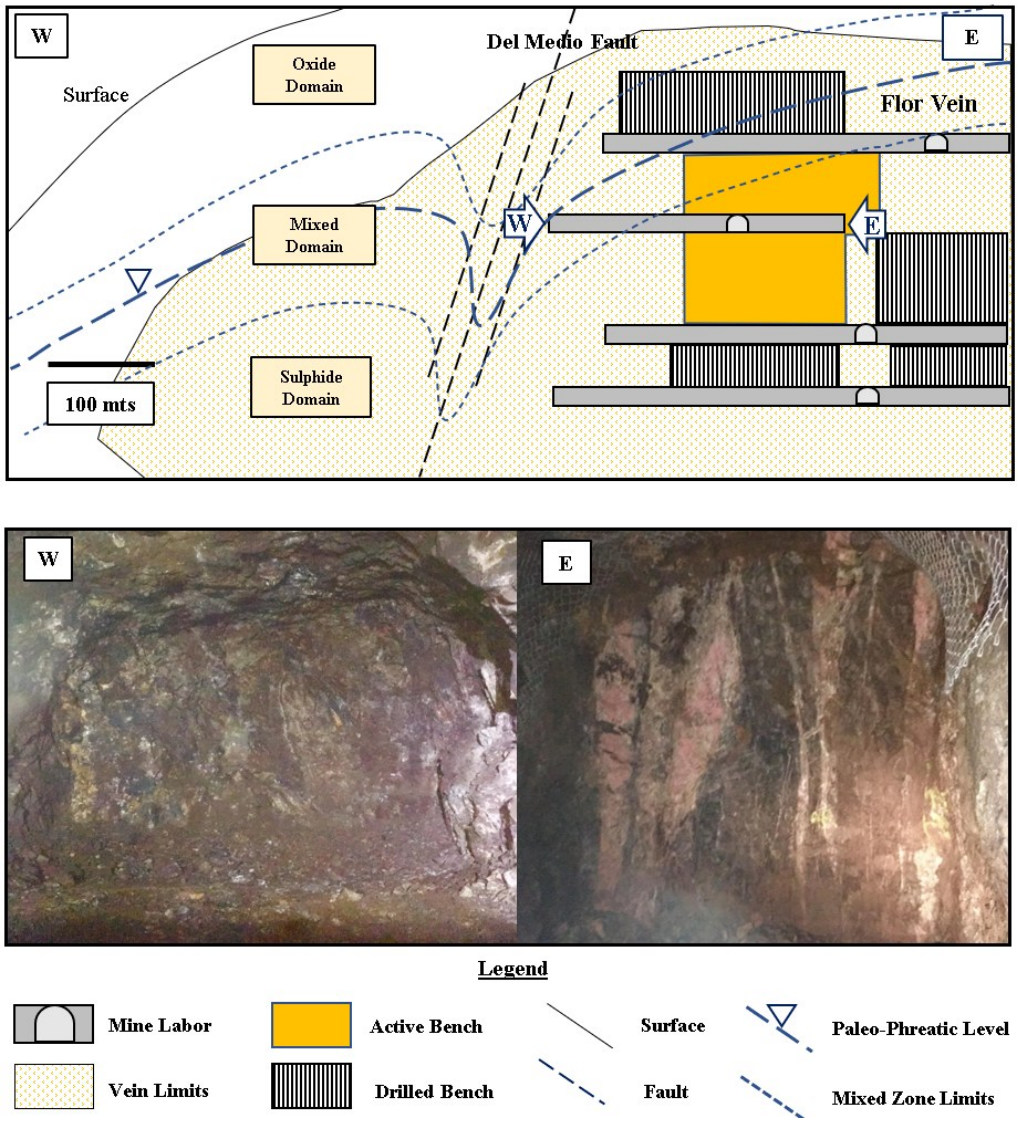

Figure 4.1.3: Flor vein workfaces, 975 level, Florida Mine. A difference in the oxidation state of the ore is observed within the same vein and level. The West workface is partially or completely oxidized compared to the East workface where the sulphides are preserved.

According to the regional scale deposit model proposed by Matthews (Matthews, 2018), base metal concentrations in the Alhué district increase at deeper levels and to the east. This increment is mainly due to a high temperature copper-iron rich fluid interpreted to have migrated through a listric fault system, acting as a feeder channel for these elements (Figure 4.1.4). This generates two main types of mineralization: 1) polymetallic suites in the western part of the district, characterized by the presence of Zn-Pb-Fe base metal sulfides, with Ag-Au-bearing quartz veins ± epidote-hornblende-magnetite chlorite, garnet, rhodonite, and tourmaline; and 2) Cu-Au sulfide-bearing quartz veins, with magnetite, chlorite, hornblende, epidote and zoisite, to the east.

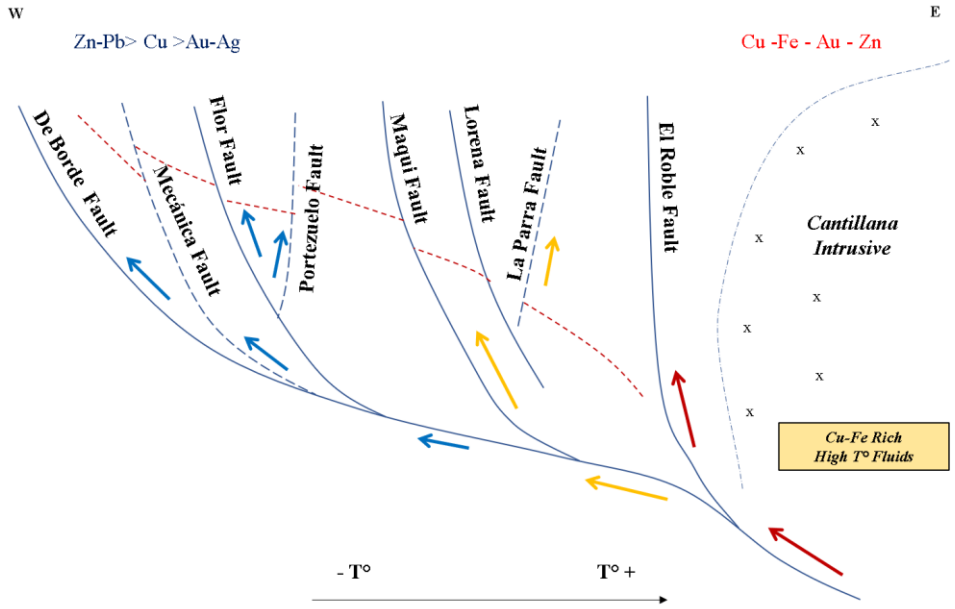

Figure 4.1.4: Schematic flow model of mineralizing solutions, Alhué district (Matthews, 2018).

These geological controls divide the deposit into four main domains (Oxide, Mixed, Low Cu Sulphide and High Cu Sulphide zones), each with different geometallurgical responses based on the resulting mineralogy (Figure 5). The primary (sulphide) zone is the largest and most important domain within the Alhué district, and consists of predominantly sphalerite, galena, chalcopyrite, and pyrite mineralization. Silver occurs as native silver, electrum, argentite, pyrargyrite and polybasite, and is strongly associated with vein-controlled quartz and sulphides (Araya, 2001). Silver has also been identified as inclusions in sphalerite and hessite grains. Iron oxide can also occur locally as magnetite in this zone, but is related to primary host-rock formation and/or epigenetic hydrothermal alteration (Gómez, 2019). This zone can be further subdivided into two subdomains, as a function of depth and Cu-Fe content (low vs. high).

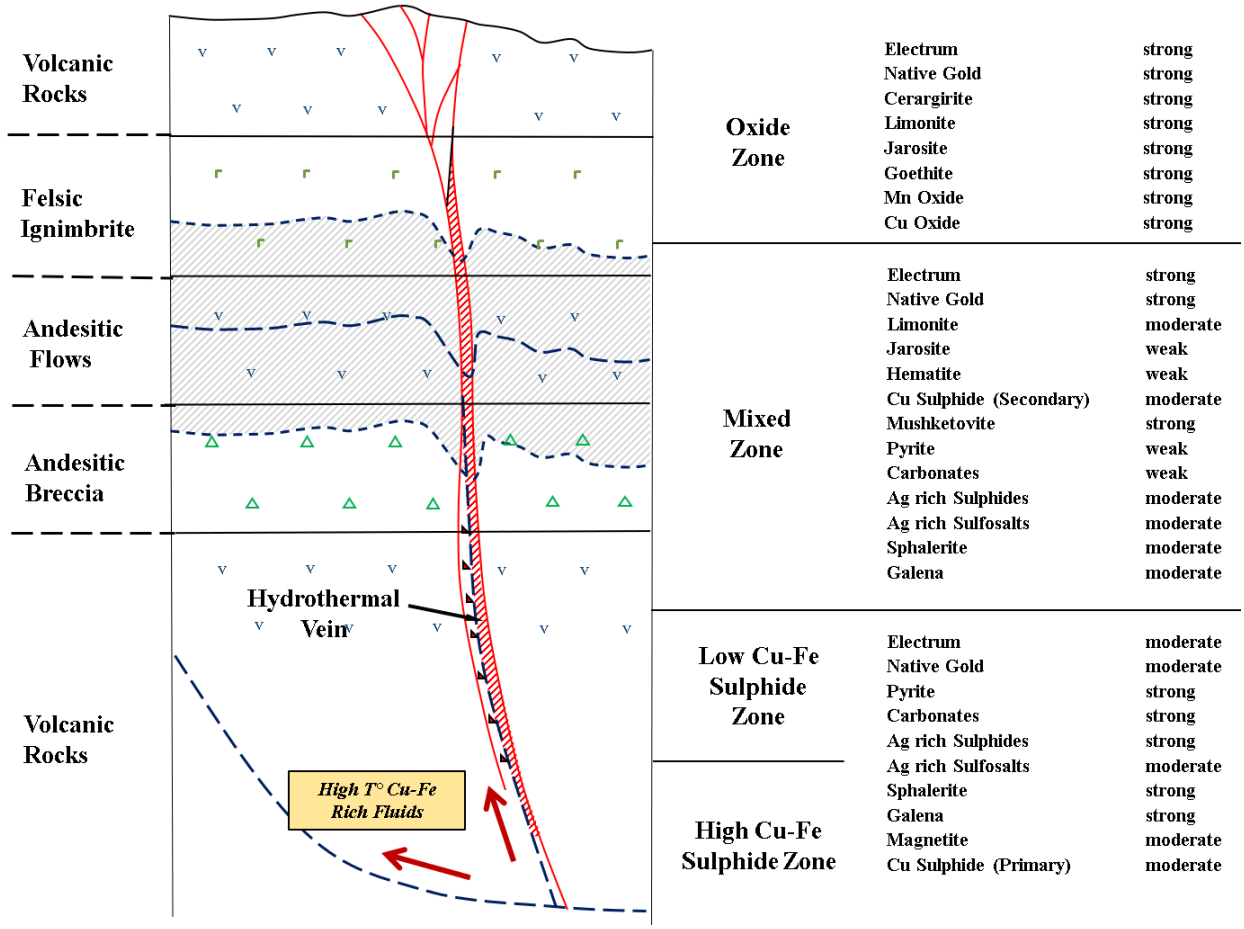

Figure 4.1.5: Schematic profile model of Alhué veins. Spatial relationship of base metals and mineralogical domains with the hydrothermal feeder, faults, and topography.

4.1.2 Mineral Processing and Process Mineralogy Alhue District

The mineral processing complex at Florida Mine is composed of two plants(Yamana Gold Inc., 2020): the concentrator-leaching plant that occupies the upper half of Figure 4.16, and the tailings treatment plant that occupies the lower half; this so-called 'tailings treatment plant' was initially for the reprocessing of historic tailings (fed by repulping and subsequent grinding), but since 2017 has been integrated with the main concentrator-leaching plant as depicted in Figure 4.1.6. Indeed, the adsorption–desorption recovery (ADR) operation now feeds into the electrowinning operation, as the barren solution is sent into the so-called tailings leach process, which itself leads into the carbon-and-pulp (CIP) operation and cycles back through the ADR. This process configuration (Figure 4.1.6) allows communal detoxification (de-cyanidation), prior to transmission into the tailings dam.

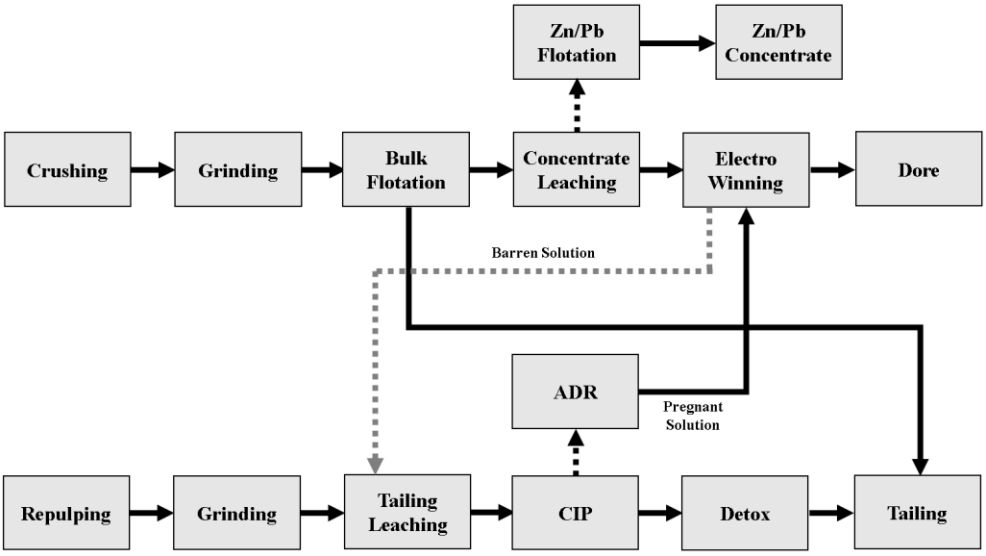

Figure 4.1.6: Simplified flowsheet of the mineral processing at the Florida Mine.

The nominal processing capacity of the concentrator-leach plant is 2400 t/day of ore, producing variable rates of dore metal and Zn-Pb concentrate (Yamana Gold Inc., 2020). The crusher is fed with three different size classes of run-of-mine ore: oversize (5–20 inches), middle size (1–4 inches), and small size (less than 1 inch); each of these streams is treated according to predetermined regimens within a series of primary, secondary, and tertiary crushing, resulting in fragments that are 100% below 0.39 inches, which form the feed stockpiles for subsequent grinding and bulk flotation. The grinding circuit is composed of three mills which can collectively exceed the nominal throughput by 25%; this provides operational flexibility to control recirculating loads, such that the bulk flotation feed has a P80 size of 120 microns. The bulk flotation consists of 15 cells, producing (1) a gold-rich concentrate that is subject to cyanidation leaching in tanks, and (2) a non-cyanided tailings stream that is send to the tailings dam. Following the concentrate leaching and subsequent electrowinning, the precious metals are precipitated as cathodic mud, which is then filtered and dried prior to smelting and final conversion into doré metal bars. Subordinately, the underflow of the concentrate-leaching thickener is filter-pressed to produce a 10% humidity cake and is subsequently fed into the zinc-lead flotation plant to produce a sulphide concentrate that is 40% Zn and 8% Pb. Moreover, the reprocessing of barren solution within the so-called tailings leaching has resulted in a 60% recovery of combined gold and silver value, which contributes to an overall recovery at the Florida Mine that exceeds 90% (Yamana Gold Inc., 2020).

4.1.3 Copper and iron minerals in cyanide solution`

Cyanide can leach different metals, with the resulting ions grouped into several categories depending on the type and strength of the bond (Mardsen & House, 2006). This interaction defines its stability in a solution, wherein iron and gold have a high affinity with the CN ion, generating a strong bond. On the other hand, copper can have different stability bond levels, from weak to medium intensity. The majority of the copper minerals are highly soluble in cyanide solution (Table 4.1.1) except for chalcopyrite, which has limited solubility (Massoud, 1997). Copper is indeed one of the major cyanide consumers because it forms various cyanocomplexes (Mardsen & House, 2006). As a result, the dissolution of copper is generally undesirable during gold and silver leaching extraction processes. This can cause higher cyanide consumption, slow the dissolution rate of gold and silver, interfere with subsequent recovery processes from the pregnant solution, and ultimately contaminate the final product. In addition, some copper minerals (e.g. chalcopyrite) are capable of removing gold from solution by reduction at the mineral surface, exhibiting reversible preg-borrowing characteristics in cyanide-deficient solutions (Mardsen & House, 2006). Chalcopyrite is the least soluble sulphide mineral that is commonly found in gold and silver deposits. Chalcocite, bornite, enargite and covellite have medium to high solubilities, and copper oxides and carbonates are all highly soluble. In addition to copper cyanide complexes, the copper sulphide minerals (e.g. chalcocite) react with cyanide to form soluble sulphide ions (S^{2-}). These ions may react with cyanide to form thiocyanate ions or form protective coatings on particle surfaces and thus hinder the cyanidation process (Mardsen & House, 2006).

Table 4.1.1: Copper mineral solubilities in 0.1% NaCN (Hedley & Tabachnick, 1958) adapted to Alhué mineralogical zones.

Mineral	Formula	Percentage of dissolved copper		Alhué Mineralogical Zones
		at 23°C	at 45°C	
Azurite	$2CuCO_3{\cdot}Cu(OH)_2$	94.5	100	**Oxide**
Chrysocolla	$Cu_2\ H_2\ Si_2O_5(OH)4$	11.8	15.7	
Malachite	$CuCO_3{\cdot}Cu(OH)_2$	90.2	100	
Chalcocite	Cu_2S	90.2	100	**Secondary Sulphide**
Covellite	CuS	--	--	
Bornite	Cu_5FeS_4	70	100	**Primary Sulphide**
Tetrahedrite	$4Cu_2S_4{\cdot}Sb_2S_3$	21.9	43.7	
Chalcopyrite	$CuFeS_2$	5.6	8.2	

On the other hand, iron-bearing sulphides that are commonly associated with gold mineralization include pyrite, marcasite, and pyrrhotite. Weathering and oxygen action can result in the formation of different iron oxides, hematite and jarosite being the most common. Oxidized iron minerals, such as hematite, magnetite and goethite, as well as the Fe-rich carbonate mineral siderite, are considered refractory to a cyanide solution. However, complex iron carbonates such as ankerite decompose to some extent in weakly alkaline (<10 pH) cyanide solutions, and form ferrocyanides Mardsen & House, 2006). Therefore, hematite, magnetite, goethite, siderite, and iron silicates are virtually insoluble in alkaline cyanide solutions Mardsen & House, 2006). Though some Fe-rich and other complex carbonates decompose in low-alkalinity solutions, they are mostly unreactive at the higher pH values usually applied for leaching (Hedley & Tabachnick, 1958).

Iron sulphides such as marcasite and pyrrhotite are more reactive than pyrite in a cyanide solution. Though pyrite is the most common sulphide mineral occurring in gold ore, it thankfully interferes less with the cyanidation process (Haque, 1992). Marcasite and pyrrhotite will react with cyanide and form iron cyano-complexes, soluble sulphide ions (S^{2-}) and thiocyanate ions as major undesirable products. It has also been reported that ferrocyanide ions have an inhibiting effect on gold cyanidation (Nicol, 1980). This can be explained by the additional consumption of oxygen and cyanide required for the formation of ferrocyanide ions. Moreover, soluble sulphide ions at very low concentrations can retard gold dissolution almost completely (Weichselbaum et al.,1989). Increased cyanide (CN) consumption related to ores containing elevated concentrations of copper and iron minerals has been a primary concern for process engineers at the Florida Mine in recent years. This has led to a restructuring of geometallurgical units to better predict consumption rates through an assessment of incoming ore feed attributes. These new geometallurgical units are (1) in alignment with the four geological domains illustrated in Figure 5, namely the Oxide, Mixed, Low Cu Sulphide and High Cu Sulphide domains, and (2) are further grouped by a combination of metallurgical behaviour, field-observed copper and iron mineralogy coupled with interpreted redox states and process impurities including CuS and FeS, all of which relate to sodium cyanide consumption. In practice at the Florida plant, it has been especially challenging to optimize plant operations when feeds are coming in simultaneously from two different geometallurgical units. Such circumstances are confronted, for example, as the Flor Vein intersects with the *Del Medio* Fault (Figure 4.1.3), causing discontinuities in the redox state and an extreme increase in cyanide

consumption. This has caused a rethinking of the approach to stockpile management, so that the plant can be fed only by blends that are well understood by the operators. Following the approach of Navarra et al. (Navarra, 2019), these stabilized feed blends are directly related to system-wide operational modes.

4.1.4 Data-Driven Simulation of the Minera Florida Cyanidation Process

For aging gold mines in particular, it often happens the process continues to run according to longstanding guidelines and settings, even when the nature of the incoming feed has changed; for the case of Minera Florida this has resulted in increases in cyanide consumption as increasing amounts of certain copper sulphides are entering the feed (Órdenes, 2021), as described below (Figure 4.1.7).

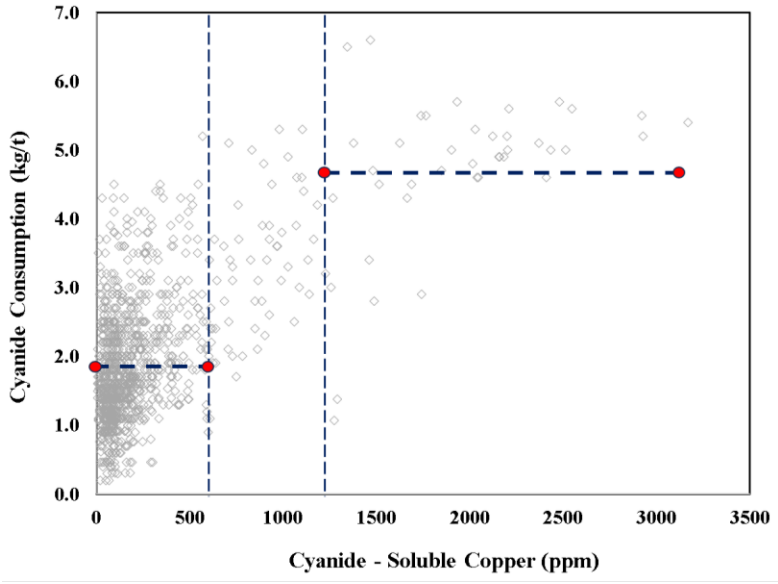

Figure 4.1.7: Summative data from Minera Florida from June 2020 to February 2021, regarding the processing of ores from the Alhué district, demonstrating that spikes in cyanide consumption (expressed in kg of cyanide per tonne of feed) are associated with higher quantities of cyanide-soluble copper carried by the feed. "Cyanide-soluble copper" includes copper from chalcocite/digenite, covellite, and bornite, but not chalcopyrite and tetrahedrite/tennantite.

The status quo tends to be maintained within aging mines because any substantial modification in processing strategy is perceived as risky, unless it is supported by metallurgical studies and potentially pilot tests, to obtain the necessary data to parametrize operational changes and possibly to justify equipment upgrades. Furthermore, these metallurgical studies require a budget (often tens of thousands of dollars) and a time-commitment of personnel, e.g. a special projects team

and/or outside consultants. Gaining support from management for experimentation and piloting can be difficult, unless we can demonstrate that we would know what to do with the data once we had it; this is a "chicken-or-the-egg" problem.

In the case of Alhue mine, how was showed on Figure 4.1.5, it had been observed that certain copper sulphides within the feeds, especially bornite Cu_5FeS_4, chalcocite Cu_2S and tetrahedrite $4Cu_2S4{\cdot}Sb_2S_3$, cause spikes in cyanide consumption (Ordenes, 2021). The faulting at Minera Florida (and presumably in similar mines) is such that within a single drift, there can be tens of meters of low-cyanide-consuming (LCC) ore, interrupted by a few meters of high-cyanide-consuming (HCC) ore, followed by a long extent of LCC ore. The LCC and HCC ores can have dramatically different visible appearance along the drift walls, and were therefore easily linked to the downstream requirement of increased cyanide. Figure 4.1.7 is a plot of operational data obtained from June 2020 to February 2021, showing the effect of the aforementioned cyanide-soluble copper (a.k.a. "cyanicidal copper"). A linear or quadratic regression is not forthcoming due to the corrective actions of expert operators and metallurgists, with R^2 values of 42.51% and 43.65% respectively. However, a comparative Student T test (see Devone, 2011 or similar) of the 929 points below 600 ppm cyanide-soluble copper and the 41 points above 1200 ppm gives over 99.99% statistical confidence that cyanide-soluble copper minerals are associated to spikes in cyanide requirement; indeed the cyanide consumption can be roughly triple on a per-tonne of feed basis. Essentially, beyond ~600 ppm of cyanide-soluble copper, the system is overwhelmed, causing surges cyanide requirements, despite the metallurgical operators' best efforts.

The analysis illustrated by Figure 4.1.7 merely confirms what was being observed by geologists and operators, but is somewhat crude, since it does not detail the dynamic responses of the operators, and therefore does not adequately support the integration/standardization of these responses. However, it motivated the quantitative approach of Órdenes et al. (2021) that could indeed represent dynamic operational responses, which itself was an adaptation of the more general DES/DRS framework of Navarra et al. (2019). Yet although the framework successfully illustrated the spiking of cyanide consumption, and was thus generally well-received, management questioned the "parametrizibility" of the model. From their perspective, the framework had only qualitatively captured the dynamical aspects of their operational challenge, and they had hoped for a statistical treatment that would be "in the same spirit" as the analysis of Figure 4.1.7, including

hypothesis testing. The DES/DRS framework is ultimately a composition of probabilistic distributions, as described in Section 3.2; the management would question how well these distributions could be (optimally) parametrized to best represent the actual real data from their process. These interactions have been a confluence of interdisciplinary expertise, which established the following consensus:

- There are numerous process variables that ideally should be represented within the framework as probability distributions, rather than fixed deterministic values.
- Process data must be used to determine which standard distributions are most representative, and what their parameter values should be.
- In the context of Minera Florida, the process variable that is currently perceived to be the most important is the head grade of the incoming ore, measured in gold-equivalent ounces per ton.

The methods presented in Section 3.2.1 are of general interest for system simulation (Altiok, 2017), and are applicable to the entire set of process variables identified by Minera Florida. The specific list is not explicitly given here, in the interest of confidentiality, but contains typical measures such as base metal grades and acid potentials, which are a common concern throughout the gold industry (Dominy et al., 2001; Ferguson et al., 1988). To balance the interests of generality and confidentiality, the sample computations of Section 4.1.7 consider the parametrization only of head grade distributions, and similar approaches can be used for other variables.

The DES/DRS framework of Navarra et al. (2019) was successfully adapted to represent spikes in cyanide consumption at Minera Florida (Ordenes et al., 2021), considering the following threshold crossing events:

- Stockout of HCC ore;
- Stockout of LCC ore;
- Reestablishment of target level for total stockpile (LCC + HCC);
- Transition to the next geological parcel.

As will be described in Section 3.2, stockouts trigger contingency processing modes. The notion of a "geological parcel" is described in (Peña-Graf, et al. 2022) and provides a basic

representation of geostatistical variation; each parcel contains a balance of HCC and LCC ore, which is the result of RNG. When detailed geospatial data (i.e., drill core samples) are available, the balance of HCC/LCC can be the result of a sequential Gaussian simulation (Pearson, 1900), which is the subject of ongoing work (Bai & Tahmasebi, 2021). For the current study, it is sufficient to consider:

- In the event that the parcel, *k - 1*, is completely excavated, a following parcel, k, is generated that will contain the next m_k tonnes of ore to be excavated;
- There is a 70% chance that parcel *k* is within the same facies as *k - 1*; if so, then the weight fraction of LCC in parcel *k*, denoted as $\boldsymbol{w_k^{LCC}}$, is generated according to a Gaussian distribution centered at $\boldsymbol{w_{k-1}^{LCC}}$, with the small standard deviation, $\sigma_{\text{interfacies}}$;
- Otherwise, if parcel *k* is in a new facies, then $\boldsymbol{w_k^{LCC}}$ is generated independently of the previous parcel, according to a Gaussian distribution centered on the orebody average and with a comparatively large standard deviation $\sigma_{\text{orebody}} > \sigma_{\text{interfacies}}$.

This basic representation considers only two ore classes (also known as geometallurgical units), such that the weight fraction of HCC is given by $w_k^{\text{HCC}} = 1 - w_k^{LCC}$. The DES/DRS framework can consider a higher number of ore classes, depending on the context, but these two classes have been sufficient to represent the Minera Florida context. Moreover, the mass mk of parcel k is generated according to a uniform distribution; other distributions have been tested for this purpose, but they have no significant effect.

Following the approaches for the DES of manufacturing systems (Altiok & Melamed, 2007), the parameterization of process-variable distributions is an extension of standard exploratory data analysis (EDA). Depending on the context, standard EDA usually includes a listing of descriptive statistics such as mean, standard deviation, extreme observations (maxima and minima), and quartile data, as well as histograms and possibly other graphical constructions (Komorowski et al., 2016). The quartile data are often used to establish criteria for outlier filtering. Figure 4 illustrates the use of maximum likelihood estimation (MLE) and goodness-of-fit statistics (GOF) in order to enhance a DES/DRS model; this type of detailing can be situated within the improvement cycle of Figure 2 if we consider that a data-driven probability distribution of a process variable is itself a submodel that replaces the deterministic representation. The conversations that followed the first

collaboration with Minera Florida (Ordenes et al., 2021) have emphasized the practical relevance of the data-driven parametrization of probabilistic distributions within gold extractive metallurgy (and ostensibly in other areas of mining and metallurgy). Without developing a convincing connection to the available plant data, the simulations may be rightly criticized for lacking a connection to production metrics, even if the most critical phenomena are well represented. Yet there seems to be an underrepresentation of journal articles detailing the contextualized application of MLE and GOF techniques within extractive metallurgical simulations. With the exception of the current work, we have failed to find such a paper.

4.1.4.1 Exploratory Data Analysis and Fitting of Gold Head Grade Distributions

Based on its current mineral processes flow sheet, Minera Florida had previously ran a detailed geometallurgical characterization program to link the vein mineralogy to the metallurgical behavior of the ore fed into the cyanidation process. This sampling campaign included 1214 ore samples from different workfaces, classified in situ and tested at the on-site metallurgical laboratory. The samples were analyzed by a shaker test to determine a range of process parameters and related cyanide consumption (Table 4.1.2).

Table 4.1.2: Summary of shaker test analytical conditions.

Parameters	Quantity
Ore Mass (g)	30
Granulometry (µm)	100% -200#
Solution Volume (ml)	60.00
Solid Percentage (%)	33.00
NaCN Concentration (g/l)	10.00
Pulp pH	11.00
Head Grade Assay	Au, Ag, Cu, *Fe
Leached Solution Assay	Cu, Fe, Free CN, *Au, *Ag
Tail Grade Assay	*Au, *Ag

From the information collected during the sampling campaign and the analytical results from the tested samples, a new geometallurgical ore classification was defined. This new ore classification is (1) in alignment with the four geological domains presented by Órdenes et al. (2021), namely the oxide, mixed, low-Cu sulfide, and high-Cu sulfide domains, and (2) are further grouped by a combination of metallurgical behavior, field observed copper, and iron mineralogy, coupled with interpreted redox states and process impurities, including CuS and FeS, all of which

relate to sodium cyanide consumption [2,11]. The presence of processed impurities (such as copper, iron, and sulfur) within the different orebodies exploited by Minera Florida, has a high potential of generating undesired reactions including the formation of thiocyanate and the dissolution of the transition metals, Cu, Fe, and Zn. Consequently, this new mineralogical scenario can inflict extra operational costs and diminished profits resulting from high levels of cyanide consumption (Hedley & Tabachnick, 1958; Habashi,1967). Following from the understanding at Minera Florida and previously published work (Órdenes, 2021), the head grades from the tested samples have been separated into two geometallurgical units; these are high-cyanide-consuming (HCC) sulphides and low-cyanide-consuming (LCC) sulphides. This is an enhancement over the previously published work which did consider the two units but did not consider the head grade distribution data. The basic descriptive statistics for the HCC and LCC geometallurgical units are given in Table 4.1.3, as part of the initial exploratory data analysis (EDA). The samples describe the ore that is forecast over the medium term, originating from sampling campaigns that were extended from production tunnels.

Table 4.1.3: Cyanide consumption per geometallurgical unit.

Variable	Statistics	High CN Consuming Sulphides	Low CN Consuming Sulphides
Cyanide soluble copper (ppm)	**N° Samples**	739	308
	Mean	310.26	176.22
	Standard Deviation	456.80	218.73
	Minimum	6.50	8.20
	Q1	80.60	65.05
	Q2	160.50	105.25
	Q3	319.65	204.53
	Maximum	3169.50	2480.20
Cyanide consumption (kg/t)	**N° Samples**	739	308
	Mean	2.24	1.75
	Standard Deviation	1.21	0.90
	Minimum	0.31	0.20
	Q1	1.40	1.10
	Q2	1.90	1.60
	Q3	2.80	2.20
	Maximum	7.40	5.70

The EDA was then extended to incorporate the gold head grade. A critical aspect of data analytics is handling the anomalous data adequately (Komorowski et al., 2016); this takes particular relevance when commodities grades are assessed, especially in gold (Filiben, 2003). Geostatisticians have proposed and used different techniques to mitigate the impact of high-grade data on mineral resource estimation; hence the same procedures can be utilized in simulations to manage head grades. Various methods generally involve some form of capping and/or high-grade influence restrictions to mitigate the disproportionate influence of true outlier values on the contained metal in a resource.

High values may arise because of sampling errors or reflect distinct geological sub-environments or domains within a mineral deposit (Kehmeier, 2022). Efforts must be directed to examining these high values and their geological context to distinguish errors from "real" high grades, investigate their characteristics, and how they relate to the mineral inventory estimates (Kehmeier, 2022). In calculating the descriptive statistics for gold head grade, a data cleansing procedure was applied to the Minera Florida data given by:

$$Lower\ limit = Q1 - 1.5 \cdot (Q3 - Q1) \tag{4.1.1}$$

$$Upper\ limit = Q3 + 1.5 \cdot (Q3 - Q1) \tag{4.1.2}$$

These criteria have resulted in the elimination of 49 outliers from High Cyanide Consuming (HCC) Sulphides and 24 outliers from Low Cyanide Consuming (LCC) Sulphides, entirely from the upper limit in both cases. The summary of the preprocessed statistics for the gold head grade of the geometallurgical sample set is summarized in Table 4.1.4. The data in this table, and throughout the remainder of the paper, were computed subsequent to the aforementioned elimination of outliers (Equation4.1.2).

Table 4.1.4: Gold head grade statistics by geometallurgical unit.

Variable	Statistics	High CN Consuming Sulphides	Low CN Consuming Sulphides
Gold Head Grade (g/t)	**N° Samples**	673	278
	Mean	5.07	3.56
	Standard Deviation	2.92	1.88
	Kurtosis	0.29	0.46
	Skewness	0.99	1.00
	Minimum	0.24	0.18
	Q1	2.81	2.11
	Q2	4.29	3.22
	Q3	6.61	4.55
	Maximum	14.39	9.04

Gold grades in vein-style gold deposits are highly variable, are often complex and erratic, but commonly show skewed positive grade distribution (Dominy et al., 2001). Their complexity is typically reflected in two components: (1) low-grade continuity and (2) diversity of ore trends. Gold grades are commonly related to variably sized ore shoots of high-grade mineralization surrounded by lower grade areas; yet ore shoots may account for a relatively small proportion of the total mineralization (Dominy et al., 2001). For the Minera Florida dataset, the histogram of gold-grades for both geometallurgical units shows a positive skewness (Sk >0.5, Table 3) and low kurtosis (Table 4.1.4), and a platykurtic shape (Figure 4.1.8). The histograms for both geometallurgical units show high variability, and high-grade tail.

Table 4.1.5 lists the candidate distributions in terms of their goodness-of-fit metrics for several candidate distributions, indicating that the Log-Normal could be an acceptable choice for representing the gold head grades, noting that it ranked highly in χ^2 and KS, third and fourth, respectively, and was the top-ranked distribution in both cases for AD; these results were obtained using the Easy Fit software developed by Math Wave Technologies.

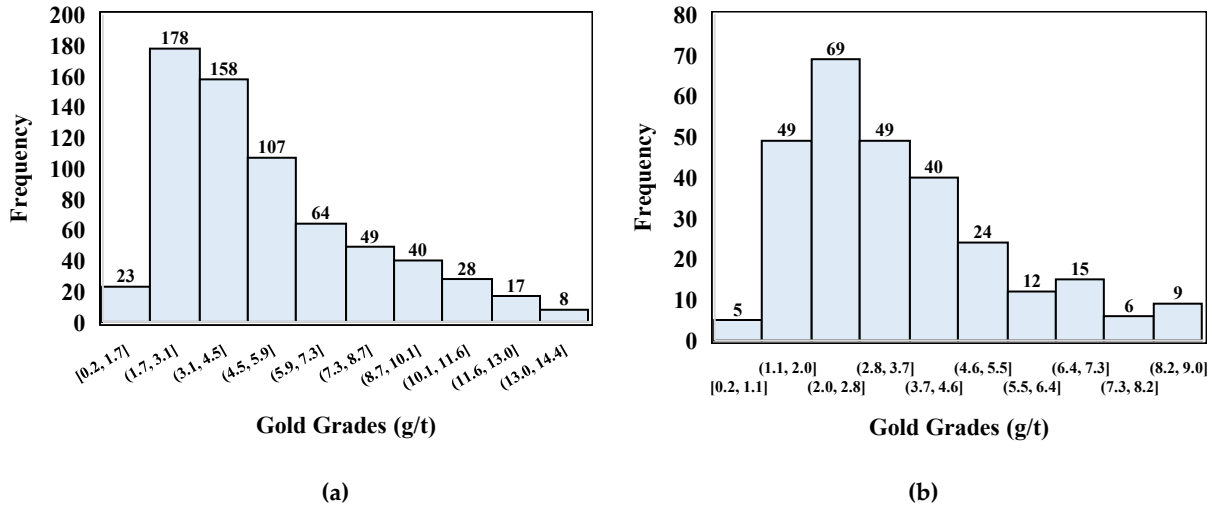

Figure 4.1.8: Gold grades histograms for (a) the HCC geometallurgical unit, and (b) the LCC geometallurgical unit.

Looking at the HCC data, a consideration may be given to the Pearson 5 distribution, for having ranked well in terms of χ^2, but its ranking was very low in KS and AD; perhaps a better case can be made for the Fatigue Life distribution (a.k.a. Birnbaum-Saunders distribution), which surpassed the Log-Normal for χ^2 and KS for HCC, although it did not perform especially well in KS and AD for LCC and is a somewhat obscure; to be fair, the Fatigue Life distribution is represented to model equipment failure times, and a flash occurrence of cyanide-consuming minerals is (debatably) like a spontaneous equipment breakdown.

Nonetheless, the case for Log-Normal is clearly the strongest candidate for HCC. Although the Inverse Gaussian and General Extreme Value distributions could be considered for LCC, these distributions are comparatively difficult to since they are not commonly used, and the more common Log-Normal was the highest ranked in AD. For general interest, the poorly ranked Gaussian distribution was included in Table 4.1.5.

The choice of the Log-Normal is further corroborated by the χ^2 and Kolmogorov-Smirnov GOF hypothesis tests, as summarized in Table 4.1.5. However, in the case of the HCC geometallurgical unit, the null hypothesis that the data is characterized by Log-Normal is rejected according to the Anderson-Darling (AD) test at the 95% significance but is nonetheless accepted by the χ^2 and Kolmogorov-Smirnov tests. As noted in Section 3.2.2, the AD emphasizes (and possibly over-penalizes) the extreme values; even after the preprocessing described by Equations

4.1.1 and 4.1.2, the HCC data includes unusually high grades exceeding 13 g/t, but this corresponds to only 1.2% of the samples.

Table 4.1.5: Ranking of distributions in accordance with GOF metrics.

High Cyanide Consuming Sulphides						
	Chi-Square		Kolmogorov-Smirnov		Anderson-Darling	
Distribution	**Statistics**	**Rank**	**Statistics**	**Rank**	**Statistics**	**Rank**
Pearson 5	8.15	1	0.050	22	4.04	25
Fatigue Life	12.09	2	0.030	3	1.46	2
Log-Normal	12.41	3	0.032	4	1.41	1
Pearson 5 (3P)	14.19	4	0.059	28	9.84	33
Dagum	14.94	5	0.040	8	2.54	10
Dagum (4P)	18.17	6	0.043	14	2.56	11
Log-Logistic (3P)	19.14	7	0.042	9	2.71	12
Log-Logistic	19.77	8	0.048	18	3.06	14
Fatigue Life (3P)	20.86	9	0.040	7	1.97	4
Gaussian	170.21	42	0.116	40	18.89	38
Low Cyanide Consuming Sulphides						
	Chi-Square		Kolmogorov-Smirnov		Anderson-Darling	
Distribution	**Statistics**	**Rank**	**Statistics**	**Rank**	**Statistics**	**Rank**
Pearson 5 (3P)	7.64	1	0.053	18	3.67	30
Inv. Gaussian	7.93	2	0.044	9	0.98	11
Fatigue Life	9.40	3	0.065	25	1.32	17
Frechet	10.52	4	0.080	30	4.65	34
Pearson 5	11.23	5	0.070	26	3.12	29
Log-Normal	11.80	6	0.044	8	0.62	1
Gamma	17.24	7	0.055	19	1.28	16
Gen. Extreme Value	17.37	8	0.041	1	0.83	2
Log-Logistic	17.44	9	0.045	10	0.84	3
Gaussian	70.27	42	0.125	39	7.10	36

But the rejection of the top-ranked AD distribution (Table 4.1.5) when subjected to the AD hypothesis (Table 4.1.6) is moot, since the actual head grades that will be received by the Florida plant will follow a distribution that is more complex than the Log-Normal and any other commonly available distribution; it depends on both the geospatial distribution of the minerals as well as the excavation sequence. This will be further discussed in Section 4.1.8 Interestingly, the Log-Normal is accepted in the case LCC for all three GOF tests.

Table 4.1.6: Summary of goodness of fit tests for the Log-Normal, α = 0.05.

High CN Consuming Sulphides	Critical Value	Observed Value	Null Hypothesis
Chi-Squared (Degrees of Freedom= 8)	15.51	12.41	H_0 is accepted for Log-Normal Distribution
Kolmogorov – Smirnov	0.034	0.031	H_0 is accepted for Log-Normal Distribution
Anderson-Darling	0.87	1.40	*H_0 is rejected for Log-Normal Distribution*
Low CN Consuming Sulphides	**Critical Value**	**Observed Value**	**Null Hypothesis**
Chi-Squared (Degrees of Freedom= 7)	14.07	11.80	H_0 is accepted for Log-Normal Distribution
Kolmogorov – Smirnov	0.053	0.045	H_0 is accepted for Log-Normal Distribution
Anderson-Darling	0.87	0.61	H_0 is accepted for Log-Normal Distribution

The GOF computations of Tables 4.1.5 and 4.1.6 considered the MLE parametrization of the solutions, computed from the cleansed data described by Table 4.1.4. Considering that the Log-Normal distribution has been selected for geometallurgical units, the corresponding parameter values are given in Table 4.1.7. As been described in this Section, the gold head grades are best represented by a log-normal distribution, for which the MLE estimation formulas (also known as "estimators") have been found to be:

$$\hat{\mu}(\boldsymbol{x}) = \frac{1}{n}\sum_{i=1}^{n} \ln x_i \tag{4.1.3}$$

$$\widehat{\sigma^2}(\boldsymbol{x}) = \frac{1}{n}\sum_{i=1}^{n} (\ln x_i - [\hat{\mu}(\boldsymbol{x})])^2 \tag{4.1.4}$$

Both expressed as a function of the observed measurement values, x, to emphasize that the parametrization is data-driven. Furthermore, it is data-driven in a dependable (rigorous) sense, i.e., the sense of maximum likeliness. Alternatively, for example, log-normal could be erroneously fitted with the logarithm of the mean, rather than the mean of the logarithm; the MLE formulation resolves these potential pitfalls. These results were provided by Easy Fit, and were verified by Equations 4.1.3 and 4.1.4 prior to being programmed into the discrete rate simulations that will now be described.

Table 4.1.7: Maximum likelihood estimation results

Maximum Likelihood Estimation (MLE)	Gold Head Grade Estimator HCC	Gold HeadGrade Estimator LCC
$\widehat{\boldsymbol{\mu}}$	4.29	3.09
$\widehat{\boldsymbol{\sigma}}^2$	1.42	1.35

4.1.5 Discrete Rate Simulation of the Alhue Mine Cyanidation Process

The mineralogical variation confronted by mines within the Alhué district may be managed by alternating between modes of operation. These modes provide an integrated response to changes in feed mineralogy and other operational conditions within the mineral value chain. Processing plants are generally designed to maximize profits while respecting technological limitations, environmental norms, and tactical constraints that align operational objectives with long-term strategic goals. The decision to alternate between modes depends on current and forecasted stockpile levels. Interestingly, the selection of thresholds that would trigger a mode change is related to the classic reorder-quantity (RQ) problem from inventory theory (Winston and Goldberg, 2004), as described in (Navarra, 2019). Most importantly, operational modes are conceived with respect to system-wide performance rather than local metrics that only consider isolated unit operations.

Even within relatively short timeframes, it is uncertain whether the decreasing feedstocks will be replenished by the incoming mined material; unexpected changes in ore feed characteristics can occur abruptly and lead to shortages of a particular ore type from a particular geometallurgical unit. For an underground mine, this variation in stockpile levels is typically intensified due to a variety of factors, including: 1) a large number of concurrent active workfaces (ore type variability); 2) ore grade-driven mine planning that does not consider geometallurgical inputs; and 3) the uncertainty caused by complex extraction methods, which rely on the coordination of many variables (e.g. ventilation, drainage, equipment availability) to meet planned production.

Specifically, at the Alhue Mine, the most significant risk to the metallurgical process is the variability in cyanide consumption related to a production imbalance from sectors with varying concentrations of impurities. The risk of stockout of a feed class is mitigated through the alternation of operational modes; that is, when a stockpile falls below a critical level, the system changes to a different (possibly less productive) mode so that the stockpile may be replenished,

prior to resuming the original mode. The approach of Navarra et al. (Sepúlveda, 2004) is to use discrete event simulation (DES) as a dynamic representation of feed stockpiles that are continually fed by mining operations, while also being continually drawn upon by the plant. The DES framework is capable of simulating extended operating periods in order to optimize the trigger points that would induce a change in operational mode, as described in the following section. Within the current context, the objective of the framework is to maximize throughput while avoiding spikes in cyanide consumption. This is in agreement with the experiences at the Florida Mine, in which a moderate decrease in throughput can be justified, if it reduces the risk of surges in cyanide consumption.

Moreover, the current sample computations consider geometallurgical units characterized as "Sulphide with high CN consumption" and "Sulphide with low CN consumption", which shall be referred to as ores 1 and 2, respectively. These tend be observed within the deeper intrusive-influenced zones of the Alhué district (Figure 4.1.5), however the actual classifications of Minera Florida consider additional attributes including the prevalence of the different copper-bearing minerals listed in Table 4.1.1.

For the deterministic analysis of operational modes, Navarra et al. developed the following equation to describe the expected mass balance (Navarra, 2019). It considers two configuration of operation, A and B, and computes the anticipated portion of time that the system should spend in under each of the configuration,

$$\left(\frac{t_A}{t_B}\right) = \left(\frac{w_{2B}\, w_{1D} - w_{1B}\, w_{2D}}{-w_{2A}\, w_{1D} + w_{1A}\, w_{2D}}\right)\left(\frac{r_B}{r_A}\right) \tag{4.1.1}$$

in which,

t_A = duration of time devoted to mode A

t_B = duration of time devoted to mode B

r_A = ore processing rate under mode A

r_B = ore processing rate under mode B

w_{1A} = weight fraction of high CN (Ore 1) consuming ore within the feed of mode A

w_{2A} = weight fraction of low CN (Ore 2) consuming ore within the feed of mode A

w_{1B} = weight fraction of high CN (Ore 1) consuming ore within the feed of mode B

w_{2B} = weight fraction of low CN (Ore 2) consuming ore within the feed of mode B

w_{1D} = weight fraction of low CN (Ore 1) consuming ore that is expected from the deposit

w_{2D} = weight fraction of high CN (Ore 2) consuming ore that is expected from the deposit

Indeed, the alternation between configuration A and B provides the mining system with a degree of freedom to accommodate the balance of ore that is coming from deposit, i.e. the deposit (w_{1D}, w_{2D}) is balanced by a combination of (w_{1A}, w_{2A}) and (w_{1B}, w_{2B}).

The overall throughput is determined by time-averaging,

$$r = \left(\frac{t_A}{t_A + t_B}\right) r_A + \left(\frac{t_B}{t_A + t_B}\right) r_B$$
$$= \left(\frac{\left(\frac{t_A}{t_B}\right)}{\left(\frac{t_A}{t_B}\right) + 1}\right) r_A + \left(\frac{1}{\left(\frac{t_A}{t_B}\right) + 1}\right) r_B \qquad (4.1.2)$$

which, upon substitution with Equation 1, can be expressed as

$$r = \left(\frac{w_{1A}\, w_{2B} - w_{2A}\, w_{1B}}{\left(w_{2B}\, \left(\frac{r_B}{r_A}\right) - w_{2A}\right) w_{1D} - \left(w_{1B}\, \left(\frac{r_B}{r_A}\right) - w_{1A}\right) w_{2D}}\right) r_B \qquad (4.1.3)$$

Table 4.1.8 contains data that is typical of the Florida Mine in confronting the boundaries between typical high and low CN consuming ores, which we take to be ore types 1 and 2, respectively. Based on these parameters (Table 4.1.1), Equation 4.1.2 gives tA/tB = 1.8 from which it can be determined that the system will (ideally) be in Mode A for 64% of the time, and Mode B for 36% of the time. Moreover, Equation 4.1.3 indicates an average throughput of 2.6 kt/d.

The alternating configuration provide an integrated response to changes in feed mineralogy and other operational conditions within the mineral value chain. Processing plants are generally designed to maximize profits while respecting technological limitations, environmental norms, and tactical constraints that align operational objectives with long-term strategic goals. For an underground mine, the variation in stockpile levels is typically intensified due to a variety of factors, including: 1) a large number of concurrent active workfaces (ore type variability); 2) ore grade-driven mine planning that does not consider geometallurgical inputs; and 3) the uncertainty caused by complex extraction methods, which rely on the coordination of many variables (e.g. ventilation, drainage, equipment availability) to meet planned production (Órdenes et al.,2021).

All of these factors add to the variability of feeds being received by the Minera Florida cyanidation plant district, which has motivated the adaptation of a DES/DRS to improve decision-making and evaluate the effects of the stockpile management in the plant performance.

To achieve the best performance of the mining system under study, alternating configurations and modes are represented within the current framework to help maintain consistency in ore feeding. The selection of a configuration depends on the forecasted timing of stockouts in HCC and LCC given their requirement for feed blending. In the case of Alhué ore, the operational policies were designed to maximize tonnage and stabilize cyanide consumption, within the regular mode of configuration A (Table 4.1.8). This mode (called "A-regular") brings the plant to its maximum productive capacity while minimizing the cyanide consumption. Nonetheless, if at the end of a production campaign the LCC stockpile is below a predetermined threshold, the plant is then reconfigured into configuration B, whose regular mode (called "B-regular") is designed to rebuild the LCC stockpile while still avoiding the risks of spikes in cyanide consumption. If a stockout occurs during a production campaign, a contingency mode is applied in which only the available type of ore is consumed to allow the depleted ore type to accumulate again before returning to the regular configuration. Thus, the mode changes from A-regular to A-contingency if there is an LCC stockout during a campaign of configuration A; similarly, the mode changes from B-regular to B-contingency if there is a HCC stockout during a campaign of configuration B.

For the current set of simulations, A-contingency consumes only HCC ore which allows the LCC stockpile to rebuild as quickly as possible, while B-contingency consumes only LCC ore which allows the HCC stockpile to rebuild (Table 7). Because contingency modes are less productive than the regular configuration, the duration of contingency segments has been set at 1 day, causing the plant to alternate between regular and contingency until the next planned shutdown. In reality, the contingency durations can be longer than a day depending on how much longer is remaining in the current production campaign. (Some discussions have been made regarding how to better represent the contingency durations, to capture the actual operational decisions that are taken, but an improved sub-model has yet to be developed in this regard).

Table 4.1.8: Description of operational configuration in relation to possible deposit forecast, including gold grades.

Parameters	Deposit	Configuration A			Configuration B		
	Average	Regular	Contingency	Mine Surging	Regular	Contingency	Mine Surging
Throughput (kt Ore/day)	-	2.7	2.3	-	2.4	1.2	-
HCC -Ore 1 in feed (%)	60	55	100	55	70	0	70
LCC -Ore 2 in feed (%)	40	45	0	45	30	100	30
Cyanide Consumption (kg/t)	2.04	2.02	2.24	2.02	2.09	1.75	2.09
Gold Head Grade (g/t)	3.81	3.75	4.29	3.09	3.93	3.09	4.29

In practice, attaining a throughput of 2.6 kt/day would require stockpiles that act as a buffer against geological variation, and to maintain stable feeds, especially avoiding feed shortages. Intuitively, larger stockpiles provide greater protection against the risk of stockout. However, larger stockpiles also require larger storage pads and handling equipment, as well as increased operating costs to manage the lifting and moving of material (Wilson, 2021). Furthermore, a deterministic analysis cannot determine the tradeoff between stockpile sizes and the risk of shortages of the different ore types.

From the data in Table 4.1.8, it can be observed that Mode A draws upon the low CN consuming feed (Ore 2) at a faster rate than is replenished by the deposit on average (i.e. 45% > 40%). In case there is a stockout of Ore 2 while the system is configured for Mode A, then a contingency mode is applied. Specifically, the system runs with only the high CN consuming ore (Ore 1), which allows the Ore 2 to be replenished, before reverting to the regular balance of 45% Ore 1 and 55% Ore 2. However, the contingency mode can only process 2.4 kt/day which equates to 85% of the regular mode capacity and causes an undesirable 30% spike in per-ton cyanide consumption. Conversely, Mode B presents a risk of stockout of the high CN consuming ore, which coincides with a 30% decrease in cyanide consumption; however, the throughput is reduced to 50% so as not to “waste” the low CN consuming ore.

The data in Table 4.1.8 demonstrate the conflicting objectives of maintaining a high throughput (close to 2.7 kt/day), while mitigating the risk of cyanide consumption spikes. Although Mode A is more productive under regular operation, it presents risks of significant spikes in cyanide

consumption in case of Ore 2 shortages. Ideally, with sufficiently large and appropriately managed stockpiles, the contingency configuration would never be applied, and the deterministically balanced value of 2.7 kt/day can be attained. Indeed, the tradeoff between the two objectives is more pronounced with smaller stockpile levels, as demonstrated in the following section, and becomes increasingly sensitive to the triggering condition of Mode B.

4.1.6 DES Computations

The main mine, as well as other mines in the Alhué district, must consider the possibility of expanding into new areas that have greater mineralogical variability, and which are increasingly dominated by ores with high contents of cyanicidal impurities (Matthews,2018; Massoud, 1997), particularly copper. Thus, the current computations consider the low cyanide consuming ore (Ore 2) to be in shorter supply. The current framework considers a forecasted average of 40% type 2, and there would in fact be variation surrounding this average, hence the need to manage stockpiles and alternate between operating modes, as described in the previous section. Over a longer timeframe, as new depths are reached, the portion of Ore 2 may continue to decrease, as suggested by Figure 4.1.5, causing Configuration B to be increasingly favored over Mode A. For demonstrative purposes, the current simulations consider a sufficiently short timeframe such that the average of 40% Ore 2 is regarded as stationary (although it would be possible to test different values, e.g. 35%, 30%, etc., or to implement a declining trend). In particular the 40% average should result in a 2.6 kt/day throughput as predicted by Equation 4.1.3, but only if the stockpile levels are sufficiently high to absorb the geological variation, and if there is an appropriately tuned trigger point to decide when to apply Mode B.

In adapting the DES framework of Navarra et al. (Navarra et al., 2019), geological variation is represented as follows:

At any moment in time, the stockpiles of Ore 1 and Ore 2 are being fed from rockfaces that are collectively called a “parcel”.

Within each parcel, a fixed portion of the ore is Ore 1, and the remaining ore is Ore 2.

Each parcel contains a total of between 10 and 40 kt of ore, following a uniform distribution.

When the excavation of a parcel is completed, a subsequent parcel is randomly generated, considering a 40% chance that the new parcel is a continuation of the same lithofacies and a 40% chance that the parcel is of a new lithofacies.

If the new parcel is a continuation of the previous lithofacies, then it contains a portion of Ore 2 that is only slightly deviated from the previous parcel; this deviation is randomly generated according to a gaussian distribution with mean 0 and standard deviation of 5.

If the new parcel corresponds to a new lithofacies, then it contains a portion of Ore 2 that is randomly generated according to a gaussian distribution with mean 0 and standard deviation 1.

The framework supports more elaborate representations of geological variations, including the confluence of geostatistical simulations and mine planning (Wilson, 2021), which is beyond the scope of the current paper. The completion of a parcel is itself a discrete event. Additional discrete events occur within the framework, including the shutdowns which are simulated to occur every thirty days, and last for one entire day. In actuality, the shutdowns at the Florida Mine can last for longer than one day, and the campaign cycles are not always regular. The DES framework can represent random variation in the cycling of shutdowns and production campaigns, including equipment breakdown. For simplicity however, the current computations consider a regular cyclic schedule of twenty-nine days of production followed by a one-day shutdown. At the moment of shutdown, a decision is made as to whether the system should be configured for Mode A or for Mode B, which is then maintained for the entirety of the subsequent production campaign. If the level of Ore 2 (i.e. the low CN consuming ore) is sufficiently low so as to present a stockout risk, then Mode B is selected; otherwise, the more productive Mode A is chosen. As indicated by Table 4.1.8, a campaign of Mode A is at risk of stockout because it consumes Ore 2 faster than the (expected) replenishment rate; similarly, a campaign of Mode B is at risk of stockout because it consumes Ore 1 faster than the (expected) replenishment rate. If the actual replenishment rates are lower than anticipated, resulting in shortages of either ore type, then the contingency modes are applied, as illustrated in Figure 4.1.9.

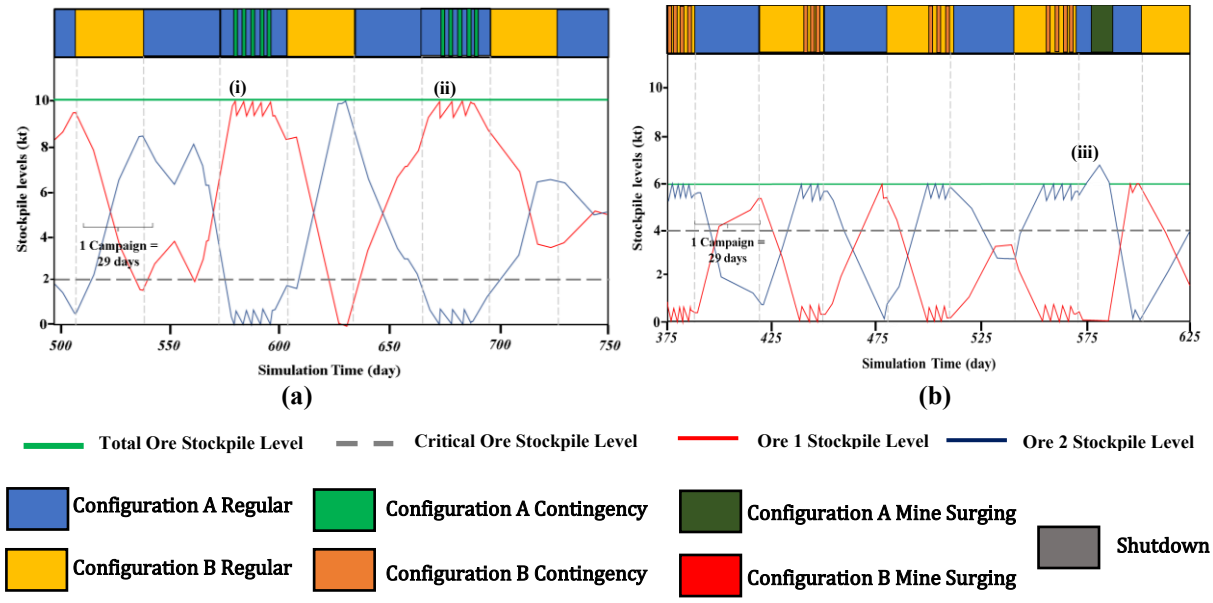

Figure 4.1.9: Discrete Event Simulations Alhue mining system (a) Stockpile evolution during simulations with control parameters set at 10,000 t for the Target Ore Stockpile Level (TOSL) and 2,000 t for the Critical LCC Stockpile Level, which shows some stockpile shortages and long timeframes without stockouts. (b) System entering in Mode A-Contingency and B-Contingency in cyclic time intervals, due to the repeating shortages of HCC and LCC ores affecting the operational stability of the plant and the final KPI results at 6,000 t for the Target Ore Stockpile Level (TOSL) and 4,000 t for the Critical LCC Stockpile Level (i) Cyclical jagged saw-tooth pattern showing the alternation between Configuration A and Configuration A Contingency. (ii) Cyclical jagged saw-tooth pattern showing the alternation between Configuration B and Configuration B Contingency. (iii) System entering in Configuration A Mine Surging, wherein the level of ore 2 type (LCC) increases above the total ore stockpile target level to provide feed directly to the plant in response to a sustained stockout of the other ore type.

Following the approach of Navarra et al. (Navarra et al., 2019), there are two operational policy parameters, a.k.a. control variables, that characterize the decision-making:

X = Target Ore Stockpile Level (TOSL)

Y = Critical Ore 2 Stockpile Level (COSL)

The Target stockpile level, computed as the sum of the available ore types (i.e. the levels of HCC and LCC). More elaborate operational modes are supported by the framework, including mid-campaign decisions to hasten or postpone the shutdown. However, the original two-parameter formulation of Navarra et al. (Navarra et al., 2019) is sufficient for demonstrative purposes. Table 4.1.9 is the result of simulating 5,500k t of excavated ore, or roughly 2000 days, under various combinations of X and Y values; each case shows the average value of 100 replicas, ± one standard deviation. For all cases it is observed that deterministically optimal throughput of 2.6 kt/day is attained, given sufficiently large Y values, as predicted in the previous section using Equation 3.

The approach toward 2.6 kt/day is better illustrated in Figure 8, which includes additional simulations.

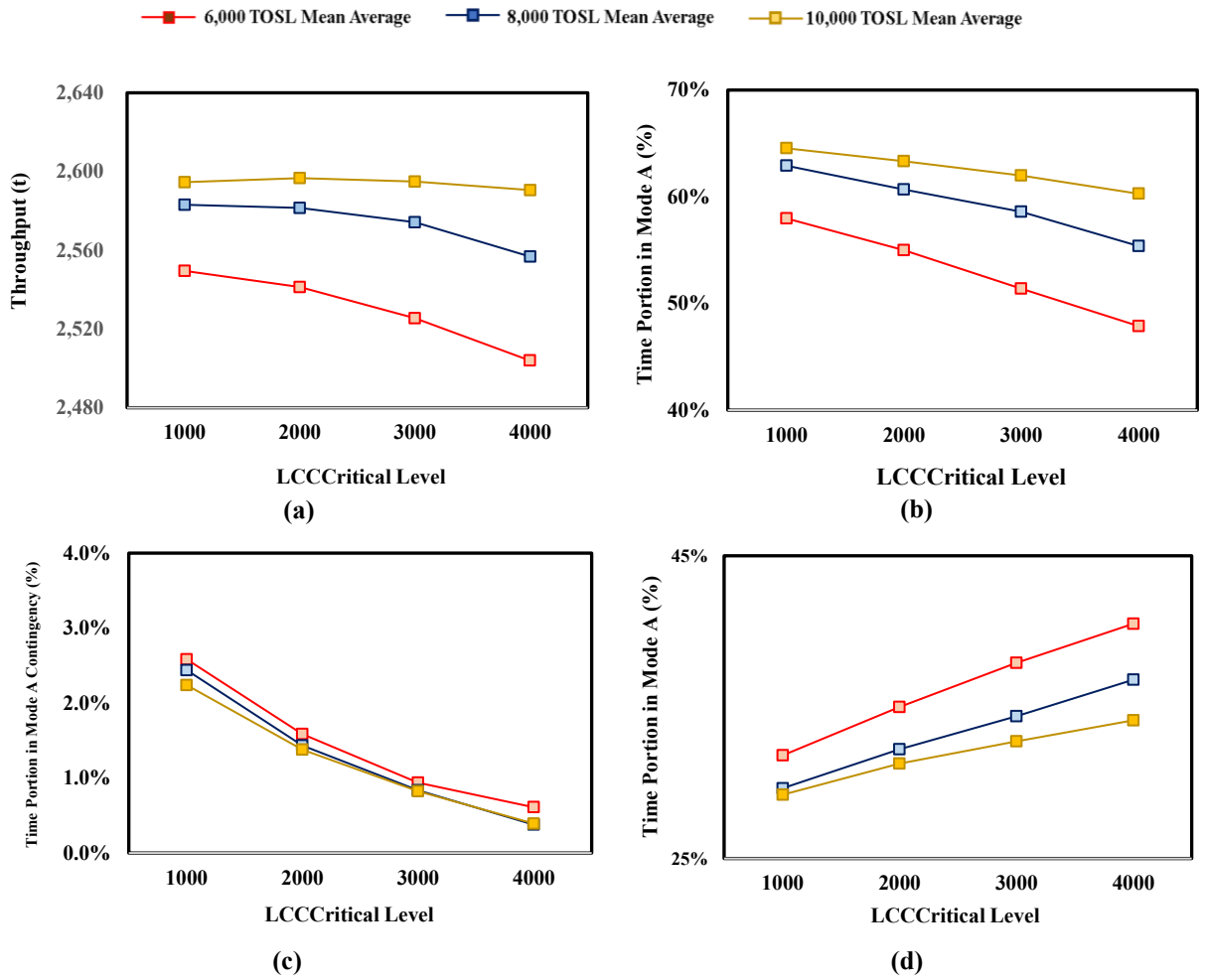

Figure 4.1.10: Discrete event simulations main statistics as a function of policy parameter target stockpile levels X = 10,000 t (Yellow line), 8,000 t (Blue line), 6,000 t (Red line), 4,000 t (Green line), considering critical stockpile levels Y = 1,000 t, 2,000 t, 3,000 t, 4,000 t. (a) Mean Average Throughput. (b) Mean average time in Mode A. c) Mean average time in Mode A Contingency. (d) Mean average time in Mode B.

The decision to alternate between modes depends on current and forecasted stockpile levels (Órdenes et al.,2021). This research follows the approach proposed by Navarra et al. (Navarra et al., 2019) wherein two operational policy parameters, a.k.a. control variables, characterize the decision-making: X = Target Ore Stockpile Level and Y = LCC Critical Stockpile Level. To coincide with the formulation of Navarra et al. (Navarra et al., 2019), the high-cyanide consuming ore is considered to be Ore 1 whereas the low-cyanide consuming ore is Ore 2; thus, when the stockpile of LCC falls below the user-specified Y value, the decision is made to convert the system

into configuration B at the following shutdown. The simulated gold head grades and the average of the gold ounces fed into the plant are presented in Figure 8. These consider the variation of the stockpile levels of the two sulphide geometallurgical units of the Alhué district (Figure 4.1.11).

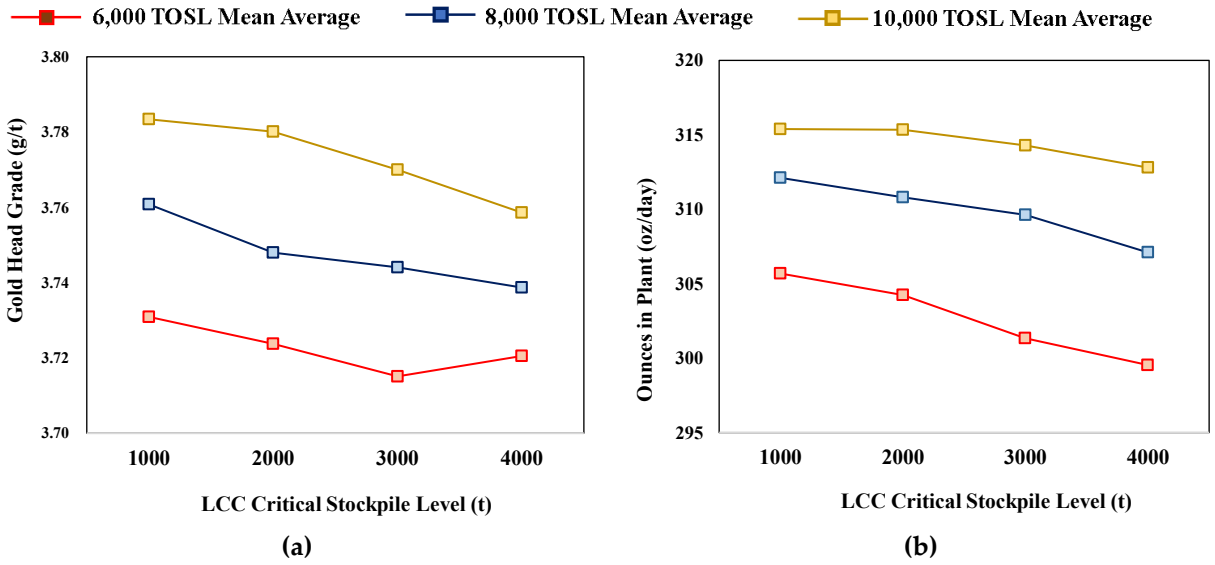

Figure 4.1.11: Discrete event simulations gold head grades statistics as a function of policy parameter target stockpile levels X = 10,000 t (Yellow line), 8,000 t (Blue line), 6,000 t (Red line), considering LCC critical stockpile levels Y = 1,000 t, 2,000 t, 3,000 t. (a) Gold head grades average under different Target Ore Stockpile Level. (b) Gold ounces average fed into plant under different Target Ore Stockpile Level.

By verifying the results, it is possible to establish that the optimal configuration for the control variables for the modelled mining system is X = Target Ore Stockpile Level = 10,000 t and Y = LCC Critical Stockpile Level= 2000 t. The dynamics reaches its best performance achieving the highest throughput (2594.79 t, Table 8) and the second-best result in fed ounces (315.35 oz/day, Table 8). Under this system configuration the key performance indicators (KPI) are maximized, as throughput and gold head grades reach values that are close to those predicted by the orebody average. Additionally, a stable sodium cyanide dosage is attained despite the process being subject to heterogeneous fed (Órdenes et al.,2021).

As for cyanide consumption, the simulation results show that it is possible to stabilize this process parameter by applying the policies of operating modes, where in most cases, the system achieves an average consumption of approximately 2.04 kg/t (Table 4.1.9).The analysis of the dynamics of the mining system, based on the inventory management strategies and modes of operation, shows that the orebody average of 3.81 g/t is attainable (considering 60% HCC ore and

40% LCC ore, Table 4.1.9). The highest production of ounces of gold is obtained when the total target inventory level is set to 10,000 tons and the critical LCC stockpile level is set to 1,000 tons, where the maximum production of 315.39 oz/day.

Table 4.1.9: Summary of discrete event simulation throughputs, cyanide consumption, simulated gold grades.

Target Stockpile Level	Critical Ore Stockpile Level	1,000 t	2,000 t	3,000 t	4,000 t
6,000 t	Mean Average Throughput (t)	2,549.51	2,541.28	2,525.46	2,503.90
	Mean Average CN Consumption (kg/t)	2.044	2.042	2.040	2.038
	Max Average Gold Head Grades (g/t)	4.03	3.96	4.02	4.00
	Mean Average Gold Head Grades (g/t)	3.73	3.72	3.72	3.72
	Min Average Gold Head Grades (g/t)	3.40	3.44	3.43	3.42
	Max Average Gold in metal (oz/day)	333.88	327.35	328.27	325.86
	Mean Average Gold in metal (oz/day)	305.69	304.24	301.34	299.54
	Min Average Gold in metal (oz/day)	276.37	278.81	275.16	272.37
8,000 t	Mean Average Throughput (t)	2,581.31	2,579.32	2,572.19	2,554.89
	Mean Average CN Consumption (kg/t)	2.047	2.046	2.045	2.045
	Max Average Gold Head Grades (g/t)	4.00	4.02	3.98	4.00
	Mean Average Gold Head Grades (g/t)	3.76	3.75	3.74	3.74
	Min Average Gold Head Grades (g/t)	3.41	3.43	3.47	3.46
	Max Average Gold in metal (oz/day)	334.60	336.12	332.48	331.50
	Mean Average Gold in metal (oz/day)	312.11	310.81	309.63	307.10
	Min Average Gold in metal (oz/day)	281.19	282.80	284.60	280.67
10,000 t	Mean Average Throughput (t)	2,592.84	2,594.79	2,592.99	2,588.51
	Mean Average CN Consumption (kg/t)	2.047	2.046	2.045	2.045
	Max Average Gold Head Grades (g/t)	4.01	4.03	4.02	4.02
	Mean Average Gold Head Grades (g/t)	3.78	3.78	3.77	3.76
	Min Average Gold Head Grades (g/t)	3.41	3.46	3.39	3.41
	Max Average Gold in metal (oz/day)	336.56	337.82	337.25	336.64
	Mean Average Gold in metal (oz/day)	315.39	315.35	314.29	312.80
	Min Average Gold in metal (oz/day)	282.40	286.57	281.37	282.47

This outcome is due to the greater availability of ore, and to a less constrained system due to decreased occurrences of LCC shortages. Conversely, the configuration that minimizes the available stock (X = 6000 t and Y = 4000 t) with a head grade result of 3.72 g/t (one of the lowest head grade results, Table 8) and throughput result of 2503.90 t (the lowest tonnage result), this system configuration produces the second lowest value of the average ounces, 299.54 oz/day. In this case the system is constrained due to the continuous LCC ore shortages under configuration A and HCC shortages under configuration B, causing decreases in throughput and lower recovery.

With a low target ore stockpile level, the system is forced to constantly change operational mode, which means that the cyanide dose must be adjusted frequently over short periods (Figure 4.1.12a) to handle the varying ore type proportions and related cyanide requirements (recall Table 4.1.8). The system achieves higher stability by maximizing the time spent in Mode A. With the exception of a few events requiring higher CN consumption due to a shortage of ore 2, this scenario allows for a stable cyanide dose over more extended periods (Figure 4.1.12.b).

Figure 4.1.12. cyanide consumption simulation plots based on modes of operation, relative ore proportions and average consumption requirement for each ore type (Ore1= 2.24 kg/t, Ore 2=1.75 kg/t). (a) Simulation trial using a TOSL of 4,000 t and COSL of 3,000 t, showing the constant cyanide dose adjustment as a function of the short time frames between each operational mode change due to system instability. (b) Simulation trial using a TOSL of 10,000 t and COSL of 2,000 t, showing a flat cyanide dose (greater system stability) as a function of the longer time frames spent in Mode A. Moreover, additional benefits from an appropriate set of the target ore stockpile level allows longer operational plant stability timeframes, supported by more extended periods in configuration A (with time in configuration A > configuration B, Figure 4.1.13a) in comparison with lower Target Ore Stockpile Level (Figure 4.1.13 b). In this context, minimizing this control variable is an operational decision that mine managers must face, considering the effects on the KPIs. For instance, having a low ore stockpile level available, the system is at risk of suffering constant ore shortage events.

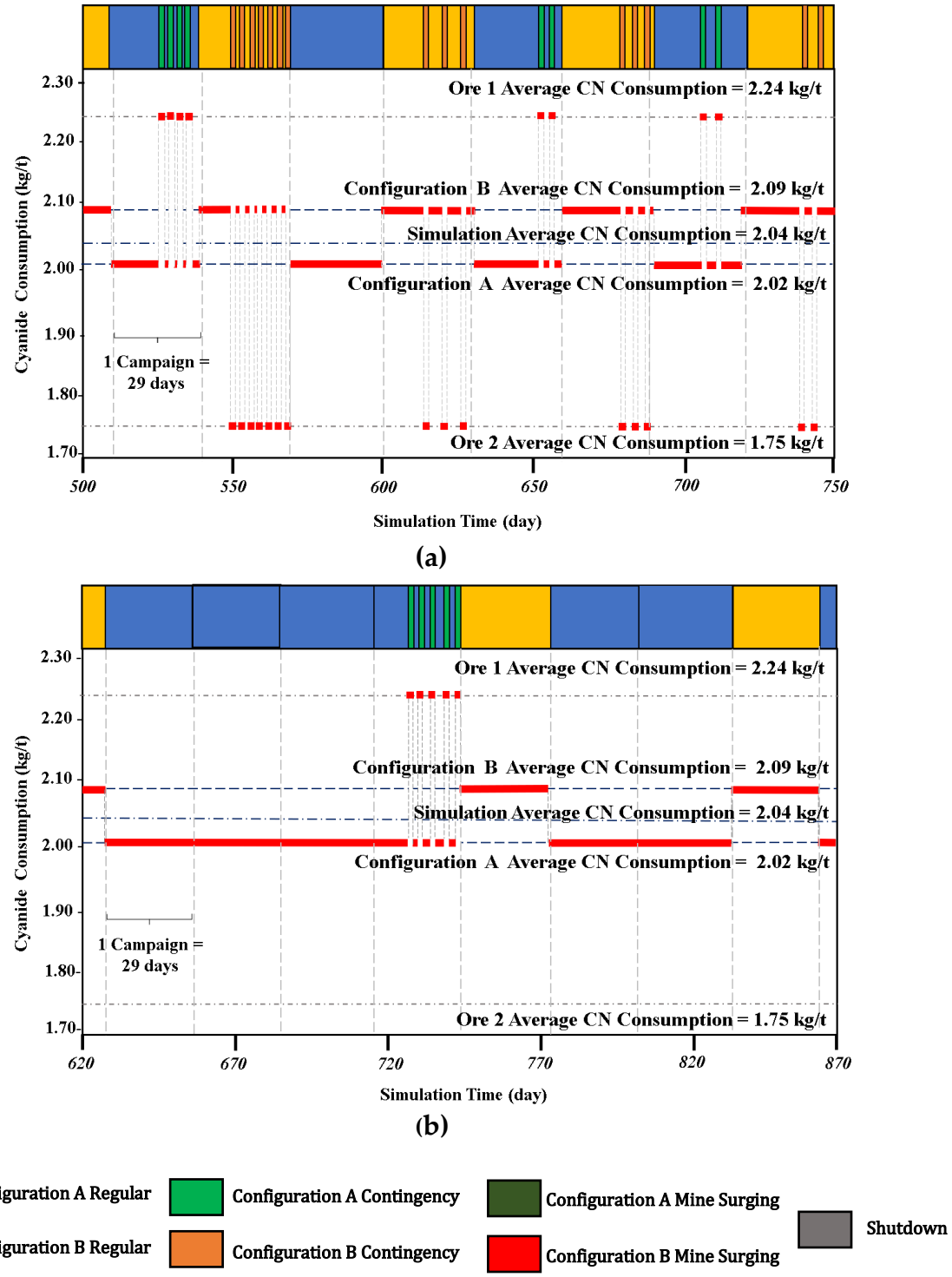

Figure 4.1.12: Cyanide consumption simulation plots based on modes of operation, relative ore proportions and average consumption requirement for each ore type (Ore1= 2.24 kg/t, Ore 2=1.75 kg/t). (a) Simulation trial using a TOSL of 4,000 t and COSL of 3,000 t, showing the constant cyanide dose adjustment as a function of the short time frames between each operational mode change due to system instability. (b) Simulation trial using a TOSL of 10,000 t and COSL of 2,000 t, showing a flat cyanide dose (greater system stability) as a function of the longer time frames spent in Mode A.

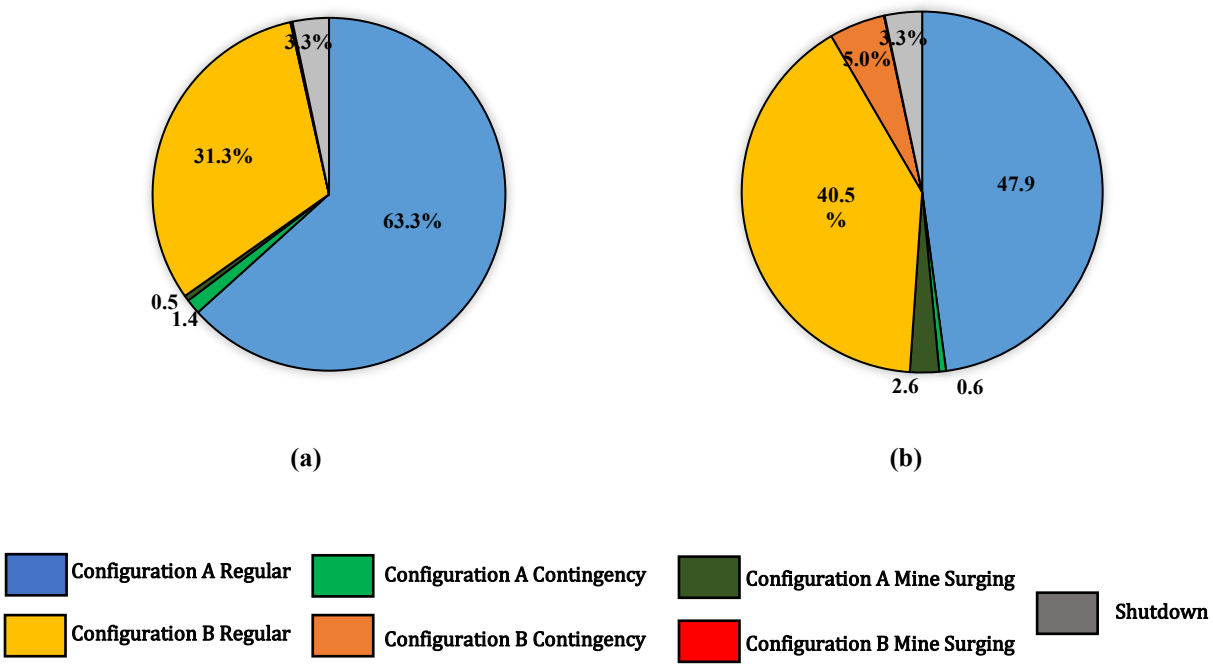

Figure 4.1.13: Time distribution of operational modes in response to geometallurgical units with CN consumption variability, for (a) Target ore stockpile level critical of 10,000 t and LCC threshold of 2,000 t, and (b) enhanced configuration using a critical value of 6,000 t and target total stockpile level of 4,000 t.

Another adverse effect generated by low mineral stockpiles is the continuous changes of modes of operation within a production campaign, from A-regular to A-contingency and B to B-contingency in cyclic time intervals, caused by the frequent stockouts (Figure 4.1.9 a). This causes lower head grades, and at the same time, adversely affects the mill productivity (Table 4.1.9). The optimal configuration of 10,000 t target ore stockpile level and 2,000 t LCC critical stockpile level, in which the ore shortage events are more likely (Figure 4.1.9 b), is compared with other stockpile levels with lower target ore stockpile level. As a result, the system occasionally enters the less productive contingency modes. This can be estimated as a 5% loss of benefit in daily ounces production, comparing the best result with the 6000 t target ore stockpile level and 4000 t LCC critical stockpile level configuration.

4.1.7 Conclusions

For the Alhué mining district, the distribution of metallurgical domains is influenced by 1) the topography of the area where the structure is located, and 2) the permeability of the host rock as a function of the major fault systems that interact with the veins. Both of these factors affect the location of the paleo-water table, which conditions the nature of mineral-groundwater interactions,

and thus, the in situ oxidation-reduction state of the minerals. Most importantly for the Florida Mine, transitioning into high CuS-FeS areas can lead to spikes in cyanide consumption, but this can be mitigated through blending in coordination with pre-established operational modes. Furthermore, a continually successful operation may require the periodic revision of geometallurgical units and reconfiguration of the operational modes, thus integrating updated geological interpretations into system-wide quantitative analyses. In particular, this study demonstrates the use of DES/DRS trials to optimize the balance of incoming high and low cyanide-consuming ores at the Alhué mining district and provide better insight into cyanide consumption dynamics within the mining system. Using blending and stockpiling practices as control measures to mitigate potential operational risks, two control variables (target total stockpile and critical levels of low CN consuming ore) were adjusted to stabilize the mass balancing of incoming plant ore feed. The logical decision would normally be to increase the target total stockpile level, particularly with respect to the critical ore level; this typically allows the system to reach higher throughputs that approach the deterministic value, thereby increasing the revenue potential and overall efficiency by optimal use of the milling plant capacity. Nevertheless, it is also possible to achieve the deterministic throughput by the opposite approach of decreasing both control variables, with the potential benefit of reduced operational costs related to stockpile storage and handling.

The target total ore stockpile parameter is vital as an operational buffer to mitigate the risk of ore shortages under geological uncertainty, which can have a direct impact on reagent consumption for mining systems subject to heterogeneous ore feeds in this stabilizing the cyanide consumption, avoiding extreme variability in this parameter. By stabilizing plant feed and target ore blends, the system benefits from extended periods of operation under the most productive set of operating policies (i.e. Configuration A), and longer time frames without adjusting the cyanide dose. This has a positive influence on plant operations by steadying process parameters and avoiding constant modifications to reagent dosages caused by rapid changes in ore feed blends. This highlights the importance of stockpile management, with a strict but balanced critical stockpile threshold, towards attaining optimal throughput for the system, minimizing the likelihood of potential ore shortages, maximizing mill productivity and improving overall reagent consumption.

Also, another objective reach with this work was to demonstrate the data-driven incorporation of gold head grades into the DES/DRS framework developed to represent the operations at Minera

Florida, and to visualize the dynamics in the system of the new variable under study. This research also confirms that the critical variable Target Ore Stockpile Level is crucial in maximizing gold head grades and tonnage, and indeed metal production. This same approach is being used to represent other process variables in simulating the Minera Florida process, in addition to gold head grades. The incorporation into the DRS framework of key performance indicators (KPIs), in conjunction with gold head grades and other process variables, helps managers to improve the decision-making under the successive detailing of system simulations (Figure 3.1). In the same direction, with a better understanding of the dynamics of the different parameters within each system, it is possible to identify potential risks that may affect these critical variables, as much as at the strategic level (long term planning) as at the tactical level (short term planning). Finally, a complement to this research in discrete rate simulation frameworks (Figure 3.1) is the parallel development of programmed routines that allows the simulation platform to draw geological attributes directly from block models and mine plans. This points toward the experimentation with the incorporation of geostatistical techniques (e.g. stochastic ore body modelling, Sequential Gaussian Simulations, kriging estimation, etc.) that allow the linking of feed variability with the geospatial aspects of the orebody and the mine plan.

4.2 Sequential Gaussian Simulation Incorporated into Dynamic Mass Balance for Simulation-based Control of Cyanide Consumption

Epithermal deposits are significant sources of gold and silver (Simmons, White, & John, 2005). Mineralization in epithermal systems can be produced from chemically distinct fluids; those of low, high, and intermediate sulphidation. These terms refer to the oxidation state of sulphur in the mineralizing fluid (Robb, 2005). Low sulphidation epithermal gold deposits are products of dilute fluids which have been reduced and have a pH of ~7, which are developed by the entrainment of magmatic components within deep circulating groundwaters and are characterized by sulphur species reduced to H_2S (Corbett & Leach, 1998). For low-sulfidation epithermal deposits, one of the most distinctive features are their open-space vein-fill textures (Herrington,2011). The mineral assemblage in low sulphidation veins is quartz ± calcite ± adularia ± illite. Electrum, acanthite, silver sulphosalts, silver selenides, and Au-Ag tellurides are the main gold- and silver-bearing minerals; in conjunction with variable amounts of chalcedony, pyrite, and/or rhodochrosite (Simmons et al., 2005).

Due to this geological interaction, supergene Cu-bearing sulphides (a.k.a. secondary enrichment copper sulphides i.e., chalcocite, digenite, covellite) can occur in the portion of the orebody that interacts with the upper limit of the water table. Critically from the metallurgical point of view, these supergene Cu-bearing sulphides result in high cyanide consumption when processed which results from their high solubility in cyanide solutions (Órdenes et al., 2021) and can therefore be called cyanicidal. This is in contrast to chalcopyrite, for instance, which is not particularly reactive to cyanide. Another consequence of this post-mineralization processes is that the original mineralogy of the deposit can be affected by weathering. This drastic change is found when the portion of the orebody located above the water table is fully oxidized.In this case, base metal ore minerals are absent because they are unstable under this redox condition and the cyanide consumption in this zone is considerably lower when the copper is absent (Órdenes, 2014). This variability can affect the process by causing spikes in cyanide consumption as related to different zones. High base metal sulphide concentrations may be subject to continual dose adjustments, lost throughput, and the accumulation of large stockpiles of complex ore. In this context, the difficulties in the mineral process can be exacerbated if the resource is excavated using underground as opposed to surface methods, due to the inflexibility inherent in underground mining operations. This inflexibility is comprised of tactical considerations such as the location of future and pre-existing mine developments, ventilation, drainage, communications, among others and in addition to site specific complex logistics that may exist in underground mining.

In 2014, Órdenes studied the impact of sulfide ore on the cyanidation of the El Peñón Au-Ag epithermal deposit in the mineral processing performance. Sulphide-rich veins which contain refractory minerals and impurities that affected the Au-Ag leaching by NaCN, effecting negatively gold and silver recoveries while significantly increasing cyanide consumption to historical levels. Moreover, this increment was attributed to the higher concentration of process impurities, remarkably copper (Cu) and manganese (Mn), in plant solutions. These impurities triggered undesired reactions, further reducing the overall process efficiency (Figure 4.2.1). To counteract the refractoriness of silver sulfosalts and stabilize Au-Ag recovery, sodium cyanide (NaCN) concentrations were increased. However, this results in the solubilization of more impurities that generate new operational problems across different process cycles and equipment.

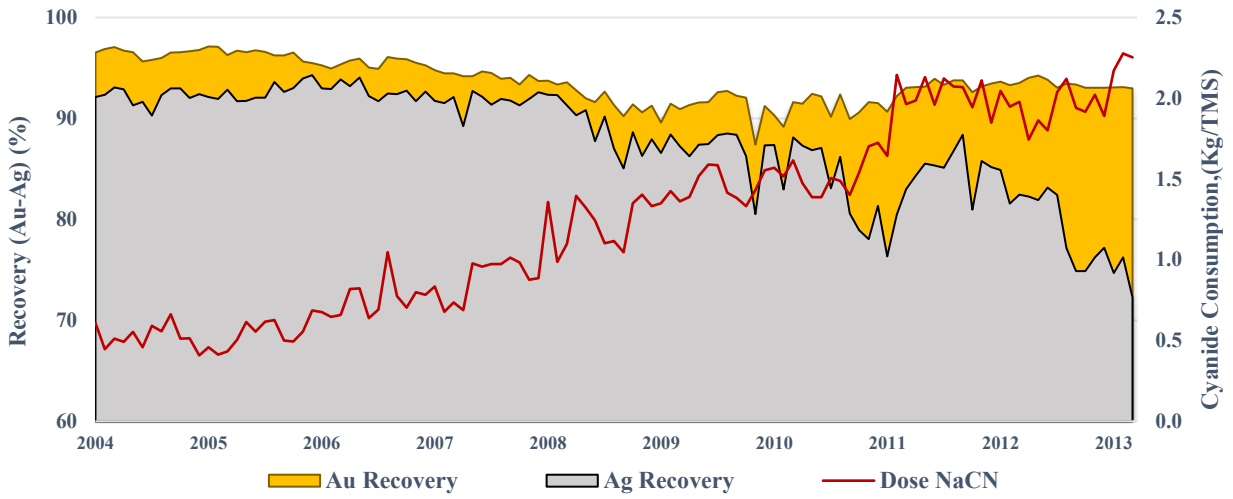

Figure 4.2.1: Results Au and Ag recovery and cyanide dose used between January 2004 to May 2013. The trend towards low recoveries is observed in September 2008 and from June 2010 onwards, which coincides with the entry into production of sulphide-rich ore veins. Also, the constant increase in the NaCN dose used, in particular since the end of 2010(Órdenes, 2014).

At El Peñón mine, veins from deeper levels entered production in 2010. Sulphide ore with higher base metals, such as Cu, Sb, Pb and Zn, and also manganese carbonate had never been processed. This radical mineralogical change led to a noticeable increase in impurities concentration of plant solutions, specially copper, which primarily impacted silver recovery (Figure 4.2.2). Copper concentration in plant solutions reach historical levels, about 1,150 ppm (Figure 4.2.2) with a peak of 1,273 ppm.

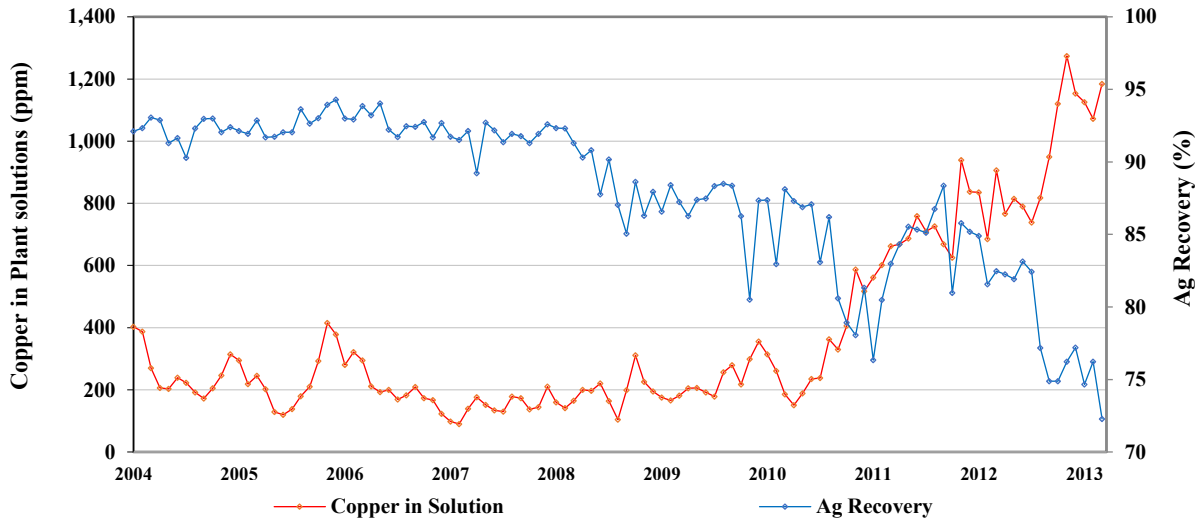

Figure 4.2.2: Soluble copper concentration in solution versus silver recovery period 2004 -2013 (Órdenes, 2014).

An industrial-scale test was carried out at the plant, which consisted of three stages. The results are summarized in Table 1. The first was the six-day feeding of ore from veins in oxidized zones, whose mineralogical and metallurgical characteristics were suitable for the cyanidation leaching process design, where Ag recoveries had results above 85% with NaCN addition of 1.38 kg/t in average, which is considered optimal and is also closer to results in previous years (Figure 1). In a second stage the plant process exclusively ore from veins sulfide zones, which had unfavorable metallurgical characteristics. As consequence, Au-Ag recovery declined severely with a marked increase in cyanide consumption, reaching a consumption spikes of 3.86 kg/t and a restriction in throughput. Finally, the ore blending was restored to a maximum limit for sulfide minerals of 30% (Table 4.2.1), Under these conditions, process performance stabilized, achieving what was considered “normal” results within the new mineralogical context.

Table 4.2.1: Results of the industrial test conducted at El Peñón processing plant in 2010, including a summary of the recoveries achieved and variation of the cyanide consumption (NaCN) during the three stages of the test (Órdenes, 2014).

Day	Oxide Ore (t)	Sulphide Ore (t)	Marginal	%Sulph Ore	Tonnage	Au (g/t)	Ag (g/t)	Rec Au (%)	Rec Ag (%)	NaCN (kg/t)
1	3,868	0	553	**0%**	**4,421**	7.51	178.76	94.40%	83.83%	**1.81**
2	3,810	0	544	**0%**	**4,354**	5.76	156.79	94.44%	86.25%	**1.38**
3	3,924	0	512	**0%**	**4,436**	4.50	142.83	93.23%	86.28%	**1.35**
4	3,903	0	634	**0%**	**4,537**	4.02	136.53	93.42%	85.53%	**1.32**
5	2,659	0	443	**0%**	**4,120**	3.90	150.25	92.56%	85.97%	**1.46**
6	3,734	0	622	**0%**	**4,356**	3.57	149.89	92.99%	86.46%	**1.84**
7	0	3630	0	**100%**	**3,630**	4.79	164.16	94.05%	88.22%	**3.86**
8	0	2932	0	**100%**	**2,932**	6.17	186.38	93.35%	86.97%	**3.41**
9	0	2723	0	**100%**	**2,723**	9.47	208.37	93.15%	84.06%	**3.67**
10	0	3483	0	**100%**	**3,483**	9.32	188.42	90.23%	76.69%	**3.73**
11	541	2848	0	**84%**	**3,389**	10.09	185.61	91.61%	74.83%	**2.95**
12	1,824	729	0	**29%**	**2,553**	10.89	237.88	91.73%	82.47%	**3.13**
13	2,253	901	0	**29%**	**3,154**	8.62	214.06	93.02%	85.52%	**2.54**
14	2,513	1043	64	**29%**	**3,620**	9.41	204.59	91.90%	84.22%	**1.93**

The goal of this report is to optimize mill performance through discrete rate simulation (DRS), which incorporates geological variation into decision-making based on the mining plan, including the establishment of trigger points to induce operational mode changes, in a context of a direct

cyanidation leaching process which is designed to process oxide Au-Ag ore. The simulated scenarios are sample calculations of different cyanide consumption situations controlled by geological features and mineralogy, which is then modelled by the well-known geostatistical technique, sequential Gaussian simulation (SGS). The current paper appears to be the only instance in which SGS is embedded within DRS, even though DRS may be the most straightforward approach to dynamic and stochastic mass balancing.

4.2.1 Geometallurgical Considerations

4.2.1.1 Low Sulphidation Au-Ag Vein Hosted Deposits

Hydrothermal deposits that form in the shallow crust are referred to as epithermal gold-silver deposits and are found typically at depths of less than 1,500 meters below the water table. They are mined for their concentrations of gold and silver, and some deposits also contain significant quantities of other metals including lead, zinc, copper, and manganese. Epithermal deposits can be high-grade or low-grade, and they can be mined using a several different methods or a combination thereof, including underground and open-pit mining. Currently, many such deposits with less than 1 part per million (ppm) of gold are mined using surface mining methods (John, et al., 2018). Hydrothermal deposits that form in the shallow crust are referred to as epithermal gold-silver deposits and are found typically at depths of less than 1,500 meters below the water table. They are mined for their concentrations of gold and silver, and some deposits also contain significant quantities of other metals including lead, zinc, copper, and manganese. Epithermal deposits can be high-grade or low-grade, and they can be mined using a several different methods or a combination thereof, including underground and open-pit mining. Currently, many such deposits with less than 1 part per million (ppm) of gold are mined using surface mining methods (John, et al., 2018).

Epithermal deposits are significant sources of gold, silver, lead, and zinc. This deposit type forms close to the surface and at relatively low temperatures (less than 300°C) in mainly continental hydrothermal environments. Epithermal deposits can be classified by the degree of alteration, sulfide and gangue assemblages, metal content, and sulphide content (Simmons et al., 2005). Epithermal gold-silver deposits have been categorized into various subtypes based on their metal content, presence of various ore and gangue minerals, and inferred composition of hydrothermal fluids required for ore formation. Traditionally, two primary categories of epithermal

deposits are distinguished in the literature: acidic and alkaline (Sillitoe, 1977). The first type of deposit is referred to as enargite-gold, alunite-kaolinite, acid-sulfate, or high sulphidation. The second type is called an epithermal deposit of adularia-sericite or low sulphidation (Camprubí et al., 2006).

A low sulphidation Au-Ag epithermal deposit, specifically, consists of quartz-adularia accompanied by ore minerals such as electrum (mostly 40-60 % by weight Au), native gold, rarely pyrite, silver sulphides and sulphosalts, and base metal sulphides (mainly lead-zinc and minor copper). Cu-sulphides are commonly present in this type of mineral deposit, note that chalcopyrite is refractory to cyanidation and closely related to the hypogenic zone. These deposits have a vertical zoning, being rich in Au-Ag and poor in base metals in the top of the mineralized zone, followed by a portion rich in silver and base metals. This is then followed by an area rich in base metals, and finally reaching a pyrite zone poor in nonferrous metals where both gold and silver are absent (Camus et al., 1991). The precipitation of gold occurs when the fluid boils as it approaches the surface generating mineralization in veins. The mineralogy of these deposits consists mainly of gold, silver, sphalerite, electrum, chalcopyrite, argentite, tetrahedrite, silver sulphosalts, pyrite, and galena. Gangue minerals such as quartz, adularia, and carbonates of different metal ions, such as Mn, Fe, and lesser amounts of Pb and Zn are associated with ore (White & Hedenquist, 1995).

4.2.1.2 Gold and Silver Extraction by Cyanidation

Cyanidation is the primary leaching process to separate the gold and silver in the ore. In general, the optimal concentration of cyanide is dictated by the properties of the ore and commonly used levels are from 0.05% to 0.30% NaCN (0.45~2.0 kg of NaCN per ton) (Azañero, 2001). The use of low concentrations of cyanide is recommended considering the low operating and technical costs due to a lower dissolution of impurities that may affect the extraction of Au and Ag (Cárdenas, 1993).

Knowing the exact mechanism of gold dissolution within a cyanide solution is of considerable importance because of the numerous reactions that take place in the dissolution of the precious metal in agitated solutions of cyanide. These reactions sometimes cause an unwanted consumption of cyanide and lime, as well as complicating the chemical processes involved (Domic, 2001). The total dissolution of gold in alkaline cyanide solutions exposed to oxygen, considering both anodic

and cathodic semi-reactions, is described more precisely by the following reactions, which occur simultaneously:

$$4Au + 8NaCN + O_2 + 2H_2O \rightarrow 4Na[Au(CN)_2] + 4NaOH \quad (4.3.1)$$

Silver sulphides react in an analogous way to gold in aqueous cyanide solutions with the following general equation:

$$2Ag_2S + 4NaCN + H_2O \rightarrow 2Na[Ag(CN)_2] + NaSH + NaOH \quad (4.3.2)$$

The majority of gold deposits occur as native metal and are nearly all present with varying quantities of silver. Early studies on the dissolution of gold in cyanide solution have shown that if the ore contains both heavy metal components (i.e., Cu, Fe, and Zn) and sulphide minerals, more cyanide and oxygen is consumed during the dissolution (Habashi, 1967). Due to the high solubility of these sulphide minerals, the concentration of cyanide used to dissolve gold in ores is usually greater than the expected value obtained from the stoichiometric ratio (Parga et al., 2012).

Gold is often associated with specific minerals, notably the following: pyrite, galena, zinc blend, arsenopyrite, stibnite, pyrrhotite, and chalcopyrite. Gold and silver predominantly occur in nature as native metals and are occasionally associated with various sulphide minerals, and interactions with these minerals can often delay the rate of gold dissolution in a cyanide solution (Aghamirian, 1997). Free cyanide forms complexes with several transition metal species which vary widely in stability and solubility via the following reaction:

$$M^{x+} + yCN^- \rightarrow M(CN)_y^{(y-x)-} \quad (4.3.3)$$

Based on the low sulphidation gangue mineralogy, it has been found that it is likely that the presence of metallic ions in a process solution consumes more cyanide due to undesired reactions. Copper-silver cyanide complexes form during the first phase of the leaching process, which can reduce the amount of cyanide available for gold recovery (Medina and Anderson, 2020). Cyanide consumption from copper could be as high as 2.3 kg of NaCN per kilogram of metal leached

(Stewart & Kappes, 2012). As mentioned in previous sections, the following reaction shows how copper sulfides can react with cyanide to form complexes:

$$4Cu_2S + 22NaCN + 5O_2 + 2H_2O \rightarrow 4Na[Cu(CN)_2] + 4Na_2[Cu(CN)_3] + 4NaCNS + Na_2SO_4 + 2NaOH \quad (4.3.4)$$

Another example of parasitic reactions with this reagent is Mn2+ contained in rhodochrosite (manganese carbonate, very common gangue mineral present in low sulphidation veins). This mineral transforms the cyanide ion into cyanate, impairing the leaching process of Au and Ag, according to the following reaction.

$$2MnCO_3 + 7NaCN + 2NaOH \rightarrow 2Na_3Mn(Na)_3 + 2Na_2CO_3 + NaCNO^- + H_2O \quad (4.3.5)$$

As cyanide consumptions continues to be one of the main economic considerations for gold mining (Hill, 1986) (Kianinia, et al., 2018) (Medina & Anderson, 2020), the operating cyanidation cost increases significantly with the sustained incremental consumption of this reagent in the forecasted ore due to impurities. Copper is a major cyanide consumer because it forms cyano-complexes. This can lead to higher cyanide consumption, slower dissolution rates of gold and silver, interference with successive recovery activities, and contamination of the final product (Marsden & House, 2006). Cyanide complexes can be broadly categorized into three main groupings, which are based on their thermodynamic stability constants k, from least to most stable:

(1) Free cyanide (HCN, CN-).

(2) Weak acid dissociable cyanide (WAD) complexes, for which log k ≤ 30 approximately:

$(Zn(CN)_4^{2-}, Cu(CN)_2^-, Cu(CN)_4^{2-}, Cu(CN)_4^{3-}, Ni(CN)_4^{2-}, Ag(CN)_2^-)$.

(3) Strong cyanide complexes, for which log k>30 approximately $Au(CN)_2^-$), ($Fe(CN)_6^{2-}$, ($Fe(CN)_6^{4-}, Co(CN)_6^{3-}$).

Cyanide forms ionic complexes with metals (Kuyucak & Akcil, 2013) and virtually all metal ions present in a solution are associated with cyanide ions. This means that at high concentrations of

metals in solution, the presence of free cyanide is inconsequential due to the occurrence of sulphide species in the mined ore (e.g., sphalerite, galena, Cu-bearing sulphides such as chalcopyrite, chalcocite, and covellite). While low-stability cyanide complexes could behave like free cyanide, albeit with slower reaction kinetics, this type of cyanide is called available cyanide. This occurs in the presence of other species with a tendency to form more stable complexes, and thus disfavors the gold extracting reactions (free cyanide + WAD cyanide). In practice, the spiking of cyanide consumption can be modeled empirically or semi-empirically, leading to gold mines experimenting with different feed and reagent blends, in the formulation of different operational modes.

Órdenes et al., (2021) proposes a simulation-based procedure to optimize the balance of incoming high and low cyanide-consuming ores in the Alhué mining district. The results of the simulations offer a more thorough understanding of cyanide consumption dynamics within the mining system and the importance of blending and stockpiling practices as control measures to mitigate potential operational risks related to unexpected rises in cyanide consumption. An increasing comprehension of geometallurgical relationships brings value to a mine, insomuch as it is incorporated in the actual operational decisions.

4.2.2 Case Study

The goal of this study is to build a model that can predict the effects of a radical change in the mineralogy of a leaching plant due to variations in redox conditions caused by geological features within the ore deposit. Geometallurgical data, derived from a low sulphidation gold and silver deposit, is presented in the context of a leaching process using cyanide solutions and is assessed for the potential to increase consumption of the sodium cyanide (NaCN) consumption. In quartz adularia veins, there are several sin-genetic minerals with gold-silver deposits that can be deleterious to the leaching process by cyanide, specifically mineral assemblages located below the paleo water table within the deposit (Figure 4.2.3).

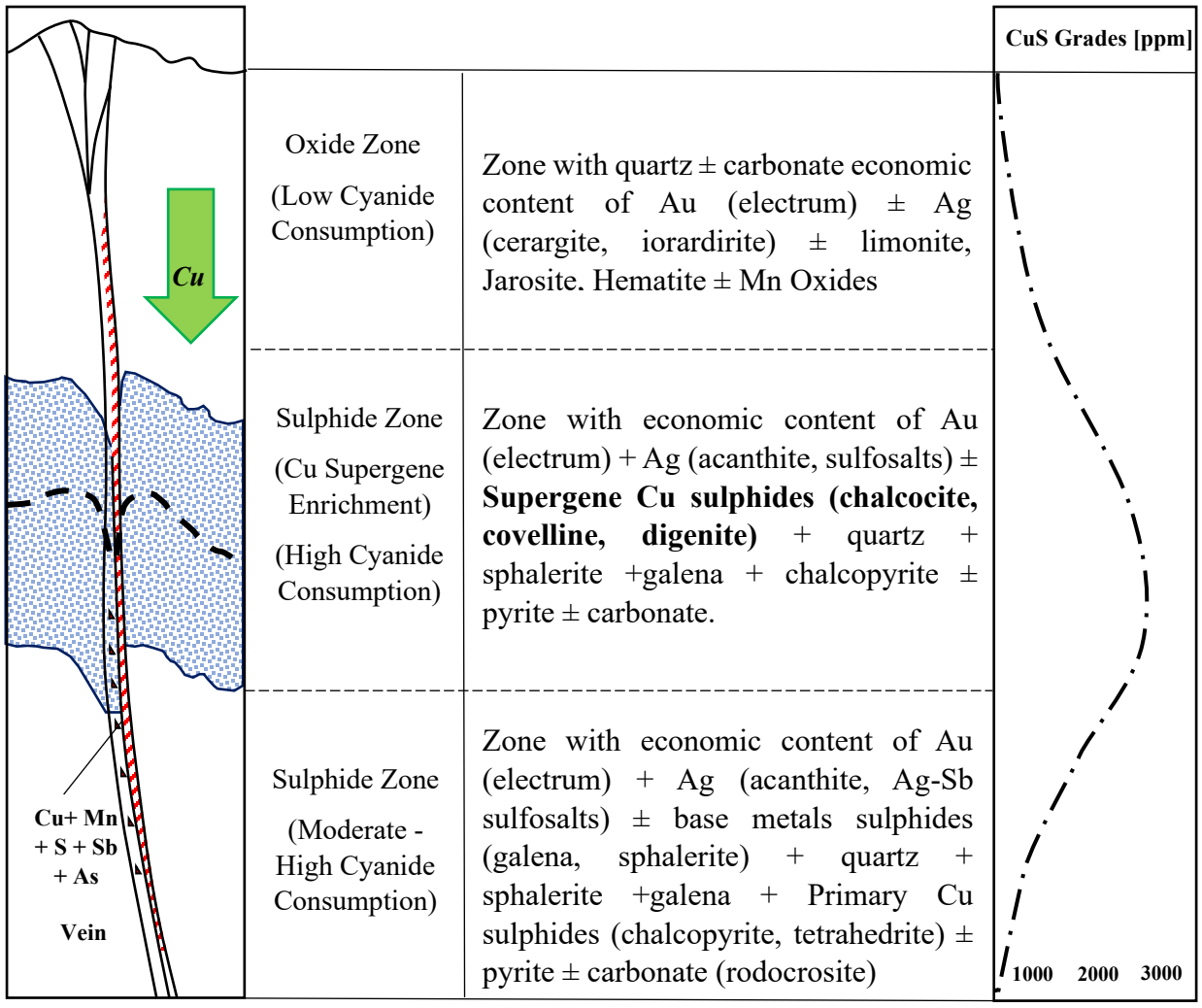

Figure 4.2.3: Schematic profile of the mineralogical distribution in low sulphidation veins and their location respect the paleo water table. Below this limit which conserve the original mineralogical species at the formation of low sulphidation system dominated by quartz + adularia > carbonates (rhodochrosite + calcite +ankerite)> and Zn-Pb Sulphides (Sphalerite + Galena)>> hypogenetic copper sulphides (chalcopyrite +tetrahedrite). Also copper from oxide zone is transported to lower levels generating supergene Cu-sulphides (chalcocite-covellite -digenite).

This mineralogical zone contains numerous potential cyanide consumers, such as copper and manganese (the two most significant described in Section 4.2.3.2), especially with the occurrence of copper primary sulphides chalcopyrite, tetrahedrite (Figure 4.2.4a) and bornite (Figure 4.2.4b), also, chalcocite, covellite (Figure 4.2.4c). For manganese the main mineral specie is rhodochrosite (Figure 4.2.4d), very common in Au-Ag low sulphidation systems.

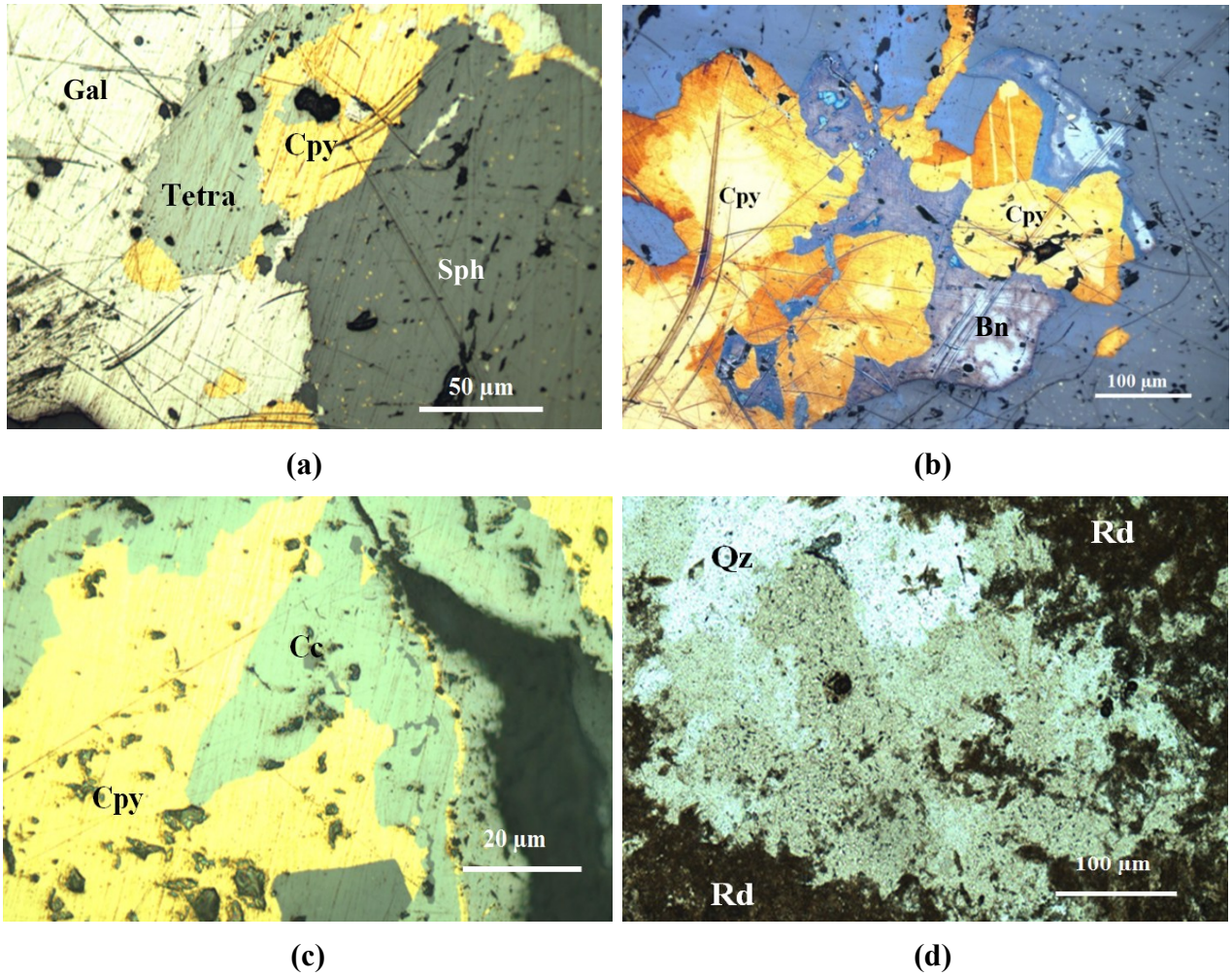

Figure 4.2.4: Cyanide consumer mineralogy (a) Chalcopyrite (Cpy) intergrow with tetrahedrite (Tetra) ; sphalerite (Sph) and Galena (b)Chalcopyrite (Cpy) intergrow with sphalerite (Sph) and bornite (Bn) (c)Chalcopyrite (Cpy) replaced by covelline (Cv) and chalcocite (Cc) (c) (d)Rodocrosite(Rd) inter growed with hydrothermal Quartz (Qz) (Ordenes, 2014).

Feeding this ore type directly into a leaching plant results in a high increment of cyanide consumption, generating a series of parasitic chemical reactions and process inefficiencies. Furthermore, operational problems related with high concentrations of manganese in the sulphide ore (Table 4.2.2) can occur in different stages, such the precipitation of gels into plant pipelines (triggered by the undesired dissolution different metallic ions due to spikes in the cyanide dosage and reacting with the lime of the process water), and/or affecting the physical and/or chemical quality of the Dore bars in the refinery (Órdenes, 2014). Additionally, supergene copper sulphides (e.g. chalcocite, digenite, covellite) have a high solubility in cyanide solutions (with more than 90% of recovery with this leaching reagent Table 4.1.1) in combination with a fast-leaching

kinetics of covellite and chalcocite/digenite (Órdenes et al., 2021), which also cyanide consumption.

Table 4.2.2: Comparison in the concentration of elements harmful to cyanidation between mineralogical zones in low sulphidation deposits (Órdenes, 2014).

	Copper (ppm)		Manganese (ppm)		Lead (ppm)		Zinc (ppm)	
	Oxide	**Sulphide**	**Oxide**	**Sulphide**	**Oxide**	**Sulphide**	**Oxide**	**Sulphide**
Average	112	951	2,665	16,163	702	7,428	677	10,159
P10	12	39	77	554	30	234	12	463
P90	210	2,476	9,990	44,431	1,811	21,670	1,533	29,280

Conversely, even though rhodochrosite (a Mn-rich carbonate) has a moderate solubility, in some areas can be highly concentrated. As shown in Section 3, this gangue mineral can oxidize cyanide to cyanate (Equation 4.3.5), which has no leaching capability and is not recovered by the process downstream (Órdenes, 2014). In contrast, oxide ore (located above the water table level) generally contains low concentrations of cyanicides (Table 4.2.1) and carbonates, most of which were leached by a post-mineral geologic process that can lead to changes in the geochemical stability under new redox conditions. Over this level, acid rain and dissolved oxygen from groundwater react with pyrite and other sulphides, generating iron oxyhydroxides and sulphuric acid. This acid seeps down into the orebody removing copper, lead, and other base metals and dissolving carbonates as it moves downwards (Habashi, 1967). Therefore, the presence of carbonates, especially Cu-sulphides, is essential in assessing cyanide utilization in the plant. For the current calculations, a bench and fill mining method (which is an adaptation of cut and fill) was computed for the mineral extraction to obtain the mining extraction sequence.

This research focuses on finding alternative options to deal with unexpected problems caused by the mineralogical variation and the potential effects on key performance indicators (KPI), specifically cyanide consumption. Furthermore, the dosage control of cyanide consumption using ore blending strategies and stockpile management policies outlined in a discrete rate simulation framework performed in Rockwell ARENA ©. Finally, it contributes to evaluating process alternatives and improving production planning, reducing uncertainties in the prediction of reagent consumption such as sodium cyanide.

4.2.3 Cyanide Consumption Simulation

Geometallurgical data was utilized for the Sequential Gaussian Simulation (SGS) to compute a hundred equiprobable sodium cyanide consumption scenarios. This database contains 338 ore samples, classified in situ (Figure 4.2.5). The samples were analyzed to determine the cyanide consumption by a roll test and the data was grouped by ore type (oxide-sulphide) based on workface observations.

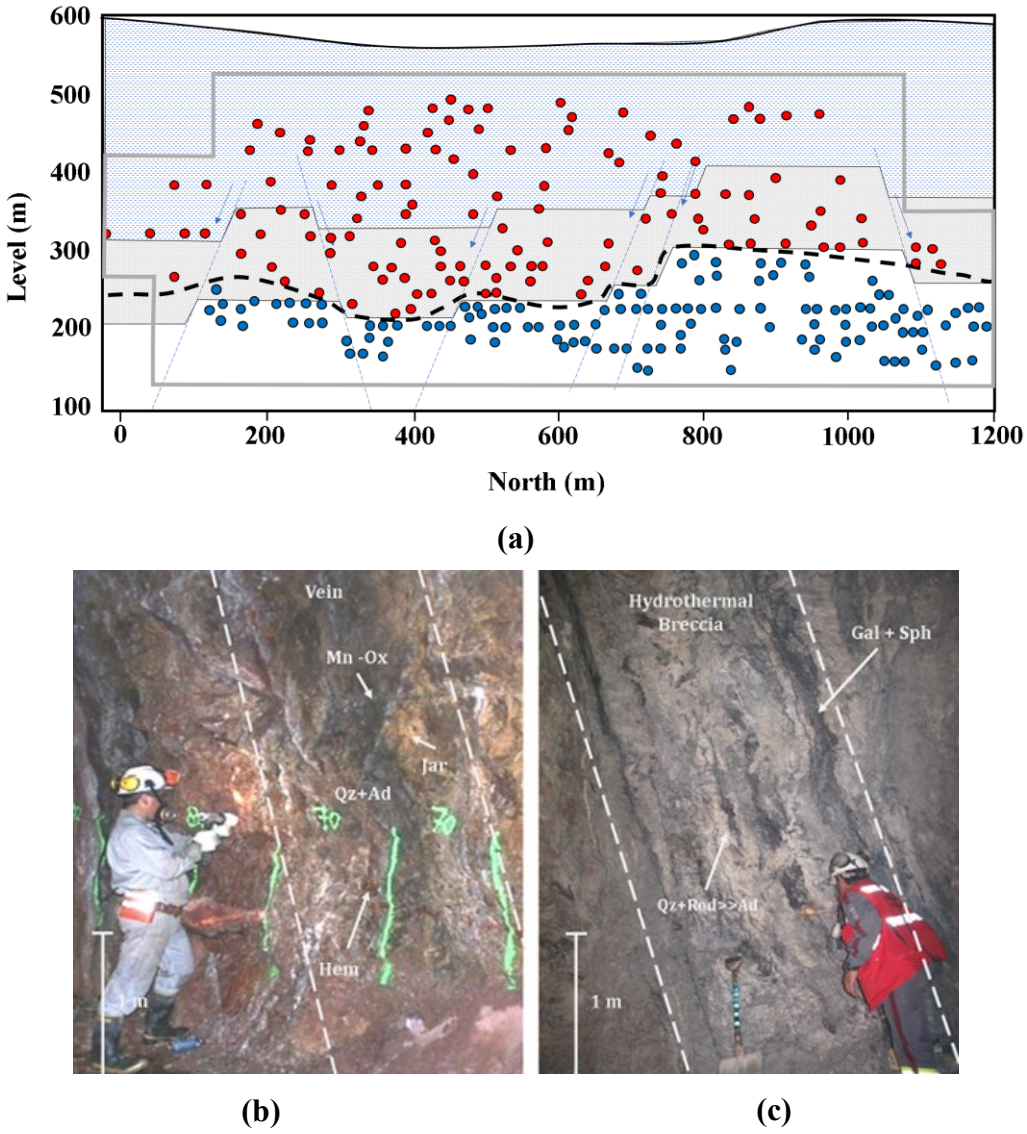

Figure 4.2.5:(a) Profile showing the location of the geometallurgical sampling data. The boundary between the two mineralogical zones was constructed by oxide-sulphide classification made from the in situ mineralogical assemblage in each sampling point. (b) Workface in oxide zone with quartz (Qz), adularia (Ad), and oxides such as jarosite(jar), hematite(hem) and manganese-oxide (Mn-Ox). (c)Workface in sulphide zone with quartz (Qz), adularia (Ad) mixed with and rhodochrosite (Rod), and sulphides such as galena (Gal), sphalerite (Sph). The black dashed line marks the limits of the oxide-sulphide zone as reference (Órdenes, 2014).

The geometallurgical sample database was statistically described for the cyanide consumption variable for the entire data set and by ore types. The NaCN average consumption for the ore body is 2.53 kg/t and a 2.26 kg/t declustered average. The result revealed that there is a strong influence from the mineralogical zone, with a notable difference in the sodium cyanide dosage based on the significant disparity in the average consumption of this reagent between the two geometallurgical units (1.61 kg/t in the oxide ore vs 3.22 kg/t of the sulphide). The result is summarized in Table 4.2.3.

Table 4.2.3: Cyanide consumption statistical summary.

Variable	Statistics	All-Data	Normal Score	Oxide Ore	Sulphide Ore
Cyanide Consumption (kg/t)	N° Samples	338	338	143	195
	Mean	2.53	0.22	1.61	3.22
	Standard Deviation	1.26	1.02	0.84	1.08
	Minimum	0.06	-2.70	0.064	0.63
	Q1	1.55	-0.45	0.98	2.57
	Q2	2.55	0.23	1.55	3.18
	Q3	3.47	0.96	2.23	3.95
	Maximum	5.61	3.14	3.49	5.61

To perform the Sequential Gaussian Simulation (SGS), a series of realizations from a random function that shares spatial continuity features from the collected data is generated. From the available geometallurgical information, a histogram of the raw data can be inferred (Histogram, Figure 4.2.6a). Following this, the simulated variable, in this case cyanide consumption, were translated into the Gaussian space through a normal score transformation using SGEMS (Figure 4.2.6b). The subsequent step in the SGS (Sequential Gaussian Simulation) procedure involves generating variograms of the weighted standard samples. This process is crucial for calculating the parameters required to estimate the block model and uncover hidden patterns within the samples.

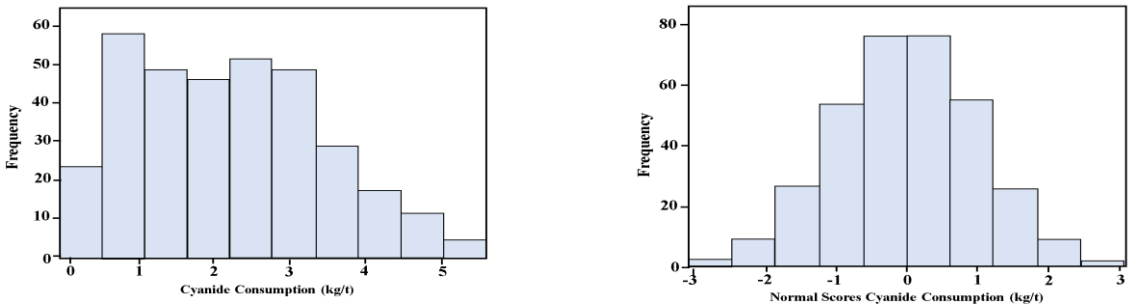

(a) **(b)**

Figure 4.2.6: (a) Declustered NaCN consumption raw data Histogram. (b) Normal Scored NaCN consumption.

The subsequent step in the SGS (Sequential Gaussian Simulation) procedure involves generating variograms of the weighted standard samples. This process is crucial for calculating the parameters required to estimate the block model and uncover hidden patterns within the samples. The histograms are shown in figure 4.2.7.

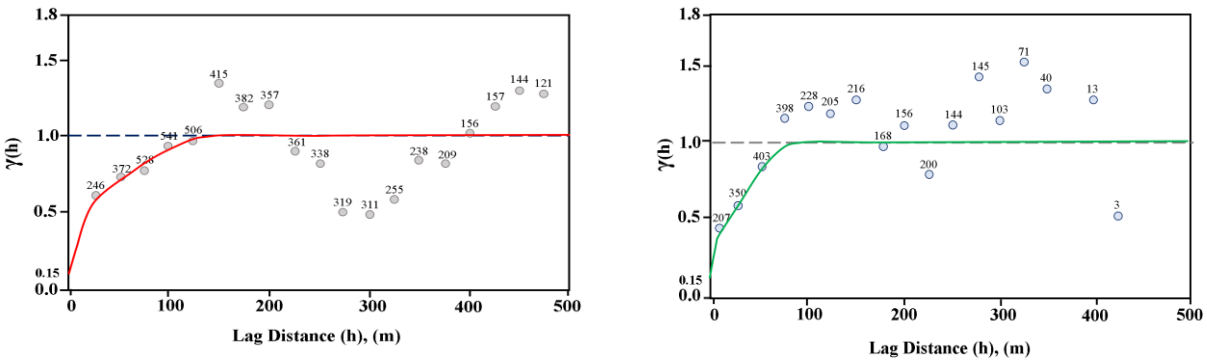

Figure 4.2.7: (a) Normal Scored NaCN consumption major range direction Variogram. (azimuth 0°, dip 35°) (b) Normal Scored NaCN consumption minor range direction Variogram (azimuth 0°, dip 125°).

The simulations were carried out in the SGEMS and GSLIB, where 100 realizations were computed based on the modelling parameters and then assessed in the variography calculation and sequential gaussian simulation algorithm. Block models were built with a common parent block size of 1m × 1 m × 1m and re-blocked to 4m × 5m × 4m. The summary of the estimation parameters for the SGS are summarized in Table 4.2.4.

Table 4.2.4: Cyanide consumption Normal Scored Variogram Parameters.

		Ranges [m]	
	Sill	Major (Az 0°/ Dip 35°)	Minor (Az 0°/ Dip 125°)
Nugget Effect	0.15		
Spherical	0.29	15	10
Spherical	0.56	150	95

Each simulation estimates values in the in the Gaussian space, which needs to be back transformed to the sample distribution to obtain the final simulated cyanide consumption scenarios (Figure 4.2.8a). These realizations represent different equiprobable cyanide consumption possibilities for the mineral body that relies on the same sample distribution histogram.

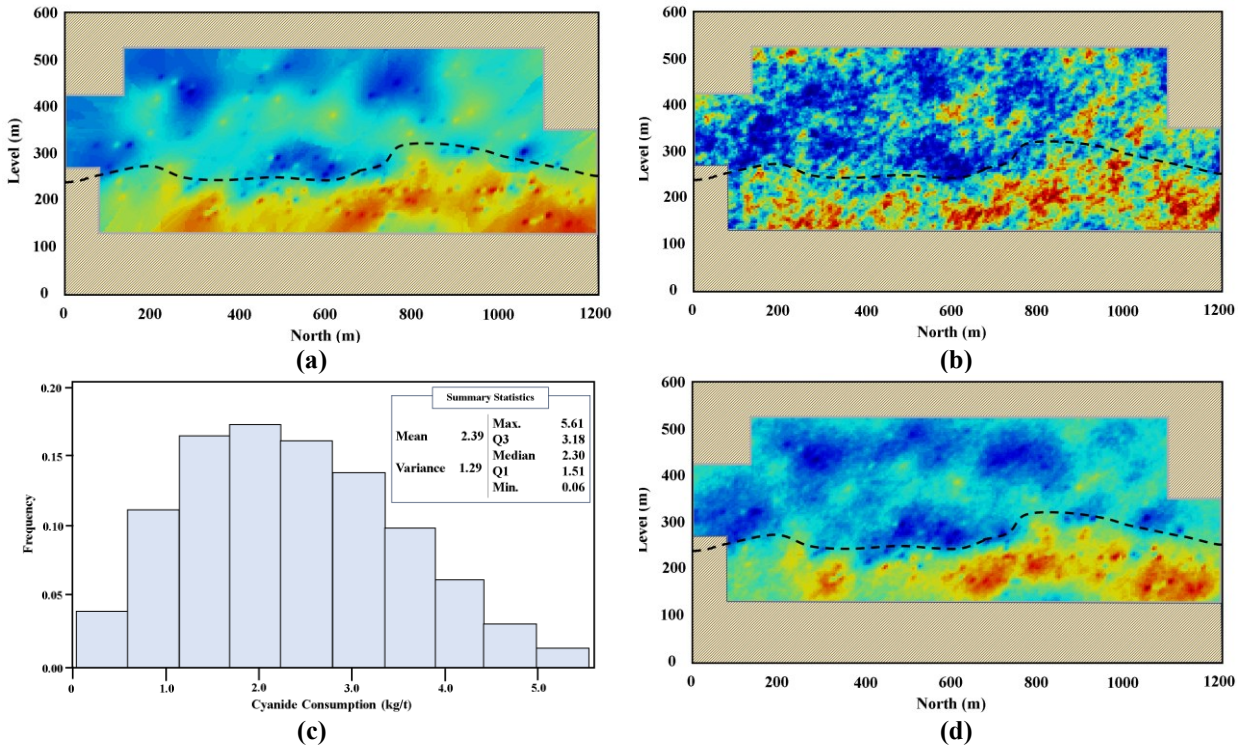

Figure 4.2.8: (a)Cyanide consumption estimated by Kriging. (b) Cyanide consumption back transformed simulations. (c)Cyanide consumption back transformed simulation 12 histogram and summary statistics. (d) E-type Cyanide Consumption. The black dashed line marks the limits of the oxide-sulphide zone as reference.

The histograms of the estimated blocks in each realization were also generated (Figure 4.2.8c) with their corresponding statistics. Unlike estimation, where a best map can be generated under some quality parameter definition (e.g. minimization of the mean square error in the case of kriging), realizations are accepted or rejected based on their ability to honor the data, geology, histogram, variogram, and any secondary information (Ortiz, 2020). The histogram of each scenario shows that each realization respects the distribution of the sample set, and, in addition, its statistical parameters are also very similar to those of the cyanide consumption test database. The new contribution of the approach of the Monte Carlo simulations framework for decision making under uncertainty is that the information generated from the geostatistical simulation and mine planning will feed the discrete rate simulations developed in the ARENA Rockwell © software. This report proposes a new method of evaluating the influence of stockpile management policies to stabilize plant reagent consumption (in specific sodium cyanide) while maintaining mine production levels. This novel contribution tries to integrate geostatistical methods (e.g., Sequential Gaussian Simulation) into operational simulations from the different scenarios to be able to evaluate a specific variable, stochastically, into the mining system.

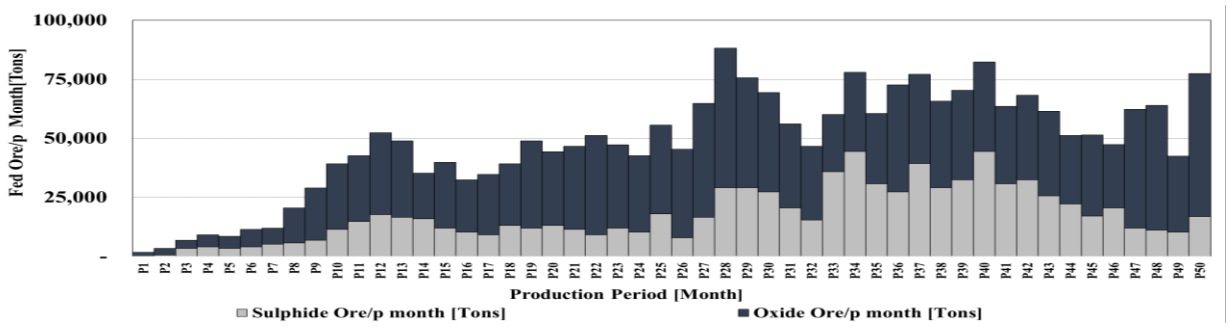

(a)

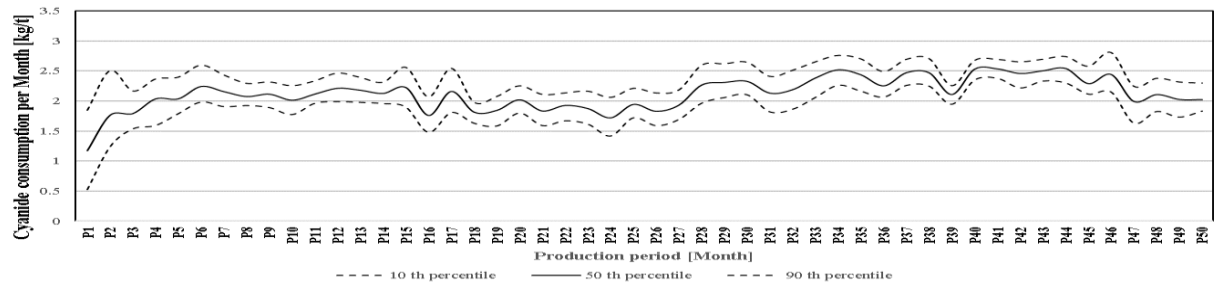

(b)

Figure 4.2.9: Geometallurgical mine plan summary (a) Ore feeding profile for fifty periods and their oxide-sulphide ore type ratio. (b) Stochastic Cyanide Consumption profile.

Based on the mining sequence, which was generated from the ore production scheduling, the result was a 50-month feeding plan, during mining periods where the oxide-sulphide ratio varies depending on the mineral zone being mined (Figure 4.2.9a). Additionally, the cyanide consumption profile was constructed, but for this variable the projected future consumption is stochastic, based on the one hundred realizations computed under the Sequential Gaussian Simulation procedure. Therefore, the cyanide dose takes the expected value (P50) of stopes extracted in a single period of production measured in the simulated block model under the different scenarios. Another advantage of stochastic modeling is that, in addition to the expected value, the 10th and 90th percentiles can be used as a potential range of variation of the consumption value (Figure 4.2.9b).

4.2.4 Sample Calculations DRS Framework

The current methodology uses Discrete Rate Simulation (DRS), a relatively simple approach to dynamic mass balancing, including spikes in cyanide consumption. The resulting framework demonstrates how spikes in cyanide consumption can be mitigated by balancing the feed from

zones with supergene Cu-bearing sulfides soluble in cyanide solutions or other consumers of this reagent. As explained in earlier sections, the transition from oxide to sulfide ore assemblages can severely affect the cyanide leaching process. During this transition, cyanide consumption can increase significantly, leading to increased processing costs and operational problems. In this context, a suitable approach might be to implement ore blending practices in conjunction with alternate modes of operation to maximize plant throughput, stabilize reagent consumption, and achieve process stability.

This study demonstrates the use of a DRS framework as an appropriate tool to reach the objectives of maximizing plant throughput, stabilizing reagent consumption, and achieving process stability. The framework is also a useful tool to evaluate and control consumption of certain reagents (e.g., sodium cyanide, flocculants, energy, lime), improve future production planning and cost projections, and reduce uncertainty in metallurgical parameters (Órdenes et al., 2021).

The framework is designed to manage the bottleneck created by the processing plant, which has a lower capacity than the mining rate. To address this, campaign cycles are set up in a regular schedule of 29 days of production followed by a one-day shutdown. During the shutdown phase, decisions are made on whether to change the operational configuration. If the level of Ore 2 (Oxides) is low enough to present a potential stockout risk during the next campaign, a mode change is triggered from Configuration A to Configuration B. On the other hand, if Ore 2 levels are above a defined threshold following a production campaign in Mode B, the operational mode returns to Configuration A. Contingency configuration is applied for one day in case a stock shortage occurs during an operating campaign. A contingency mode implies that the plant only utilizes the available ore type (refer to Table 4.2.4 & Table 4.2.5).

The characteristics of the operational configurations, described in Table 4.2.5, were used for the present set of computations. Configuration A is designed to maximize the mill capacity, using all the oxide available and feeding all the ore to the plant that is mined in the period. In this first stage, the stockpile management policies were designed to handle the sulphide ore that would be reached in the early mine development. The mine productivity shows an increment in the latter half of the mining schedule (Stage 2, period 27 onwards) due to a larger number of active

production workfaces and bench stopes prepared for extraction. For this stage the blending strategies (Table 4.2.6) increase the tonnage of the Configuration A and B (due to the higher ore production rate), with a different proportion of oxide-sulphide (60% - 40% for config. A), but in this case Configuration B is designed to consume a larger portion of sulphide and at the same time help to recover the level of the critical ore in a short time frame (55% sulphides – 45% oxide).

Table 4.2.5: Stockpile Blending Strategy Stage 1.

	Configuration A			Configuration B		
	Regular	Contingency	Mine Surging	Regular	Contingency	Mine Surging
Throughput (kt /day)	2,000	1,300	-	1700	850	-
(%) Sulphide Ore	20	100	20	45	0	45
(%) Oxide Ore	80	0	80	55	100	55

Table 4.2.6: Stockpile Blending Strategy Stage 2.

	Configuration A			Configuration B		
	Regular	Contingency	Mine Surging	Regular	Contingency	Mine Surging
Throughput (kt /day)	2,750	1790	-	2,340	1170	-
(%) Sulphide Ore	40	100	40	55	0	55
(%) Oxide Ore	60	0	60	45	100	45

Configuration A is a more productive operational state that exhibits roughly the same throughput of the processing plant before encountering the mineralogical change. Configuration B is considered more stable and allows for stockpile replenishment. Both operational modes consider blends of Ore 1 (sulfide ore) and Ore 2 (oxide ore) in different proportions. Since the plant is better adapted for oxide mineralogy, Mode A utilizes a larger proportion of Ore 2 compared to Configuration B. Configuration B is an operational policy designed to re-establish the levels of the critical ore (oxides show lower average cyanide consumption and are more stable using a direct leaching process). Furthermore, this configuration avoids large accumulations of this ore type, generating a non-processable ore stock and avoiding a potential loss. A simplified (deterministic) analysis of the optimal throughput of the simulated processing plant considers two operational policy parameters to characterize decision-making following the approach of Navarra et al. (Wilson et al., 2021), based on the following system variables:

$$X = \text{Target Ore Stockpile Level}$$

$$Y = \text{Critical Ore 2 Stockpile Level}$$

The aspired ore stockpile level is determined by the sum of the accessible ore types, and the critical Ore 2 stockpile level is analogous to the oxide ore availability.

4.2.5 Discrete Rate Simulations Results

To assess the potential impact of the new operational policies on cyanide consumption in response to the mineral transition, 100 scenarios were tested with different values for the two policy parameters, which are described in Tables 2 and 3. In the case of stage 1, the critical ore level (Y) ranging between 1,000 t and 2,000 t is considered; with target ore stockpile level (X) values of 4,000 t, 5000 t and 6,000 t. For stage 2, critical ore stockpile levels vary between 2,000 t and 6,000 t, while the target ore considers three different levels for the stockpile of 8,000 t, 10,000 t and 12,000 t. Each scenario was simulated for approximately 1,500 days of operation using reagent consumption scenarios generated by the SGS Figure 4.2.10 summarizes the results.

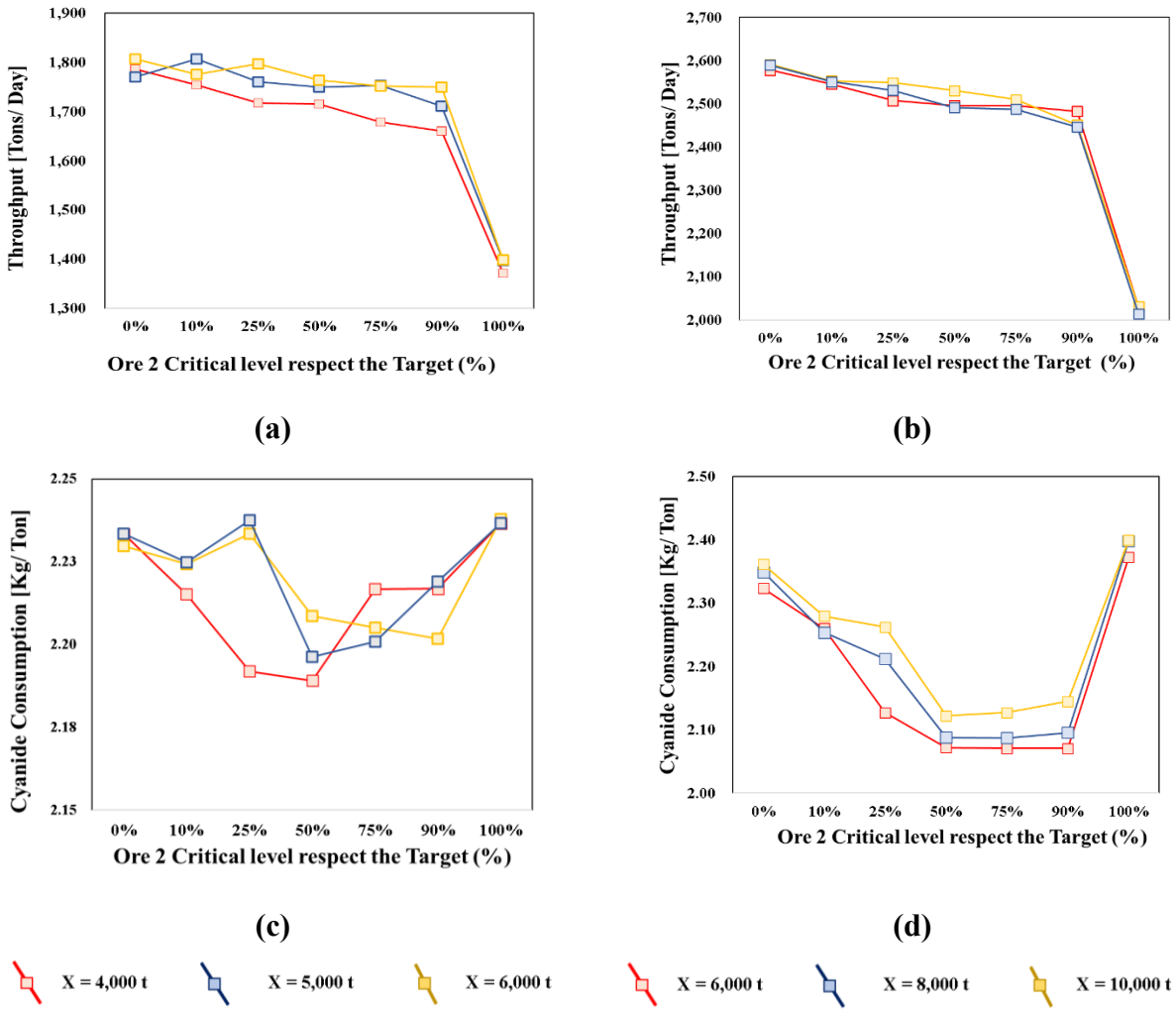

Figure 4.2.10: Results simulations based on system variables (X = Target Ore Stockpile Level and Y = Critical Ore 2 Stockpile Level) (a) Average daily throughput for first production stage. (b) Average daily throughput for second production stage. (c) Daily cyanide consumption average for first production stage. (b) Daily cyanide consumption average for second production stage.

The analysis of the mining system dynamics, based on stockpile strategies, shows that cyanide consumption is reached when no critical ore ha low availability in some cases reaching a maximum value of 2.38 kg/t. The result also show that is possible control the cyanide average consumption increasing the level of critical ore, in this case oxide (low cyanide consumer ore). The summary of the results is shown in tables 4.2.7 and 4.2.8.

Table 4.2.8: Summary of discrete event simulation throughputs, cyanide consumption, stage 1

Target Stockpile Level	Critical Ore Stockpile Level	0%	10%	25%	50%	75%	90%	100%
4,000 t	**Mean Average Throughput (t)**	1,786	1,754	1,718	1,716	1,679	1,660	1,371
	Max Average CN Consumption (kg/t)	2.34	2.31	2.30	2.30	2.33	2.33	2.35
	Mean Average CN Consumption (kg/t)	2.23	2.22	2.19	2.19	2.22	2.22	2.24
	Min Average CN Consumption (kg/t)	2.09	2.09	2.03	2.03	2.07	2.08	2.10
5,000 t	**Mean Average Throughput (t)**	1,770	1,806	1,760	1,749	1,753	1,711	1,398
	Max Average CN Consumption (kg/t)	2.35	2.35	2.36	2.31	2.31	2.31	2.35
	Mean Average CN Consumption (kg/t)	2.23	2.22	2.24	2.20	2.20	2.22	2.24
	Min Average CN Consumption (kg/t)	2.09	2.08	2.09	2.04	2.05	2.08	2.10
6,000 t	**Mean Average Throughput (t)**	1,807	1,776	1,797	1,764	1,752	1,749	1,398
	Max Average CN Consumption (kg/t)	2.35	2.34	2.35	2.31	2.31	2.30	2.35
	Mean Average CN Consumption (kg/t)	2.23	2.22	2.23	2.21	2.21	2.20	2.24
	Min Average CN Consumption (kg/t)	2.09	2.09	2.09	2.04	2.05	2.05	2.10

Table 4.2.9: Summary of discrete event simulation throughputs, cyanide consumption, stage 2

Target Stockpile Level	Critical Ore Stockpile Level	0%	10%	25%	50%	75%	90%	100%
6,000 t	**Mean Average Throughput (t)**	2,578	2,546	2,508	2,496	2,496	2,483	2,031
	Max Average CN Consumption (kg/t)	2.45	2.37	2.21	2.16	2.16	2.16	2.51
	Mean Average CN Consumption (kg/t)	2.32	2.26	2.13	2.07	2.07	2.07	2.37
	Min Average CN Consumption (kg/t)	2.16	2.17	1.93	1.94	1.94	1.94	2.25
8,000 t	**Mean Average Throughput (t)**	2,590	2,551	2,531	2,491	2,488	2,446	2,014
	Max Average CN Consumption (kg/t)	2.45	2.34	2.33	2.17	2.17	2.17	2.51
	Mean Average CN Consumption (kg/t)	2.35	2.25	2.21	2.09	2.09	2.10	2.40
	Min Average CN Consumption (kg/t)	2.21	2.19	2.11	1.97	1.96	1.97	2.26
10,000 t	**Mean Average Throughput (t)**	2,591	2,553	2,549	2,531	2,510	2,451	2,031
	Max Average CN Consumption (kg/t)	2.50	2.39	2.37	2.23	2.22	2.23	2.51
	Mean Average CN Consumption (kg/t)	2.36	2.28	2.26	2.12	2.13	2.14	2.40
	Min Average CN Consumption (kg/t)	2.25	2.15	2.13	1.97	1.96	2.04	2.27

The simulation results show that it is possible to stabilize cyanide consumption by applying the new operational policies. The system achieves optimal performance in the scenario with a throughput of 1,772 tonnes per day (tpd) and an average consumption of approximately 2.23 kilograms per tonne (kg/t) for stage 1, and 2,525 tpd and 2.26 kg/t for stage 2 (Figure 4.2.11). Applying stockpile management policies is possible to find the variables values that maximize the throughput and minimize the reagent consumption.

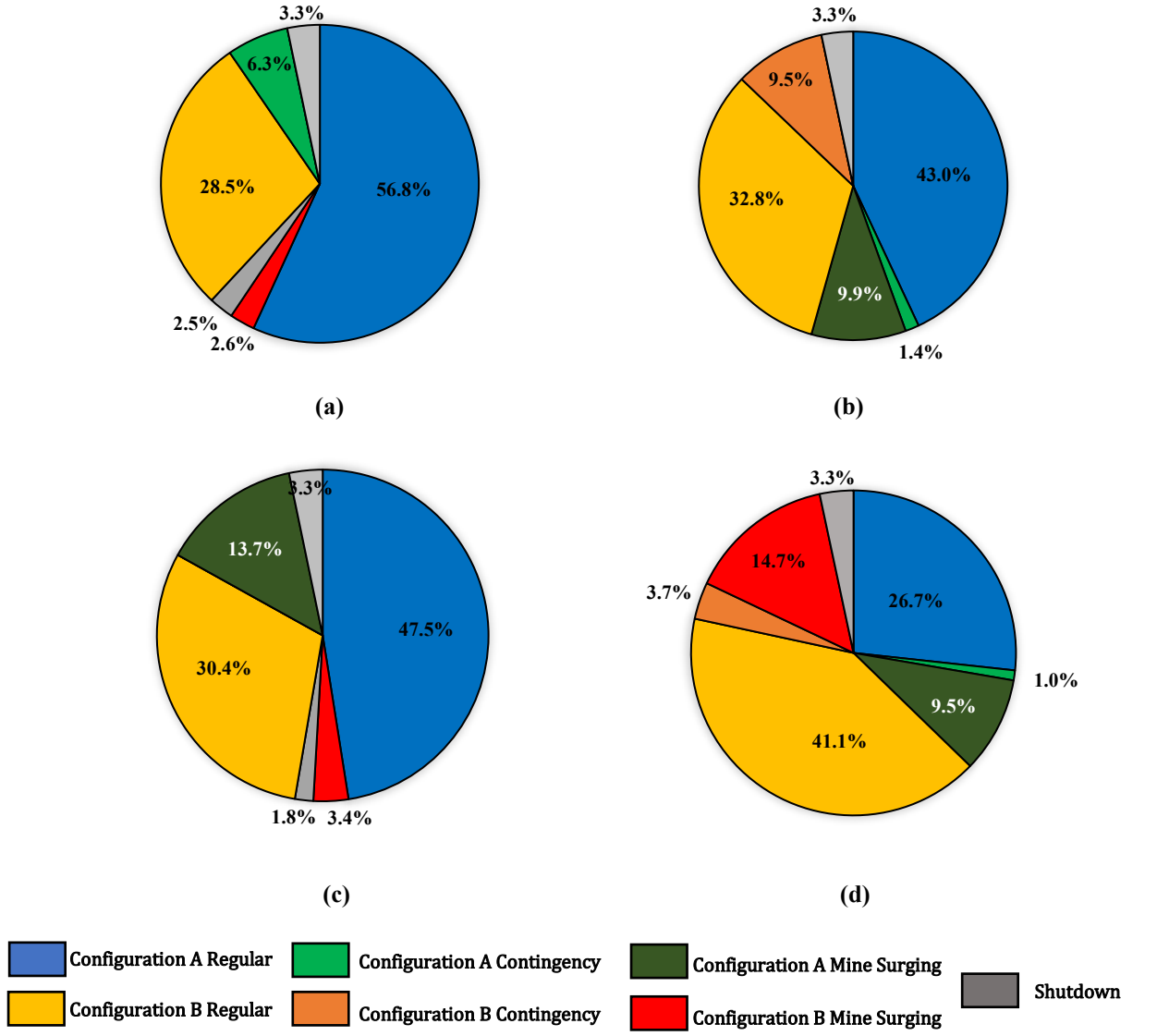

Figure 4.2.11: Time distribution of operational modes in` response to geometallurgical units with CN consumption variability, for (a) Target ore stockpile level for stage 1 of 6,000 t and Critical Ore Stockpile Level threshold of 1,500 t (25%), and (b) Stage 1 system variable configuration using a target value of 6,000 t and critical stockpile level of 4,500 t (75%). (c) Target ore stockpile level for stage 2 of 10,000 t and Critical Ore Stockpile Level threshold of 2,500 t (25%), and (ii) Stage 2 system variable configuration using a target value of 10,000 t and critical stockpile level of 7,500 t (75%).

Figure 4.2.12 summarizes the average amount of time spent in Configuration A (highly productive) versus Configuration B (replenishing mode). An appropriately set target ore stockpile level can provide additional benefits, such as longer operational plant stability periods, supported by longer periods in mode A (with time in Configuration A greater than Configuration B, Figure 4.2.9a for stage 1 and c for stage 2) compared to a lower Target Ore Stockpile Level (Figure 4.2.10b for stage 1 and d for stage 2). In this context, minimizing this control variable is an operational decision that mine managers must make, considering the effects on key performance indicators (KPIs). For instance, having a low ore stockpile level available increases the likelihood of the system experiencing frequent ore shortages.

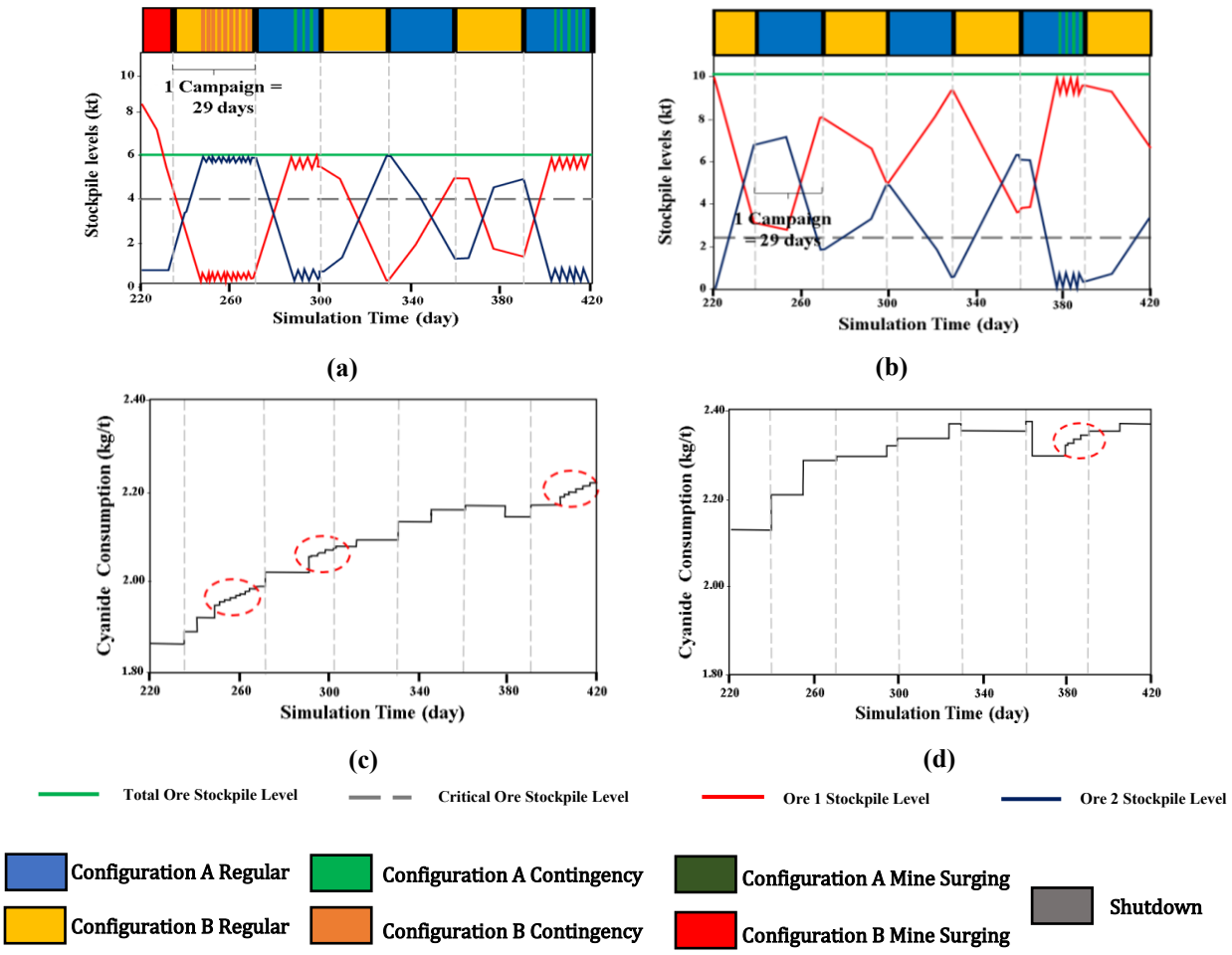

Figure 4.2.12: Cyanide consumption simulation plots are based on modes of operation, relative ore proportions, and average consumption requirement for each ore type. (a) Stage 2 simulation trial using a X= 6,000 t and Y= 4,500 t (75%), showing the continual cyanide dose adjustment (small stairs shape, dashed ovals) as a function of the short time frames between each operational mode change due to a constant shortage of one operational stockpile generating system instability. (b) Stage 2 simulation trial using a X=10,000 t and Y= 2,500 t (25%), showing a static cyanide

dose for longer periods (indicating greater system stability) as a function of the increased time spent in Configuration A.

A low target ore stockpile level forces the system to constantly change its operational configuration. This means that the cyanide dosage must be adjusted frequently over short periods (Figure 4.2.11a) to accommodate the changing ore type proportions. The system achieves greater stability by maximizing the time spent in Configuration A. This scenario allows for a stable cyanide dose over longer periods (Figure 4.2.11b), with the exception of events that require higher CN consumption due to a shortage of ore 2 (oxide ore). The lack of one of the operational stockpiles (ore 1 or 2) in combination with a low target stockpile level forces the system to enter contingency configuration more frequently, which has negative effects on throughput and uncontrolled cyanide consumption (Figure 4.2.12).

The use of stockpiles to mitigate geological variability has economic implications. In Stage 1, the total stock level has a significant influence on reagent consumption costs. As shown in Figure 4.2.13a, managing the total stockpile level can lead to lower reagent consumption, which in turn reduces overall process costs. Importantly, this reduction in stockpile levels in stage 1 does not severely impact on the performance of the plant, as shown in Table 6, and can help to decrease the operating stockpiles managing cost. For Stage 2, the total stockpile level has a lesser impact, while the critical ore stocks play a more significant role in cost reduction. By increasing the proportion of critical ore stocks to up to 50% of the total stockpile, substantial savings can be achieved, particularly in cyanide consumption. For instance, as depicted in Figure 4.2.13b, increasing the level of the critical ore can save approximately $KUSD 500 annually (assuming a cyanide price of $2.5 USD/kg of NaCN) from $MUSD 5.25 to $MUSD 4.75. This demonstrates the strategic importance of managing critical ore stockpiles to optimize costs and improve the overall efficiency of the plant.

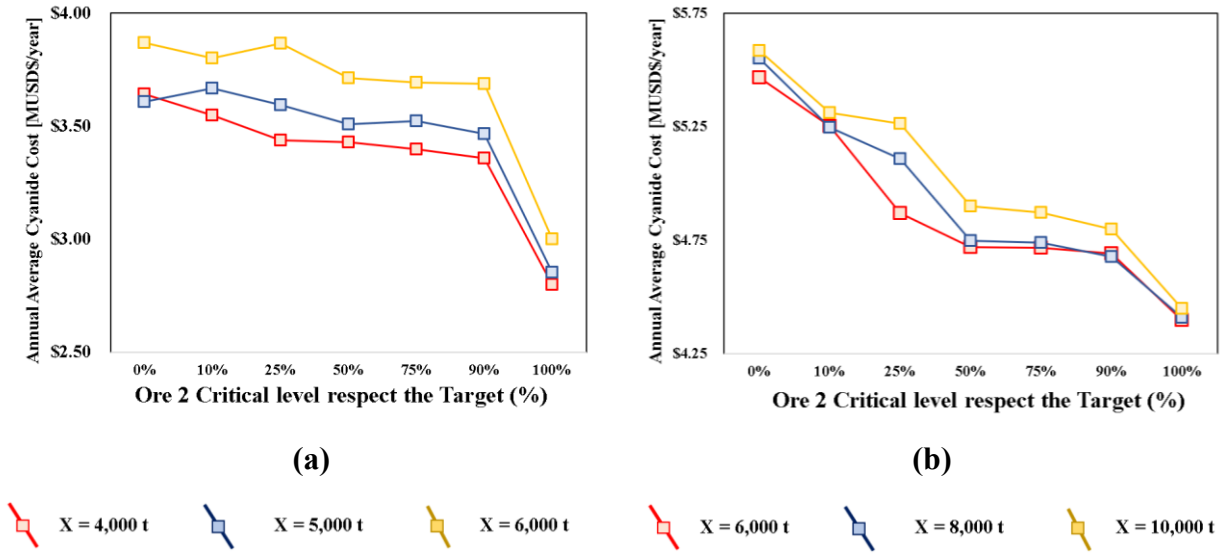

Figure 4.2.13: Annual sodium cyanide cost plots based on modes of operation, average throughput, and average cyanide consumption. (a) Stage 1 (b) Stage 2.

4.2.6 Conclusions and Future Work

Using discrete-rate simulation (DRS) trials in combination with stochastic simulations can provide better insights into cyanide consumption dynamics within a mining system by optimizing the balance of incoming ore. The use of simulations provides a reliable input to model the geological uncertainty by testing possible values from the sample dataset while honoring its probability of occurrence (histogram distribution). The addition of a mine plan schedule following the requirements of a defined mining method enables a significant contribution to improve the optimization with more realistic data that responds to the spatial variability and geological uncertainty. This can be a useful tool for decision making, especially to calculate the minimum stockpile requirements for mineral process plant stability and giving more degrees of freedom to the mine operation stages.

The target ore stockpile level (control variable X) is a significant parameter for mitigating the risk of ore shortages under geological uncertainty. It acts as a "buffer" against geological variability by providing a reserve of ore that can be used to maintain production when ore supplies are disrupted. Therefore, is important in the mine planning stages to consider the stockpile policies and include this parameter as an input of the planning process. Additionally, it is of use to take this further and consider a minimum stockpile volume which is calculated in the mine evaluation or planning stages. The Critical Ore Stockpile Level (control variable Y) is also relevant in avoiding

cascading delays in the event of an ore stockout and contributes to mineral process stability, also is vital to control the cyanide average consumption of the system. It is important to find the level that stabilizes the mining system, based in the simulations this number is at least 25% of the total stock, without this stockpile policy the system enters a constant instability that especially affects the consumption of cyanide. At the other extreme only having mineral of the critical type (in this case oxide) the system has few degrees of freedom that mainly affect the throughput.

Blending and stockpiling are effective control measures that can be used to mitigate potential operational risks, maximize mill productivity, improve overall reagent consumption, and help the plant maintain a stable process. All combined, decreasing the likelihood of unexpected events generated by harmful impurities or other geological features. This tool can be used to model reagent consumption for a mining project under evaluation, but in this case using stochastic modelling technics, it will help to make decisions based on a probabilistic input instead of a deterministic one (conventional estimation methods).

The future work is to feed the DES/DRS framework with the new modeled variables from the block model estimated (e.g., head Grades, metal recovery, hardness, filtration rates, etc.), experiment with other geostatistical technics such as direct block support simulation (DBSIM) and incorporate processing cost into the evaluation framework. Finally, evaluate this new information into the DES/DRS framework in order to obtain a simulated net present value (NPV) or cashflow.

Chapter 5

DRS Framework applied to Mining Project Evaluation

5.1 Discrete Rate Simulation for Geostatistically Informed Economical Evaluation of Narrow Vein Au-Ag Mining and Processing.

Mine project development includes irreversible long-term decisions with high costs (Savolainen et al., 2021). Additionally, price fluctuations and restricted production plans are difficulties that mining companies must face in the development of a mining project. New mining projects face several challenging risk-related aspects related to uncertainty about mineral resources, which are not present in other engineering projects (Al-Bakri, et al., 2023). The success or failure of a mining prospect is often determined by how key variables are managed and optimized while levels of risk and uncertainty are minimized. The geological characteristics of the mineral deposit, such as its size, shape, grade, and depth, play a crucial role in determining the risk of a mining project due to the high percentage of uncertainty present. Hence, implementing intelligent decision-making tools (supported by investments in data acquisition and processing) can be critical to ensuring the competitiveness of mines and new projects. In this context, developing digital platforms that incorporate stochastic simulation techniques can help to evaluate potential business opportunities, in the project evaluation (e.g. between the Exploration and Prospecting stages, Figure 5.1. 1).

Mine development includes irreversible long-term decisions with high costs (Savolainen et al., 2021). Additionally, price fluctuations and restricted production plans are difficulties that mining companies must face in the development of a mining project. New mining projects face several challenging risk-related aspects related to uncertainty about mineral resources, which are not present in other engineering projects (Al-Bakri, et al., 2023). The success or failure of a mining prospect is often determined by how key variables are managed and optimized while levels of risk and uncertainty are minimized. The geological characteristics of the mineral deposit, such as its size, shape, grade, and depth, play a crucial role in determining the risk of a mining project due to the high percentage of uncertainty present. Hence, implementing intelligent decision-making tools (supported by investments in data acquisition and processing) can be critical to ensuring the

competitiveness of mines and new projects. In this context, developing digital platforms that incorporate stochastic simulation techniques can help to evaluate potential business opportunities, in the project evaluation (e.g. between the Exploration and Prospecting stages, Figure 5.1.1).

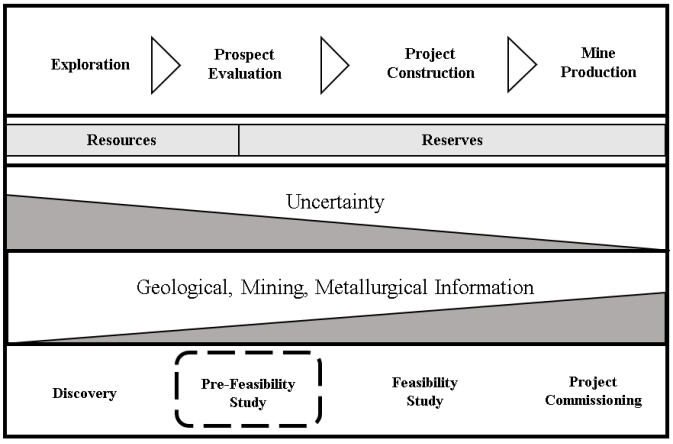

Figure 5.1.1: Mine life cycle and uncertainty related to levels of information.

The aims of the present study are to model the effects of orebody geometry in the cash flow of a mining project developing within Au-Ag narrow veins hosted in different lithologies, to estimate ore tonnage production using ore blending strategies and stockpile management policies. This is outlined in a discrete rate simulation framework implemented within the software Rockwell ARENA ©, evaluating the influence of blending and processing policies in the Net Present Value variation. This research focuses on finding alternative options to deal with unexpected variations in plant throughput.

5.1.1 Mining Economic Evaluation

Mining project evaluation assesses the performance, outcomes, and overall effectiveness of a mineral resource. Evaluations occur at different stages throughout the project lifecycle, such as during planning, production, and after project completion. In the mining project evaluation, assessing the feasibility, profitability, and potential risks associated with a deposit under study is crucial to making informed decisions and ensuring economic viability. This process involves collaboration of different technical disciplines (geology, mining, geometallurgy, and metallurgy) to obtain the economical parameters of the global process as well as to establish the viability of a business plan. Also, it is possible to incorporate sensitivity analysis into the main variables that

affect the project outcome, such as metal prices, constrained outbound supply chains, and shortages of key consumables (Bassan & Knights, 2008).

Mining project evaluation must consider quantifying and qualifying the mineral resource present in the mining project area and assessing the technical aspects, such as evaluating different mining methods based on the orebody characteristics, equipment requirements, and project infrastructure. Additionally, a comprehensive financial analysis must be completed to determine the economic viability of the project by estimating the capital costs, operating costs, and revenue projections. This financial analysis includes variables such as commodity prices, market demand, and potential risks. For a mining project evaluation, strong economic knowledge is an important complement to technical mining knowledge, in every step of the mining process (Runge, 2011). This stage demands a multidisciplinary approach, involving fields such as geology, mining engineering, economics, environmental engineering, law, and other relevant subjects. In summary, the evaluation process varies depending on the characteristics of the orebody, location, and other deposit-specific factors, and qualified professionals with expertise in mining project evaluation must be involved to ensure a thorough assessment. A feasibility study takes into account various aspects of the proposed mining project, including market analysis, technical feasibility, financial projections, operational requirements, legal and regulatory considerations, and environmental impact. Herein lies the importance of developing digital tools that can process a larger amount of data to facilitate and accelerate the process of evaluation of new projects, expansion of capacities, and re-evaluation of mineral bodies previously left out of the reserve inventory.

The standard principles of economics used generally on a broad scale are also applied to the mining industry. Four standard metrics that are well understood by economists and commonly applied to mining project evaluation are: (1) Net Present Value (NPV), (2) Rate of Return on Investment (IRR), (3) Payback Period, and (4) Competitive Cost (De la Vergne, 2008). Net Present Value is the most widespread valuation method for resource stocks and, in theory, is best suited to non-producing resource companies, given the nature of the development timeline (Perrott-Humphrey, 2011). The first step in analyzing a mining project is to determine the present value of the future cash flows it will generate and to compare this present value with the required investment [9] (Perrott-Humphrey,2011). NPV may be described as a rational attempt to put a dollar value on the mineral property (Brennan & Schwartz, 1985). An accurate definition is that NPV is the

difference between the present value of the positive and negative cash flows (also described as a measure of liquidity), discounted to the present time at a predetermined interest rate (De la Vergne, 2008).For the case study presented in this section, the calculation of the net present value incorporated results from discrete rate simulations, which extends the original variables incorporated into the framework developed by Navarra (2019) and complemented by Órdenes et al. (2022) that integrates head grades.

5.1.2 Case Study

Epithermal deposits are shallowly formed vein, stockwork, disseminated, and replacement deposits that are mined primarily for their gold and silver content, and are typically known for their high gold grades amenable to mining by underground methods. Indeed, many bulk tonnage deposits with as little as 1 part per million (ppm) gold or less are presently being exploited by open-pit mining (John et al., 2018). Epithermal Au-Ag deposits are a very important source of noble metals, commonly developed in association within volcanic arcs at convergent plate margins, as well as in intra-arc, back-arc, and post-collisional rift settings. Many important deposits are tertiary and younger in age and are concentrated mainly around the Pacific Rim (Simmons et al., 2005). Epithermal veins are a product of hydrothermal systems, which involve hot water, or other hydrothermal fluids heated by geological internal heating processes. Veins had a strong structural control, so fluids rich in gold and silver move through fractures, faults, and other permeable pathways in the host rock, forming ore bodies at relatively shallow depths, typically within 1-2 km below the surface. When these structures have suitable chemical conditions, valuable minerals like gold and silver precipitate lead to the formation of epithermal veins.

In general, epithermal deposits are associated with areas with volcanism related to active continental margins and island arches. Therefore, the rocks that commonly host this type of deposit are volcanic rocks of varied composition, as precious metal mineralization develops in zones of high paleo-permeability, hosted within sequences of coeval volcanic and underlying basement rocks (Órdenes, 2014). Also, other geological structures such as anticlines and synclines can create traps and conduits for hydrothermal fluids, concentrating mineralization in specific areas or zones. For example, the intersection of faults and folds may provide favorable sites for the formation of ore shoots. A fictional Au-Ag sub-vertical vein was modeled by SIS, and the gold and silver content was modelled using the traditional kriging estimation method. An Au-Ag leaching plant

will be fed with two different ore types (geometallurgical units classified based on host rock lithology) from the ore body, rhyolitic and andesitic hosted ore (Figure 5.1.2).

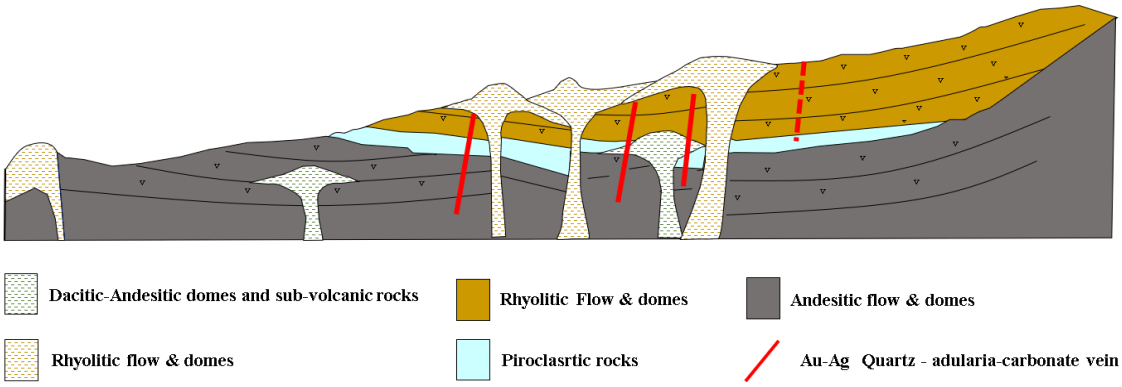

Figure 5.1.2: Schematic Geological profile of gold and silver epithermal veins hosted in volcanic complexes (Órdenes, 2014).

Based on tests of filtration and sedimentation rates (Table 5.1.1), a remarkable difference in behavior can be established between ore hosted in different types of volcanic rock. The source of clay minerals in epithermal vein systems is a combination of the alteration produced by hydrothermal fluids and their interaction with the host rock (Pirajno, 1992). The presence of hydrothermal clays will depend on the type of rock that hosts the Au-Ag-rich fluids. Warren et al. (2004) mentioned that in epithermal deposits, the replacement minerals form from conversion of precursor phases (from the host rock composition) and reflect the interaction of these precursor phases and hydrothermal fluids.

Table 5.1.1: Solid-liquid separation tests summary results.

Variable	Statistics	Andesitic Host Rock	Rhyolitic Host Rock
Filtration Rates [Ton/m^2*h]	**N° Samples**	299	1070
	Mean	1304	2320.4
	Standard Deviation	1432.7	1930.2
	Minimum	5	5
	Q1	189	675.6
	Q2	686.3	1852.9
	Q3	2098.4	3474.2
	Maximum	5558.7	7940.9
Sedimentation Velocity [Ton/h]	**N° Samples**	294	1029
	Mean	10.0	18.6
	Standard Deviation	7.4	12.3
	Minimum	0.2	0.2
	Q1	4.2	9.4
	Q2	7.7	16.8
	Q3	14.3	24.1
	Maximum	31.2	53.4

Excessive clay content can hinder the flow of materials in various processing equipment types, such as pipes, chutes, and conveyors, and the subsequent processing of ores with a high percentage of clay is a significant challenge for mineral processing engineers (Cheng & Peng, 2018). Clay properties vary widely depending on mineral composition, particle size, and surface charge. These minerals have high water absorption properties, which can lead to excessive water consumption during mineral processing. Lower settling rates of clay minerals can be attributed to their fine particle size, anisotropic particle shape, and low density, resulting in very low terminal velocities of solids. In separation methods, the presence of clay minerals can reduce the separation efficiency of minerals due to their fine particle size and adhesive nature. The presence of even a small amount of clay minerals has the potential to exacerbate the reduction of the filtration rates significantly due to the unique properties of clay minerals, such as anisotropic shape, very fine particle size, and swelling characteristics (Basnayaka et al., 2018). Clay minerals, such as montmorillonite, kaolinite, and bentonite, have small particle sizes and high surface areas, which can lead to a reduction in permeability caused by deposition of colloidal particles in porous media (a.k.a. clogging in mineral filtration systems), reducing filtration efficiency and flow rates. Very fine particles inhibit the filtration rate as they reduce the porosity and permeability of the build-up filter cake, resulting in low filterability (Besra et al., 1999). Furthermore, tailing slurries of hydrometallurgical processes can potentially reduce the efficiency of the thickening process, attributing to the lower settling rates of clay particles (McFarlane, 2005). It has been reported that smectite-group clays are detrimental due to the swelling of clay particles since swelled smectite clays have meagre settling rates and increase the viscosity of thickener underflow, causing pumping difficulties (Mpofu, 2005). Dealing with the negative effects of clays in processing can lead to lower throughput and higher operating costs. This variability can lead to inconsistent filtration performance, making achieving reliable and predictable results challenging. These costs may arise from increased maintenance, downtime for cleaning, and the need for additional filtration media or equipment.

5.1.3 Host Rock Vein Lithology Simulated by SIS

Lithology data was utilized for the application of Sequential Indicator Simulation to model the rocks that host the vein and compute thirty equiprobable realizations. The outcomes of this modeling exercise were instrumental in drawing meaningful conclusions regarding the variability

of the geometallurgical behavior observed during the solid-liquid separation stage across various ore types within the plant. In the present case study, the lithology of two veins was stochastically modeled using SIS. The first ore body is predominantly hosted in rhyolitic rock, with 61% of samples confirming a rhyolitic composition. The second ore body is primarily hosted in andesitic rock, with 57 % of samples indicating an andesite rock. To perform Sequential Indicator Simulation, a series of realizations from a random function (that shares the spatial continuity features from the collected data) are generated. These realizations are constructed by transforming measurements of rock types into binary code representations. Subsequently, variograms are computed for each distinct category, facilitating a comprehensive understanding of the spatial correlation and variability present within the lithological formations, which allowed for determination of the kriging estimation parameters necessary for the estimation of the block mode for each modelled structure. This approach enhances the predictive capabilities of the modeling process and aids in optimizing operational strategies within the plant environment. The variography of the lithology for both veins is presented in Figure 5.1.3.

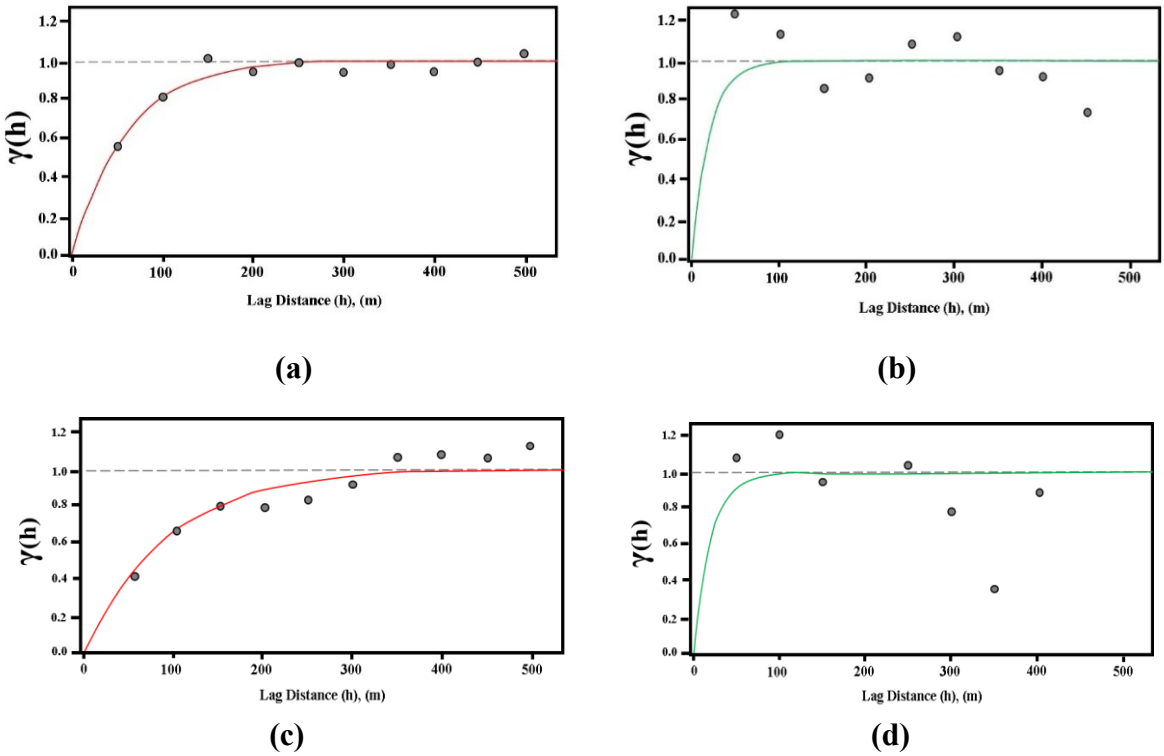

Figure 5.1.3: Lithology Variograms (a) Major range direction Variogram Vein A. (b) Minor range direction Variogram Vein B. (c) Major range direction Variogram Vein B. (d) Minor range direction Variogram Vein B.

The host rock simulations were computed using the SGEMS software, where 30 realizations were generated based on the modelling parameters assessed in the variography calculation (Figure 5.1.4) and sequential indicator simulation (SIS) algorithm. The estimation parameters for the SIS are summarized in Table 5.1.2.

Table 5.1.2: Variograms parameters host rock lithologies for vein A and B

	Vein A	
	Major	**Minor**
Ranges [m]	192	60
Azimuth/Dip [°]	0/5	180/85
	Vein B	
	Major	Minor
Ranges [m]	315	60
Azimuth/Dip [°]	0/5	180/85

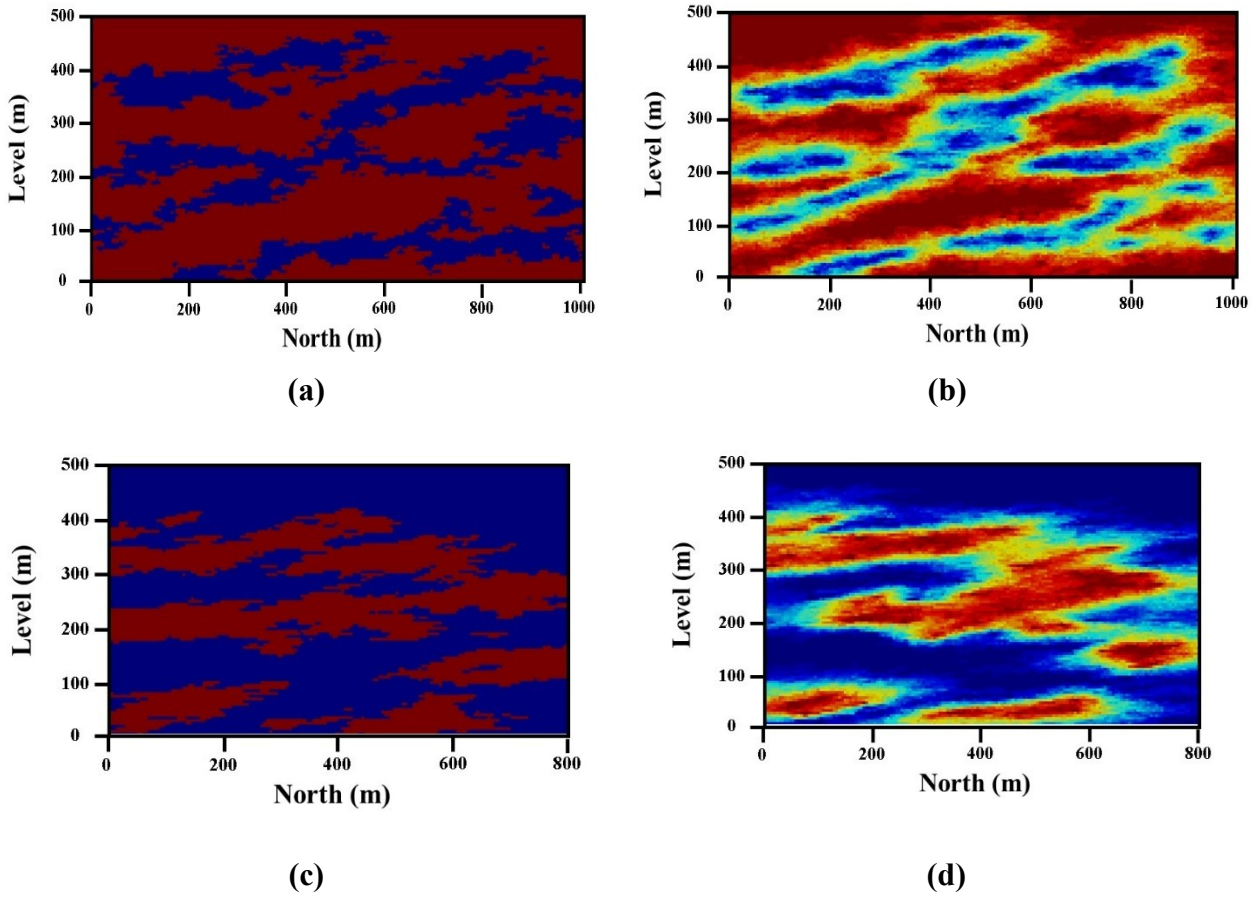

Figure 5.1.4: Veins modeled by Sequential Indicator Simulation (a) Vein A - simulation 5 (b) E-type host rock vein A (c) Vein B - simulation 1 (d) E-type host rock vein B.

Geological data was used to create a detailed resource model of two Au-Ag veins, including 3D geological and block model, in which the grades were estimated by ordinary kriging.

Table 5.1.3: Statistic summary for Au and Ag grades for vein A and B

Statistics Vein A	Au (g/t)	Ag (g/t)	Au (g/t) caped (p95)	Ag (g/t) caped (p95)
N° Samples	129	129	122	122
Mean	3.60	125.68	3.48	116.62
Standard Deviation	3.19	126.64	2.83	99.13
Minimum	2.48	87.04	2.48	87.04
Q1	0.10	5.63	0.10	5.63
Q2	1.55	49.66	1.55	49.66
Q3	2.46	87.04	2.46	87.04
Maximum	4.16	138.75	4.16	138.75
Statistics Vein B	**Au (g/t)**	**Ag (g/t)**	**Au (g/t) caped (p95)**	**Ag (g/t) caped (p95)**
N° Samples	123	123	117	117
Mean	4.79	140.28	4.27	125.29
Standard Deviation	2.52	116.20	2.92	106.05
Minimum	0.18	1.41	0.21	1.41
Q1	1.31	69.71	1.41	68.94
Q2	2.52	116.20	2.92	116.20
Q3	5.67	178.87	5.79	171.45
Maximum	63.43	571.90	16.87	355.60

The main parameters for the sub-level stoping mining method (described in Appendix A) were chosen at regular levels in intervals of 20 m. A density of 2.50 g/cm^3 was used for the volume – tonnage conversion. A 4-year feeding plan was developed based on the mining sequence for ore production scheduling, during which the rhyolitic-andesitic ore type ratio varies depending on the vein zone being mined. The cut-off grade utilized was 2.80 g/t of Aueq for reserve inventory determination. Table 4 summarizes the financial parameters used to be inputted in the discrete rate simulation framework:

Table 5.1.4: Net Present Value calculation input parameters.

Parameter	Value
Discount Rate (%)	8
Gold Price [US$/Oz]	1,150.0
Silver Price [US$/Oz]	14.00
Gold Refinery Cost [US$/Oz]	11.20
Silver Refinery Cost [US$/Oz]	0.13
Mine Cost [per ton]	63.32
Plant Cost [per ton processed]	29.42
General & Administrative Cost [per ton processed]	6.75
Gold recovery (%)	94.5
Silver recovery (%)	86.5
Initial Investment [MUSD$]	100

Block models were constructed with a standardized parent block size of 5m × 5m × 5m. Each simulation aimed to model the geometry of the two distinct geological units, as illustrated in Figure 5.1.4. These realizations depict various equiprobable distributions of lithology that serve as the host formations for the orebody under study. Simulations generate a range of lithological distributions, reflecting the inherent variability and uncertainty present in geological formations. These diverse realizations provide valuable insights into the potential spatial configurations of the host lithologies within the orebody, aiding in geological interpretation and resource estimation efforts. SIS supports a comprehensive characterization of geological units and underpins a robust modeling of orebody geometry, allowing informed decision-making in mining and exploration activities. The new contribution of the approach of the DRS framework will use stochastically generated models, as mine planning inputs will feed the discrete rate simulations developed in ARENA Rockwell © software. This paper presents a new approach to evaluating the influence of stockpile management policies to stabilize the performance of solid separation equipment such as bulk thickeners and tail filtration while maintaining mine production levels. This novel contribution tries to integrate conditional simulation techniques (Sequential indicator simulations) into long-term dynamic evaluation, and from the different scenarios, to be able to evaluate a different variable stochastically into the mining system. Based on the mining sequence, which was generated from ore production scheduling, the result was a 4-year feeding plan. During mining periods (Monthly), the rhyolitic-andesitic ore ratio varies depending on the mineral zone being mined (Figure 5.1.5).

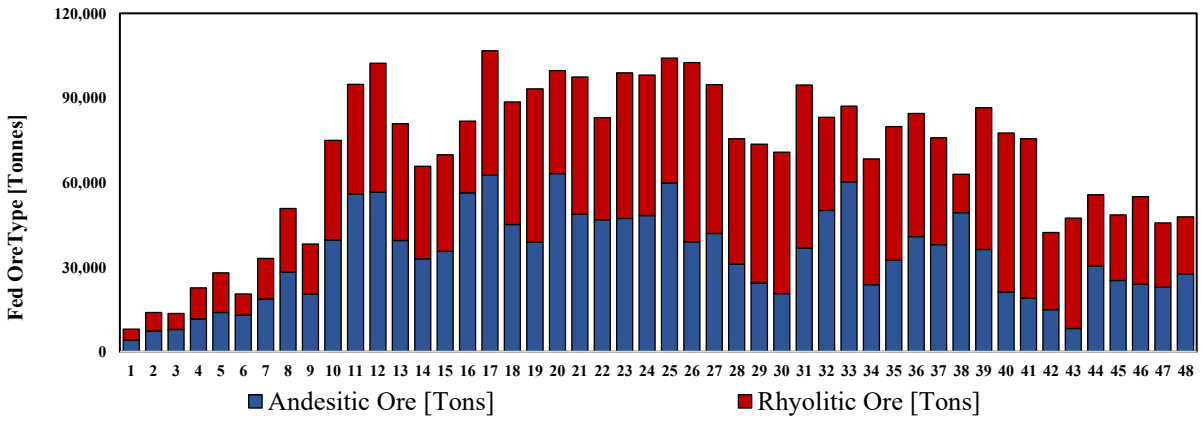

Figure 5.1.5: Deterministic ore profile based on host rock type simulated (ore types) with 48-months.

Additionally, the tonnage profile was constructed, but for this variable the projected future throughput is stochastic, based on the realizations computed under the SIS procedure. Therefore, the throughput takes the expected value (P50) of stopes extracted in a single production period measured in the simulated block model under the different scenarios. Stochastic modeling can provide a complete vision about the modelled parameter, as the 10th and 90th percentiles can be used as a potential range of variation of the ore type (Figure 5.1.6).

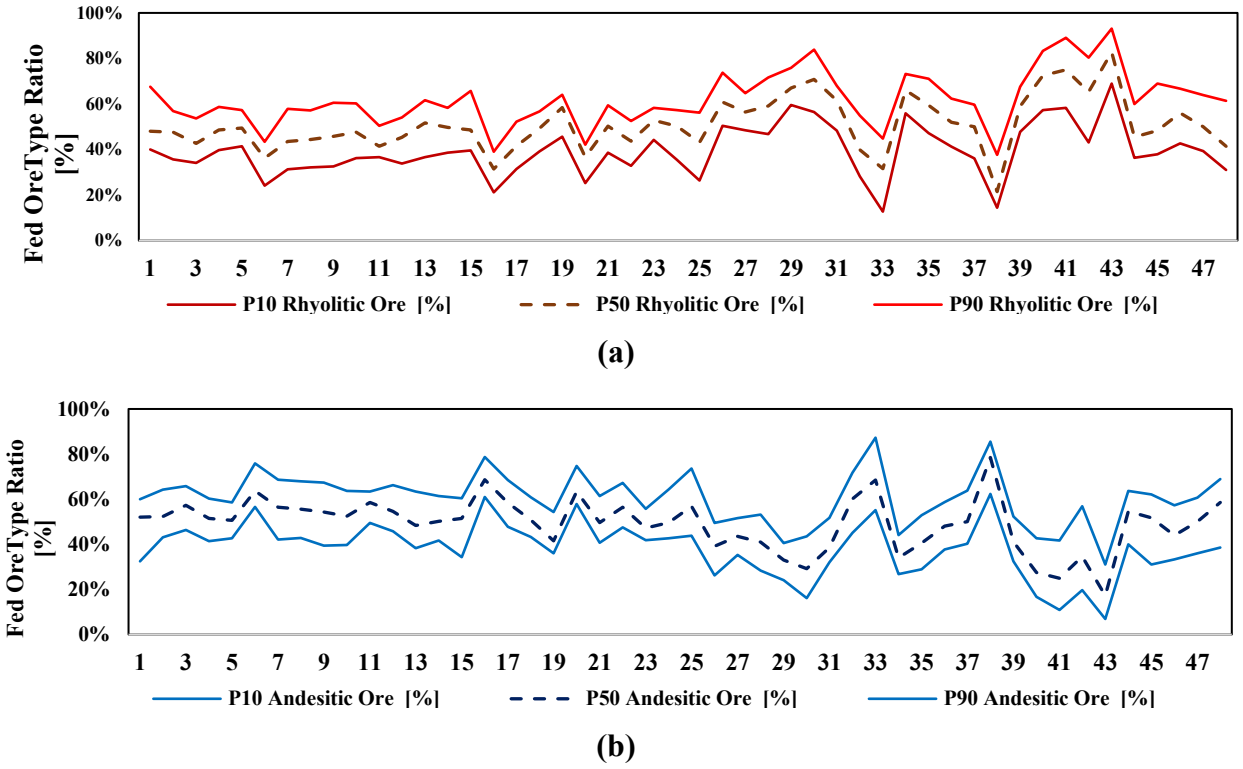

Figure 5.1.6: Mine Production Risk profile showing 10th (Lower solid), 50th (dashed) and 90th (Upper solid) percentiles for Ore percentage. (a)Rhyolitic hosted ore. (b)Andesitic hosted ore.

5.1.4 Application of the DRS Framework

The current methodology features Discrete Rate Simulation (DRS), a simple approach to dynamic mass balancing to model throughput behavior and the performance of the plant. In this context, a suitable approach might be to implement ore blending practices in tandem with alternate modes of operation to maximize plant throughput. This study highlights the implementation of a framework using discrete rate simulations as a digital tool to optimize the uncertainty related to significant mass fluctuations in ore feeds and additionally with the opportunity to directly visualize the effects in the cash flow. The framework is designed such that the processing plant acts as a

bottleneck with mining rates exceeding plant capacity. As such, monthly campaign cycles are configured in a regular schedule of 29 days of production followed by a one-day shutdown. The characteristics of the operational configuration that were used for the current set of calculations are described in Table 4. Configuration A is designed to maximize the mill capacity, using all the rhyolitic ore available (i.e. the ore with high filtration and sedimentation rate) and feeding all the ore produced in the period. In this first stage, the blending policies are designed to handle the andesitic ore that will be reached in the early mine development. Configuration B is designed to consume a larger portion of low filtration and sedimentation rate ore and at the same time help to recover the level of the critical ore in a short time frame (52% andesitic - 48% rhyolitic). Operational level decisions on when to change operational modes are made during the shutdown phase. If the level of rhyolitic ore (Ore 2) is low enough to present a potential stockout risk during the next campaign, a mode change is initiated from Configuration A to Configuration B. On the other hand, if rhyolitic ore levels are above a defined threshold following a campaign in Configuration B, the operational mode reverts to Configuration A. If stock shortage occurs during a campaign, contingency configurations are applied with a one-day duration. A contingency configuration involves that the plant can be fed with the only ore type available, depending on if the shortage is from rhyolitic or andesitic ore (Table 5.1.5).Configuration A has the highest productivity while Configuration B is considered stable and allows for stockpile replenishment and is particularly designed to allow the rhyolitic-hosted ore stockpile to recover to a higher level so that subsequently the plant can return to the most productive configuration. Both operational configurations consider blends of andesitic ore (Ore 1) and rhyolitic ore (Ore 2) in different proportions. Considering the filtration stage adapted to a high-rate filtration ore, Configuration A utilizes a larger proportion of Ore 2 compared to Configuration B. Configuration B is an operational policy designed to reestablish the levels of the critical rhyolitic ore, and this operation mode is designed to prevent large accumulation of this low filtration rate ore (Andesitic type) generating a stock of non-processable ore, decreasing the risk of a potential loss of throughput.

Table 5.1.5: Stockpile Blending Strategy for the low-rate filtration ore.

	Configuration A			Configuration B		
	Regular	Contingency	Mine Surging	Regular	Contingency	Mine Surging
Throughput (kt /day)	2,600	1,300	2,600	2,210	1,105	2,210
(%) Andesitic Hosted Ore	45	100	100	45	0	0
(%) Rhyolitic Hosted Ore	55	0	0	55	100	100

A simplified (deterministic) analysis of the optimal throughput of the simulated processing plant considers two operational policy parameters to characterize decision-making following the approach of Navarra et al. [11], based on the following system variables:

X = Target Ore Stockpile Level

Y = Critical Ore 2 Stockpile Level

The target ore stockpile level considers the sum of both ore types, and the critical Ore 2 stockpile level corresponds the level of rhyolitic ore below which Mode B will be activated at the next shutdown.

5.1.5 Results and Discussion

The results of this integrated framework that includes net present value (NPV) demonstrate its potential to evaluate the economic implications and related risk factors, under different operational configurations and stockpile management policies. Table 5.1.6 summarizes the resulting statistics produced from the stochastic simulations performed in the DRS framework developed for the study case. All dollar quantities can be taken as US dollars.

Table 5.1.6: Discrete Rate Simulations Results Summary.

Target Stockpile Level (X)	Critical Ore Stockpile Level (Y)	10%	25%	50%	75%	90%
8,000 TOSL	Mean Average Throughput (t)	2,363	2,359	2,347	2,344	2,337
	Mean Average Gold Head Grades (g/t)	2.14	2.17	2.19	2.16	2.17
	Mean Average Silver Head Grades (g/t)	59.85	60.66	61.24	60.45	60.72
	Percentile 90 NVP (MUSD$)	319.11	329.18	351.48	321.16	321.66
	Average NVP (MUSD$)	**258.97**	**260.49**	**265.73**	**262.72**	**263.59**
	Percentile 10 NVP (MUSD$)	258.97	260.49	265.73	262.72	263.59
10,000 TOSL	Mean Average Throughput (t)	2,386	2,382	2,370	2,361	2,359
	Mean Average Gold Head Grades (g/t)	2.18	2.18	2.23	2.21	2.21
	Mean Average Silver Head Grades (g/t)	60.68	61.25	62.27	61.83	61.98
	Percentile 90 NVP (MUSD$)	307.59	316.66	336.73	309.30	309.75
	Average NVP (MUSD$)	**262.18**	**263.77**	**272.67**	**271.93**	**271.59**
	Percentile 10 NVP (MUSD$)	215.50	216.51	218.74	214.43	214.48
12,000 TOSL	Mean Average Throughput (t)	2,387	2,388	2,377	2,363	2,357
	Mean Average Gold Head Grades (g/t)	2.20	2.21	2.25	2.24	2.24
	Mean Average Silver Head Grades (g/t)	61.66	61.89	62.98	62.95	62.77
	Percentile 90 NVP (MUSD$)	322.74	323.64	348.64	343.12	350.14
	Average NVP (MUSD$)	**272.25**	**269.36**	**278.59**	**277.71**	**275.61**
	Percentile 10 NVP (MUSD$)	222.34	222.44	221.53	220.92	221.70

The analysis of the dynamics of this study shows that based on the control variables, this mining system reaches the maximum throughput when the total target stockpile level is set to 12,000 tonnes (Figure 5.1.7), and the critical high filtration rate ore (Ore 2) stockpile level is set to 25% with respect to the Target Level (Y=3,000 t). Conversely, the configuration that minimizes the available stock is Target Level set on 8,000 [t] and a Critical Ore Level of 90% with respect to X (Y = 7,200 [t]).

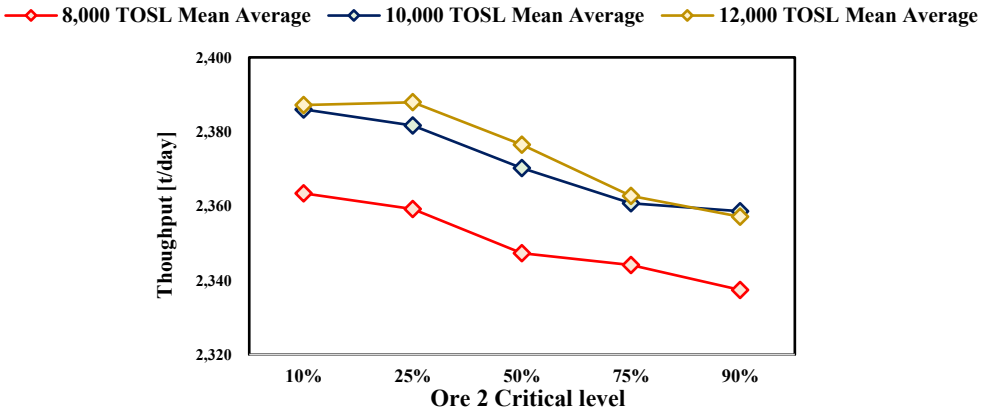

Figure 5.1.7: Throughput average results under different Target Ore Stockpile Levels.

Gold and silver head grade DRS simulation results show that the system maximize the grades in both metals when the total target inventory level is set to 12,000 tonnes (Figure 10), and the critical Ore 2 stockpile level is set to 50% with respect to the Target Stockpile Level (Y= 6,000 t). With this configuration, the mining system has an average head grade of 2.25 g/t (Figure 5.1.8a), Au and 62.98g/t Ag (Figure 5.1.8b).

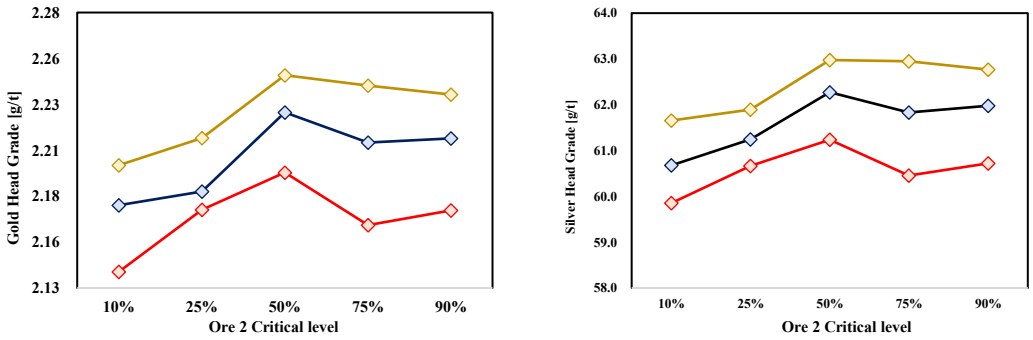

Figure 5.1.8: (a)Gold head grade average results under different Target Ore Stockpile Levels. (b) Silver head grade average results under different Target Ore Stockpile Levels.

Configuration A can suffer stockout because it consumes higher tonnages of Ore 2 faster than the replenishment rate. Likewise, a campaign in Configuration B is at risk of stockout because it consumes Ore 1 faster than the replenishment rate. If the actual replacement rates are lower than anticipated, resulting in shortages of either ore type, then the contingency modes are applied, as illustrated in Figure 11. The depletion in the inventory of one of the operational stockpiles (Ore 1 or Ore 2) in combination with a low target stockpile can make contingency configurations more likely, which can result in reductions in throughput and other complex scenarios for mineral processing like uncontrolled reagent consumption (Quelopana et al. 2023).

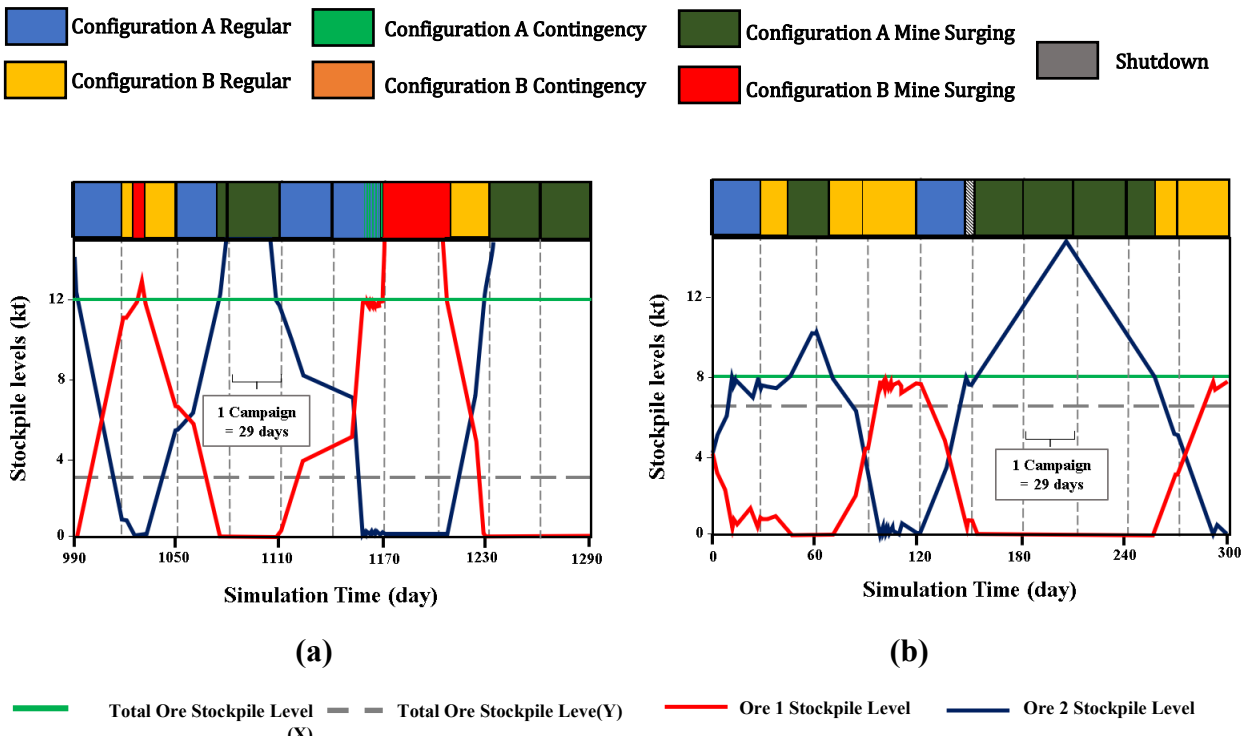

Figure 5.1.9 (a) Simulation trial using a X= 12,000 t and Y= 3,000 t (10%), %), showing longer periods (greater system stability) as a function of the longer time spent in Configuration A (b) Simulation trial using a X= 8,000 t and Y= 7,200 t (90%), showing shorter periods (lower system stability) as a function of the switching Configuration A and B, and more frequent activation of the Configuration B Contingency

Establishing an appropriate target ore stockpile level and critical ore reserve level can extend plant operational stability periods, providing complementary benefits to the mining system performance. A higher frequency of consecutive production campaigns in which the plant is configured in configuration A (total production time in configuration A > configuration B) can be achieved if a high total ore reserve is obtained with a low stock of critical ore. This combination of control variables gives the system more degrees of freedom, allowing for a longer total time in

configuration A. In contrast, setting a low target ore stockpile level in combination with a high critical ore level (90% of the total), the degrees of freedom of the system are reduced, reducing plant performance. With this setting of control variables, the system is extremely constrained and obligated to constantly change its operational configuration (Órdenes, 2022), which can lead to a lower average plant throughput (Table 5.1.6).

The maximum net present value (NPV) occurs when the system parameters are set with the Target Stockpile Level to 12,000 t and a Critical Inventory Level of 10% with respect to the target inventory level (Y = 6,000 t). With this configuration, the system reaches a maximum NPV of MUSD$278.59(Figure 12). In contrast, the configuration that obtains the lowest NPV of MUSD$258.97 is with a target inventory of 8,000 t and a critical inventory level of 90% with respect to the target inventory level (Y = 7,200 t). Results show that the NPV reaches the maximum value with a X= 12,000 t, for every Critical Ore Level (Y) value.

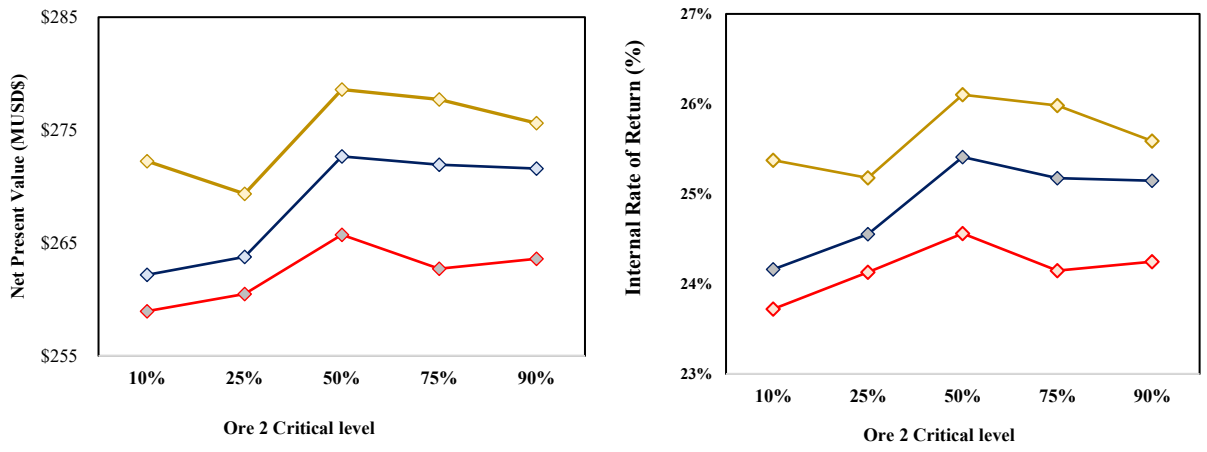

Figure 5.1. 10:(a) Net Present Value (NPV) average with different Target Ore Stockpile Levels in in $MUSD. (b) Internal Rate of Return (IRR) average under different Target Ore Stockpile Levels.

In this particular case, the critical ore stockpile level (X) impacts the average grade of ore processed in the plant. When the critical stockpile level is high represents the 50% of the total stockpile the system reaches the maximum ore grade. In the other hand, when the X level is low, the average grades of gold and silver are affected, typically resulting in a detrimental impact on the NPV. This is particularly pronounced when the critical ore level constitutes 25% or less of the total stockpile.

5.1.6 Case study Conclusions

The DES/DRS framework was developed to represent underground mining operations at an Au-Ag mine and evaluate the financial impact of the change of the ore metallurgical behavior in the solid - liquid stage. With this update, a new capability was added to the DRS framework developed by Navarra et al. (2019), directly connecting the factors that influence the NPV computations that can be used for resource evaluation and mine planning process. This new approach is especially practical for evaluating a new ore type and assessing the potential of incorporating new sectors into the mining plan. Additionally, this framework can assist in evaluating the integration of a new process in the plant and comparing its performance with the current process.

A series of simulations were run to observe the effects of the selected control variable levels on throughput and potential stockout risk, in response to geological uncertainty generated by the ore types. Within these computations the system control variable Target Ore Stockpile Level (X) is crucial in maximizing the NPV, performance of a mining project, and metal production. This variable indeed must be considered in long and mid-range mine planning due to the potential impact for mining system performance. However, the Target Stockpile Level (X) needs to be carefully estimated because the beneficial effects of increasing the target level are limited. In the A high target level can constrain the system, reducing its degrees of freedom and potentially generating a negative effect on throughput.

On the other hand, the variable of the Critical Ore 2 Stockpile Level (Y) system turns out to be relevant to maximize NPV and IRR. By controlling this level, it is possible to reach the maximum head grades; however, their increase can have negative effects on throughput. This means that the best option is to find a balance between performance and head laws to determine the optimal system configuration. If this level is too high, it will adversely affect both throughput and grades and consequently NVP. On the other hand, If the level is low, the plant can increase its throughput, but this implies meeting the higher throughput demand lower grade ore needs to be fed, rising the processing costs, reducing the revenue thereby affecting the NPV negatively.

Assessing stockpile levels by decision makers can be crucial to improving the performance of the processing plant, avoiding unexpected changes in ore behavior in the process. With an

accurate setup of these parameters, anomalous events in the process can be mitigated, such as unexpected changes in the filtration rates, and sudden increases in process impurities. The future work is related to adapting this framework to different mining systems, for example, to evaluate new technologies incorporated into a mining system such as an ore sorter or new cycles into the plants. With this new framework, it will be possible to conduct a comprehensive economic analysis, allowing for a trade-off evaluation between the current process performance and the proposed new capacity. This analysis will provide valuable insights into the overall economic benefits and potential costs associated with implementing changes to the mining operation.

Chapter 6

Discussion and Final Conclusions

6.1 DRS Frameworks applied to Underground Mining Systems

Geological variability affects mine operation and mineral processing efficiency, making its understanding essential to mining. When an engineering team begins evaluating the potential of a mining asset, ore characterization is the first and fundamental step in mining project evaluation. Variability manifests through a diversity of potential sources, including orebody geometry, mineralogical composition, lithology, rock texture, and geochemistry. Variability is particularly significant to when decisions regarding geological exploration, mining method selection, and mineral processing design. Also, directly influences the estimation the quality, quantity, and distribution of the available resources. A comprehensive understanding of these variables is vital, as it enables better management of technical issues and identification of new opportunities in developing mining projects.

The integration of different techniques, such as geological mapping, deposit sampling, three-dimensional geological modeling, and numerical simulation, allows geologists and engineers to understand the complexity of ore deposits. This understanding enables mine planning teams to develop strategies for sustainable and profitable mining and mineral processing activities, allowing for informed decisions at all stages of the mining cycle. By enhancing the understanding of an orebody's main characteristics, mining companies can improve their processes to maximize resource profitability, minimize environmental impacts, and ensure long-term operational viability. Developing tools to improve knowledge of geological variability is essential not only for resource geologists but also for all stakeholders in the mining value chain. The integration of quantitative methods into a DRS/DES framework makes it feasible to evaluate issues arising from variations in future ore body characteristics, thereby maximizing plant performance.

In the initial part of this research, Navarra's (2019) quantitative framework was expanded by introducing additional variables into the evaluation framework. This development enabled two significant contributions: (1) the integration of new data, such as geological inputs (head grades, lithology) and geometallurgical (mineral process reagents) into the DES/DRS framework (2) the visualization of the dynamics of the system of the incorporated variables. The first case study was conducted in a real operational context, specifically the Alhue Au-Ag (Pb-Zn) deposit in Chile. This study underscored the critical role of feed-blending in mitigating an unexpected increase in cyanide consumption. In this particular case, it was crucial when an increased weight fraction containing a high proportion of cyanicidal sulphides could imbalance the cyanide dosing. A proactive tactic for preventing spikes in cyanide consumption was proposed, based on geometallurgical input data, to maintain a well-defined feed strategy. Additionally, operating modes were controlled by varied blending based on operational stockpiles and clear policies for alternating between these configurations. Specific operational modes were also included in case a particular ore stockpile was not being replenished as anticipated (due to lower yields from the orebody), thus preventing the stockpile level from dropping below a critical threshold. This triggered a temporary shift to another operating mode designed to allow for stockpile replenishment while avoiding additional process complications, such as spikes in cyanide consumption. Such measures were demonstrated to lead to fewer unexpected high cyanide consumption events, thereby reducing the likelihood of these occurrences, promoting a stable feed with minimal stockout events, reducing fluctuations in reagent consumption, and enhancing operational stability at the beneficiation plant.

The second stage of this research focused on integrating the quantitative framework with block models developed using stochastic simulation methods. As detailed in Chapters 2 and 3, this approach, derived from the Monte Carlo method, enabled the generation of multiple equiprobable realizations of geometallurgical variables, notably cyanide consumption and other geometallurgical variables that can have a detrimental effect in the mineral process, as demonstrated in this thesis. This integration allowed the DES/DRS framework to be directly informed by simulated block models, representing an expansion of Navarra's (2019) framework by incorporating data from three-dimensional geological models.

The current work also incorporated financial variables, specifically net present value (NPV) and internal rate of return (IRR), into the framework presented in this thesis. This new integration allows for the early visualization of how different geometallurgical variables influence key financial performance indicators. By utilizing this digital development, it becomes possible to iterate and identify the areas where the greatest risks affecting the mining business lie. As a result, the tool enables a more informed allocation of resources, allowing for targeted and efficient characterization of the deposit, thereby optimizing decision-making and mitigating risks in mining projects. In this same context, having a virtual model of the process that incorporates financial indices provides a powerful tool for iterating in response to fluctuations in uncontrolled variables, such as metal prices, which could jeopardize a project's profitability. With this framework, potential adjustments to the project—such as re-evaluating production plans or modifying processes in response to new metal price projections—can be quickly and effectively evaluated. The integration of financial indices into the DRS framework not only enhances adaptability to volatile market conditions but also ensures that projects under evaluation can be optimized efficiently.

Additionally, this study demonstrated the utility of DRS/DES simulations, informed by different data sources, in optimizing the balance of incoming ores with varying metallurgical behaviors. This approach not only improves the efficiency of mineral processing but also contributes to more informed and strategic decision-making in mining operations, effectively addressing operational concerns. The ability to visualize a variable dynamic directly from the block model offers a significant comparative advantage, enhancing the understanding of the variable behavior under a specific (or deterministic) mining plan. This facilitates management through simulations to explore better alternatives and make informed decisions regarding geometallurgical or other variables.

Moreover, it enables feedback on stockpile management policies and ore blending strategies, which is crucial to maintaining overall system performance or ensuring that any necessary adjustments are based on solid technical foundations. This enhanced quantitative framework can now incorporate data from different sources, for instance early-stage sampling campaigns and use this information for pre-feasibility studies, and also incorporate more detailed geological information from block models developed through different stochastic simulation methods, such

as sequential Gaussian simulations (SGS), sequential indicator simulations (SIS), the turning bands method (TBM), or block support simulation (DBSIM). Such simulations enable the evaluation of different scenarios, significantly reducing the risks associated with processing ore at the beneficiation plant. Utilizing these detailed analyses allows for the development of effective control strategies along the mine-plant profile, thus optimizing the performance of the mineral processing stage. Incorporating additional variables, such as energy consumption, that significantly impact economic profitability enhances the utility of simulation techniques. These simulations enable the exploration of various system scenarios, aiding in the visualization of risks that encompass multidisciplinary aspects, which is crucial for evaluating the sustainability of mining projects. Understanding system dynamics can help improve the handling of harmful contaminants, optimize mineral process reagents (e.g., cyanide consumption as studied in this sequence of works), improve process water management, and decrease carbon footprint (i.e., optimize energy consumption).

The integration of predictive models from geometallurgical sampling can significantly enhance decision-making and planning processes in mining operations. To generate these predictive models, systematic sampling campaigns and detailed laboratory analyses are essential. However, these processes are often time-consuming and costly, requiring substantial resources to achieve a degree of predictive accuracy that allows for informed decision-making. In many cases, these models are generated deterministically, which can introduce potential risks, especially when decisions are made, and the project is already underway. Such risks may arise from unforeseen variability or inaccuracies in the models. With the development of this digital tool, it becomes possible to model different scenarios, offering a more flexible and risk-aware approach.

By utilizing an extensible simulation framework prior to the approval of metallurgical studies, this tool raises a better interaction with management, which can lead to the approval of additional resources for new studies. Moreover, this approach allows for continuous improvement of the simulation framework, as it can incorporate new models and sub-models over time. As a result, decision-makers benefit from more detailed and accurate simulations, reducing risk and improving the overall planning and execution of mining projects. In context, here lies the value of this contribution, with the possibility of compute different and more complex scenarios while the

amount of information grows during the drilling campaigns and geological sampling, a making decision related of the following campaigns, exploration or mine expansions.

A promising direction for future research linked to these developments is the utilization of simulation results as inputs for automated control and dosing systems for reagents (e.g., cyanide, sulfuric acid, lime). A refined understanding of the dynamics of various key system indicators makes it possible to identify potential risks affecting these critical variables, both at the strategic level (for long-term planning) and at the tactical level (for short-term planning). Furthermore, the scope of simulations can be expanded to include estimates of a plant's projected operating costs.

Future work involves incorporating additional variables, modeled from block model estimates, such as metal recovery, hardness, and seepage rates, into the current framework. Many of these geometallurgical variables are more complex to model, and traditional geostatistical methods like kriging may not be sufficient to capture their intricacies. Kriging, being a linear estimator, has limitations when it comes to modeling nonlinear interactions and multifractal behaviors that are often observed in natural geological phenomena. To enhance the capabilities of the framework presented in this thesis, it will be necessary to explore alternative geostatistical modeling methods, such as higher-order statistics. Unlike traditional kriging, higher-order geostatistics incorporates higher-order moments (such as skewness and kurtosis) and considers complex, nonlinear spatial relationships between variables. These methods can capture intricate spatial patterns and interactions that kriging might miss, providing a more accurate representation of geological and geometallurgical variability.

This holistic approach not only ensures economic efficiency but also enhances environmental sustainability and operational stability. This model can be improved by incorporating methodologies that account for mining operation uncertainties such as equipment performance failures and equipment scheduling (including drilling, loading and hauling, underground rock support, etc.). For instance, the output from a stochastic mine plan can be integrated into a discrete event/rate simulation framework to evaluate its performance under various operational scenarios. This integration can help identify potential bottlenecks or inefficiencies within the mine plan. Although stochastic mine planning and discrete event simulations focus on different aspects—the former on broader strategic planning and the latter on detailed operational processes—they work

synergistically to provide a comprehensive approach to managing mine operations under uncertainty. This whole picture point of view approach not only improves operational efficiency but also enhances decision-making, ensuring more resilient and adaptive mining operations.

The integration of artificial intelligence (AI) and automation in mining operations is of increasing interest within the mining industry and represents a new field of research. The integration of the framework developed for the mining context with artificial intelligence (AI) opens up a wide range of possibilities for enhancing efficiency in planning, operations, occupational safety, and environmental sustainability. By leveraging artificial intelligence analytical and predictive capabilities, this relationship can lead to smarter, resilient, and environmentally responsible mining operations. AI is particularly useful in mining, allows utilizing extensive amounts of data from diverse sources such as sensor readings, engineering reports, and maintenance logs to improve operational efficiency and decision-making. For instance, Wilson et al. (2022) implemented an artificial neural network within a DES framework to assess system performance across a conceptual regionalized mine-to-mill profile, specifically targeting marginal underground gold mining operations. Similarly, Peña-Graf et al. (2022) developed a framework that combines discrete event simulation with a customized machine learning (ML) model for ore type classification, which subsequently informed the design of stockpile management policies and discrete event simulations. While the potential for AI and automation in mining is substantial, the actual implementation of these technologies is still in development. Many mining companies are currently in the experimental phase of adopting AI applications. The successful integration of AI in mining will require significant investments in data management, computer capability, training, and potential changes to mining processes.

6.2 Final Conclusions

Ore is a multi-component, inherently complex and exhibits great variability due to their geological characteristics. Changes in mineralogy during mineral processing can have significant effects on the efficiency and results of the plant. For instance, rock texture and the presence of some mineral phases affect flotation circuits, clays are complex in the dewatering because their water-holding properties that decrease the efficiency of the solid-separation process; impurities can lead to higher reagent consumption affecting the leaching stage. Understanding these changes

and their impacts is crucial to optimizing mineral processing operations, reducing costs and potential environmental impacts. It is highly likely that in an operating mine there will be significant variations in the ore characteristics during its mine life. This information is critical to designing more effective and efficient processing methods, which can be tailored to the specific requirements of each type of ore. These insights also enable the development of predictive models that anticipate how minerals will behave in various processing scenarios, thereby reducing the risks associated with variability and improving overall operational efficiency in mining projects. Herein lies the main objective achieved in this thesis, it is the development of quantitative tools that allow informed decisions to be made to deal with the complexities related to significative changes in the characteristics of the minerals that will enter the processing plant.

The quantitative discrete events/rates framework developed in this research was linked with block models using geostatistical techniques such as stochastic simulation (Sequential Gaussian and Sequential Indicator Simulations). This integration enables a dynamic system evaluation informed by three-dimensional data, honoring the spatial distribution and geological characteristics of the ore body. This framework also allows for more flexible use of different types of data, which are often underutilized due to a lack of adequate processing tools. Additionally, it can be used to evaluate critical variables for mining operations and mineral processing. The framework facilitates the processing of geological data and enables the use of the results for operational decision-making, with the potential to extend to higher decision-making levels.

This platform has the potential to merge different methodologies, relate results to various stages of the process, identify bottlenecks in the production chain, and visualize future risks due to significant changes in the geological characteristics and mineral processing variables of the ore body. The integration of technologies that efficiently, quickly, and reliably process a mining operation’s data can significantly impact business outcomes, process optimization, and contribute to reducing the environmental impacts of mining activities.

The DES/DRS framework can serve as a valuable tool for guiding exploration, continuous improvement, and reengineering projects. Its results can facilitate informed decision-making for drilling campaigns, the purchase of new equipment or the resizing of existing equipment, and/or significant modifications in the mineral process. As mentioned, the global transition to clean

energy sources and the projected costs of the necessary materials have initiated a race to obtain the various primary materials needed to achieve the ambitious goal of carbon neutrality. Therefore, the diversity of materials (different elements, types of deposits) and the prospect of a growing number of new projects—whether in exploration, operation, or re-evaluation of old mines—give this framework significant potential to expand in multiple directions. This scenario necessitates flexible tools that enable faster decision-making to greenlight projects. In this context, quantitative tools like the one presented in this thesis can be instrumental in helping mining companies streamline and enhance their analysis and evaluation of mining projects.

References

Al-Bakri, A., Ahmed, H., Ahmed, H., & Hefni, M. (2023). Evaluation studies of the new mining projects. Open Geosciences, 15(1), 20220466. https://doi.org/10.1515/geo-2022-0466

Aghamirian, M. (1997). Reactivity of sulfide minerals and its effect on gold dissolution and its electrochemical behaviour in cyanide. Kingston, Ontario, Canada: Queen's University.

Alabert, F. (1987). The practice of fast conditional simulations through the LU decomposition of the covariance matrix. Mathematical Geology, 19(5), 369-386.

Alpagut, M., & Çelebi, N. (2003). System dynamics applications in the mining industry. In 181 International Mining Congress and Exhibition of Turkey-IMCET 2003 (pp. 181–186). ISBN 975-395-605-3.

Altiok, T., & Melamed, B. (2007). Output analysis. In Simulation modeling and analysis with Arena (Chap. 4, pp. 55–64). Elsevier.

Anderson, E. (2021). On-line metallurgical mass balancing and reconciliation (Master's thesis, Umeå University, SE-901 87 Umeå, Sweden). Department of Physics.

Anderson, T., & Darling, D. (1954). A test of goodness of fit. Journal of the American Statistical Association, 49(268), 765–769.

Araya, J. (2001). Informe geológico y evaluación de recursos distrito minero Alhué (Memoria de Título, Universidad de Chile, Santiago, Chile).

Ascough, J., Green, T., Ma, L., & Ahjua, L. (2005). Key criteria and selection of sensitivity analysis methods applied to natural resource models. In Proceedings of MODSIM 2005 International Congress (pp. 170-176).

Awuah-Offei, K., Osei, B., & Askari Nasab, H. (2011). Modeling truck-shovel energy efficiency under uncertainty. Research Report Three 2010/2011, Mining Optimization Laboratory (MOL), paper 301, 171-190.

Baccini, P., & Brunner, P. (1991). Metabolism of the anthroposphere. Springer.

Bai, T., & Tahmasebi, P. (2022). Sequential Gaussian simulation for geosystems modeling: A machine learning approach. Geoscience Frontiers, 13(1). https://doi.org/10.1016/j.gsf.2021.101001

Bala, B., Fatimah, M., & Kusairi, M. (2017). System dynamics: Modelling and simulation. Springer Singapore. https://doi.org/10.1007/978-981-10-2045-2

Balusa, B., & Gorai, A. (2019). A comparative study of various multi-criteria decision-making models in underground mining method selection. Journal of The Institution of Engineers (India): Series D, 100(1), 105–121. https://doi.org/10.1007/s40033-018-0165-7

Basnayaka, L., Subasinghe, N., & Albijanic, B. (2018). Influence of clays on fine particle filtration. Applied Clay Science, 156, 45-52. https://doi.org/10.1016/j.clay.2018.01.008

Bassan, J., & Knights, P. (2008). Application of advanced analytics in mining - Safer, smarter, sustainable operations. In Australian Mining Technology Conference.

Besra, L., Sengupta, D. K., & Roy, S. K. (1999). Particle characteristics and their influence on dewatering of kaolin, calcite and quartz suspensions. International Journal of Mineral Processing, 59, 89–112. https://doi.org/10.1016/S0301-7516(99)00025-0

Beucher, H., & Renard, D. (2016). Truncated Gaussian and derived methods. Comptes Rendus Geoscience, 348(7), 510-519. https://doi.org/10.1016/j.crte.2015.11.006

Brackebusch, F. (1992). Cut-and-fill stoping. In H. L. Hartman (Ed.), SME Mining Engineering Handbook (2nd ed., pp. 1743-1748). Society for Mining, Metallurgy, and Exploration.

Brailsford, S., & Hilton, N. (2001). A comparison of discrete event simulation and system dynamics for modelling health care systems. In J. Riley (Ed.), Planning for the future: Health service quality and emergency accessibility. Operational Research Applied to Health Services (ORAHS), Glasgow Caledonian University.Biermé, H., Moisan, L., & Richard, F. 2015. A

Turning-Band Method for the Simulation of Anisotropic Fractional Brownian Fields. *Journal of Computational and Graphical Statistic*s, 24(3), pp. 885–904.

Birol, F. (2022). The role of critical minerals in clean energy transitions. IEA, Paris, France.

Bluekamp, P. (1981). Block cave mining at the Mather Mine. In D. R. Stewart (Ed.), Design and operation of caving and sublevel stoping mines (pp. 321-327). SME-AIME.

Boom, R., Twigge-Molecey, C., Wheeler, F., & Young, J. (2015). Metallurgical plant design. Canadian Institute of Mining, Metallurgy and Petroleum.

Brady, B., & Brown, E. (1999). Rock mechanics for underground mining. Chapman and Hall.

Brennan, M., & Schwartz, E. (1985). Evaluating natural resource investments. The Journal of Business, 58(2), 135-157. https://doi.org/10.1086/296294

Brewis, A. (1995). Narrow vein mining 1: Steep veins. Mining Magazine, 173, 116-130.

Brillinger, D. R., & Rosenblatt, M. (1967). Computation and interpretation of k-th order spectra. In Spectral analysis of time series (pp. 189-232).

Brooker, P. (1985). Two-dimensional simulation by turning bands. Mathematical Geology, 17(1), 81-90. https://doi.org/10.1007/BF02099949

Bueno, M., Foggiatto, B., & Lane, G. (2011). Geometallurgy applied in comminution to minimize design risk. Ausenco, 144 Montague Road, South Brisbane, Australia.

Bullock, R. L. (2011). Room-and-pillar mining in hard rock. In P. Darling (Ed.), SME mining engineering handbook (3rd ed., pp. 1327-1338). Society for Mining, Metallurgy, and Exploration.Brunner, P. H.; & Rechberger, H. 2004. Practical Handbook of Material Flow Analysis; CRC Press/LewisPublishers: Boca Raton, FL.

Cai, Y., Xing, Y., & Hu, D. (2008). Review of sensitivity analysis. Journal of Beijing Normal University (Natural Science), 1, 9-16.

Caers, J., & Zhang, T. (2004). Multiple-point geostatistics: A quantitative vehicle for integration of geologic analogs into multiple reservoir models. In Integration of outcrop and modern analog data in reservoir models.

Camprubí, A., Gonzales-Partida, E., Levresse, G., Tritlla, J., & Carrillo-Chávez, A. (2006). Depósitos hidrotermales de alta y baja sulfuración: Una tabla comparativa. Boletín de la Sociedad Geológica Mexicana, LVI(N1), 10-18.

Cardozo, F., Petter, C., & Rodrigues, N. (2022). Monte Carlo simulation risk analysis for underground mining projects. Tecnologia em Metalurgia, Materiais e Mineração, 19.

Carter, W., & Aliste, N. (1962). Geology and ore deposits of the Ñilhue quadrangle, Aconcagua province. Boletín Instituto Investigaciones Geológicas, 189.

Cavalcante, I. M., Frazzon, E. M., Forcellini, F. A., & Ivanov, D. (2019). A supervised machine learning approach to data-driven simulation of resilient supplier selection in digital manufacturing. International Journal of Information Management, 49, 86-97. https://doi.org/10.1016/j.ijinfomgt.2019.03.004

Chen, X., & Peng, Y. (2018). Managing clay minerals in froth flotation—A critical review. Mineral Processing and Extractive Metallurgy Review. https://doi.org/10.1080/08827508.2018.1433175

Chilès, J., & Delfiner, P. (1999). Geostatistics: Modeling spatial uncertainty. Wiley Series in Probability and Statistics.

Chilès, J., & Delfiner, P. (2012). Geostatistics: Modeling spatial uncertainty (2nd ed.). Wiley Series in Probability and Statistics.

Chiquini, A. (2018). Mineral resources evaluation with mining selectivity and information effect (Master's thesis, University of Alberta, Department of Civil and Environmental Engineering).

Coddington, P. D. (1993). Analysis of random number generators using Monte Carlo simulation. Northeast Parallel Architectures Center, Syracuse University, 111 College Place, Syracuse, NY, U.S.A.

Copco, A. (2007). Mining methods in underground mining (2nd ed.). Atlas Copco, Sweden.

Corbett, G., & Leach, T. M. (1998). Southwest Pacific Rim gold-copper systems: Structure, alteration, and mineralisation. Economic Geology, Special Publication, 6.

Cotton, W. B. (1998). Geology and ore deposits of the Maqui Vein, Alhué Mining District, Coast Range of Central Chile (Master's thesis, University of Colorado).

Dai, H., Li, N., Wang, Y., & Zhao, X. (2022). The analysis of three main investment criteria: NPV, IRR, and payback period. In Proceedings of the 2022 7th International Conference on Financial Innovation and Economic Development (pp. 185-189). Atlantis Press. https://doi.org/10.2991/aebmr.k.220307.028

Damiron, C., & Krahl, D. (2015). A global approach for discrete rate simulation. In Proceedings of the Winter Simulation Conference.

Damiron, C., & Nastasi, A. (2008). Discrete rate simulation using linear programming. In Proceedings of the Winter Simulation Conference (pp. 740-749).

Darling, P. (2011). SME mining engineering handbook (3rd ed.). Society for Mining, Metallurgy, and Exploration (SME), U.S.A.

Davis, M. W. (1987a). Production of conditional simulations via the LU triangular decomposition of the covariance matrix. Mathematical Geology, 19(2), 91–98.

Dehghani, H., Ataee-pour, M., & Esfahanipour, A. (2014). Evaluation of the mining projects under economic uncertainties using a multidimensional binomial tree. Resources Policy, 39, 124-133. https://doi.org/10.1016/j.resourpol.2013.12.001De Iaco, S. & Maggio, S. 2011. Validation Techniques for Geological Patterns Simulations Based on Variogram and Multiple-Point Statistics. Math Geosci 43, pp. 483–500.

De la Vergne, J. (2008). Hard rock miner's handbook (3rd ed.). McIntosh Engineering.

Deutsch, C. (1992). Annealing techniques applied to reservoir modeling and the integration of geological and engineering (well test) data (Ph.D. thesis). Stanford University, Stanford, California.

Deutsch, C. V. (2002). Geostatistical reservoir modeling. Oxford University Press.

Deutsch, C. V., & Cockerham, P. W. (1994). Practical considerations in the application of simulated annealing to stochastic simulation. Mathematical Geology, 26(1), 67-82. https://doi.org/10.1007/BF02065873

Deutsch, C. V., & Journel, A. G. (1992). GSLIB: Geostatistical software library and user's guide. Oxford University Press.

Deutsch, C. V., & Journel, A. G. (1997). GSLIB: Geostatistical software library and user's guide (2nd ed.). Oxford University Press.

Deutsch, C. V., & Journel, A. G. (1998). GSLIB: Geostatistical software library and user's guide (2nd ed.). Oxford University Press.

Deutsch, C. V., & Wang, L. (1996). Hierarchical object-based stochastic modeling of fluvial reservoirs. Mathematical Geology, 28(7), 857-880. https://doi.org/10.1007/BF02065988

Devore, J. L. (2011). Inferences based on two samples. In Probability and statistics for engineering and the sciences (8th ed., pp. 345–390). Cengage Learning.

Devore, J. L. (2011). The analysis of variance. In Probability and statistics for engineering and the sciences (8th ed., pp. 391–418). Cengage Learning.

Dimitrakopoulos, R., & Fonseca, M. B. (2003). Assessing risk in grade-tonnage curves in a complex copper deposit, Northern Brazil, based on an efficient joint simulation of multiple correlated variables. Application of Computers and Operations Research in the Minerals Industries. South African Institute of Mining and Metallurgy.

Dimitrakopoulos, R., Mustapha, H., & Erwan, G. (2010). High-order statistics of spatial random fields: Exploring spatial cumulants for modeling complex non-Gaussian and non-linear phenomena. Mathematical Geosciences, 42(5), 565-589. https://doi.org/10.1007/s11004-010-9298-3

Dindarloo, S., & Siami-Irdemossa, E. (2016). Merits of discrete event simulation in modeling mining operations. In SME Annual Meeting (Feb. 21-24), Phoenix, AZ.

Dominy, S. C., Annels, A., Camm, G., Cuffley, B., & Hodkinson, P. (1999). Resource evaluation of narrow gold-bearing veins: Problems and methods of grade estimation. Mining Technology IMM Transactions Section A, 108, 52-70.

Dominy, S. C., Phelps, R. F. G., Sangster, C. J. S., & Camm, G. S. (1998). Shrinkage stoping of narrow veins—Problem or profit? In R. K. Singhal (Ed.), The 7th Mine Planning and Equipment Selection (pp. 105–110). Calgary, Canada.

Doran, P. (2013). Chapter 4 - Material balances. In P. M. Doran (Ed.), Bioprocess engineering principles (2nd ed., pp. 87-137). Academic Press.

Driss, G., Addaim, A., & Abdessalam, A. (2018). Enhanced Box-Muller method for high-quality Gaussian random number generation. International Journal of Computing Science and Mathematics, 9(287). https://doi.org/10.1504/IJCSM.2018.10013648

Dungan, J. L. (1999). Conditional simulation. In A. Stein, F. van der Meer, & B. Gorte (Eds.), Spatial statistics for remote sensing (pp. 135–152). Kluwer.

Emanuele, B. (2006). Measuring uncertainty importance: Investigation and comparison of alternative approaches. Risk Analysis, 26(5), 1337-1353. https://doi.org/10.1111/j.1539-6924.2006.00811.x

Emery, X. (1984). The turning bands method for simulation of random fields using line generation. Centre de Géostatistique, Fontainebleau, France.Emery, X., 2006. A disjunctive kriging program for assessing point-support conditional distributions. Computers & Geosciences 32 (7), pp. 965–983.

Emery, X. (2008). A turning bands program for conditional co-simulation of cross-correlated Gaussian random fields. Computers & Geosciences, 34(1), 1850–1862. https://doi.org/10.1016/j.cageo.2008.02.003

Engelbrecht, A. P., Cloete, I., & Zurada, J. M. (1995). Determining the significance of input parameters using sensitivity analysis. In J. Mira & F. Sandoval (Eds.), From natural to artificial neural computation (Vol. 930, pp. 403-412). Springer. https://doi.org/10.1007/3-540-59497-3_168

Fahl, S. (2017). Benefits of discrete event simulation in modeling mining processes (Master's thesis, University of Alberta, Edmonton, Canada).

Ferguson, K. D., & Erickson, P. M. (1988). Pre-mine prediction of acid mine drainage. In W. Salomons & U. Förstner (Eds.), Environmental management of solid waste (pp. 24–41). Springer.

Fogg, G., Lucia, F., & Sengen, R. (1991). Stochastic simulation of inter-well scale heterogeneity for improved prediction of sweep efficiency in a carbonate reservoir. In L. Lake, H. Caroll, & P. Wesson (Eds.), Reservoir characterization II (pp. 355-381). Academic Press.

Fowler, A., & Davis, C. (2011). Quantifying uncertainty in a narrow vein deposit: An example from the Augusta Au-Sb mine in Central Victoria, Australia. In 8th International Mining Geology Conference 2011.

Galli, A., Beucher, H., Le Loc'h, G., Doligez, B., & others. (1994). The pros and cons of the truncated Gaussian method. In Geostatistical simulations (pp. 217-233). Springer. https://doi.org/10.1007/978-94-015-8264-4_15

Gbadam, E.; Awuah-Offei, K. & Frimpong, S. (2015). Investigation into Mine Equipment Subsystem Availability and Reliability Data Modeling Using Discrete Event Simulation, Society for Mining, Metallurgy and Exploration.

Giel, R., Plewa, M., & Mlynczak, M. (2017). Analysis of picked up fraction changes on the process of manual waste sorting. Procedia Engineering, 178, 349-358. https://doi.org/10.1016/j.proeng.2017.01.073

Glacken, I. (1996). Change of support by direct conditional block simulation. In Fifth International Geostatistics Congress, Wollongong.

Goovaerts, P. (1996). Kriging vs. stochastic simulation for risk analysis in soil contamination. In Proceedings of the 1st European Meeting on Geostatistics for Environmental Applications (pp. 247-258), Lisbon, November 18-19, 1996.

Goovaerts, P. (1997). Geostatistics for natural resources evaluation. Oxford University Press.

Gómez, A. (2019). Fluidos mineralizantes del distrito minero Alhué, Chile (Master's thesis, Universidad de Chile, Santiago, Chile).

Groen, E. A., Bokkers, E. A. M., & Heijungs, R. (2017). Methods for global sensitivity analysis in life cycle assessment. International Journal of Life Cycle Assessment, 22, 1125-1137. https://doi.org/10.1007/s11367-016-1217-3

Guilbert, J. M., & Park, C. M. (1986). The geology of ore deposits. W.H. Freeman and Co.

Guo, B., Peng, Y., & Espinosa-Gomez, R. (2014). Cyanide chemistry and its effect on mineral flotation. Minerals Engineering, 66-68, 25-32. https://doi.org/10.1016/j.mineng.2014.04.008

Habashi, F. (1967). Kinetics and mechanism of gold and silver dissolution in cyanide solution. Bulletin 59, Montana Bureau of Mines.Haque, K.E.1992. The role of oxygen in cyanidation leaching of gold ore, CIM. Bulletin, Canada, pp. 3 1-3 8.

Han, S., Jung, M., Lee, W., Kim, S., Lee, K., Lim, G.-T., Jeon, H.-S., Choi, S. Q., & Han, Y. (2021). Diagnosis and optimization of gold ore flotation circuit via linear circuit analysis and mass balance simulation. Minerals, 11(1065). https://doi.org/10.3390/min11091065

Hedley, N., & Tabachnick, H. (1958). Chemistry of cyanidation. Mineral Dressing Notes 23. New York: American Cyanamid Company.

Herrington, R. (2011). Geological features and genetic models of mineral deposits. In P. Darling (Ed.), SME mining engineering handbook (3rd ed., Vol. 2, pp. 1365-1373). Society for Mining, Metallurgy and Exploration.

Himmelblau, D. (1967). Basic principles and calculations in chemical engineering (2nd ed.). Prentice Hall.

Jackson, S., Fredericksen, D., Stewart, M., Vann, J., Burke, A., Dugdale, J., & Bertoli, O. (2003). Geological and grade risk at the Golden Gift and Magdala gold deposits, Stawell, Victoria, Australia. In Proceedings of the 5th International Mining Geology Conference.

John, D. A., Vikre, P. G., du Bray, E. A., Blakely, R. J., Fey, D. L., Rockwell, B. W., & Graybeal, F. T. (2018). Descriptive models for epithermal gold-silver deposits: U.S. Geological Survey Scientific Investigations Report 2010–5070–Q. https://doi.org/10.3133/sir20105070Q

Journel, A. (1974). Geostatistics for conditional simulation of ore bodies. Economic Geology, 69(5), 673-687. https://doi.org/10.2113/gsecongeo.69.5.673

Journel, A. G. (1983). Nonparametric estimation of spatial distributions. Journal of the International Association for Mathematical Geology, 15(3), 445–468. https://doi.org/10.1007/BF01031292

Journel, A. G. (1989). Fundamentals of geostatistics in five lessons (Vol. 16). American Geophysical Union.

Journel, A. G. (1996). Modelling uncertainty and spatial dependence: Stochastic imaging. International Journal of Geographical Information Systems, 10, 517–522. https://doi.org/10.1080/02693799608902101

Journel, A. G., & Huijbregts, C. J. (1978). Mining geostatistics. Academic Press.

Journel, A. G., & Isaaks, E. H. (1984). Conditional indicator simulation: Application to a Saskatchewan uranium deposit. Mathematical Geology, 16(7), 685-718. https://doi.org/10.1007/BF01029339

Journel, A. G., & Kyriakidis, P. C. (2004). Evaluation of mineral reserves: A simulation approach. Oxford University Press.

Journel, A. G., & Zhang, T. (2006). The necessity of a multiple-point prior model. Mathematical Geology, 38(5), 591-610. https://doi.org/10.1007/s11004-006-9031-2

Kehmeier, R., Acuña, E., Hartman, B., & Zeise, J. (2016). Management of extreme high-grade assay in mineral resource estimates. SME Annual Conference & Expo.

Khosrowshahi, S., & Shaw, W. (2001). Conditional simulation for resource characterization and grade control - Principles and practice. Journal of the Southern African Institute of Mining and Metallurgy, 23, 285-292.

Kleijnen, J. (2012). Design and analysis of Monte Carlo experiments. In J. E. Gentle, W. K. Hardle, & Y. Mori (Eds.), Handbook of computational statistics (pp. 529–547). Springer. https://doi.org/10.1007/978-3-642-21551-1_18

Komorowski, M., Marshall, D. C., Salciccioli, J. D., & Crutain, Y. (2016). Exploratory data analysis. In Secondary analysis of electronic health records (Chapter 15). Springer Nature.

Kumral, M., & Asli Sari, Y. (2017). Simulation-based mine extraction sequencing with chance constrained risk tolerance. Simulation, 93(6), 527-539. https://doi.org/10.1177/0037549716679496

Kuyucak, N., & Akcil, A. (2013). Cyanide and removal options from effluents in gold mining and metallurgical processes. Minerals Engineering, 50-51, 13-29. https://doi.org/10.1016/j.mineng.2013.05.027

Lancaster, S. T., & Bras, R. L. (2002). A simple model of river meandering and its comparison to natural channels. Hydrological Processes, 16, 1–26. https://doi.org/10.1002/hyp.1036

Lavoisier, A. (1789). Traité élémentaire de chimie, présenté dans un ordre nouveau, et d'après des découvertes modernes (1st ed.). Cuchet.Laing, T. & Pinto, A. 2023. Artisanal and small-

scale mining and the low-carbon transition: Challenges and opportunities*, Environmental Science & Policy*, Volume 149.

Iooss, B., & Saltelli, A. (2017). Introduction to sensitivity analysis. In Handbook of uncertainty quantification (pp. 1103-1122). Springer. https://doi.org/10.1007/978-3-319-11259-6_31

Le, S. (2021). The applications of NPV in different types of markets. In 2021 3rd International Conference on Economic Management and Cultural Industry (ICEMCI 2021) (pp. 1054-1059). Atlantis Press. https://doi.org/10.2991/assehr.k.211209.171

Li, D., Jiang, P., Hu, C., & Yan, T. (2023). Comparison of local and global sensitivity analysis methods and application to thermal hydraulic phenomena. Progress in Nuclear Energy, 158. https://doi.org/10.1016/j.pnucene.2023.104585

Liu, D., Guoqing, L., Nailian, H., & Zhaoyang, M. (2019). Application of real options on the decision-making of mining investment projects using the system dynamics method. IEEE.

Maidstone, R. (2012). Discrete event simulation, system dynamics, and agent-based simulation: Discussion and comparison. System (2012), 1-6.

Malek, A., Kawsary, M., & Hasanuzzaman, M. (2022). Chapter 10 - Economic assessment of solar thermal energy technologies. In M. Hasanuzzaman (Ed.), Technologies for solar thermal energy (pp. 293-322). Academic Press. https://doi.org/10.1016/B978-0-12-824254-0.00010-5Mantoglou, A., Wilson, J.L. 1982. The turning bands method for simulation of random fields using line generation by a spectral method. Water Resources Research 18 (5), pp. 1379–1394.

Mariethoz, G., Renard, P., & Straubhaar, J. (2010). The direct sampling method to perform multiple-point geostatistical simulations. Water Resources Research, 46(W11536). https://doi.org/10.1029/2008WR007621

Marsden, J., & House, C. (2006). The chemistry of gold extraction (2nd ed., pp. 503-651). The Society for Mining Metallurgy and Exploration Inc.

Massey, F. J., Jr. (1951). The Kolmogorov-Smirnov test for goodness of fit. Journal of the American Statistical Association, 46(253), 68–78. https://doi.org/10.1080/01621459.1951.10500769

Massoud, M. (1997). Reactivity of sulfide minerals and its effect on gold dissolution and its electrochemical behaviour in cyanide solution (Doctoral dissertation, Queen's University, Kingston, Ontario, Canada).

Matheron, G. (1963). Principles of geostatistics. Economic Geology, 58(8), 1246-1266. https://doi.org/10.2113/gsecongeo.58.8.1246

Matheron, G. (1973). The intrinsic random functions and their applications. Advances in Applied Probability, 5(3), 439-468. https://doi.org/10.2307/1425829

Matheron, G. (1982). Pour une analyse krigeante des données régionalisées. Centre de Géostatistique, Fontainebleau, France.

Mathey, M. (2022). Simulation of production processes and associated costs in mining using the Monte Carlo method. Journal of the Southern African Institute of Mining and Metallurgy, 122(12), 697–704. https://doi.org/10.17159/2411-9717/2087/2022

Matthews, S. (2018). Geología del distrito minero Alhué (Internal presentation). Minera Florida, Alhué, Chile.

McFarlane, A. J., Bremmell, K. E., & Addai-Mensah, J. (2005). Optimising the dewatering behaviour of clay tailings through interfacial chemistry, orthokinetic flocculation, and controlled shear. Powder Technology, 160(1), 27-34. https://doi.org/10.1016/j.powtec.2005.04.046

McGrath, P. (2005). Improving operations in the mining industry with business process management technology. In Application of Computers and Operations Research in the Mineral Industry (APCOM), Tucson.

Medina, D., & Anderson, C. G. (2020). A review of the cyanidation treatment of copper-gold ores and concentrates. Advances in Mineral Processing and Hydrometallurgy, 10(7).

Mirakovski, D., Krstev, B., Krstev, A., & Petrovski, F. (2009). Mine project evaluation techniques. Natural Resources and Technologies, 3(3).

Mittal, S., Zeigler, B. P., Martin, J. L. R., Sahin, F., & Jamshidi, M. (2008). Modeling and simulation for systems of systems engineering. In M. Jamshidi (Ed.), System of systems engineering: Innovations for the 21st century (Chapter 5, pp. 101–149). Wiley.

Mizuno, T., & Deutsch, C. (2022). Sequential indicator simulation (SIS). In J. L. Deutsch (Ed.), Geostatistics Lessons.

Montaldo, D. (1977). A system dynamics model of an underground metal mine (Master's thesis, Massachusetts Institute of Technology).

Montgomery, D. C., & Runger, G. C. (2010). Sampling distributions and point estimation of parameters. In Applied statistics and probability for engineers (5th ed., pp. 223–250). John Wiley & Sons.

Mpofu, P., Mensah, J. A., & Ralston, J. (2005). Interfacial chemistry, particle interactions, and improved dewatering behaviour of smectite clay dispersions. International Journal of Mineral Processing, 75(1-2), 155–171. https://doi.org/10.1016/j.minpro.2004.10.005

Mungall, J. E. (2014). Geochemistry of magmatic ore deposits. In H. D. Holland & K. K. Turekian (Eds.), Treatise on geochemistry (2nd ed., Vol. 13-8, pp. 195–218). Elsevier. https://doi.org/10.1016/B978-0-08-095975-7.01108-6

Muravjovs, A., Tolujevs, J., & Yatskiv, I. (2016). The use of discrete rate simulation paradigm to build models of inventory control systems. In 2016 International Conference on System Modeling & Research in Logistics and Operations (pp. 650-655). https://doi.org/10.1109/SMRLO.2016.115

Murphy, M., Parker, H., Ross, A., & Audet, M. (2004). Ore-thickness and nickel grade resource confidence at the Koniambo Nickel Laterite Deposit in New Caledonia. In Banff 2004 Seventh International Geostatistics Conference (43 p.).

Navarra, A. (2019). Automation and control of mining systems. McGill University, Montreal (unpublished).

Navarra, A. (2020). MIME 527 Course Notes - Chapter II: Blasting and excavation operations. Montreal (unpublished).

Navarra, A. (2023). Discrete event simulation for the integrated management of mining and metallurgical systems. In Proceedings of the 62nd Conference of Metallurgists, COM 2023.

Navarra, A., Alvarez, M., Rojas, K., Menzies, A., Pax, R., & Waters, K. (2019). Concentrator operational modes in response to geological variation. Minerals Engineering, 134, 356–364. https://doi.org/10.1016/j.mineng.2019.01.028

Navarra, A., Grammatikopoulos, T., & Waters, K. (2018). Incorporation of geometallurgical modelling into long-term production planning. Minerals Engineering, 120(1), 118-126. https://doi.org/10.1016/j.mineng.2018.02.002

Navarra, A., Marambio, H., & Oyarzún, F. (2017). System dynamics and discrete event simulation of copper smelters. Mining, Metallurgy & Exploration, 34, 96–106. https://doi.org/10.1007/s42461-018-0030-9

Navarra, A., & Waters, K. (2016). Concentrator utilization under geological uncertainty. Canadian Metallurgical Quarterly, 55(4), 470-478. https://doi.org/10.1080/00084433.2016.1207943

Nelson, M. (2011). Site environmental considerations. In P. Darling (Ed.), SME mining engineering handbook (3rd ed., Vol. 2, pp. 1365-1373). Society for Mining, Metallurgy, and Exploration.

Nicol, M. J. (1980). The anodic behavior of gold. Gold Bulletin, 13(3), 105-111. https://doi.org/10.1007/BF03215464Nieto, A. 2010. Key Deposit Indicators (KDI) and Key Mining Method Indicators (KMI) in Underground Mining Method Selection. Transactions of the Institution of Mining and Metallurgy, Section A: Mining Technology, 328, pp 381-396.

Órdenes, J. (2014). Influencia de la mineralogía de la veta Bonanza en el proceso hidrometalúrgico de extracción de Au y Ag, Yacimiento El Peñón. Antofagasta: Universidad Católica del Norte, Facultad de Ingeniería y Ciencias Geológicas.

Órdenes, J., Toro, N., Quelopana, A., & Navarra, A. (2022). Data-driven dynamic simulations of gold extraction which incorporate head grade distribution statistics. Metals, 12, 1372. https://doi.org/10.3390/met12081372

Órdenes, J., Wilson, R., Peña-Graf, F., & Navarra, A. (2021). Incorporation of geometallurgical input into gold mining system simulation to control cyanide consumption. Minerals, 11, 1023. https://doi.org/10.3390/min11101023

O'Regan, B., & Moles, R. (2006). Using system dynamics to model the interaction between environmental and economic factors in the mining industry. Journal of Cleaner Production, 14(8), 689-707. https://doi.org/10.1016/j.jclepro.2005.08.012

Orioli, A., & Di Gangi, A. (2015). The recent change in the Italian policies for photovoltaics: Effects on the payback period and levelized cost of electricity of grid-connected photovoltaic systems installed in urban contexts. Energy, 93, 1989-2005. https://doi.org/10.1016/j.energy.2015.10.100

Ortiz, J. M. (2020). Introduction to sequential Gaussian simulation (Annual Report 2020, Paper 2020-01). Predictive Geometallurgy and Geostatistics Lab, Queen's University, Kingston (ON).

Ortiz, J. M., & Deutsch, C. V. (2004). Indicator simulation accounting for multiple-point statistics. Mathematical Geology, 36(5), 545-565. https://doi.org/10.1023/B:MATG.0000037736.00489.b5

Ortiz, J., & Peredo, O. (2010). Multiple point geostatistical simulation with simulated annealing: Implementation using speculative parallel computing. Proceedings of the Geostatistical Association of Australasia.

Panagiotou, G. N. (1999). Discrete mine system simulation in Europe. International Journal of Mining Reclamation and Environment, 13(2), 43–46. https://doi.org/10.1080/09208119908944224

Pamparana, G., Kracht, W., Haas, J., Díaz-Ferrán, G., Palma-Behnke, R., & Román, R. (2017). Integrating photovoltaic solar energy and a battery energy storage system to operate a semi-autogenous grinding mill. Journal of Cleaner Production, 165, 273-280. https://doi.org/10.1016/j.jclepro.2017.07.092

Pakalnis, R. T., & Hughes, P. B. (2011). Sublevel stoping. In P. Darling (Ed.), SME mining engineering handbook (3rd ed., Vol. 2, pp. 1365-1373). Society for Mining, Metallurgy, and Exploration.

Parga, J., Rodríguez, M., Vázquez, V., Valenzuela, J. L., & Moreno, H. (2012). Recovery of silver and gold from cyanide solution by magnetic species formed in the electrocoagulation process. Mineral Processing and Extractive Metallurgy Review, 33(6), 363-373. https://doi.org/10.1080/08827508.2011.625870

Paravarzar, S., Emery, X., & Madani, N. (2015). Comparing sequential Gaussian and turning bands algorithms for cosimulating grades in multi-element deposits. Comptes Rendus Geoscience, 347(1), 84-93. https://doi.org/10.1016/j.crte.2014.12.001

Pearson, K. (1900). X. On the criterion that a given system of deviations from the probable in the case of a correlated system of variables is such that it can be reasonably supposed to have arisen from random sampling. The London, Edinburgh, and Dublin Philosophical Magazine and Journal of Science, 50(302), 157–175. https://doi.org/10.1080/14786440009463897

Peña-Graf, F. A., Grammatikopoulos, T., Kabemba, A., & Navarra, A. (2021). Integrated feed management of mineral processing plants with application to chromite processing. Canadian Metallurgical Quarterly, 60(3), 130–136. https://doi.org/10.1080/00084433.2021.1902102

Peña-Graf, F., Órdenes, J., Wilson, R., & Navarra, A. (2022). Discrete event simulation for machine-learning enabled mine production control with application to gold processing. Metals, 12(225). https://doi.org/10.3390/met12020225

Perrott-Humphrey, F. (2011). Market capitalization. In P. Darling (Ed.), SME mining engineering handbook (3rd ed., Vol. 2, pp. 1365-1373). Society for Mining, Metallurgy, and Exploration.

Pirajno, F. (1992). Hydrothermal alteration. In Hydrothermal mineral deposits (pp. 89-134). Springer. https://doi.org/10.1007/978-3-642-75671-9_5

Price, A. (2014). Discrete-event haulage simulation: Making better decisions with reduced uncertainty. In P. Runge (Ed.), Pincock Minarco Perspectives (Issue No. 123).

Pyrcz, M. J., Boisvert, J. B., & Deutsch, C. V. (2009). ALLUVSIM: A program for event-based stochastic modeling of fluvial depositional systems. Computers & Geosciences, 35(8), 1671–1685. https://doi.org/10.1016/j.cageo.2008.09.012

Pyrcz, M. J., & Deutsch, C. V. (2014). Geostatistical reservoir modeling (2nd ed.). Oxford University Press.Vann, J., Bertoli, O. & Jackson, S., 2002. An overview of geostatistical simulation for quantifying risk. In: S. M. Searston & R. J. Warner, eds. Proceedings of the Quantifying Risk and Error Symposium. Perth (WA): Geostatistical Association of Australasia, pp. 1–12.

Radzicki, J., & Taylor, R. (2008). Origin of system dynamics: Jay W. Forrester and the history of system dynamics. In U.S. Department of Energy's Introduction to System Dynamics.

Raychaudhuri, S. (2008). Introduction to Monte Carlo simulation. In S. J. Mason, R. R. Hill, L. Mönch, O. Rose, T. Jefferson, & J. W. Fowler (Eds.), Proceedings of the 2008 Winter Simulation Conference (pp. 91–100). https://doi.org/10.1109/WSC.2008.4736059

Razavi, S., Jakeman, A., Saltelli, A., Prieur, C., Iooss, B., Borgonovo, E., Plischke, E., Lo Piano, S., Iwanaga, T., Becker, W., Tarantola, S., Guillaume, J. H. A., Jakeman, J., Gupta, H., Melillo, N., Rabitti, G., Chabridon, V., Duan, Q., Sun, X., Smith, S., Sheikholeslami, R., Hosseini, N.,

Asadzadeh, M., Puy, A., Kucherenko, S., & Maier, H. R. (2021). The future of sensitivity analysis: An essential discipline for systems modeling and policy support. Environmental Modelling & Software, 137, 104954. https://doi.org/10.1016/j.envsoft.2021.104954

Reggelin, T., & Tolujew, J. (2011). A mesoscopic approach to modeling and simulation of logistics processes. In Proceedings of the Winter Simulation Conference (WSC '11) (pp. 1513–1523). https://doi.org/10.1109/WSC.2011.6147875

Ren, W. (2005). Short note on conditioning turning bands realizations. Centre for Computational Geostatistics, University of Alberta, Canada.

Richmond, A. J. (2012). Conditional simulation of a folded lode-style gold deposit. In Narrow Vein Mining Conference 2012 (pp. 149–153). Perth, Australia.

Rivalin, L., Stabat, P., Marchio, D., Caciolo, M., & Hopquin, F. (2018). A comparison of methods for uncertainty and sensitivity analysis applied to the energy performance of new commercial buildings. Energy and Buildings, 166, 489-504. https://doi.org/10.1016/j.enbuild.2018.02.009

Rodriguez, J. D., Perez, A., & Lozano, J. A. (2010). Sensitivity analysis of k-fold cross validation in prediction error estimation. IEEE Transactions on Pattern Analysis and Machine Intelligence, 32(3), 569-575. https://doi.org/10.1109/TPAMI.2009.187

Rosenblatt, M. (1985). Stationary processes. In Stationary sequences and random fields (pp. 1–34). Birkhäuser.Roy, S. S., Reparaz, O., Vercauteren, F., & Verbauwhede, I. 2014. Compact and Side Channel Secure Discrete Gaussian Sampling. Cryptology ePrint Archive.

Runge, I. (2011). Economic principles for decision making. In P. Darling (Ed.), SME mining engineering handbook (3rd ed., Vol. 2, pp. 1365-1373). Society for Mining, Metallurgy, and Exploration.

Sadehi, M., Houdouin, D., & Bazin, C. (2018). Mineral processing plant data reconciliation including mineral mass balance constraints. Minerals Engineering, 123, 117–127. https://doi.org/10.1016/j.mineng.2018.03.010

Samara, N. (2009). Heavy metals concentrations in biosolids of Al-Bireh sewage treatment plant and assessment of biosolids application impacts on crop growth and productivity (Master's thesis, Birzeit University).

Savolainen, J., Rakhsha, R., & Durham, R. (2021). Simulation-based decision-making system for optimal mine production plan selection. Mineral Economics. https://doi.org/10.1007/s13563-021-00297-w

Sepúlveda, F. (2004). Caracterización geológica y antecedentes microtermométricos de la veta Lorena, distrito minero Alhué, región metropolitana, Chile (Memoria para optar al título de geólogo, Universidad de Chile).

Shishvan, M., & Benndorf, J. (2016). The effect of geological uncertainty on achieving short-term targets: A quantitative approach using stochastic process simulation. Journal of the Southern African Institute of Mining and Metallurgy, 116(3), 259-264. https://doi.org/10.17159/2411-9717/2016/v116n3a9

Sillitoe, R. H. (1977). Metallic mineralization affiliated to subaerial volcanism: A review. In Volcanic processes in ore genesis (pp. 99-116). Institution of Mining and Metallurgy-Geological Society of London.

Simmons, S. F., White, N., & John, D. (2005). Geological characteristics of epithermal precious and base metal deposits. Economic Geology, 100th Anniversary Volume, 485-522.

Simon, H. (1957). Rationality and decision making. In Models of man. John Wiley.

Simoni, M., Drielsma, J., Ericsson, M., Gunn, A., Heiberg, S., Heldal, T., Nassar, N., Petavratzi, E., & Müller, D. B. (2023). Mass-balance-consistent geological stock accounting: A new approach toward sustainable management of mineral resources. Environmental Science & Technology. https://doi.org/10.1021/acs.est.3c02437

Skorstad, A., Hauge, R., & Holden, L. (1999). Conditioning in a fluvial reservoir model. Mathematical Geology, 31(7), 857–872. https://doi.org/10.1023/A:1007590204917

Srivastava, M. (2018). In B. S. Daya Sagar, Q. Cheng, & F. Agterberg (Eds.), Handbook of mathematical geosciences: Fifty years of IAMG (pp. 1-23). Springer. https://doi.org/10.1007/978-3-319-78999-6

Stephan, G. (2011). Cut-and-fill mining. In P. Darling (Ed.), SME mining engineering handbook (3rd ed., Vol. 2, pp. 1365-1373). Society for Mining, Metallurgy, and Exploration.

Stewart, M., & Kappes, D. (2012). SART for copper control in cyanide heap leaching. Journal of The Southern African Institute of Mining and Metallurgy, 112, 1037-1043.

Stewart, P., & Trueman, R. (2008). Strategies for minimising and predicting dilution in narrow vein mines—The narrow vein dilution method. In Proceedings of the Narrow Vein Mining Conference (pp. 1-14), Ballarat, VIC, Canada.

Strebelle, S. (2000). Sequential simulation drawing structures from training images (PhD thesis). Stanford University, USA.

Strebelle, S. (2002). Conditional simulation of complex geological structures using multiple-point statistics. Mathematical Geology, 34(1), 1–21. https://doi.org/10.1023/A:1014009426274

Tahmasebi, P. (2018). Multiple point statistics: A review. In B. S. Daya Sagar, Q. Cheng, & F. Agterberg (Eds.), Handbook of mathematical geosciences: Fifty years of IAMG (pp. 77-100). Springer. https://doi.org/10.1007/978-3-319-78999-6_4

Tang, V., & Vijay, S. (2001). System dynamics: Origins, development, and future prospects of a method. Massachusetts Institute of Technology, Cambridge, MA.

Terlunen, S., Horstkemper, D., & Hellingrath, B. (2014). Adaption of the discrete rate-based simulation paradigm for tactical supply chain decisions. In Proceedings of the 2014 Winter Simulation Conference (WSC '14) (pp. 2060–2071). IEEE Press. https://doi.org/10.1109/WSC.2014.7020052

Thomas, H. (1958). Geología de la Cordillera de la costa entre el Valle de la Ligua y la Cuesta Barriga. Instituto de Investigaciones Geológicas, Boletín Nº 2, 86 pp.

Upadhyay, S., Askari Nasab, H., Tabesh, M., & Badiozamani, M. (2015). Simulation and optimization in open pit mining. In K. Bandopadhyay (Ed.), Application of computers and operations research in the mining industry (pp. 120-130). Society for Mining Metallurgy & Exploration (SME).

Verbrugge, B., Lanzano, C., & Libassi, M. (2021). The cyanide revolution: Efficiency gains and exclusion in artisanal- and small-scale gold mining. Geoforum, 126, 267-276. https://doi.org/10.1016/j.geoforum.2021.08.005

Vives, A. (2015). Evaluación técnica y económica de una mina subterránea utilizando relleno cementado (Memoria para optar al título de Ingeniero Civil de Minas, Universidad de Chile, Santiago, Chile).

Wang, X., Wang, W., Tao, F., & Liu, A. (2021). New paradigm of data-driven smart customisation through digital twin. Journal of Manufacturing Systems, 58(Part B), 270-280. https://doi.org/10.1016/j.jmsy.2020.06.012

Weichselbaum, J., Tumility, J. A., & Schmidt, C. G. (1989). The effect of sulfide and lead on the rate of gold cyanidation. In The AusIMM Annual Conference (pp. 221-224).

Wells, W. (2002). Using simulated annealing in geostatistics (Honors thesis). Edith Cowan University. https://ro.ecu.edu.au/theses_hons/542

White, N. C., & Hedenquist, J. W. (1995). Epithermal gold deposits: Styles, characteristics, and exploration. Society of Economic Geologists Newsletter, 23, 1-13.

Wilson, R., Mercier, P. H. J., & Navarra, A. (2022a). Integrated artificial neural network and discrete event simulation framework for regional development of refractory gold systems. Minerals, 123–154. https://doi.org/10.3390/mining2010008

Wilson, R., Perez, K., Toro, N., Parra, R., Mackey, P. J., & Navarra, A. (2022b). Mine-to-smelter integration framework for regional development of porphyry copper deposits within the Chilean context. Canadian Metallurgical Quarterly, 61, 48–62. https://doi.org/10.1080/00084433.2022.2071750

Wilson, R., Toro, N., Naranjo, O., Emery, X., & Navarra, A. (2021). Integration of geostatistical modeling into discrete event simulation for development of tailings dam retreatment applications. Minerals Engineering, 164, 106814. https://doi.org/10.1016/j.mineng.2021.106814

Wills, B. A., & Finch, J. (2016). Sampling, control, and mass balancing. In B. A. Wills & J. A. Finch (Eds.), Wills' mineral processing technology (8th ed., pp. 41-90). Butterworth-Heinemann. https://doi.org/10.1016/C2014-0-02764-5

Winston, W., & Goldberg. (2004). The EOQ with uncertain demand: The (r,q) and (s,S) models. In Operations research: Application and algorithms (pp. 895-902). Cengage Learning.

Wittwer, J. W., Chase, K. W., & Howell, L. L. (2004). The direct linearization method applied to position error in kinematic linkages. Mechanism and Machine Theory, 39(7), 681-693. https://doi.org/10.1016/j.mechmachtheory.2003.11.003

Yamana Gold. (2020). Annual report 2020. Available online: [Link accessed on 15 September 2021].

Zhang, T. (2006). Filter-based training pattern classification for spatial pattern simulation (Ph.D. thesis). Stanford University, USA.

Zhang, T., Switzer, P., & Journel, A. (2006). Filter-based classification of training image patterns for spatial simulation. Mathematical Geology, 38(1), 63–80. https://doi.org/10.1007/s11004-005-9003-4

Zio, E. (2013). Monte Carlo simulation: The method. In The Monte Carlo simulation method for system reliability and risk analysis (pp. 1-19). Springer. https://doi.org/10.1007/978-1-4471-4588-2_1

Appendix A

A.1 Cut and Fill

Cut-and-fill is an open-stope mining method that is considered ideal for steeply dipping and irregular high-grade deposits found in weak host rock (which is an advantage for dilution control and mining flexibility). The idea is excavating small stopes of high-grade ore and then backfilling with cemented tailings to artificially support the rock and nearby mine openings. Concrete forms are built at the entrance to each room, followed by filling the recently excavated stope with cemented mill tailings slurry, which is pumped into the mine (Brackebusch, 1992). Cut-and-fill mining is extremely flexible, and several combinations of mining methods and fill materials can be used to cope with specific mining situations (Stephan, 2011).

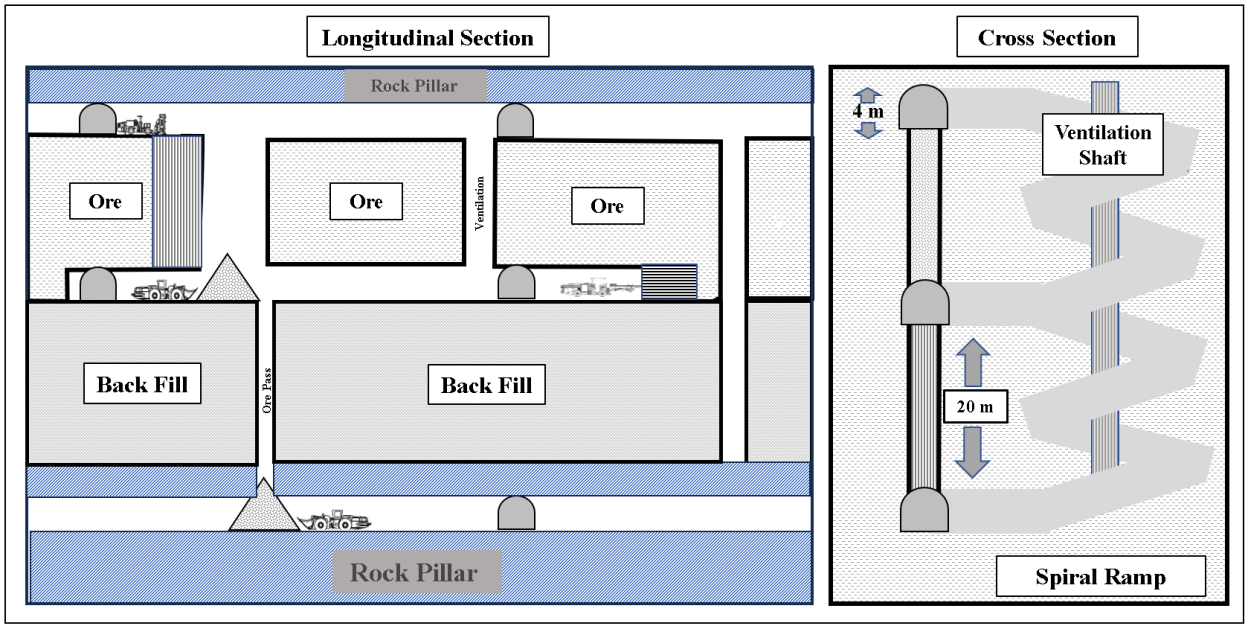

Figure A.1.1: Schematic profile of the Cut and Fill mining method.

This method presents high ore recovery and is the most selective and flexible underground mining method available. Most of the work requires excavating stopes and backfilling them, while

a small labors portion is utilized by developing and connecting passageways and tunnels. Is suitable for orebodies with irregular geometry and scattered mineralization, where high grade sections can be mined separately, and low-grade rock left in the stopes (Copco, 2007), therefore, it is easy to bypass a section of low-grade ore and target the areas with higher revenue potential (high grades). If prices rise in the future, the operators can always return to unmined blocks to recover what was left behind. Cut-and-fill is preferred in specific scenarios, particularly where the ore value is high, and the primary objective is to achieve a high ore recovery rate with minimal dilution. (Stephan, 2011). In cut and fill mining, the operation is highly mechanized, labor-intensive and some tasks are conducted on top of freshly blasted rock. The operating cost is quite high due in large part to the backfill, low productivity and development rate (Darling, 2011). Additionally, ventilation systems and massive ground control measures are required increasing the potential operation cost, therefore, cut-and-fill mining can be unsuitable for low-grade orebodies (Hamrin, 1980).

For the current work, a bench and fill mining method (which is an adaptation of cut and fill) was computed for the mineral extraction to obtain the mining extraction sequence. The spatial characteristics (e.g., size, shape, orientation) and the degree of boundary uniformity of the orebody are the initial aspects to consider when opting for a cut-and-fill method (Stephan, 2011). The right mining method selection imply ensure the revenue surpass the costs of extraction and the recovery process of a saleable metal and narrow-vein type deposits are particularly challenging to mine profitably (Drake et. Al, 2020). For narrow high-grade veins, cut and fill and its adaptations (e.g., bench-and-fill, long hole-stopping, and drift-and-fill) are the most common methods selected for this orebody geometry. The main economic downside is the cost of backfill production and placement (Darling, 2013). The main parameters for the mining method and ore development (production tunnels of 4m x 4m workface area) at regular levels in intervals of 20 m (Figure A.1.2).

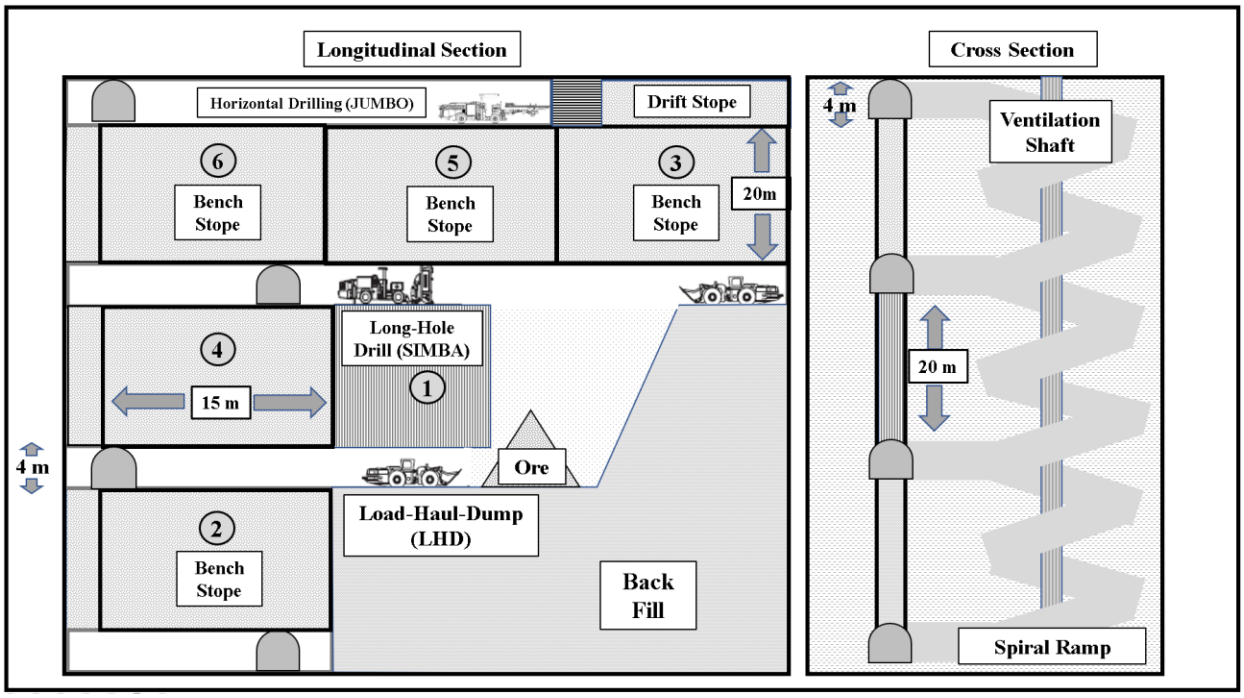

Figure A.1.2: Schematic profile of the bench-and-fill mining method.

A.2 Sub-level Stoping

Sub-level stoping is an underground mining method used to extract ore from a steeply dipping or vertical ore body. It involves the extraction of ore in a series of horizontal slices (a.k.a. sublevels) within the deposit. The method is widely used for mining narrow, high-grade ore bodies, particularly those with a significant dip and is commonly used to extract gold and silver. Once the development is completed, sublevels are established at regular vertical intervals within the ore body. These sublevels are typically accessed by ramps or raise boreholes. The distance between sublevels depends on the height of the ore zone and the desired size of the mining blocks (stopes). Ore is extracted using a cycle of drilling and blasting, followed by mucking of the ore by a loader and transported the crushed ore to either an ore-pass or a truck to carry the ore further to a crusher, before it is sent up to the surface via the shaft. A typical longitudinal and cross-sectional view of the sublevel stoping method is shown in Figure A-1. This mining method offers several advantages, including high ore recovery rates, the ability to mine high-grade ore bodies economically, and the flexibility to adapt to variable orebody geometries. Overall, sublevel stoping is a widely used underground mining method that allows for efficient and selective extraction of ore from steeply dipping or vertical deposits. However, it also presents challenges such as the need for proper ventilation, ground control measures, and efficient material handling systems.

Conveyors and ore passes can be used in conjunction with a truck-loader configuration to ensure a streamlined material handling system. If the rock mass is jointed or weak, the stopes are backfilled once all of the material is extracted to promote stability throughout the mine. Backfill also allows for tailings of the processed ore to be used as a component of paste backfill, allowing it to be disposed of underground instead of a tailings pond that could fail and contaminate nearby water sources. Otherwise, sublevel stoping, in the absence of consolidated backfill, employs pillars to separate the individual stopes to reduce the potential for wall slough (Pakalnis & Hughes, 2011). An extraction pattern based on sublevel stoping mining method was utilized to obtain an extraction sequence.

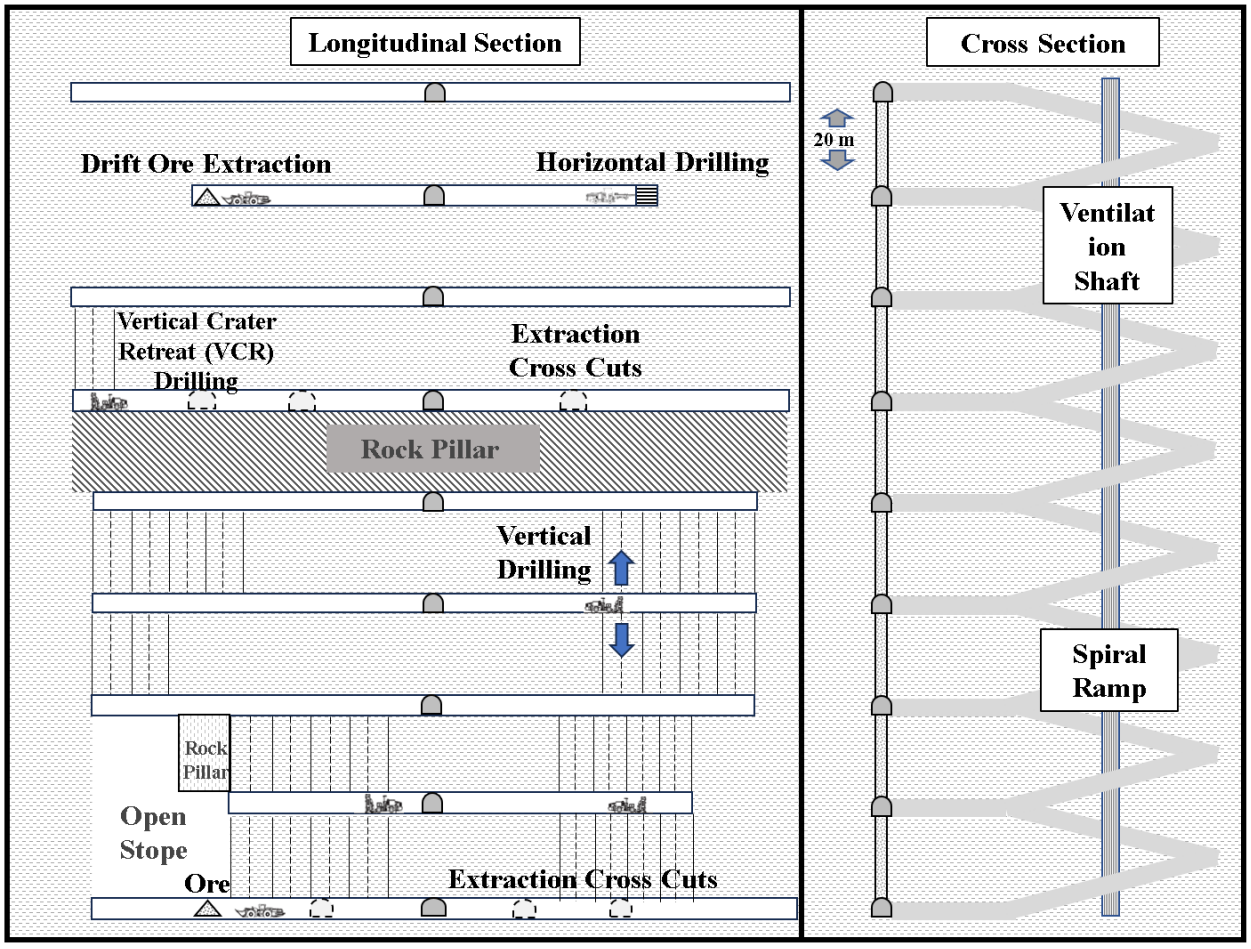

Figure A.2.1: Schematic profile of the sublevel stoping mining method.